Molecular regulation of BRD3

in forward programming of Megakaryocytes

Maria Isabel Marques Rosa

University of Cambridge

Newnham College

This dissertation is submitted for the degree of Doctor of Philosophy

September 2018

Declaration

This dissertation is the result of my own work and includes nothing which is the outcome of work done in collaboration except as declared in the Preface and specified in the text.

It is not substantially the same as any that I have submitted, or, is being concurrently submitted for a degree or diploma or other qualification at the University of Cambridge or any other University or similar institution except as declared in the Preface and specified in the text. I further state that no substantial part of my dissertation has already been submitted, or, is being concurrently submitted for any such degree, diploma or other qualification at the University of Cambridge or any other University or similar institution except as declared in the Preface and specified in the text.

It does not exceed the prescribed word limit for the relevant Degree Committee.

Isabel Rosa
September 2018

"Quando de lá vimos, é que para lá havíamos de ir"

"The moment when one finishes a journey, is when they are truly ready to start."

Ernesto Rosa, my Dad

Table of contents

List of figures

Introduction

Appendix

List of tables

Material and Methods

Results

Appendix

Table of Abbreviations

ACS	Acute coronary syndrome
ADP	Adenosine diphosphate
AGM	Aorta-gonad-mesonephros
AMR	Ashwell-Morell receptor
ATAC-seq	Assay for transposase-accessible chromatin with sequencing
BET	Bromodomain and extra terminal
BRD	Bromodomain protein
BD	Bromodomain module
CBFβ	Core binding factor β
ChIP-seq	Chromatin immunoprecipitation followed by massively parallel DNA sequencing
CRISPR/Cas9	Clustered regularly interspaced palindromic repeats and associated Cas9 enzymes
CRISPRi	CRISPR interference
cMpl	Thrombopoietin receptor
crRNA	CRISPR RNA
c-kit	SCF tyrosine kinase receptor
CTCF	CCCTC-binding factor
CMP	Common myeloid progenitor
CLOUD-HSPC	Continuum of Low primed UnDifferentiated HSPC
DNA	Deoxyribonucleic acid
DSB	Double strand break
dCas9	Dead Cas9
DMSO	Dimethyl sulphoxide
EB	Erythroblast
ESC	Embryonic stem cell
EPO	Erythropoietin
EKLF	Erythroid Krüppel-like factor
EDTA	Ethylenediaminetetraacetic acid
FACS	Fluorescence activated cell sorting
FLI-1	Friend of leukemia integration 1
FoP	Forward programming
GATA-1	GATA binding factor 1
gDNA	Genomic DNA
GMP	granulocyte-monocyte progenitor
HATs	Histone acetyltransferases
HDACs	Histone deactylases
HDR	Homologous directed recombination
HSPC	Haematopoietic stem pluripotent cell
HSC	Haematopoietic stem cell
IMS	Invaginated membrane system
IMDM	Iscove's Modified Dulbecco's Media

iPSC	Induced pluripotent stem cell
imMKCL	Immortalized MK progenitor cell line
Jak2	Janus kinase 2
KO	knockout
LD	Linkage disequilibrium
LT-HSC	Lon-term haematopoietic stem cell
Ly-bi HSC	lymphoid-biased haematopoietic stem cell
MAPK	Mitogen-activated protein kinase
MARS-seq	Massive parallel single cell RNA-seq
MK	megakaryocyte
MK-FoP	Megakaryocytes forward programming
MEP	megakaryocyte-erythrocyte progenitors
My-bi HSC	Myeloid-biased haematopoietic stem cell
MLP	multipotent lymphoid progenitors
MPV	Mean platelet volume
MPP	multipotent progenitors
NURF	Nucleosome remodeling factor
NHEJ	Non-homologous end joining
ORF	Open reading frame
PLT	Platelet count
PDW	Platelet distribution width
P-TEFb	Positive transcription elongation factor b
Pol II	Polymerase II
PTS	Paris-Trousseau syndrome
PAM	Protospacer adjacent motif
PI3K	Phosphoirositol 3 kinase
P-Sp	Para-aortic splanchnopleura
RUNX1	Runt-related transcription factor 1
RNA	Ribonucleic acid
RNA-seq	Ribonucleic acid sequencing
rTetR	Reverse tetracycline repressor
SCF	Stem cell factor/kit-ligant/steel-factor
STAT	Signal transducer and activator of transcription
ST-HSC	Short term haematopoietic stem cell
SOC media	Super Optimal broth with Catabolite repression
SNP	Single nucleotide polymorphism
sgRNA	Single guide ribonucleic acid
TAL1	T-cell acute lymphocytic protein 1
TBE buffer	Tris/borate/EDTA buffer
TF	Transcription factor
TSS	Transcription starting site
tracrRNA	Trans-activating ribonucleic acid
TPO	thrombopoietin
VEGF	Vascular endothelial growth factor
vWF	Von Willebrand factor
WT	Wild type
ZFN	Zinc finger nucleases

Abstract

Platelets are one of the most abundant cell type in the blood, and they play a crucial role in the process of homeostasis. Platelet traits, such as platelet count (PLT) and mean platelet volume (MPV) are highly heritable and stable within individuals, but the molecular mechanisms controlling these traits are poorly understood. Genome-wide association studies (GWAS) have identified BRD3 as a regulator of platelet traits. BRD3, along with BRD2, BRD4 and BRDT, is classified within the bromodomain and extra terminal (BET) family, specialised in recognising and binding to acetylated lysine residues.

In this project, I studied the functions of BRD3 during megakaryopoiesis, the process that leads to platelet formation. Because platelets do not have nucleus, megakaryocytes are the best model to study chromatin interactors associated with platelet traits. I used CRISPR/Cas9 to generate a BRD3 KO iPSc model. These cells were capable to differentiate into MKs, using a forward programming protocol, demonstrating that BRD3 is not essential for MK differentiation. I found that a subset of genes was differentially expressed in the absence of BRD3, despite genome-wide chromatin accessibility and H3K27ac signatures remaining unaltered. In order to investigate whether there was a compensatory effect among BET proteins, I designed BRD2 and BRD4 KO iPSCs, as well as combinations of BET KOs. BRD2 KO generated MK progenitors, indicating that the protein is also dispensable in MK generation. Interestingly, using an inhibitor that recognises all BET proteins, MK progenitor differentiation was impaired, but not late megakaryopoiesis, suggesting that some BET proteins might play a critical role in early MK differentiation.

Overall, these results indicate that BRD2 and BRD3 are dispensable in megakaryocytes differentiation, and probably, that BRD4 might be essential due to its role in mesoderm differentiation. Together, this work starts to unveil the requirement of BET during megakaryopoiesis.

Chapter 1

Introduction

1.1 Haematopoiesis

The human body produces over 100 billion blood cells every day. This process is known as haematopoiesis. Blood cells are highly specialised cells that have three main functions. (1) Transport of gases, nutrients, hormones and waste products. (2) Protection against pathogens. (3) Regulation of fluids and pH levels. The haematopoietic system is highly controlled, and the dysregulation of its functions can result in catastrophic outcomes for the body. Hence, understanding the complex molecular mechanisms that control the blood differentiation and function is imperative for the improvement of health care of patients suffering from blood diseases.

1.1.1. Embryonic haematopoiesis

Haematology studies on animal models, such as mouse and zebrafish, generated a great amount of knowledge on the events that characterise haematopoietic development (Jagannathan-Bogdan and Zon 2013). It is accepted that vertebrate haematology is developmentally conserved with differences mainly in the temporal sequence of differentiation, probably due to differences in individual gestation periods (Tavian and Peault 2005). Until the 1970s, it was assumed that the yolk sac was the main blood-forming tissue during embryogenesis, and blood precursor cells would migrate to the fetal liver and bone marrow (M. A. S. Moore and Metcalf 1970). Currently, it is known that the differentiation process from a pluripotent cell stage to progenitor blood cells happens in several different tissues in the embryo (figure 1.1.1). There are two main waves of embryonic haematopoietic differentiation; the primitive wave of haematopoiesis happens exclusively extra-embryonically in the yolk sac (Lux et al. 2008), whilst the definitive haematopoiesis takes place in the yolk sac and intra-embryonically.

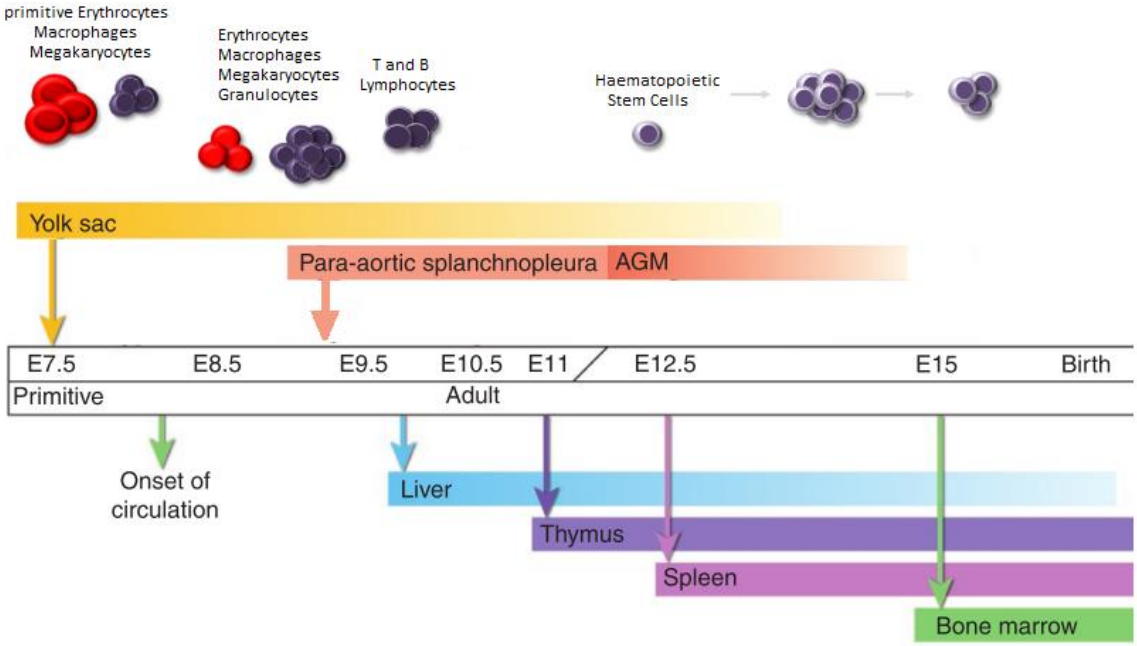

Figure 1.1.1 Sequential waves of embryonic haematopoiesis. Schematic representation of haematopoietic development during mouse embryogenesis with the embryonic day of emergence (middle), type of progenitors generated (top) and the location of each wave of haematopoiesis (bottom). Mouse haematopoiesis mimics the human haematopoiesis process during embryogenesis. Schematics adapted from (Lacaud and Kouskoff 2017; Dzierzak and Speck 2008).

In the primitive haematopoiesis, shortly after gastrulation, mesoderm cells migrate away from the primitive streak and form several populations with distinct developmental fates including blood cells (Huber et al. 2004). In the yolk sac, mesoderm cells expressing the receptor for vascular endothelium growth factor (VEGFR$^+$ or CD309), in the posterior primitive streak, differentiate into blood precursor cells, denominated blood islands (Garcia-Martinez and Schoenwolf 1993; Lugus et al. 2009; Ferkowicz and Yoder 2005). These blood precursors have a limited self-renewal and differentiation potential, and their primary function is to facilitate oxygenation of the rapidly dividing embryo. Primitive macrophages, megakaryocytes, and erythroid cell types have been reported at this early embryonic stage (Tober et al. 2007; Palis et al. 1999).

The second wave of early haematopoiesis is characterised by the development of immature myeloid and lymphoid cells, as well as the appearance of the first haematopoietic stem cells (HSCs). The erythro/myeloid progenitors identified at the embryonic stage are still immunophenotypically immature as the surface markers, transcription factors and lineage potential are present in unique proportions when compared with their adult counterparts (McGrath et al. 2015). The first lymphoid cell precursors (B and T cells) have been observed at this stage where haemogenic endothelial cells (CD144$^+$/CD41$^-$) differentiated into T-cell precursors, and successfully generated mature T-cells upon

transplantation, confirming T-cell progeny from haemogenic endothelium (Yoshimoto et al. 2012). The generation of the first B cells has been identified in the yolk sac and in the para aortic splanchnopleura (P-Sp) (Yoshimoto et al. 2011). The P-Sp region is the first intra-embryonic region where blood cells emerge, and it develops into the aorta–gonad–mesonephros (AGM) from which the haemogenic endothelium is known to derive (A Medvinsky and Dzierzak 1996).

Time-lapse imaging techniques and cell-tracking methods have contributed to tracing HSC progeny to haemogenic endothelium. A temporally restricted genetic tracing strategy, using an inducible VE-cadherin ($CD144^+$) Cre-line, has shown that first HSCs arise exclusively from endothelium (Zovein et al. 2008) located in both the yolk sac and the AGM (A Medvinsky and Dzierzak 1996; Godin, Dieterlen-Lièvre, and Cumano 1995). High-resolution imaging of live zebrafish embryos confirmed the migration of endothelial cells from the AGM to the sub-aortic space, and their transdifferentiation into multipotent haematopoietic stem/progenitor cells (HSPCs). This is a process regulated by transcription factors Runx1 (Kissa and Herbomel 2010) and GATA-2 (Tsai et al. 1994; Ling et al. 2004).

The onset of circulation is a determinant factor that allows the distribution of HSCs throughout the organism (North et al. 2009; Hirsch et al. 1996; Potocnik, Brakebusch, and Fässler 2000). The first HSCs and the endothelial precursors share a similar surface expression signature, differing in the presence or absence of CD45 expression (Dzierzak and Speck 2008; Taoudi et al. 2008). It is believed that $CD45^+$ HSCs migrate and colonise the fetal liver where they undergo expansion (Alexander Medvinsky, Rybtsov, and Taoudi 2011). HSCs are then established in the spleen and thymus, and just before birth, the bone marrow. Osawa *et al.* first demonstrated that the transplant of single HSCs harbours the potential to generate the entire repertoire of differentiated blood cells (multilineage potential) for long periods of time (Osawa et al. 1996).

1.1.2. Adult haematopoiesis, an evolving model

HSCs are rare cells with the ability for self-renewal, and differentiation into all the blood progenitors and lineage restricted blood cells. Due to the high demand of differentiated blood cells; the self-renewal, maintenance, and lineage determination of HSC is a controlled process that meets the constant supply of progenitors throughout life. HSC are found mainly in the stem cell niche in the bone marrow, but can also be found in fetal liver, cord blood and peripheral blood (Bluteau et al. 2013). The distinct properties of HSC, such as cell-surface markers, differentiation potential and cell-cycle status change remarkably throughout life, depending on the niche and development-stage. Thus, actively dividing HSCs are found in the fetal liver and quiescent HSCs in the bone marrow (Stuart

H. Orkin and Zon 2008); and older HSCs are biased toward myeloid lineages (Sudo et al. 2000; W. W. Pang et al. 2011). HSCs self-renewal ability has also been categorised into short term (ST-HSC) and long-term (LT-HSC) depending on the cells lifespan (C. E. Muller-Sieburg et al. 2004a; Weissman, Anderson, and Gage 2001; Reya et al. 2001). The recent discoveries on HSCs intrinsic properties led to a greater understanding of the mechanisms regulating differentiation of blood cells.

The model describing the differentiation of blood cells is commonly known as the haematopoietic tree. The evidence used to build this classical model was based on antibodies staining and fluorescence-assisted cell sorting (FACS) which allows the isolation of cells expressing combinations of surface markers (Morrison and Weissman 1994). Functional and molecular characterisation of these populations was achieved mainly by *in vitro* colony assays and transplantation experiments (F. Notta et al. 2011). The classical hierarchical model describes how HSCs give rise to all blood cell types in a stepwise manner, where a given cell has a more restricted lineage than its precursor (figure 1.1.2). In this model, HSCs either self-renew or differentiate into multipotent progenitors (MPP) (Osawa et al. 1996; Kent et al. 2009; Weksberg et al. 2008). MPPs lose self-renewal capability, but directly commit to two separate branches; the common myeloid progenitors (CMPs) and the multipotent lymphoid progenitors (MLPs) (Koichi Akashi et al. 2000; Kondo, Weissman, and Akashi 1997). On the myeloid branch, CMPs give rise to granulocyte-monocyte progenitors (GMP) and megakaryocyte-erythrocyte progenitors (MEPs). GMPs differentiate into granulocytes (neutrophils, eosinophils and basophils) and monocytes, cells involved in fighting infections. MEPs are the precursor cells of erythrocytes and megakaryocytes, and consequently platelets. The lymphoid branch generates lymphoid cells (such as B and T lymphocytes) and innate lymphoid cells (such as natural killer cells), but also has the potential to differentiate into the granulocytes (GMP) lineage.

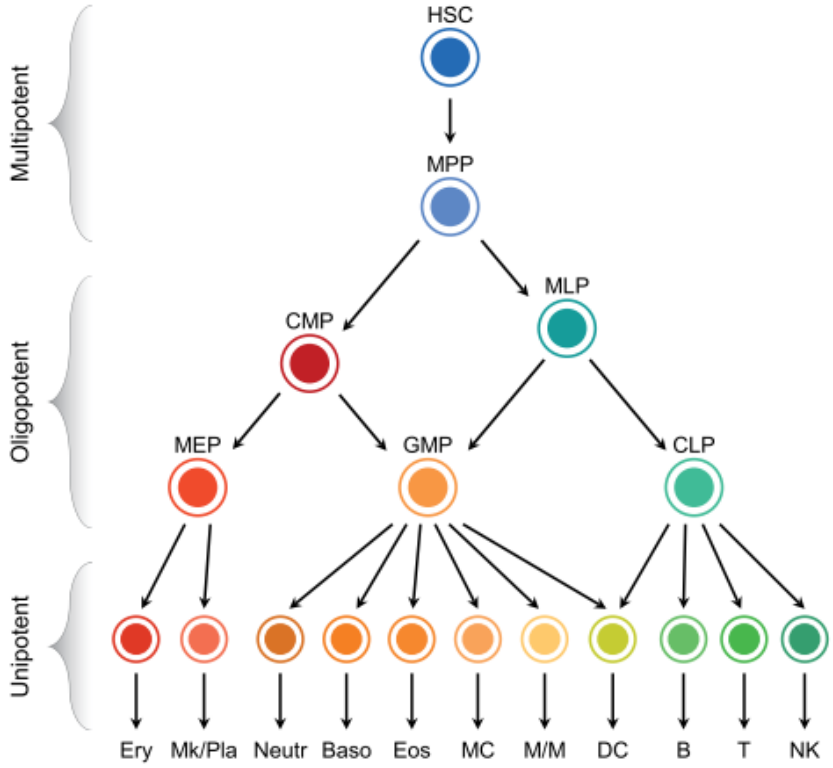

Figure 1.1.2 Diagram of canonical haematopoietic tree. An illustration of the ontological differentiation events derived from a haematopoietic stem cell (HSC). The common myeloid progenitor (CMP) and multipotent lymphoid progenitor (MLP) are derived from a direct bifurcation from the HSC and multiple pluripotent progenitor (MPP). CMP further differentiates into the myeloid lineage cells (megakaryocytes, MK and erythroblasts, EB) and into the granulocyte-monocyte progenitor (GMP). The MLP matures into the lymphoid lineage (common-lymphoid progenitor, CLP, and lymphoid cells) and can give rise to the granulocyte-monocyte lineage. The haematopoietic differentiation process happens in the bone marrow where haematopoietic (HSC) and all the progenitor cells develop. The differentiated cells are then released in the bloodstream and tissues. Those include erythrocytes (Ery), megakaryocytes and platelets (MK/Pla), neutrophils (Neutr), basophils (Baso), eosinophils (Eos), master cells (MC), monocytes/macrophages (M/M), dendritic cells (DC), B cells (B), T cells (T) and natural killer cells (NK). Figure from (Antoniani, Romano, and Miccio 2017).

The haematopoietic tree was devised based on population studies of cell transplant experiments in immunocompromised mice, which have been crucial in studying HSCs biology (Osawa et al. 1996). However, differences in mature cell outputs from single HSCs transplants remained unexplained until recently. Methods based on population level characterisation disregard important details, such as differences in transcriptional states within the same cell population; or whether the detected changes happen only on a few cells or a subpopulation. These issues be come critical when analysing rare cells, such as HSCs. The canonical haematopoietic model explains the relationship between progenitors and mature cells, as a hierarchical progression, based on the following assumptions; (1)

cells are phenotypically classified into distinct compartments with shared homogeneous surface marker signatures; (2) all cells in a compartment retain the differentiation potential of that category; and (3) when a cell differentiates, the progeny cannot regain the previous compartment potential. Currently, it is recognised that seemingly homogeneous populations of blood cells, based on cell surface markers, can contain an array of intermediate cell types with different transcriptomic profiles and capability to differentiate into divergent cell outcomes (Moignard et al. 2013).

The advent of modern technologies, based on single cell profiling, shone light on the heterogeneity of HSC populations. Currently, it is recognised that individual HSCs exhibit promiscuous multilineage-primed states prior to lineage commitment (M. Hu et al. 1997; K. Akashi et al. 2003; Miyamoto et al. 2002). These primed differentiation programmes are thought to be epigenetically fixed and transmitted to the next generation through self-renewal (Christa E Muller-Sieburg et al. 2012; W. W. Pang, Schrier, and Weissman 2017; Müller-Sieburg et al. 2002; C. E. Muller-Sieburg et al. 2004b; Sieburg et al. 2006). Müller-Sieburg *et al.* classified the HSC populations in myeloid-biased (My-bi) HSCs, lymphoid-biased (Ly-bi) HSCs or balanced HSCs that generate lymphoid and myeloid lineages in the same ratio. It has also been shown that My-bi HSCs generate defected lymphoid cells (C. E. Muller-Sieburg et al. 2004b) and, accordingly, Ly-bi HSCs have impaired ability to differentiate into myeloid lineage. More recently, the hypothesis that lineage-primed HSCs gradually acquire lineage status has gained strength with the CLOUD-HSPCs concept (Velten et al. 2017). Continuum of Low primed UnDifferentiated haematopoietic stem-and progenitor-cells (CLOUD-HSPCs) are HSC-like cells ($Lin^{-}CD34^{+}$), characterised by the expression of stemness signature in combination with phenotypic blood multi-progenitor transcriptomic signatures. Verten *et al.* demonstrated, by multiplexed index sorting and single-cell RNA-sequencing that distinct lineages emerge from CLOUD-HSPCs without passing through stable progenitor stages. Interestingly, this study also showed that the earliest priming events express myeloid/lymphoid or megakaryocyte/erythrocyte signatures, which suggests that these might be the first priming events on adult haematopoiesis.

The identification of lineage-primed HSCs and multi-lineage precursor cells calls for an updated haematopoietic model that capture the inherent flexible and pluralistic nature of the blood cells differentiation. The attempts to re-design the haematopoiesis model have been few and shy, probably reflecting the recognition that our understanding of the transcription networks regulating blood differentiation is only starting to unveil.

1.2 Megakaryopoiesis

1.2.1. Megakaryopoiesis development

1.2.1.1. Early MK lineage commitment

HSCs undergo lineage commitment steps, to differentiate into megakaryocytes, in a process denominated megakaryopoiesis. Recently, the model stating bifurcation of lymphoid versus myeloid lineages has been challenged, as new data suggests that MK fate determination is triggered at earlier differentiation stage. Single-cell profiling studies revealed that the HSC priming happens at earlier stages than previously thought, and primitive HSC subsets express myeloid transcriptional profiles. Multiplexed qPCR revealed that populations of progenitor cells, sorted based on cell surface markers and considered homogeneous populations, are actually heterogeneous sub-populations with diverse differentiation potential revealing an early myeloid/lymphoid separation (Guo et al. 2013). In this study, single cell gene clustering showed that the megakaryocyte-erythroid lineage is closer to HSCs than the lympho/myeloid lineages, suggesting a staggered lineage commitment. Primed HSC subsets are thought to be developmentally regulated as lymphoid-biased HSCs are found mainly early in life, and myeloid-biased HSCs predominantly populate the HSC niche later in life (W. W. Pang et al. 2011; Christa E Muller-Sieburg et al. 2012). Interestingly, studies based on single cell transcriptome data, identified MK and platelet transcriptomes as the most common in aged HSCs, demonstrating an age-related biased differentiation towards myeloid commitment (Grover et al. 2016). Sanjuan-Pla *et al.* reinforced the concept of platelet-primed HSCs by demonstrating that Von Willebrand factor expressing HSCs (VWF^+ HSCs) generate mainly platelets and myeloid cells upon transplantation in mice (Sanjuan-Pla et al. 2013). Studies based on surface markers demonstrated that a subset of adult HSC expresses integrin CD41, previously thought to be present only on embryonic HSCs (Gekas, Graf, and Pampori 2013). It was also shown that $CD41^+$ HSCs possess long-term repopulation capacity in transplantation experiments, yielding a myeloid-biased progeny which aligns with the hypothesis of age-related myeloid-biased HSCs.

Megakaryocytes directly and independently branch from a multipotent cell, such as HSC or MPP, rather than an oligopotent progenitor. Rising from the hypothesis that myeloid lineage commitment is not gradual and might not progress through CMP stage; Notta *et al.* devised a sorting strategy to examine cellular heterogeneity within the $CD34^{+}$ compartment (HSC), and map the origins of myeloid cells at different stages of development (fetal liver, neonatal cord and bone marrow) (Faiyaz Notta et al. 2016). In this study, based on 11 cell markers, progenitors expressing myeloid-erythroid-MK signatures were prominently found in the fetal liver, as opposed to the bone marrow. The study also showed that, in bone marrow, MK lineage commitment happens exclusively within the multipotent cell compartment (figure 1.2.1). This data challenges the classical progeny of MKs in adult haematopoiesis, by suggesting that MK lineage commitment happens earlier than CMP progenitor stage.

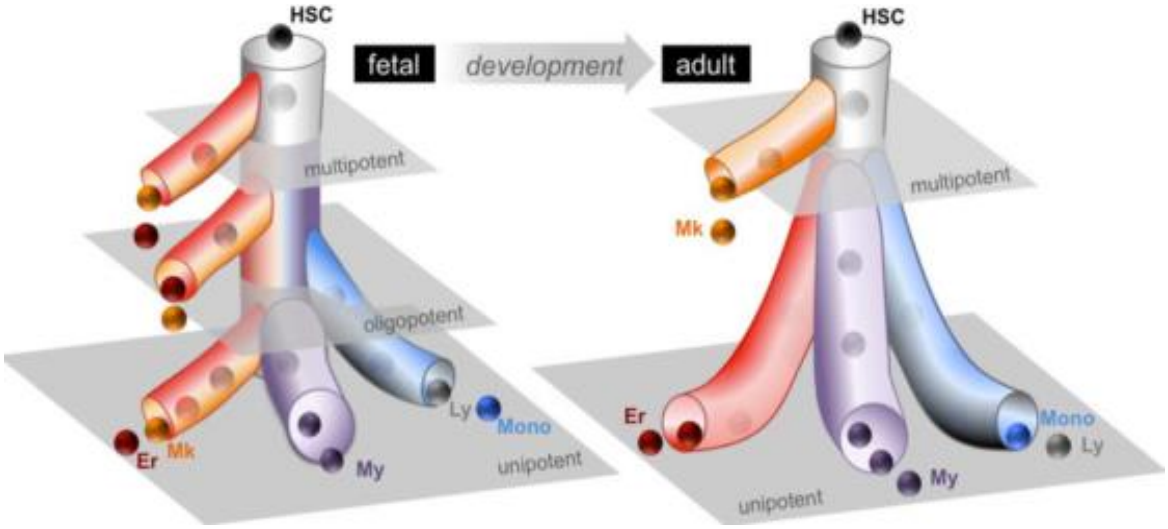

Figure 1.2.1 Redefined model of human blood lineage formation. Graphical representation of a redefined haematopoiesis model including lineage potential of progenitor subsets. This model hypothesises a developmental shift in the progenitor potential from a three-tier at embryonic stage (multipotent, oligopotent and unipotent cells) to a two-tier hierarchy by adulthood where MKs derive directly from HSCs. Figure from (Faiyaz Notta et al. 2016).

Common myeloid progenitor (CMP) population is not, as previously thought, a population of cells that directly derives from a naïve HSC, but instead a flexible and complex population expressing dynamic transcriptional states. A study combining massively parallel single-cell RNA-seq (MARS-seq) with indexed FACS sorting identified 19 transcriptionally distinct subpopulations within the CMP

population ($Lin^{-}c\text{-}Kit^{+}Sca1^{-}$) (Paul et al. 2015). This study demonstrated that myeloid progenitors are cells primed towards individual fates (MKs, erythrocytes, monocytes, neutrophils, eosinophils, basophils or dendritic cells), defining an early transcriptional commitment in the cell development. In the same study, the authors also index-sorted 8 subpopulations within the megakaryocyte/erythroblast progenitors (MEP). One of these subpopulations presented a MK signature and the other 7 subpopulations showed clear erythrocyte characteristics varying from early progenitor to mature erythrocytes signatures, suggesting a developmental progression within the MEP population. Importantly, a subpopulation was identified, within the CMP population, remarkably expressing MK-related genes which is a strong indication that MKs might diverge from erythrocytes prior to MEP stage. This observation falls in line with the identification of myeloid-primed HSCs, suggesting that MK lineage commitment derives directly from HSCs and not from a CMP progenitor.

1.2.1.2. MK maturation and proplatelet formation

Megakaryocytes (MKs) are large (50-100 µm) and rare cells which represent only 1% of the myeloid lineage. MKs major function is the production and release of platelets, a process denominated thrombopoiesis. Every day, an average of 10^{11} platelets are released into the bloodstream, making platelets one of the most common cells in the body. Until recently, it was thought that thrombopoiesis happened exclusively in the bone marrow, but there is evidence that MKs also reside, and produce platelets, in the lungs (Slater, Trowbridge, and Martin 1983; Lefrançais et al. 2017). The assembly and release of platelets is a stepwise maturation process that involves MK polyploidisation by endomitosis, MK maturation and proplatelet formation.

MK maturation starts with endomitosis, a process primarily thrombopoietin-driven by which MKs become polyploid (Deutsch and Tomer 2013; Kenneth Kaushansky 2005). Similarly to other cells, MKs undergo a normal 2N DNA replication. Although, cytokinesis (cell division) is absent, and MKs begin accumulation of DNA content (up to 128N) in a single polylobulated nucleus. The lack of cell division happens due to a defect in late cytokinesis which results in a defective cleavage furrow, necessary for physical cell separation (Geddis et al. 2007; L. Lordier et al. 2008). Endomitosis is accompanied by a cell size increase to accommodate the new nucleic genomic DNA load. This increase in DNA cargo is related to the capacity to generate platelets (Mattia et al. 2002).

During MK maturation, the cells increase the cytoplasmic protein and lipid content that lead to the formation of secretory granules. These granules include dense granules, lysosomes and α-granules.

The granule production is followed by the development of the invaginated membrane system (IMS). The IMS is a complex system of tubules present in the cytoplasm and continuous with the plasma membrane. This structure requires a significant reorganisation of the mature MKs, and it is thought to function as a reservoir for proplatelet formation (Schulze et al. 2006).

Mature MKs form cytoplasmic protrusions that progressively elongate to form beaded structures, the proplatelets (Machlus, Thon, and Italiano 2014). Proplatelets are long branching protrusions extended and released by fragmentation of mature MKs into the sinusoidal blood vessels (Junt et al. 2007). These structures are loaded with platelet-specific granules, RNAs and proteins required for the posterior platelet maturation (Thon et al. 2010). The factors that trigger proplatelets release are still unclear, although a few mechanistic theories have been proposed, such as the positioning of the MKs on the vascular interface and their exposure to gradients of blood components; the presence of podosomes in the process of proplatelets extension (Schachtner et al. 2013); and the shear forces of blood flow (Junt et al. 2007). Proplatelets in the blood stream undergo a final maturation step, driven by microtubule-based forces, to become fully functional platelets (Thon et al. 2012).

1.2.2. Megakaryopoiesis regulation

1.2.2.1. Transcriptional regulation

During megakaryopoiesis, the MK-primed HSC gradually acquire lineage maturity through a coordinated network of transcriptional factors, cytokine signals, and epigenetic cues. Single-cell transcriptome studies revealed that the MEP population comprises distinct populations differentially primed to MK or erythroid lineage (Psaila et al. 2016). However, despite the distinct lineage priming at MEP stage, MKs and erythrocytes share considerable gene expression signatures (L. Chen et al. 2014). MK and erythroid lineages share many critical TFs, and although both differentiation processes are accurately regulated, it is acceptable to speculate that could be a functional overlap in TF function (Doré and Crispino 2011). The main regulators controlling megakaryopoiesis intrinsic gene expression programmes include GATA-1 (S H Orkin et al. 1998), FOG-1 (Pope and Bresnick 2010), TAL1 (H. Chagraoui et al. 2011), FLI1 (Kawada et al. 2001), and RUNX (Growney et al. 2005).

1.2.2.1.1. GATA-1

GATA-1 (GATA-binding factor 1) is a zinc-finger transcription factor (TF), that promotes transcriptional activation by recruiting coregulators to chromatin via its N- and C-domains, as well as

2 zinc fingers DNA domains (Kaneko et al. 2012). GATA-1 has been associated with regulation of both early and late megakaryopoiesis, and it is considered a master regulator due to its interactions with multiple MK-specific TF and cofactors. In mice, GATA-1 is required for MK-erythroid lineage commitment (Iwasaki et al. 2003), and the ablation of GATA-1 results in impaired early maturation of megakaryocyte-erythroid progenitors (Stachura, Chou, and Weiss 2006). Abnormal MK proliferation was observed in GATA-1-null MKs, indicating that GATA-1 controls MK cell cycle (S H Orkin et al. 1998) and therefore, a major player in MK growth, as well as lineage commitment. At later stages of megakaryopoiesis, downregulation of GATA-1 results in polyploidisation disruption, reduced number of circulating platelets, and defective haemostasis activation responses in mice (Muntean et al. 2007; Meinders et al. 2016; Vyas et al. 1999). GATA-1 interacts with FOG-1 (Friend of GATA-1), a zinc finger TF directly associated with regulation of MK-specific gene activity (Pope and Bresnick 2010). The GATA-1/FOG-1 complex is maintained from embryonic stage throughout the megakaryocyte/erythrocyte maturation (Tsang et al. 1997; Chang et al. 2002). In humans, a genetic defect in GATA-1 N-terminal zinc-finger (amino acid change from methionine to valine) inhibits its interaction with FOG-1, leading to MK maturation defects and thrombocytopenia (Nichols et al. 2000). A SNP in the same GATA-1 domain has also been reported to cause an abnormal size and number of dysmorphic platelets that present a weak functional profile in aggregation studies (Freson et al. 2001). Mutations in GATA-1 exon 2 (N-terminal transactivation domain), leading to premature stop codons, are commonly found in children with transient myeloproliferative disorder (TMD) and acute megakaryblastic leukemia (AMKL) (Greene et al. 2003).

1.2.2.1.2 TAL-1

TAL-1 (T-cell acute lymphocytic leukemia protein 1) belongs to a basic helix-loop-helix (bHLH) protein family which is incapable of intrinsically binding to DNA. Therefore, proteins containing the bHLH domain rely on interaction with other TFs to regulate gene transcription (Hsu et al. 1994). TAL-1 is a haematopoietic TF with important regulatory functions at both embryonic and adult haematopoiesis. Studies in mice demonstrated that TAL-1 regulates establishment of haemogenic endothelium, as well as haematopoietic commitment (Shivdasani, Mayer, and Orkin 1995; Lancrin et al. 2009; D'Souza, Elefanty, and Keller 2005). TAL-1 role in regulation of early lineage commitment of MK/erythroid cells was further demonstrated by chromatin immunoprecipitation (ChIP) experiments showing that TAL-1 is required prior to GATA-1 binding (Kassouf et al. 2010; Palii et al. 2011). TAL-1 function at late haematopoiesis has also been demonstrated as TAL-1-null mice fails to differentiate both erythrocytes and MKs (Schlaeger et al. 2005), and TAL-1 knockdown affects MK polyploidisation and platelet count (Hedia Chagraoui et al. 2011). In line with these results, overexpression of TAL-1

in human embryonic stem cells (hESC) increases differentiation of MK-erythroid progenitors (Yung et al. 2011).

1.2.2.1.3. FLI-1

FLI-1 (Friend leukemia integration 1) belongs to the ETS transcription factors family (Karim et al. 1990). FLI-1 role in early haematopoiesis has been reported (F. Liu et al. 2008), although FLI-1 regulation is mainly associated with late lineage development. This TF was first identified as a regulator in megakaryopoiesis for its role on regulation of glycoprotein IX promoter, a sub-unit of von Willebrand receptor (Bastian et al. 1999). Mice lacking FLI-1 present defective megakaryopoiesis development (Kawada et al. 2001). Despite binding to both early and late megakaryopoiesis-specific genes, ablation of FLI-1 only affects late megakaryopoiesis (L. Pang et al. 2006); and inducible deletion of FLI-1 presents a thrombocytopenia phenotype (Starck et al. 2010). In humans, FLI-1 hemizygous deletion leads to Paris-Trousseau syndrome (PTS), an abnormally leading to dysmegakaryopoiesis and thrombocytopenia (Stevenson et al. 2015; Di Paola 2015). It has been shown that overexpression of FLI-1 in $CD34^{+}$ cells from PTS patients, restores normal megakaryopoiesis (Raslova et al. 2004). Lastly, FLI-1 has been shown to interact with GATA-1 to synergistically activate MK-specific promoters at terminal differentiation of MKs (Eisbacher et al. 2003).

1.2.2.1.4. RUNX1

RUNX1 (Runt-related transcription factor 1) is a member of the RANT TF family, and together with its heterodimeric partner, CBFβ, regulates a broad spectrum of myeloid and lymphoid genes. Mouse model of RUNX1 KO is embryonically lethal, and a conditional KO results in MK reduced polyploidisation and platelets abnormal cytoplasmic development (Growney et al. 2005). This phenotype has been explained due to RUNX1 role in the switch from mitosis to endomitosis, required for MK polyploidisation and platelets cytoskeleton rearrangements (Larissa Lordier et al. 2012). Interestingly, a similar phenotype in observed in GATA-1 KO mice (Vyas et al. 1999). The transcriptional regulation of MKs by both GATA-1 and RUNX1 is a result of their direct physical association (Xu et al. 2006), required for polyploidisation regulation by switching MK mitosis to endomitosis (Larissa Lordier et al. 2012). Both TFs, RUNX1 and GATA-1, are co-expressed during activation of MK-specific promoters (Elagib et al. 2003), highly expressed during megakaryocytic differentiation and equally switched off during early erythroid maturation (Lorsbach et al. 2004). In humans, RUNX1 mutations lead to acute myeloid leukemia with characteristic thrombocytopenia and impaired platelet function (Heller et al. 2005).

1.2.2.2. Microenvironment and signalling regulation

Megakaryocytes development happens in highly specialised microenvironment, where gradients of growth factors and cytokines are tightly regulated. Microenvironmental signals drive transcriptional differences that influence MKs size, ploidy level and function. The direct influence of the microenvironment in MK maturity was studied by Slayton *et al.* where neonatal liver haematopoietic stem cells, that generally produce small MKs with low DNA content, produced adult-size and ploidy MKs when transplanted into an adult microenvironment (Slayton et al. 2005). *In vitro* models of megakaryopoiesis have explored the influence of cytokines signalling in MK differentiation. Despite significant differences in methodology, the successful models generally replicate MK generation by exogenous supplementation of thrombopoietin (TPO) and human stem cell factor (SCF) (Q. Feng et al. 2014; Moreau et al. 2016).

1.2.2.2.1. Thrombopoietin

Thrombopoietin (TPO), produced in hepatocytes, is the main cytokine regulating MK differentiation. TPO belongs to the four-helix bundle family of proteins, which includes erythropoietin (EPO) and leukemia inhibitory factor, amongst others. TPO binds to receptor cMpl (CD110) (Bartley et al. 1994). cMpl does not have intrinsic kinase activity, instead it associates with the cytoplasmic tyrosine kinase Janus kinase 2 (Jak2). This association triggers the cMpl internalization and dimerization (deactivation), as well as the phosphorylation (activation) of Jak2 (Drachman, Griffin, and Kaushansky 1995). Multiple signalling pathways are activated following cMpl-Jak2 association; including signal transducer and activator of transcription (STAT), mitogen-activated protein kinase (MAPK) and phosphoinositol-3 kinase (PI3K) pathways, as reviewed by Geddis *et al.* (Geddis, Linden, and Kaushansky 2002).

TPO regulates late megakaryopoiesis and platelet production via a feedback-loop mechanism in which TPO levels are gauged by platelet numbers in circulation (Kuter and Rosenberg 1995). cMpl, TPO receptor on the surface of platelets, binds to TPO in circulation, which is degraded following binding. The decrease in TPO concentrations results in the reduction of platelet production. Consequently, the decrease of circulating platelets increases TPO concentrations, thus, driving MKs to release more platelets into the bloodstream. TPO feedback-loop is the main mechanism controlling platelet release in normal health conditions, although TPO concentration can also be influenced by other factors in disturbed conditions such as inflammation. For example, thrombocytosis induced by inflammatory mediator IL-6 results in increased levels of TPO in plasma (Kaser et al. 2001). TPO circulating concentration can also be regulated by ageing platelets. These

become desialylated and bind to the hepatic Ashwell-Morell receptor (AMR) which induces TPO transcription, and consequent production of platelets (Grozovsky et al. 2015).

TPO signalling regulates early and late megakaryopoiesis. Mice lacking either TPO or its receptor show deficiencies in early haematopoietic progenitor cells as well as late-stage MK differentiation (Kimura et al. 1998). It has been shown that ablation of TPO avoids MK maturation in murine bone marrow cells (K Kaushansky et al. 1995) and causes severe thrombocytopenia (F J de Sauvage et al. 1996). Similarly, mice deficient in TPO receptor, cMpl, show low ploidy MKs and severe thrombocytopenia (Alexander et al. 1996). Soon after the identification of TPO, the study of megakaryopoiesis improved significantly due to the development of *in vitro* models based on TPO supplementation(Bartley et al. 1994; Frederic J. de Sauvage et al. 1994; Lok et al. 1994). Despite being important for MK differentiation, it has previously been shown that TPO on its own does not sustain MK cell maintenance (Ryu et al. 2001).

1.2.2.2.1. Stem Cell Factor

Stem cell factor (SCF, known as kit-ligand or steel-factor) is a cytokine that binds to c-Kit, a tyrosine kinase receptor (CD117). SCF was first discovered when mutations on the gene locus resulted in phenotypes affecting haematopoiesis (Zsebo et al. 1990). In that study, mice with mutated SCF locus presented anaemia as well as deficiencies in master cell phenotypes, and haematopoiesis could not be restored. Another study showed that mutations in the SCF receptor, c-Kit, cause a similar phenotype (Reith et al. 1990).

SCF regulates almost every step of megakaryopoiesis. At early stage, SCF promotes HSC self-renewal potential (Bowie et al. 2007). SCF also regulates MK growth, especially at late maturation stage. A study testing the effect of megakaryopoiesis-specific cytokines on TPO-induced apoptosis has found that only SCF reduced apoptosis in MK cells (Kie et al. 2002). The study also showed that SCF enhances MK maturation *ex vivo* when used in conjunction with TPO by increasing MK polyploidisation levels.

1.2.3. Platelets

In normal conditions, the bloodstream has 150-400 x 10^9 circulating platelets per litre of blood (Sylman et al. 2018; Smock and Perkins 2014). Platelets are anucleated cells, containing secretory vesicles and the translational machinery necessary for protein synthesis. The secretory vesicles in

platelet cells include α-granules, dense granules, lysosomes and t-granules (Machlus, Thon, and Italiano 2014). The most abundant granules in platelets, α-granules, contain proteins important in haemostasis, such as P-selectin, fibrinogen and vWF. Dense granules contain membrane transporters and high concentration of calcium; lysosomes are loaded with enzymes involved in protein, carbohydrates and lipid degradation; and t-granules store disulphide isomerase, a protein required for thrombus formation (Kim et al. 2013). Although, granules formation has not yet been fully characterised, it is clear that their contents are directly inherited from MKs. Similarly, the platelet transcriptome is mainly derived from MKs, and therefore, it provides an insight into the transcriptional profile of MKs. However, extrapolation of transcriptional data from MKs to platelets should be performed with caution. Firstly, MKs package mRNA in a selective manner, and disparity in mRNA and protein expression has been found between MKs and platelets (Cecchetti et al. 2011). Secondly, platelets might be able to receive RNA transcripts from other cells, as an intracellular RNA transfer mechanism has been reported (Risitano et al. 2012). Lastly, it is acceptable to speculate that the microenvironmental impact could trigger alternative pathways, inducing differences in translation or protein function.

Platelets have been reported to be involved in immunity processes (Semple, Italiano, and Freedman 2011; Thomas and Storey 2015) and angiogenesis (W. Feng et al. 2011) , but their most well studied role is in the haemostasis process and thrombus formation. Due to their small size, platelets circulate close to the luminal surface of the endothelium, which facilitates their response to changes in endothelial integrity. The sub-endothelium vWF forms a bridge between collagen, exposed at the compromised endothelium site, and the platelet membrane receptors GP Ib-IX-V, GP Ia/IIa and GPVI (López 1994; Nieswandt and Watson 2003). Platelet activation leads to a cytoskeleton rearrangement transforming the discoid platelet into a spiny spherical cell (Shin et al. 2017). The platelet shape change is followed by the release of chemical activation factors, such as adenosine diphosphate (ADP) and thromboxane A2, which escalate platelet adhesion response. Following the initial activation, platelets release thrombin which escalates the formation of the thrombus. Thrombin converts fibrinogen to fibrin, resulting in the formation of a network of fibrin fibres (Heemskerk, Bevers, and Lindhout 2002). This structure helps to stabilise the platelet mass which results in a strengthened barrier to blood loss. Following a haemostasis episode, platelet count rapidly increases due to increased cell demand.

Platelet traits, such as platelet count (PLT) and mean platelet volume (MPV), are highly heritable (Qayyum et al. 2012). During steady state thrombopoiesis, platelet mass is tightly controlled with PLT and PMV being inversely correlated (Bessman 1984). Interestingly, these traits also directly

correlate with MK ploidy level, as a decrease in PLT, and corresponding increase in PMV, leads to higher MK ploidy (Stenberg et al. 1991; Mazur et al. 1988). Platelet size is directly related to function; therefore, it is critical that normal platelet differentiation is maintained. Dysregulation of thrombopoiesis can lead to 1) the production of low platelet numbers leading to bleeding disorders, such as thrombocytopenia, or 2) over reactive platelets leading to acute coronary syndrome (ACS). ACS identifies various diseases, caused by pathological platelet thrombosis, leading to the formation of intracoronary occlusion. ACS includes conditions such as partial coronary occlusion (unstable angina) and total coronary occlusion (myocardial infarction) (Smith et al. 2015). Myocardial infarction has been correlated with platelet traits such as MPV and platelet distribution width (PDW), which refers to the size variability in platelet population (Chu et al. 2010; KLOVAITE et al. 2011a). Hence, it is important to understand the transcriptional mechanisms controlling these traits. One way of identifying possible genomic variants regulating these traits is by performing genome-wide association studies (GWAS), which identifies the association between genome variants and disease phenotypes.

1.2.4. Genome-wide association studies (GWAS)

Genome-wide association studies (GWAS) have transformed our understanding of genetic variation as the studies are based on unbiased scanning of the genome in a population, revealing previously unknown patterns of inheritance. Previously to GWAS, the identification of genome loci causative of disease was based on linkage analysis (Botstein and Risch 2003). Despite this method being successful at mapping variants affecting Mendelian diseases (Koenig et al. 1987; Kerem et al. 1989), its use was limited on mapping loci underlying complex diseases (Lander and Schork 1994). In contrast, GWAS determine the association between hundreds of thousands of variants within a population and a trait, series of traits or disease status; thereby identifying variants associated with specific trait or disease susceptibility (MacArthur et al. 2017; M. J. Li et al. 2016). The major drawback of GWAS is that the association between a genetic variant and a trait does not directly relate to causation, and therefore is not informative of the mechanism whereby the variant regulates the phenotypic differences. Hence, the identified variants can have a direct effect on the trait, i.e. a change in an amino acid affecting the protein function or stability (Butler et al. 2017); or the variant can indirectly affect a trait by being in linkage disequilibrium (LD) with a functional variant. Linkage disequilibrium (LD) refers to the correlation among DNA variants as a result of evolutionary forces (Hill & Robertson 1968).

The statistical power of GWAS is proportional to the population sample size. In order to increase statistical power, larger studies including GWAS from various cohorts can be integrated into meta-analysis. Although, the main challenge of meta-analysis lye on the normalisation of the methodology and analysis criteria used to generate individual databases. In order to overcome this drawback, GWAS of larger cohorts have been performed, using a single analysis platform, and it has been shown that this strategy leads to a gain of statistical power over meta-analysis (Astle et al. 2016). GWAS of large cohorts improve the detection of rare variants (minor allele frequency <1%), which map predominantly in or near coding regions, and have larger phenotypic effect sizes. Although, 70-90% of the identified variants map to non-coding regions of the genome (Astle et al. 2016; Wood et al. 2014a; Maurano et al. 2018). This fact could be due to co-inheritance of variants in strong linkage disequilibrium (LD) with the sentinel (the most significant) variant; or due to variants being located in cis-regulatory elements (Gallagher and Chen-Plotkin 2018). In conclusion, GWAS have the ability to determine association between traits and variants, and also estimate variance explained by sets of single nucleotide polymorphisms (SNPs) (He et al. 2015); look for potential causal SNPs within a locus, (fine-mapping, Mendelian randomization)(Spain and Barrett 2015; Wood et al. 2014b; Robinson et al. 2016); identify SNPs related to multiple traits (pleiotropy) (Willer et al. 2013); and carry out pathway analysis (Willer et al. 2013).

Mechanisms controlling platelet traits are poorly understood, and GWAS have been a critical tool in the study of such mechanisms. GWAS studies have been performed to study variants associated with platelet traits (Astle et al. 2016; Oh et al. 2014; Schick et al. 2016), and platelet function (Qayyum et al. 2015) in different populations. In the quest to learn about how genome variants influence PMV and PLT, a meta-analysis of GWAS was performed on 67,000 individuals (Gieger et al. 2011). This study identified 68 genomic loci associated with PLT and MPV, of which 11 loci had not previously been associated with haematopoiesis. One of these association is the BRD3 gene, which encodes for one of the Bromodomain and Extra Terminal (BET) proteins. Following the GWAS identification of these genes, a reverse genetic screen was performed in zebrafish, where BRD3 protein expression was knocked down by morpholino to investigate the phenotypic result of BRD3 ablation (Bielczyk-Maczyńska et al. 2014b). The association between BRD3 and platelets was confirmed when the BRD3 morpholino-knockdown resulted in reduced number of thrombocytes and erythrocytes, but normal cell generation of all other cell lineages assessed. The reduced thrombocyte number was partially restored with *in vitro* transcription of RNA-encoding human BRD3. This study also shown that JQ1 inhibition (a BET inhibitor) resulted in ablation of thrombocyte formation when administered at early stages of embryo formation, but not at later stages. The authors hypothesised that BRD3 is required

for thrombocyte differentiation from HSCs, but not thrombocyte maintenance. Although, it is important to note that JQ1 inhibits other proteins of the same family, and not only BRD3.

Astle *et al.* performed a GWAS in a large study of 174K healthy participants included in two large cohorts - UK Biobank (Sudlow et al. 2015) and INTERVAL (C. Moore et al. 2014) - and identified 29.5 million genetic variants associated with 36 blood cell traits (Astle et al. 2016). In this study, common variants in the BRD3 coding sequence (rs2157770 (A/G); rs459571 (C/T)) were associated with MPV and PDW, respectively. Figures 1.2.2 and 1.2.3 show BRD3 locus zoom plots for MPV and PDW generated in that study. Each plot represents the association between single nucleotide variants (SNVs) and the platelet trait (MPV and PDW, respectively). The association is measured as a p-value of association. It is interesting to note that the pattern of association for MPV and PDW is rather distinct, which suggests that the mechanism by which the variations affect these platelet traits may be different.

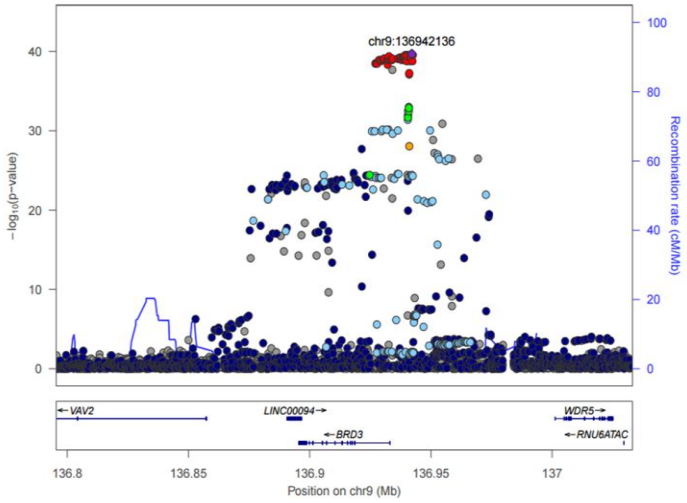

Figure 1.2.2 BRD3 locus zoom plot with SNP association for volume of platelets. This plot represents the telomere of the long arm of chromosome 9 with the genes indicated in the lower box (BRD3 coding region). The dots represent single nucleotide variants (SNVs) and the x-axis (left) is the p-value (minus log10) of association between mean platelet volume (MPV) and the individual SNVs. The height of each dot represents the strength of evidence for the association (rather than effect size). Dots are coloured according to the LD (linkage disequilibrium between the causal variant and the lead variant (labelled).

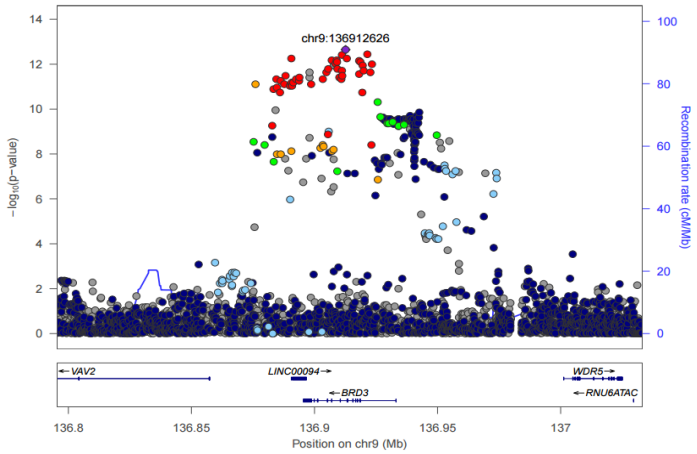

Figure 1.2.3. BRD3 locus zoom plot with SNP association for distribution width of the volume of platelets. This plot represents the telomere of the long arm of chromosome 9 with the genes indicated in the lower box (BRD3 coding region). The dots represent single nucleotide variants (SNVs) and the vertical axis (left) is the P-value of association between platelet distribution width of volume (PDW) and the individual SNVs. The height of each dot represents the strength of evidence for the association (rather than effect size). Dots are coloured according to the LD (linkage disequilibrium) between the causal variant and the lead variant (labelled).

The aforementioned GWAS identified variants associated with platelet traits. Although, the validation of such associations is a critical step to understand the role of such variants in transcriptional regulation of MKs and platelets, and its consequence on cellular traits. Therefore, the main aim of this thesis is to explore the role of BRD3 during megakaryopoiesis regulation.

1.3 Bromodomains

1.3.1. Bromodomain modules

Bromodomain modules (BDs) are evolutionary conserved modules that selectively recognise and bind to acetylated lysines. These protein-interaction modules were named after the *Drosophila* gene *brahma*, where the BD sequence was first identified (Haynes et al. 1992). BD structure is formed by four α-helices (αZ, αA, αB and αC) bound by flexible loop regions (AB, BC and ZA loops) (figure 1.3.1). Several conserved residues are characteristic of BDs; in particular an asparagine (Asn) residue at the BC loop that forms a hydrogen bond with Kac, promoting the binding of acetylated peptide to the hydrophobic pocket within the four helices (Owen et al. 2000). Interactions with acetylated peptides are initiated and stabilised by the surrounding charged surface, where extensive hydrogen bonds are established.

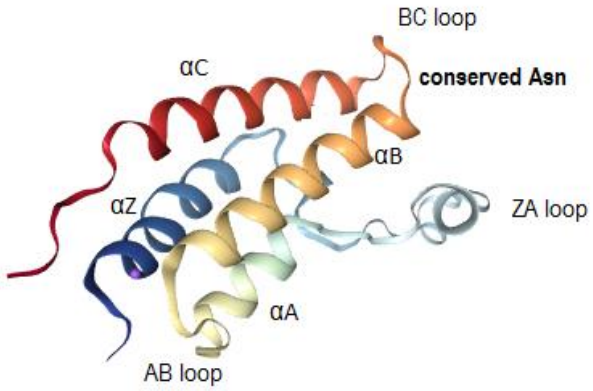

Figure 1.3.1. Structure of bromodomain modules. The structure of the first bromodomain (123 amino acids) of BRD3 (BRD3(1)). Bromodomains contain four α-helices (αZ, αA, αB and αC) bound by flexible loop regions (AB, BC and ZA loops). A conserved Asn residue in the BC loop region is responsible for docking BD modules to acetylated Lys (Kac) peptides. Image generated on RCSB PDB (Research Collaboratory for Structural Bioinformatics, Protein Database) website.

In humans, the bromodomain modules are shared by 46 known proteins containing a total of 61 BD modules. Bromodomain proteins (BRDs) have been classified in eight distinct families, based on

structure based alignments (Filippakopoulos et al. 2012b). In this thesis, I focus on the Bromodomain and Extra Terminal (BET) family of proteins described below.

1.3.1.1. Bromodomain and Extra Terminal family

There are four members of the Bromodomain and Extra Terminal (BET) family: BRD2, BRD3, BRD4 and BRDT. These are ubiquitously expressed in the human body, with the exception of BRDT, which is expressed only in testis cells. BET proteins have a highly conserved and homologous structure containing: 2 N-terminal bromodomain modules (BDs) displaying high levels of sequence conservation, an extra terminal recruitment domain (ET), and other conserved motifs (A, and B). Proteins BRD4 and BRDT also contain a C-Terminal Motif (CTM) (figure 1.3.2).

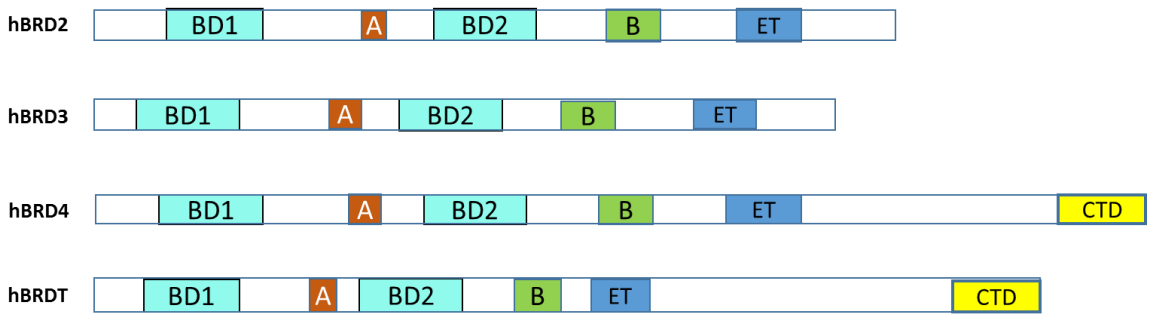

Figure 1.3.2 BET protein structure homology. BET proteins share a very similar and highly conserved structure. Proteins are constituted by two bromodomains (BD1 and BD2) with lysine acetylation recognition functions. Motifs A, B and ET are required for localisation, dimerization and protein interactions, respectively. BRD4 and BRDT contain a C-terminal domain (CTD) with protein-protein interaction functions. Adapted from (Pablo Garcia-Gutierrez and Garcia-Dominguez 2015).

BD1 and BD2 modules are both acetyl-lysine recognition sites. Interestingly, the similarity among the first bromodomain (BD1) sequences in all BET proteins is higher than between BD1 and BD2 within the same protein (Filippakopoulos et al. 2012a). This fact could explain the functional overlap observed among some BET proteins (Stonestrom et al. 2015). Motif A, located between both BD modules, contains a region of 12 amino acids that acts as a nuclear localisation signal. It has been shown that *in vitro* deletion of the A motif causes mislocalisation of the proteins (Fukazawa and Masumi 2012). Motif B is required for homo and hetero dimerization (P. Garcia-Gutierrez, Mundi, and Garcia-Dominguez 2012); and the ET domain is important for interaction with other proteins (Rahman et al. 2011). BRD4 and BRDT are longer proteins which also contain a C-terminal motif (CTM). This motif is important for protein-protein interaction as it has been shown to interact with P-TEFb, facilitating effective

transcription (Schröder et al. 2012). Bromodomain proteins form complexes with diverse protein partners due to the ability to initiate interactions by the ET or CTM domains (Rahman et al. 2011). These large protein assemblies have important roles in transcriptional programmes.

1.3.2. Bromodomain proteins (BRDs) in transcription

Bromodomains integrate protein complexes with functions in chromatin remodelling, highlighting the critical roles of BRDs in transcription regulation. BRDs are subunits of histone acetyltransferases (HATs) and anchor the HAT complex to acetylated chromatin, where other HAT subunits remodel the surrounding chromatin (Nagy and Tora 2007). As acetylation readers, BRD elements also recruit remodelling complexes to acetylated chromatin regions. These complexes alter the contact between DNA and histones, allowing the movement of nucleosomes. An example is SWI/SNF remodelling complex which is found at promoters of actively transcribed genes (Khavari et al. 1993; W. Wang et al. 1996). These functions are not exclusive and some BRD-containing complexes can perform several functions where the BRD-element plays critical roles. One example is the BRD-containing p300/CBP complex which has HAT activity (Arany et al. 1994), acetylates transcription factors such as GATA1 (Boyes et al. 1998) and can bind to acetylated p53 (Mujtaba et al. 2004).

Many transcription proteins contain several BD modules or a combination of BD with other effector domains. This feature allows targeted recognition of histone PTMs combinations, alluring to the precision of the transcription process. An example of a double bromodomain protein is TAF1, a subunit of TFIID with important functions in transcription initiation (Cianfrocco et al. 2013). TAF1 contains two tandem copies of bromodomains, and in this configuration, it binds with greater affinity to double acetylated lysines that are appropriately spaced (Jacobson et al. 2000). BD domains are also found in combination with other effector domains with transcription regulatory functions. The subunit of the NURF chromatin remodelling complex, BPTF, is one example where bromodomain and PHD finger domains co-exist. PHD finger domains recognise methylated lysines, and it has been shown that NURF binds to both H4K16ac and H3K4me3 in the same nucleosome (Ruthenburg et al. 2011). The interpretation of histone patterns by specialised multi-domain proteins is an important regulatory mechanism that is just starting to be understood.

1.3.3. BET proteins in transcription regulation and cell cycle progression

BET proteins, a bromodomain family, directly regulate transcription initiation and elongation by interacting with RNA polymerase II. BRD4 has a direct effect at all stages of transcription. This protein has been reported to phosphorylate RNA polymerase II, promoting transcription initiation (Devaiah et al. 2012). Transcription elongation is also regulated by BRD4 by recruitment of the transcription elongation factor, P-TEFb, to gene promoters (Jang et al. 2005). Additionally, BRD4 assists Pol II physical progression through hyperacetylated nucleosomes by interacting with acetylated histones (Kanno et al. 2014). BRD2 also associates directly with RNA polymerase II (Crowley et al. 2002); and both BRD2 and BRD3 have been shown to facilitate transcription of RNA Pol II though nucleosomes (LeRoy, Rickards, and Flint 2008a). Similarly to other BET proteins, BRD2 recognises acetylated histones and recruits transcriptional cofactors (Kanno et al. 2004), as well as transcription factors and other chromatin remodelling complexes (Denis et al. 2006) with impact on transcription and cell development.

BET proteins are essential in cell cycle control. Both BRD2 and BRD4 remain bound to chromatin during mitosis which suggests these proteins might have a role in maintaining epigenetic memory (Dey et al. 2003; Kanno et al. 2014). This is thought to be a transcription priming mechanism for a set of genes essential upon cell division (Maruyama et al. 2002). BRD2 and BRD4 have also been reported to control cell cycle progression. Mochizuki et al. have shown that BRD4 regulates G1-S phase progression (Mochizuki et al. 2008). In this study, BRD4 KD cells arrested at G1 phase as opposed to normal cell cycle progression observed in control cells. Arrest in G1 phase coincided with dysregulation of G1 gene signatures which were re-established following overexpression of BRD4 in KD cells. Furthermore, chromatin immunoprecipitation in control cells revealed recruitment of BRD4 to promoters of the G1 genes dysregulated in BRD4 KD. Together this shows that BRD4 regulates G1 gene expression, and progression to S phase, by binding to promoters of G1-characteristic genes. BRD2 has been shown to control S phase progression through regulation of cyclin A expression (Maruyama et al. 2002). Immunoprecipitation of BRD2 has revealed that the protein is present at cyclin A promoter during S-phase; and overexpression of BRD2 accelerates cell cycle through increased expression of cyclin A and transcriptional activation marks (H4 acetylation) at cyclin A promoter. BET proteins regulate cell progression at both gene promoters and bodies (LeRoy et al. 2008b), but also influence cell identity by regulation of non-coding regulatory regions.

BET proteins regulate transcription at enhancers. Recent studies, investigating the role of BET proteins in regulation of oncogenes, found that BRD4 co-localises with Mediator at enhancer regions (Lovén et al. 2013a). In this study, BET inhibition resulted in loss of BRD4 preferentially at enhancers, with consequent transcription elongation defects on genes regulated by those enhancers. In a different study, on adipose and muscle cells, it has been demonstrated that BRD4 co-localises with lineage-specific TFs at active enhancers (J.-E. Lee et al. 2017). In line with the previous study, BRD4 deletion prevented enrichment of Mediator and RNA polymerase II at enhancers; consequently preventing cell-specific gene signatures and differentiation (Bhagwat et al. 2016a). BRD2 has also been found to play a role on enhancer-driven transcription. In a study on differentiation of mouse T cells, BRD2 associated with the CTCF-cohesin complex that supports loop formation during cis-regulatory enhancer assembly (Cheung et al. 2017). BRD3 association with active enhancers has not been reported, in fact this is the less investigated of all the BET proteins.

1.3.4. BET inhibition

The hydrophobic nature of the acetyl-lysine recognition site in BET proteins presents an opportunity for the development of antagonist compounds. BET inhibitors are highly potent and selective molecules, capable of displacing BETs from chromatin with disruptive consequences on the transcriptional programs (Anand et al. 2013; Chapuy et al. 2013). However, despite the high selectivity over non-BET bromodomain proteins, the current BET inhibitors bind indiscriminatingly to the BET family due to the similarity among protein sequences (Filippakopoulos et al. 2010; Picaud et al. 2013). The first compounds developed to target BET proteins were I-BET and JQ1. I-BET is a benzodiazepine derivative capable of downregulating expression of inflammatory genes (Nicodeme et al. 2010). JQ1 is a triazolothienodiazepine compound first reported to halt cell cycle progression and induce apoptosis in human tumour cell lines (Filippakopoulos et al. 2010). Currently, there are several BET inhibitors used in research, and some are being tested in clinical trials for oncological diseases (Doroshow, Eder, and LoRusso 2017). The efficacy of these drugs is due to the general transcription repression of oncogenes and cell cycle arrest; in particular, c-Myc, a gene associated with cell growth, cell cycle progression and apoptosis that is frequently dysregulated in oncogenesis. BET inhibition often results in downregulation of c-Myc (Delmore et al. 2011b), probably due to the eviction of BRD4 from the c-Myc locus and consequent absence of PTEFb recruitment (Jang et al. 2005). It has been suggested that BET inhibition is particularly efficient at targeting tumour cells due to the eviction of BRD4 from oncogenic driver super-enhancers (Lovén et al. 2013b). Invariably unwanted effects have been observed during clinical trials for BET inhibitors with the most

commonly reported being thrombocytopenia (low platelet count), highlighting the role of BET proteins in platelet development (Berthon et al. 2016; Amorim et al. 2016). The pharmacological inhibition of BET proteins has shown therapeutic activity in a variety of pathologies (Prinjha, Witherington, and Lee 2012), and it represents an invaluable tool in the study of functional interactions between BET proteins and other regulatory factors.

1.3.5. BRD3-GATA-1 interaction

BRD3 directly binds to GATA-1 during erythroid-MK differentiation. Acetylation of the TF GATA-1 is essential for chromatin-binding at GATA1-activated and repressed genes (Boyes et al. 1998; J. M. Lamonica, Vakoc, and Blobel 2006). The first bromodomain of BRD3 recognises and binds to the acetylated lysines on the C-terminal of GATA1 (K312 and K315), adjacent to the zinc finger domains (Gamsjaeger et al. 2011). Lamonica *et al.* showed that acetylation of GATA-1 is essential for BRD3 association with chromatin (Janine M Lamonica et al. 2011). Additionally, the study showed that BET inhibition disrupted both BRD3 and GATA-1 chromatin occupancy, and therefore it was suggested that BRD3 promotes GATA-1 stable association with chromatin. However, this study has described the interaction between BRD3 and GATA1 in a simplistic and isolated way, which could lead to misinterpretation. Firstly, the inhibition experiments assume a targeted effect on BRD3, rather than the nonspecific targeting of all BET proteins characteristic of BET inhibitors. Secondly, the study assumes that both BRD3 and GATA1 are the only factors involved in this interaction. Therefore, the effects of other BET proteins or the possibility of a multiprotein complex containing BRD3, has been overlooked.

A different study investigated the effects of BET proteins on GATA-1 regulated genes during erythropoiesis, and concluded that BRD3 is dispensable for GATA-1 gene activation during erythropoiesis (Stonestrom et al. 2015). Stronestrom *et al.* showed that, despite high level of co-occupancy between BRD3 and GATA-1, displacement of BRD3 does not affect GATA1-mediated erythroid transcription. Interestingly, the depletion of BRD2 and BRD4 blunted several of the erythroid GATA1-regulated genes. These results show that BRD3 is not essential for erythroid GATA1-mediated gene transcription, and suggest that BRD3 might be recruited differently from BRD2 and BRD4. In addition, it was also reported that BRD3 and BRD2 could functionally overlap during erythropoiesis, as the overexpression of BRD3 on BRD2 KOs partially restored normal phenotype. This was the first time that a BET functional overlap was reported, and it highlights the complex system of transcription mechanisms.

1.4 Model systems to study megakaryopoiesis

The rarity of megakaryocytes, and the difficult accessibility to the bone marrow are the main obstacles in the study of megakaryopoiesis. Current megakaryopoiesis models include: animal models; immortalised cell lines with MK dysfunctional phenotypes, and stem cell derivation models. Each of these options presents a reliable research tool, but require careful consideration depending on the end application, as each model has its own drawbacks. Here, I briefly summarise advantages and disadvantages of each of these models, with particular focus on stem cell models as this has been my chosen model in this project.

1.4.1. Animal models

Animal models present the possibility to study megakaryopoiesis as part of a whole organism. Considering that the haematopoietic system is evolutionarily well conserved in mammals, animal models present a reliable resource to study physiological aspects of MK and platelet formation. Animals, such as mice and zebrafish, have been the basis of some important advances in the study of haematopoiesis as reviewed by (Schmitt, Lizama, and Zovein 2014). Some of the advantages offered by animal models rely on the ability to generate transgenic animals to mimic human disease phenotypes, and on the relatively short life span allowing transgenerational studies. However, the major limitation of animal models is that some human disease phenotypes are poorly replicated in animals (Seok et al. 2013).

1.4.2. Immortalised cell lines

Immortalised cell lines with dysfunctional phenotypes are an alternative model to study megakaryopoiesis. These are patient-derived cancerous cells that are adapted for *in vitro* culturing. Examples of this model are the CHRF-288-11 cell line derived from a solid tumor expressing MK and platelet characteristic markers (Fugman et al. 1990); the Dami cell established from peripheral blood of patients with megakaryoblastic leukemia (Greenberg et al. 1988); or IST-IU derived from narrow of a patient with leukemia (Sledge et al. 1986). These models hold a faithful genetic background for the disease, but they are cancerous and also omit the effects of environmental cues. Patients with rare bleeding disorders are ultimately the reason why it is important to study MKs and platelet

formation. These patients present an invaluable source of scientific information as the genome and epigenome of the cells contain the details that we, as scientists, are trying to unveil. However, often it is not ethically feasible to collect tissue samples from patients with bleeding disorders (blood or skin biopsies) for cell line generation.

1.4.3. Stem cell models

A stem cell is an unspecialised cell, capable of replicating into an identical daughter cell through cell division (self-renewal), and capable of differentiating into multiple cell types upon environmental stimuli (pluripotency). There are different classifications of stem cells based on the level of potency retained. 1) Totipotent cells are capable of generating all cells and tissues in the body. 2) Pluripotent cells retain the capability to differentiate into all embryonic tissues. 3) Multipotent and oligopotent cells are able to generate all or a limited number of lineages, respectively. 4) Unipotent (also called progenitor) are cells capable of differentiating into one lineage only.

Induced pluripotent stem cells (IPSCs) are an irreplaceable tool in the modern study of biology. In 1981, Martin G.R. and Martin Evans published two independent studies demonstrating isolation, *in* vitro culturing and pluripotency of embryonic stem cells (ESC) from mouse blastocysts (Martin 1981; Evans and Kaufman 1981). These experiments paved the way to the development of stem cell-based models. Despite the inherent potential of embryonic stem cells, the use of these cells remained surrounded by ethical controversy, fuelling the development of iPSC technology (Volarevic et al. 2018). In 2006, Yamanaka reported the induction of pluripotency from somatic cells (mouse fibroblasts) (Takahashi and Yamanaka 2006). The reprogramming of fully differentiated (somatic) cells into iPSCs was achieved through overexpression of four TFs: Oct3/4, c-Myc, Sox2 and Klf4. Currently, iPSCs are extensively used in scientific research due to their numerous advantages. 1) The potential to derive iPSCs from somatic patient lines, which not only allows the study of individual mutations, but also could present an autologous cell therapy alternative preventing immune rejection potential. 2) Morphological and growth similarities to ESCs. 3) Differentiation potential into somatic cells. This is due to the iPSC pluripotency levels, meaning that all 3 germ layers can be derived from iPSCs. The differentiation potential can be tested based on expression levels of pluripotency genes; or by cell differentiation towards the 3 germ layers (either by spontaneous or directed differentiation) (Buta et al. 2013). Although, in iPSC- based therapies, pluripotency of iPSCs is verified by the formation of teratomas following iPSC injection into immunocompromised mice, the hallmark for functional pluripotency (W. Zhang 2014).

When iPSCs were first generated, the process was extremely laborious and inefficient, and the tumorigenic potential associated with overexpression of c-Myc was a concern (Nakagawa et al. 2008). In the past decade, several methods have been developed to counteract these pitfalls, and alterations included: parental somatic cell type, reprogramming factors used, delivery methods and culture conditions. Several methods have been developed for the generation of iPSCs as review by (González, Boué, and Belmonte 2011). Currently, iPSCs could present a practical alternative to the *in vitro* differentiation of megakaryocytes and various protocols have been developed as described in the next section.

1.4.4. *in vitro* models of megakaryopoiesis

The development of in vitro models of megakaryopoiesis enables the molecular study of MKs differentiation and presents an attractive potential source of platelets for transfusion. The generation of MKs in the laboratory is a recent achievement as the first report on the differentiation of hES-derived MKs was published just over a decade ago. In that first protocol, Gaur *et al.* reported a method, based on TPO supplementation, which enabled the differentiation of hESC into high ploidy (2N-32N), $CD41a^{+}/CD42b^{+}$ MKs (GAUR et al. 2006). This protocol was simple, but the efficiency of differentiation was low (0.1-0.4 MKs per input hESC).

An alternative protocol was presented by Takayama *et al.* where supplementation with vascular endothelial growth factor (VEGF) promoted the formation of embryonic stem cell-derived sacs (ES-sacs) (Takayama et al. 2008). Haematopoietic progenitors in the ES-sacs were induced to MKs upon TPO supplementation. This protocol enable the production of 2-5 MKs per ESC which still presents a low yield, and was considerably laborious.

The first study, showing functional hESC-derived platelets contributing to *in vivo* thrombus formation following laser injury in a mouse model, was published in 2011 (Lu et al. 2011). The production of haemangioblasts, as a result of cytokines supplementation, was followed by exogenous administration of TPO, SCF and IL-11 to obtain platelet-producing MKs. This protocol presented two important advantages in comparison with previous ones: the cells were differentiated in feeder and serum-free conditions, and the MK yield was considerably higher (100 MK per hESC). A similar protocol on directed differentiation was reported in 2014 where iPSCs were differentiated

into MKs, and produced HLA-ABC-negative platelets as a potential source of universal platelets for transfusion (Q. Feng et al. 2014).

Another interesting protocol was published by Nakamura *et al.* where pluripotent stem cell-derived progenitors generated stable immortalised MK progenitor cell lines (imMKCLs). This was achieved through the overexpression of BMI1 and BCL-XL, to suppress senescence and apoptosis, respectively; and the controlled expression of c-Myc to promote proliferation (Nakamura et al. 2014). Despite allowing long-term cultures, this protocol has a demanding upfront cell requirement (4 platelets produced per imMKC).

Lastly, a forward programming protocol has recently been reported based on the overexpression of three key haematopoietic TFs (GATA1, TAL1 and FLI1) (Moreau et al. 2016). The cells are initially cultured in a 3D format to generate mesodermal embryoid bodies upon supplementation of BMP4. This step is followed by culturing embryoid bodies in suspension with TPO and SCF supplementation until cells present a MK-specific phenotype. This protocol enables the production of 2E+5 MKs per input hiPSC in a xeno-free manner and allows culturing of MKs for up to 120 days. A new version of this protocol has been developed where the initial 3D culturing system was replaced by a 2D cell monolayer. The advantages of the new system are the lower cost, justified by the removal of expensive 3D culturing plates; and the maintenance of the 2D conditions in which iPSCs are normally cultured. This version is explained in detail in the results session as this was the model I used to perform the experiments reported in this thesis.

Despite the advances made in the field of *ex vivo* MK differentiation strategies, the current protocols present the following disadvantages. 1) The MKs generated are not yet able to achieve high polyploidisation, resulting in low pro-platelet release when compared with human adult MKs. 2) The pro-platelets generated present inappropriate and premature activation confirming cell immaturity. An important advantage of all aforementioned *in vitro* models is the possibility to genetically engineer cell lines with variants to mimic MK-related disease phenotypes. The ability to genetically engineer cells has recently been improved with the adaptation of the Clustered Regularly Interspaced Palindromic Repeats (CRISPR) and CRISPR-related proteins (Cas) or CRISPR/Cas system.

1.4.3. Genetic manipulation system- CRISPR/Cas9

CRISPR/Cas is a bacterial adaptive immunity system that has recently been adapted to allow cellular genetic manipulation. In bacteria, CRISPR/Cas9 is used as a defence mechanism against invading viruses and plasmids (Barrangou et al. 2007). Upon phage infection, short DNA fragments from the invader's genome (protospacers) are incorporated into the bacteria's CRISPR loci. Following a second encounter with the phage invader, the CRISPR loci are transcribed, and the CRISPR RNA generated (crRNA) integrates the protospacers. The crRNAs hybridise with trans-activating RNA (tracrRNA) to guide the Cas9 to the specific foreign DNA, next to a protospacer adjacent motif (PAM). The foreign DNA is cleaved by Cas9, inactivating the bacteriophage infection. Although this process is generally extremely efficient; bacteriophages are known to adapt very rapidly and circumvent CRISPR/systems. One hypothesis to explain such resistance is the existence of anti-CRISPR genes or other genetic elements capable of inactivating CRISPR/Cas systems (Bondy-Denomy et al. 2013). The balance between CRISPR/Cas9 systems in bacteria and the phage resistance might have contributed to the evolution of the variety of CRISPR/Cas systems currently known.

The adaptation of the CRISPR/Cas system as a genetic engineering tool is recent, but the precision and ease of use explain how it became a ubiquitous method in modern molecular biology. The bacterial immune system was adapted so the crRNA and tracrRNA are fused into a single guide RNA (sgRNA) which flags the target genomic DNA. Similarly to the original bacterial CRISPR/Cas system, the sgRNA-targeted loci is then cleaved by the Cas9 protein at 3-4bp upstream from the PAM sequence. Upon Cas9 cleavage (double strand break, DSB), the DNA is repaired by either non-homologous-end-joining (NHEJ) or homologous directed recombination (HDR). NHEJ happens at higher frequency and it is error-prone, generating insertions and/or deletions (indels) in the repaired loci. The HDR is a high-fidelity mechanism that happens at lower frequencies. This disadvantage can be overcome by exogenous supplementation of repair templates, which are incorporated in the genome by Watson-Crick base-pairing. The technology has been used in cell lines manipulation, transgenic mice manipulation, and even in human gene therapy as reviewed by (Sander and Joung 2014).

New mutant versions of Cas9 have been developed to enable CRISPR/Cas9 system repurposing. The Cas9 binding and catalytic units that be separately manipulated. The catalytic activity is controlled by two distinct endonuclease domains: the HNH nuclease domain which cleaves the complementary strand to the sgRNA; and the RuvC nuclease domain cleaves the non-complementary strand. Each of these domains can be inactivated by single point mutations. Thus, Cas9 D10A (active RuvC) and H840

(active HNH) mutants are termed nickases due to their ability to nick only one DNA strand. The enzyme is designated dead Cas9 (dCas9) when both catalytic domains are inactivated, and the enzyme completely lacks endonuclease activity. This is a convenient feature for experiments aiming at disrupting transcription, as dCas9 can be directed to gene promoters, impeding binding of polymerase II (Qi et al. 2013). dCas9 can also be fused to enzymatic domains, such as repressor or activator domains. This variation of the system is referred to as CRISPR interference (CRISPRi), and depending on the domain fused to the dCas9 enzyme, it can be used with gene up-regulation or silencing intentions (Hilton et al. 2015; Thakore et al. 2015). Other uses of CRISPR/Cas9 include epigenome editing where Cas9 is used to recruit chromatin modifying enzymes to specific loci (Lei et al. 2017; X. S. Liu et al. 2016); live cell chromatin imaging where fluorescently labelled dCas9 is directed to target regions (B. Chen et al. 2013; P. Qin et al. 2017); or genetic and epigenetic screens where thousands of sgRNAs target a population of cells with the aim of identifying the genes responsible for a particular phenotype (Doench 2017). In this thesis, CRISPR has been used to generate KO cell clones and CRISPRi was attempted to generate knockdown clones to investigate the regulatory roles of BRD3 and other BETS in gene transcription during megakaryopoiesis.

1.5 Chromatin and gene transcription

Every cell in the body contains the same genetic information, yet cells are able to differentially express (or repress) genes, resulting in cellular and tissue differentiation. Complex and timely interactions between chromatin and specialised proteins, such as transcription factors and cofactors, are the basis of gene transcriptional regulation networks. Disruption of these interactions often result in cellular diseased states. Therefore, defining the epigenetic elements regulating haematopoiesis is critical to understand the onset and development of disease, such as haematopoietic disorders.

1.5.1. Chromatin structure organisation

Chromatin is a very dynamic structure, consisting of DNA and proteins, where the basic unit is the nucleosome. Each nucleosome is formed by ~147 base pairs of DNA folded around an octamer of four core histone proteins H2A, H2B, H3 and H4 (Luger et al. 1997). In the nucleosome core, the histones are arranged in H3-H4 tetradimer and H2A-H2B dimers. Linker histone H1 acts as a DNA stabiliser by condensing the DNA and the string of repeating nucleosome units (Izzo, Kamieniarz, and Schneider 2008).

Histones are proteins containing a globular (spherical) domain and a positively charged NH_2-terminus ("tail") protruding from the nucleosome unit. Histone tails are subjected to reversible residues modifications - posttranslational modifications (PTMs) - including acetylation, methylation, phosphorylation, ubiquitination, sumoylation, ribosylation and biotinylation (Cubeñas-Potts and Matunis 2013; Meas and Mao 2015; Rossetto, Avvakumov, and Côté 2012; Greer and Shi 2012; Eberharter and Becker 2002). These modifications alter the interaction between histones and the DNA, affecting chromatin conformation and accessibility. Chromatin can be characterised as euchromatin or heterochromatin. Euchromatin is characterised by a high level of histone acetylation, where the DNA sequence is more accessible to transcription factors and RNA polymerase II. These features are associated with active chromatin, displaying PTM-rich sites that are actively transcribed, or regulate transcription, such as enhancers (Heintzman et al. 2009; Barski et al. 2007). Heterochromatin presents a condensed architecture, enriched in histone trimethylation leading to transcriptional silencing (Kouzarides 2007). Heterochromatin has been classified in facultative heterochromatin, including regions that are differentially expressed during development and then

become silenced, such as the X-chromosome in female cells (Jeppesen and Turner 1993); and constitutive heterochromatin containing regions permanently silenced and characterised by H3K9me2/3 signatures and low acetylation levels (Trojer and Reinberg 2007).

Each histone tail modification exerts an effect on the chromatin structure, but it is the combinatorial effect of PTMs that dictates the overall chromatin state and functional outcome. Several models have been proposed to explain regulation of transcription by histone PTMS, including: the signalling network model (Schreiber and Bernstein 2002), charge neutralisation model (Roth and Allis 1992) and histone code model (Strahl and Allis 2000). The histone code model is the most widely accepted, and it postulates that synergistic combinations of histone PTMs drive distinct biological functions (Gardner, Allis, and Strahl 2011). Although the histone code provides an explanation for the current knowledge of chromatin regulation, it is becoming clear that this is a simplistic view of the histone PTMs role in transcriptional regulation. Recent studies uncovered previously unknown chromatin details involved in transcription regulation mechanisms, such as histone PTMs asymmetry within the nucleosome leading to bivalent functions (Voigt et al. 2012), or the identification of novel histone PTMs (Arnaudo and Garcia 2013). Overall, chromatin structure directly impacts the interactions between transcription regulators and DNA. Therefore, understanding the network of factors regulating histone PTMs will improve the knowledge of the processes regulating gene transcription.

1.5.2. Transcriptional regulation

Cell identity is defined by the set of genes transcribed at any given time. The expression of protein-coding genes relies on several steps, including transcription initiation, elongation, mRNA processing and translation. Transcription initiation is regulated by the association between 2 types of cis-elements: the gene promoter and distal regulatory elements, such as enhancers, silencers and insulators (Z. Hu and Tee 2017; Ogbourne and Antalis 1998; Fourel, Magdinier, and Gilson 2004). Promoters define the transcription starting site (TSS), gene directionality, and contain the docking sites for all the transcriptional machinery (Smale and Kadonaga 2003; Lenhard, Sandelin, and Carninci 2012). Cis-acting regulatory elements are brought together by trans-acting DNA-binding transcription factors. The interactions between distal elements, particularly enhancers, and TFs are of most importance for transcription initiation regulation in a temporal and spatial manner (Whyte et al. 2013).

Characteristic epigenetic features are common in cis-regulatory elements and support their role in transcriptional regulation. Firstly, the absence of nucleosomes results in highly accessible DNA which promotes binding of TFs and cofactors at these regions (Hihara et al. 2012). Secondly, nucleosomes surrounding these highly accessible regions are often characterised by specific histone modifications. As examples, enhancer chromatin signatures are often characterised by high levels of H3k4me1 and low levels of H3k4me3, while promoters are marked by H3K4me3 (Hon, Hawkins, and Ren 2009; Heintzman et al. 2007a; Barski et al. 2007). Additionally, the distinction between inactive and active enhancers can be based on H3k27ac marks (Creyghton et al. 2010). Lastly, regulatory elements presenting active signatures are generally populated by transcriptional factors, cofactors and activators (Heintzman et al. 2009).

Enhancers are cis-elements with structural characteristics that influence precise spatiotemporal transcription regulation. Enhancers contain multiple TF binding sites. The combinatorial TF occupancy evolves during cell development resulting in precise regulation patterns (Lin et al. 2010; Sandmann et al. 2006; Sandmann et al. 2007). In addition to variation in TF occupancy during cell development, epigenetic information at enhancers changes in complexity during differentiation. Heintzman *et al.* demonstrated that enhancers are marked with cell-specific histone PTMs patterns, which are strongly correlated to cell-specific gene signatures (Heintzman et al. 2009). These gene signatures can be activated through long-range interactions between the enhancers and the gene promoters, independently of the distance, or orientation between the 2 elements (Clapier and Cairns 2009; Geyer, Green, and Corces 1990). Several models have been proposed to explain the interactions between distal enhancers and promoters as reviewed in (Mora et al. 2016), although the DNA-looping model is the most widely accepted. In this model, DNA loops are formed between enhancers and promoters, where both elements are in closer proximity to each other than intervening sequences. The DNA loops are formed with intervention of TFs and other intermediate cofactors. For example, during transcription initiation, the Mediator complex recruits cohesin, which stabilises DNA loops between enhancers and promoters (Kagey et al. 2010). Additionally, CTCF has also been reported to stabilise DNA loops (S. S. P. Rao et al. 2014).

TFs intervene in the establishment of long-range interactions between promoters and enhancer regions. The mechanisms by which TFs regulate such interactions have been object of various studies as reviewed in (Spitz and Furlong 2012). Although, these interaction mechanisms are still unclear, particularly as the recruitment of TFs themselves might be regulated by other cofactors (Janine M Lamonica et al. 2011). In this thesis, I focus on the regulatory mechanisms of BRD3 during

megakaryopoiesis. BRD3 is recruited by acetylated GATA-1 to chromatin during erythropoiesis (Janine M Lamonica et al. 2011). GATA-1 is also an important TF in megakaryopoiesis, as described in section 1.2.4.1.1. However, the role of BRD3 in megakaryopoiesis has never been studied.

1.5.2.1. Histone lysine acetylation (Kac), a mark of active chromatin

Lysine acetylation (ε-*N*-acetylation or Kac) is a reversible protein post-translational modification (PTM) that consists on the addition of an acetyl group to the side-chain nitrogen of lysine. Histone acetylation has been one of the most studied histone modifications due to its impact on chromatin conformation (Verdin and Ott 2015a). Lysine acetylation neutralises residue charge, reducing electrostatic attraction between histones and the negatively charged DNA. The change in chromatin configuration provides accessibility for transcriptional machinery with downstream impact on gene transcription (Clayton, Hazzalin, and Mahadevan 2006). This conformational plasticity is the consequence of enzyme-mediated reactions, controlled by chromatin modifier enzymes.

Chromatin modifiers act in a spatial and temporal manner to deposit ("writers") or remove ("erasers") histone modifications. These enzymes are classified into categories, depending on the PTM regulated. Histone acetyltransferases (HATs) acetylate residues on histone tails, and histone deacetylases (HDACs) remove the acetyl group (K. K. Lee and Workman 2007; Haberland, Montgomery, and Olson 2009). In addition to "writers" and "erasers", there are proteins responsible for interpreting the signalling marks on histones, called "readers" (figure 1.5.1). These highly specialised enzymes play important roles in regulation of the transcriptional machinery, and often target a particular amino acid residue. Bromodomains, the family which BRD3 belongs to, are chromatin "readers" specialised in recognising lysine acetylation in chromatin and TFs (Zhou et al. 1999; Zeng and Zhou 2002). Several of these acetylation regulatory enzymes have been characterised as being critical in normal haematopoiesis as reviewed in (Glozak and Seto 2007). The abnormal function of such proteins is often causative of malignant states which makes them amenable to be targeted by small molecule drugs.

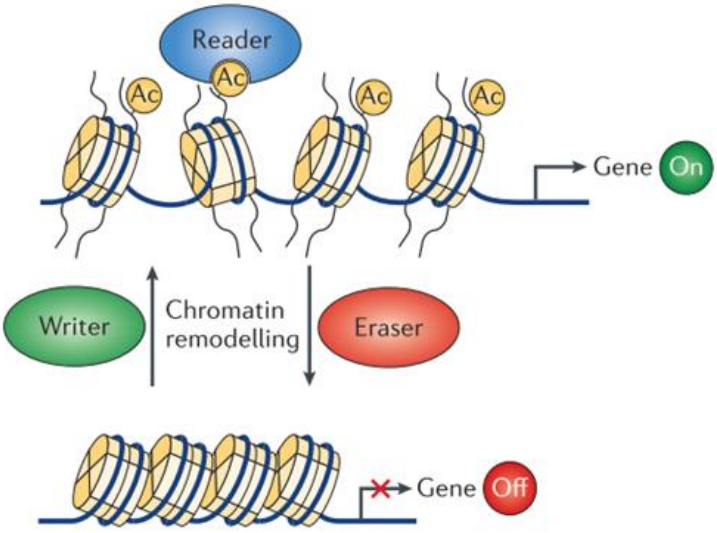

Figure 1.5.1 Enzymatic regulation of histone acetylation. Histone tails become acetylated upon addition of acetyl group to the histone tail by "writer" enzymes (HATs). Acetylation changes chromatin into a transcriptionally active conformation (euchromatin). "Reader" enzymes, such as bromodomain proteins, interpret acetylation and trigger recruitment of transcription factors and cofactors. "Eraser" enzymes (HDACs) are responsible to return the chromatin to its inactive state (heterochromatin). Adapted from (Verdin and Ott 2015b).

Lysine acetylation is found widely spread across the entire proteome, highlighting its central role in signalling networks and transcription activation (Kori et al. 2017). As the structure of acetylated chromatin is altered to a more relaxed state (euchromatin), it becomes transcriptionally active and accessible to RNA polymerases and transcription factors (Marushige 1976; Hebbes, Thorne, and Crane-Robinson 1988). Functional interaction between the transcription factors, harbouring acetyl-binding domains, and acetylated histone residues leads to transcription activation (Shogren-Knaak et al. 2006). Therefore, The effect of acetylation on transcription can happen in two ways: by altering the interactions between histone and DNA resulting in a modified chromatin structure; or by recruiting other proteins relevant to transcription (Josling et al. 2012).

The influence of Kac on transcription is broader than chromatin structure effects. Choudhary C. *et al.* were the first to show, by high-resolution mass-spectrometry, that lysine acetylation is associated with regulation of chromatin remodelling, cell cycle, splicing or nuclear transport (Choudhary et al. 2009). DNA-protein binding interactions are also affected by lysine acetylation levels. For example, the highly conserved lysine-rich motifs within the zinc finger domain of GATA1 become acetylated, triggering cell differentiation (J. M. Lamonica, Vakoc, and Blobel 2006; Boyes et al. 1998). Protein-protein interactions can also be mediated by acetylation. Erythroid Krüppel-like factor (EKLF), an

erythroid-specific transcription factor, has been shown to require Kac for interactions with other transcriptional regulatory proteins (X. Chen and Bieker 2004). Other functions such as DNA repair (Celic et al. 2006), chromatin compaction (Shogren-Knaak et al. 2006) and protein stability have been associated with acetylation.

Histone acetylation marks, or combinations of marks, have been associated with particular epigenetic states. Acetylation marks at H3k9, H3k14 and H3k27 have been found to accumulate at transcription starting sites of active genes (Z. Wang et al. 2008). Enhancer chromatin signatures are often characterised by high levels of H3k4me1 and low levels of H3k4me3 (Heintzman et al. 2007b). Additionally, acetylation marks allow the distinction of enhancers in inactive and active states (Creyghton et al. 2010).

1.6 The aims of my project

BRD3 was identified in a GWAS as one of the genes regulating platelet traits. However, the mechanisms by which BRD3 regulates platelet formation have remained unknown. As platelet *in vitro* models generate a low platelet yield, this project explores the role of BRD3 in megakaryocytes (platelet progenitors) differentiation. Therefore, the overarching goal of this project was to explore the role of BRD3 during megakaryopoiesis. As the project progressed, my work was divided in 4 main aims:

1) The first aim of this project was to generate and validate a model system to study BRD3 during MK differentiation. To achieve this goal, I generated an iPSC model, using CRISPR/Cas9 technology. The model validation was achieved by characterisation of iPSC BRD3 KO cells and investigation of the BRD3 KO capability to produce *in vitro* MKs.

2) The second aim of this project was to explore the role of BRD3 on regulatory elements during megakaryopoiesis. BET proteins occupy transcription regulatory elements in a cell-specific manner, and active regulation can be characterised by characteristic chromatin signatures. Active regions present a euchromatin (accessible) conformation and are highly acetylated. Therefore, I investigated how active chromatin signatures change in the absence of BRD3, and the consequences of those changes on gene transcription.

3) The third aim of this project was to investigate the effects of ablating BET protein complexes during megakaryopoiesis. BET proteins BRD2, BRD3 and BRD4 associate in transcriptional complexes involved in regulation of peripheral blood cells (Dawson et al. 2011). Such complexes can be targeted with BET inhibitors which indiscriminately target BRD2, BRD3 and BRD4. Therefore, I used BET inhibition at different stages of MK differentiation to investigate whether BET proteins (individually or in the complex) have an important regulatory role in Megakaryopoiesis. By comparing of BET inhibition and BRD3 KO results, I aimed at uncovering the differences in BET protein requirements during megakaryopoiesis.

4) The last aim of my project was to understand individual requirements of BET proteins, namely BRD2 and BRD4, during megakaryopoiesis. These 2 proteins have been shown to play active roles in cell cycle development and blood cell differentiation, such as erythropoiesis. I designed iPSC BET KO models to study individual BRD2 and BRD4 protein requirements on MK differentiation.

Chapter 2

Material and Methods

2.1. Cell culture

2.1.1. iPSC

Unless otherwise stated, all iPSC manipulation protocols were performed following Professor Vallier's protocols (Vallier and Pedersen 2008).

A1ATD1-c was derived from skin fibroblasts with the monocistronic iPS reprogramming kit (Vectalys), consisting of four retroviral vectors encoding: OCT4, SOX2, KLF4, v-MYC. This line was derived from a patient with an alpha1 anti-trypsin gene mutant, which has been corrected to match a reference genotype (Yusa et al. 2011).

The iPSC line S4-SF5 was derived from human fibroblastic cells by Sendai virus infection (CytoTune, LifeTechnologies) with the Yamanaka's factor (OCT4, SOX2, KLF4, MYC). The derivation was completed in Professor Vallier's laboratory on mouse embryonic fibroblasts (MEF) cells and adapted to feeder-free conditions from passage 20 (Rouhani et al. 2014).

2.1.1.1. AE6++ medium (for iPSC culture)

500ml Dulbecco's modified eagle's medium (DMEM)/F12 (cat. 11330-032, Thermo Fisher Scientific)
3.6ml 7.5% sodium bicarbonate (cat. 25080094, Thermo Fisher Scientific)
5ml L-ascorbic acid 2-phosphate, final concentration 320 ug/ml (cat. A8960, Sigma-Aldrich, Gillingham, UK)
10ml 50x insulin transferrin selenium (cat. 41400045, Thermo Fisher Scientific)
5µg/ml recombinant FGF2 (cat. 233-FB, R&D systems)
10µg/ml recombinant activin A (cat. 338-AC, R&D systems)

2.1.1.2. Cell maintenance

iPSC were grown in cell culturing plates (various sizes, from Corning) pre-coated with 10µl/ml vitronectin VTN-N (cat. A14700, Thermo Fisher Scientific) in D-PBS (cat. D8537, Sigma-Aldrich). The VTN-N coating facilitated cell adhesion as cells were cultured in a feeder-free format. $AE6^{++}$ media was pre-incubated at 37°C. Feeding was carried out 6 times a week. Antibiotics were not used. Aseptic technique was performed and plates were only opened inside a sterile laminar flow cabinet in a dedicated stem cell facility. Cells were incubated between manipulations at 37°C, 5% CO_2 (controlled temperature and pH).

2.1.1.3. Passage (culture propagation)

Cells required passage approximately every 5 days, usually when cells reached ~80% confluence. Adherent cells were washed once with 2ml D-PBS. Standard passage for cell maintenance involved incubating cells in 1ml of 50µM ethylene-diamine-tetra-acetic acid (EDTA, CIMRCK) in D-PBS$^{-/-}$ (without Mg2+/Ca2+) (PBS-EDTA) for 2 minutes (or until cells dissociation was observed under the microscope). EDTA was aspirated and 1ml D-PBS$^{-/-}$ was added to the well to gently wash the cells monolayer. Care was taken to avoid dislodging the cells. Wells were replenished with 1 ml of AE6^{++} media and gently pipetted over the cells to lift small cell clumps into suspension. The cell suspension was split into VTN-N pre-coated plates. Splitting rations varied between 1:5 and 1:20 depending on the starting cell density and the requirements of upcoming experiments.

2.1.1.4. Passage (single cells for experiment set up)

For experiments initiation, cells were seeded as single cells using TrypLE (cat. 12563029, Thermo Fisher Scientific) for dissociation. IPSC culture media was removed and cells were washed with 1ml D-PBS. 1ml room temperature TrypLE was added and plates incubated at 37^{o}C until cells were completely dissociated (as observed under the microscope). TryplE was aspirated and cells were collecte d in 10ml AE6^{++} media supplemented with 10uM of Y-27632 to aid cell survival. Cell suspension was centrifuged (200g, 3 minutes) and pellet was ressuspended in 1ml AE6^{++} media containing 10µM ROCK inhibitor (Y-27632) and seeded at the required density in vitronectin-coated tissue culture plates.

2.1.2. HEK293T (ATCC CRL-11268)

HEK293T manipulation was performed following ATCC recommendations.

2.1.2.1. Media recipe

500ml DMEM - high glucose (cat. D6429, Sigma-Aldrich)

55ml heat-inactivated fetal bovine serum (cat. F9665, Sigma-Aldrich)

5.5ml 10,000U/ml penicillin-streptomycin (cat. 15140-122, Thermo Fisher Scientific)

5.5ml minimal essential medium non-essential amino acids (cat. 11140-035, Thermo Fisher Scientific)

0.6ml 8mg/ml tylosin solution (cat. T3397, Sigma-Aldrich)

2.1.2.2. Cell maintenance

Cells were maintained in uncoated 10cm^{2} tissue culture plates in 10ml HEK293T complete media. Media was warmed to 37^{o}C prior to contact with cells and was changed two times per week. Cells were incubated between manipulations at 37^{o}C, 5% CO_2.

2.1.2.3. Cell passage

At >50% confluent, cells were gently washed with D-PBS to remove serum (present in the media) before incubation with 2ml trypsin for 3-5 minutes at 37^{o}C, until cells were dissociated. HEK293T complete media was added to the dish to neutralise the trypsin and collect the cells. Cells were homogenised, counted with a haemocytometer and reseeded in uncoated dishes at the required density. Maintenance of HEK293T was performed following the method described on ATCC website.

2.1.3. Thawing cells

To initiate a culture from frozen stock, frozen vials were thawed in a water bath at 37^{o}C until a small piece of ice remained. Vials were sprayed with 70% ethanol, and contents transferred to a 15ml falcon. Complete media (10ml) was added drop wise, and the cell suspension was centrifuged (200g, 3 minutes). The pellet was ressuspended gently in 1ml of complete media containing 10µM final concentration of Y-27632 (ROCK inhibitor, cat. Y0503, Sigma-Aldrich) and seeded in a 6 well plate. The contents of each well were replenished with 1.5ml of complete media. 24 hours later the medium was replaced with complete media without Y-27632.

2.1.4. Cryopreservation

Cells were dislodged using EDTA (50µM) in PBS (without Mg2+/Ca2+), and ressuspended in freezing media consisting of 0.1ml DMSO (cat. D8418, Sigma-Aldrich) and 0.9ml knockout serum replacement medium (cat. 10828028, Thermo Fisher Scientific). The cell mix was transferred to a cryovial and placed in a Mr Frosty freezing container containing isopropyl alcohol (cat. I9516, Sigma-Aldrich). This was placed in a -80^{o}C freezer for 24hr before transferring into a -150^{o}C freezer for longer term storage. These steps were undertaken quickly because DMSO is toxic to cells at room temperature.

2.1.5. Forward programming (FoP) to generate iMK

Moreau *et al.* published the protocol used in my experiments (Moreau et al. 2016). Alterations have been made by Dr Cedric Ghevaert's lab to the published protocol to improve yield, chiefly the single cell seeding of iPSC, culture in standard tissue culture flasks rather than an Aggrewell dish, and the removal of Ly-294002 (PI3 kinase inhibitor) from the protocol. The protocol used in this study is as follows.

2.1.5.1. Reagents

1X TrypLE Select (cat. 12563029, Thermo Fisher Scientific)

AE6^{++} media (cat A1517001, Thermo Fisher Scientific)

Vitronectin VTN-N (cat. A14700, Thermo Fisher Scientific)

Nunc 6- and 12-well uncoated tissue culture plates (Thermo Fisher Scientific)

Recombinant FGF2 (cat. 233-FB, R&D Systems)

BMP4 (cat. 314-BP-010, R&D Systems)

Rock inhibitor Y-27632 (cat. Y0503, Sigma-Aldrich)

rhTPO (cat. 01417-050, CellGenix)

rhSCF (cat. PHC2116, Thermo Fisher Scientific)

Protamine Sulphate (cat. P4505, Sigma-Aldrich)

D-PBS (cat. D8537, Sigma-Aldrich)

TrypLE (cat. 12563029, Thermo Fisher Scientific)

CellGro-SCGM (cat. 0020802-0500, CellGenix,)

Viral Vectors (Vectalys), see figures 2.1, 2.2 and 2.3 for vector maps.

pTRIPU3-TAL1 (batch pV.2.3.107_p16_01_1, titre $5.5x10^9$TU/ml)

pWPT-hFLI1 (batch pV.2.3.993_p15_11_2, titre $1.5x10^9$TU/ml)

pWPT-hGATA (batch pV.2.3.1073_p15_10_1, titre $2.6x10^9$TU/ml)

PBE flow buffer (D-PBS, 0.5% BSA and 2% PFA

2.1.5.2. MK Forward Programming (FoP) protocol

(Day -1) ~$1x10^5$ cells are collected using PBS+EDTA method and reseeded as small clumps onto a vitronectin coated well of a 12-well plate, in $AE6^{++}$ media, and allowed to reattach for 24 hours. Single cells can also be seeded, following the same protocol as described above for iPSCs. All subsequent steps of this protocol must be performed in a CL2 viral laboratory.

(Day 0) Cells are transduced with the appropriate volume of recombinant lentivirus to get the desired multiplicity of infection (MOI). Conventional forward programming requires GATA1, TAL1 and FLI1 lentiviruses, thawed on ice, all used at an MOI 20. All lentiviruses used were produced commercially (Vectalys). Lentivirus mix is added to 0.5ml mesoderm-inducing medium: AE6 + FGF2 20ng/ml + BMP4 10ng/ml (R&D) + Protamine sulphate 10µg/ml. For transduction of multiple wells a master mix was prepared. Cells and transduction mix are left to incubate for 24 hours.

(Day 1) Cells are washed 1x PBS before 0.5ml fresh mesoderm-inducing media (without protamine sulphate) was added and incubated for 24 hours.

(Day 2) Medium was changed to 0.5ml MK-1 media: CellGro SCGM (CellGenix) + Human TPO 20ng/ml (CellGenix) + Human SCF 25ng/ml (Life Technologies), for MK differentiation. Cells were left for 48

hours before fresh medium was added. The first medium addition required 0.5ml MK media with 2x concentration of cytokines (MK-2 media). Subsequent medium changes (50% exchange) involved careful removal of half the medium by tilting the plate and collecting only medium, not cells, before adding half the volume fresh medium (2x cytokines).

(Day 9/10) The supernatant of each well was collected into a 15ml falcon tube and the well rinsed 1x PBS (0.5ml), before being pooled with the supernatant. To collect the adherent cell fraction 300µl TrypLE was added to wells and incubated for 10 mins at 37°C, 5% CO_2. The TrypLE-cell mix was added to the corresponding falcon tube and quenched with 10 ml PBS before being centrifuged 300g, 5min, room temperature. Cell pellet was then re-suspended in 0.2ml MK-2 media (TPO 20ng/ml, SCF 25ng/ml). A small aliquot of cells were used for flow cytometry analysis to monitor MEP and MK markers. Remaining cells were re-plated onto 6 well plates in a total of 2ml MK-2 media. At this stage it is safe to remove cells from the CL2 viral laboratory to be subsequently handled in a standard CL2 TC laboratory. Medium was refreshed every 48-72 hours, (50% exchange).

(Day 20/21) Cells were collected and stained again to monitor MK maturation by flow cytometry. Cells can be re-plated and maintained long-term by refreshing the MK-2 media every 3 days (50% exchange) and checking MK purity every 7-10 days. Cell density can be adjusted once an accurate cell count has been obtained. Optimal cell density is 2E+5-1.5E+06 cells/ml. Cells can be split 1:5 when cell density exceeds 1.5E+06 cells/ml. Forward programmed MKs (FoP-MKs) can be frozen in IMDM 20% FBS 5% DMSO ideally at 0.5-1E+6 cells per vial. Upon thawing, these cells can be placed back in MK-2 media (TPO 20ng/ml, SCF 25ng/ml), refreshing every 2-3 days. In my experiments, I have stopped cultures at day 20, once MK markers were expressed.

2.2. Molecular techniques

2.2.1. DNA visualisation

Snapgene software was used to visualise DNA manipulation including primer positions, cloning, Sanger sequencing alignments, restriction digestion and CRISPR Cas9 gene editing strategies. Sequences were obtained from Ensembl or manufacturers of plasmids and oligonucleotides.

2.2.2. Genomic DNA extraction

All molecular protocols described were followed according to (Sambrook *et al*, 2011).

Genomic DNA (gDNA) extraction from cell cultures was performed using the Wizard Genomic DNA Purification Kit (cat. A1125, Promega) following the manufacturer's instructions.

2.2.3. Genotyping

All PCR were performed using the high-fidelity Phusion polymerase (NEB M0530) following the manufacturer's instructions on a GeneAmp PCR System 9700 thermal cycler. Primers used for BRD2, BRD3 and BRD4 PCR (i.e. for confirmation of mutations in KO clones and Sanger sequencing) are listed in table 2.2.1. Primers were purchased as lyophilised desalted oligonucleotides (Sigma-Aldrich) and ressuspended to 10uM in water. PCR was carried out at standard conditions (98 ^{0}C-30 sec, 30 cycles of (98 ^{0}C-10 sec, 65-70 ^{0}C-30 sec, 72 ^{0}C-30 sec), 72 ^{0}C-5 min, 4 ^{0}C-∞).

1% Agarose gels were used for visualisation of PCR products. 1g of agarose gel was dissolved by heating in 100ml 1x TBE buffer. When cool, 0.1µl/ml of SYBR Safe DNA gel stain (cat. SS3102, Thermo Fisher Scientific) was added. PCR products were mixed at 1:6 ratio with 6X Orange loading dye (cat. R0631, Thermo Fisher Scientific). Samples were run alongside a 1kb Generuler DNA ladder (cat. SM0311, Thermo Fisher Scientific). Gels were run at 90mV for 30-60 minutes and DNA was imaged with a Syngene Chemi Genius. Following successful PCR confirmation on gel electrophoresis, DNA was purified using the Qiaquick PCR purification kit (cat. 28104, Qiagen) and quantified by spectrophotometry using the Labtech Nanodrop Spectrophotometer at 260nm. Products were either used for Sanger sequencing at Source Bioscience, Cambridge, UK or cloning purposes.

Locus targeted	Exon targeted	Primer	sequence
BRD2	Exon 4	BRD2KO.PCR8.FWR	TGTGTGAGAGTCGGGGATCG
	Exon 4	BRD2KO.PCR8.REV	CAGGCCCTAGGCCATTACCA
	Exon 4	BRD2KO.PCR9.FWR	GCAGGGGCCTCCCTGTGGAT
	Exon 4	BRD2KO.PCR9.REV	TGGCCCCCTTCTTGTGGCTGT
BRD3	Exon 2	BRD3.E2.FWR	CAGTGGTTGGAGAGTCGTTC
	Exon 2	BRD3.E2.REV	CCAGTGAGGCAGAAGAAGG
BRD4	Exon 2	BRD4 E2 Fwd1	ACTCTGCCTCCTCTGTTGGTTTGT
	Exon 2	BRD4 E2 REV	AGATCTGTGGGCCTTCCTTTCTCC

Table 2.2.1 Successful PCR primers for BRD2, BRD3 and BRD4 genotyping of KO clones.

2.2.4. Restriction endonuclease digestion

Restriction digestion was performed following protocols recommended on the NEB online tool. All enzymes were purchased from NEB and used in optimal buffer supplied. Restriction digests were routinely set up on ice and performed at 37°C for 1 hour. 1% TBE gels were used to analyse DNA fragments SYBR safe DNA gel stain (Invitrogen) was added to visualise DNA or for DNA extraction. 6x Orange G loading buffer (Sigma) was added to DNA samples before loading into a gel.

2.2.5. Gel purification of DNA from agarose gels

Gel purification was done following the manufacturer instructions for the QIAquick gel extraction kit (Qiagen). Dephosphorylation of restriction digested products was performed with either Antarctic phosphatase (NEB), as per manufacturer instructions. PCR products intended for cloning were purified using the QIAquick PCR purification kit (Qiagen), following manufacturer instructions. Ligations were performed with T4 DNA ligase (NEB).

2.2.6. Transformation of high-efficiency competent E.coli

Competent *E.coli* cells (NEB) were thawed on ice for 10min before aliquoting 10µl into transformation tubes on ice. 1-5µl containing 1pg-100pg were added to the cell mixture and the tube gently flicked twice. Transformation mixture was placed on ice for 30min to stabilise bacterial membrane and increase the interaction between the calcium cation (in the buffer) and negatively charged DNA. Heat shock, at 42°C for 30sec, was performed to allow incorporation of the exogenous DNA into the cells (as heat shock changes the fluidity of the membrane). Following heat shock, the tubes were immediately placed on ice for 5minutes to return membrane stability to its steady state and reduce DNA transport. 950µl of SOC media (NEB) were added to the cell mixture and tubes incubated at 37° C for 60min with vigorously shaking (250rpm). Selection agar plates were warmed to 37° C in the bacteria incubator. The cell mixture was centrifuged and 13,000rpm for 2min and 500µl of supernatant removed. Pellet was ressuspended in the remaining supernatant (SOC medium) and spread onto selection plates. Plates were incubated at 37^0 C overnight.

2.2.7. Expansion and purification of plasmids

Vectors for expansion were transformed into NEB 5α competent *E.coli* (cat. C2987, NEB). Plates were incubated overnight and clones expanded in LB media containing appropriate selection (depending on vector used). The Qiaprep miniprep kit (cat. 27104, Qiagen) was used to purify plasmids from <5ml

bacterial cultures. The Promega Pureyield Maxiprep (cat. A2393, Promega) was used to purify plasmids from larger bacterial cultures. All plasmids were eluted in nuclease-free water.

2.2.8. Flow cytometry

Single cell suspensions were obtained either by collecting supernatant of suspension cultures or by enzymatically treating (TryplE) monolayer cultures. Pellets were ressuspended in blocking buffer containing 2% BSA in PBS and incubated for 20min at 4°C. The staining was carried out at 4°C in the dark with a mastermix of antibodies diluted in PBS at recommended concentrations (see table 2.2.2). The reaction was washed and collected with PBE flow buffer and fixed with 0.2% formyl saline. An unstained mix was used to visualise cells and set gates. Single stained mixes were used to perform compensation. Flow cytometry was performed on the Beckman Coulter Gallios Cytometer and analysed using Kaluza Analysis v.1.5a (Beckman Coulter). This protocol was obtained from (Moreau et al. 2016).

Antibody	Fluorochrome	Assay concentration	Catalogue Number	Manufacturer
CD41a	APC	1:10 dilution	559777	BD Biosciences
CD41a	FITC	1:10 dilution	555469	BD Biosciences
CD42b	PE	1:10 dilution	555473	BD Biosciences
CD235a	FITC	1:1000 dilution	559943	BD Biosciences
CD34	APC	1:10 dilution	345804	BD Biosciences
CD43	PE	1:10 dilution	553271	BD Biosciences
Tra-1-60	PE	1:100 dilution	12-8863-80	Thermo Fisher
SSEA4	Alexa fluor 488	1:100 dilution	53-8843-41	Thermo Fisher

Table 2.2.2. Flow cytometry antibodies used for characterisation of FoP differentiating cells and pluripotency.

2.2.9. Cell sorting

Cells were dissociated using TrypLE and either stained with antibodies (for MK sorting based on surface markers), or unstained (if transfected with plasmids containing a fluorescent marker). Cells were sorted on the BD FACSDiva 8.0.1 by the NIHR Cambridge BRC Cell Phenotyping Hub. Viable single cells were either collected bulk (MKs for processing) or plated in single wells of a 96 well plate with ROCK inhibitor for 24 hours (for KO generation experiments).

2.2.10. CRISPR/Cas9

2.2.10.1. Single guide RNA (sgRNA) design

CRISPR experiments were performed following (F. Ran et al. 2013)

sgRNA sequences were designed using Wellcome Trust Sanger Institute CRIPSR tool. This tool helps identify guide sequences that minimize identical genomic matches to reduce the risk of cleavage away from target sites (off-target effects). The sgRNAs consist of a 20 nucleotide sequence (protospacer) upstream of an NGG sequence (protospacer adjacent motif or PAM) at the genomic recognition site. The PAM sequences were not included in the sgRNAs. The identified sgRNAs were aligned to the human genome on BLAST (Basic Local Alignment Search Tool) and the sequences with lower possible off-target effects were selected. Reverse complement for each guide was calculated and BbsI overhangs designed to allow ligation into the BbsI restriction sites into Cas9 plasmids. The sgRNAs were purchased as lyophilised desalted oligonucleotides (Sigma-Aldrich) and cloned according to previously described protocol (F. A. Ran, Hsu, Wright, et al. 2013). The strategy to create deletions in the required locus relied on the delivery of two sgRNAs (one on each strand) and a Cas9nickase to create one nick at each targeted site. This method minimises off-target effects as it uses 2 sgRNAs on the target site. The vectors used were pSpCas9n(BB)-2A-PURO (PX462), pSpCas9n(BB)-2A-GFP(PX461 from Addgene) and pSpCas9n(BB)-2A-tomato (modified by Dr Annette Muller).Vector maps are shown in appendix section 6.1.1 and sgRNA sequences in table 2.2.3.

Locus targeted	sgRNA	sequence
BRD2	sgRNA.BRD2.KO.10	caccgTTAATAGTACCCATGTCCAT
	sgRNA.BRD2.KO.10.comp	aaacATGGACATGGGTACTATTAAc
	sgRNA.BRD2.KO.11	caccgACTTGAAAACAATTATTATT
	sgRNA.BRD2.KO.11.comp	aaacAATAATAATTGTTTTCAAGTc
	sgRNA.BRD2.KO.12	caccgAATGTAACAGTTGGTGAACA
	sgRNA.BRD2.KO.12.comp	aaacTGTTCACCAACTGTTACATTc
	sgRNA.BRD2.KO.13	caccgCAACTGTTACATTTACAACA
	sgRNA.BRD2.KO.13.comp	aaacTGTTGTAAATGTAACAGTTGc
BRD3	sgRNA.BRD3.KO.2	caccgAGTCGCCCCCGCGGGG
	sgRNA.BRD3.KO.2.comp	aaacCCCCGCGGGGGCGACTc
	sgRNA.BRD3.KO.3	caccgTGTGAACCCACCCCCCCGG
	sgRNA.BRD3.KO.3.comp	aaacCCGGGGGGGGTGGGTTCACAc

	sgRNA.BRD3.KO.8	caccgCCCCGCGGGGGCGACTGTCG
	sgRNA.BRD3.KO.8.comp	aaacCGACAGTCGCCCCCGCGGGGc
BRD4	sgRNA.BRD4.KO.1	caccgGATTTCTCAATCTCGTCCCA
	sgRNA.BRD4.KO.1.comp	aaacTGGGACGAGATTGAGAAATCc
	sgRNA.BRD4.KO.2	caccgTTCCCAAATGTCTACAACAC
	sgRNA.BRD4.KO.2.comp	aaacGTGTTGTAGACATTTGGGAAc
	sgRNA.BRD4.KO.8	caccgTGCCCCTTCTTTTTTGACTT
	sgRNA.BRD4.KO.8.comp	aaacAAGTCAAAAAAGAAGGGGCAc
	sgRNA.BRD4.KO.9	caccgCCCCGGGAGGGAGCAGAAGA
	sgRNA.BRD4.KO.9.comp	aaacTCTTCTGCTCCCTCCCGGGGc
	sgRNA.BRD4.KO.10	caccgGGGGGCGAGGACTTCATCGC
	sgRNA.BRD4.KO.10.comp	aaacGCGATGAAGTCCTCGCCCCCc
	sgRNA.BRD4.KO.11	caccgACCCTTCATTGCCACCCAGG
	sgRNA.BRD4.KO.11.comp	aaacCCTGGGTGGCAATGAAGGGTc
	sgRNA.BRD4.KO.12	caccgCACTACCCCAGCAGCCATCA
	sgRNA.BRD4.KO.12.comp	aaacTGATGGCTGCTGGGGTAGTGc
	sgRNA.BRD4.KO.13	caccgCAGGGCAGCGGCTCGGTTGC
	sgRNA.BRD4.KO.13.comp	aaacGCAACCGAGCCGCTGCCCTGc

Table 2.2.3 sgRNA oligos used for generation of BET KOs. SgRNAs (capital letters) were designed with overhangs (small letters) compatible with plasmid overhangs resulting from digestion with BbsI enzyme.

2.2.10.2. Plasmid preparation containing sgRNAs and Cas9

A published protocol for CRISPR/Cas9 genome editing was followed (F. A. Ran, Hsu, Wright, et al. 2013). In brief, sgRNAs were phosphorylated, annealed, diluted at 1:200 and ligated into the corresponding linearised plasmid (appendix 6.1.1). Plasmids were transformed into E.coli and expanded, as previously described (section 2.2.6). No inserts and no plasmid controls were used, as well as a PUC19 control. Expansion was carried out in LB medium and maxi preps performed using Pure Yield Promega system (#A2392). Insertion of sgRNAs was carried out by restriction digestion (see plasmid maps in appendix 6.1 for details on restriction enzymes used), followed by Sanger sequencing with U6 forward primer GGGCAGGAAGAGGGCCTAT.

2.2.10.3. Cloning into pGEM-T Easy

Cloning was required to identify all the alleles in each clone. This allows the identification of heterozygous and homozygous indels through Sanger sequencing. Cloning was performed into the pGEM-T Easy Vector System II (cat. A1380, Promega) following the manufacturer's instructions.

In brief, PCR amplicons were purified as described above, and A-tailed using the Phusion polymerase kit and dATP (cat. N8080241 and R0141 respectively, Thermo Fisher Scientific) to allow ligation. The amplicons were purified again and ligated into PGEMT-Easy (3:1 and 5:1 molar ratio) in ligation buffer according to the instructions manual. The plasmids were transformed into E.coli competent cells and plated on Fast-Media Amp XGal agar plates (cat. fas-am-x, Invivogen). Successful ligation of amplicons into the pGEM-T Easy vector interrupts the *LacZ* gene which alters the colour of the resulting *E.coli* colonies from blue to white, allowing selection for sequencing. Between five and ten colonies were picked, and plasmids were purified by miniprep and sent for Sanger sequencing using the T7F primer TAATACGACTCACTATAGGG.

2.2.10.4. Nucleofection of hiPSC lines and derivation of antibiotic resistant strains

In preparation for and up to 7 days prior to nucleofection, plates (6 well format) were coated with vitronectin. Proliferating iPSC cultures were pre-treated with ROCK inhibitor Y27632 (10uM) for 24h pre-nucleofection. Cultures were dislodged from the wells using 0.5mM EDTA in PBS (without Mg^{2+}/Ca^{2+}) to generate small clumps of cells. One million cells per condition were aliquoted into Eppendorf tubes and pelleted at 200g for 3min. Human stem cell nucleofection kit (Lonza) was used according to manufacturer instructions. Mastermixes, containing 100ul of solution I, II and 10ug (total) of the plasmids, were prepared before ressuspending the cell pellets in the respective conditions. Nucleofections were completed using program B-016 on nucleofector 2b device (Lonza). Immediately post nucleofection, cells were ressuspended in 500µl of pre-warmed DMEM/F12 culture media supplemented with ROCK inhibitor and seeded onto the iMEFs monolayer. At 24hr post nucleofection, the wells were replenished with iPSC culture media and, 48hr post transfection, the antibiotic selection was started and carried out for 2 days (puromycin at 1ug/ml). Individual surviving clones were manually isolated and expanded in iPSC medium.

2.2.10.5. T7 endonuclease assay

This assay is designed to detect heteroduplex DNA that result from annealing DNA strands modified after CRISPR/Cas9 mediated cut, and this way, estimate success of sgRNA targeting. HEK293T cells were transfected with sgRNAs and Cas9 and cultured for 2 days before performing gDNA extraction. A PCR was performed with primers designed for the CRISPR/Cas9 targeted region. This step was followed

by a hybridisation step where 200ng of PCR products were diluted to 17 µl of water and 2 µl of NEB buffer2 and incubated at the following conditions (95 ^{0}C-5 min, 95-85°C at -2°C/s for 1 min, 85-25°C at -0.1°C/s for 1 min, 4°C ∞). This step was followed by a digestion with T7 endonuclease, where 10 µl of the previous reaction was digested with 0.5 µl of T7 endonuclease (NEB M0302) for 15 min at 37 ^{0}C. Mismatched nucleotides were digested in that reaction and resulting products were visualised in a 1% agarose gel.

2.2.11. Lentiviral infection

HEK293T cells were used to produce lentivirus stocks. The cultures were seeded in 10cm dishes at 4x10^{6}cells per plate. The infection packaging system, formed by 2 plasmids, was combined with 20µg of the vector of interest and 5.6µg of PEI in DMEM basal media and incubated at room temperature for 20min before being added to the HEK293T culture media. 24hr post infection, the media was removed and plates replenished with DMEM supplemented with 10% foetal bovine serum (FBS). That media was harvested 24hr later and filtered through a 45µm syringe filter before adding polybrene (8µg/ml). The filtered mixture containing virus was used to infect proliferating hiPSC and this infection step was repeated later on the same day. Infected hiPSC were fed with DMEM/F12 supplemented with LAA (300ug/ml), FGF2 (5ug/ml) and Activin-A (10ug/ml) for 2 days before starting antibiotic selection.

2.2.12. Romanowsky staining

25x10^{5} FoP-MKs were plated on a cytospin cassettes using a Shandon Cytospin 4 machine and stained with a Rapid Romanowsky stain (BioRad HS705). The stain process consists in submerging the slides into each solution (fixative, azure and eosin) for 40 sec. Slides were dried overnight and coverslips were applied.

2.2.13. Western Blotting

Cell pellets were washed with PBS (without Mg^{2+}/Ca^{2+}) before being snap-frozen and stored at -80˚C. Pellets were lysed in NP-40 lysis buffer and supernatant collected by centrifugation at 13,000rpm for 15min at 4°C. The extracted protein concentration was determined by Bradford assay and whole-cell lysates were ran on a precast 4%-12% Bis-Tris polyacrylamide gel and transferred to PVDF membrane. Blocking was achieved using 5% milk in TBS-T (200nM Tris (pH 7.6), 1370mM NaCl, 1% Tween 20). Antibodies against protein of interest were used. Blots were imaged on the SRX-101A processor.

antibody	*dilution*	*Antibody details*
rabbit anti-human BRD3	1:1000	Bethyl # A302-368A
Rabbit anti-human BRD2	1:5000	Bethyl #A700-008
mouse anti-human β-actin	1:10,000	AbCam # Ab6276
mouse anti-rabbit HRP	1:10,000	AbCam # ab99702
rabbit anti-mouse HRP	1:10,000	AbCam # ab6728

Table 2.2.5 **Antibodies used in western blots for confirmation of BET KOs**.

2.2.14. Crystal violet staining assay

Cultures were washed with PBS and wells replenished with 2.5% glutaraldehyde for fixation at room temperature for 15 minutes. This method crosslinks all proteins and preserves morphological structure. Cell monolayers were washed twice with PBS and stained with 0.5% crystal violet solution for 10 minutes. Plates were immersed into a beaker to wash the stain and drained upside down. To solubilise the stain, the wells were washed with 1% SDS. Absorbance was read at 450nm.

2.2.15. ATAC-seq

The ATAC-seq protocol followed has been obtained from (Buenrostro et al. 2015).

Open chromatin ATAC-seq libraries were generated from freshly prepared cells using a previously published protocol (Buenrostro et al. 2013). The cell samples were spun and washed with cold PBS. Lysis was performed with cold lysis buffer (10 mM Tris-HCl, pH 7.4, 10 mM NaCl, 3 mM $MgCl_2$ and 0.1% IGEPAL CA-630) for 15min. Pellets were spun, before digestion (25 µL 2× TD buffer (20 mM Tris-HCl, pH 8.00, 10 mM Magnesium Chloride), 2.5 µL transposase and 22.5 µL nuclease-free water) at 37 ^{0}C for 30 min in the water bath. The samples were then purified using Zymo DNA purification kit before PCR to amplify and tag the fragments with Illumina-compatible adapters (table 2.2.6). PCR reaction (25 µL of template, 12.5 µL water, 10 µL Phusion buffer, 1 µL dNTP, 0.5 µL primer #1, 0.5 µL primer #2, 0.5 µL Phusion). PCR conditions were as follows: 72 °C for 5 min; 98 °C for 30 s; and thermocycling at 98 °C for 10 s, 63 °C for 30 s and 72 °C for 1 min. For iPSC and MKs, 100K cells were used with 10 amplification cycles for PCR. Libraries cleaned up with Zymo DNA concentrator kit were quantified using a qPCR Library Quantification Kit (Kapa Biosystems), pooled and sequenced with a

50bp single-end protocol on an Illumina Hiseq 2500 (Cancer Research UK Cambridge Institute, Cambridge, UK).

ID	Adaptor Sequence
Ad1	n/a
Ad2.1	TAAGGCGA
Ad2.2	CGTACTAG
Ad2.3	AGGCAGAA
Ad2.4	TCCTGAGC
Ad2.5	GGACTCCT
Ad2.6	TAGGCATG
Ad2.7	CTCTCTAC
Ad2.8	CAGAGAGG
Ad2.9	GCTACGCT
Ad2.10	CGAGGCTG
Ad2.11	AAGAGGCA

ID	Adaptor Sequence
Ad2.13	GTCGTGAT
Ad2.14	ACCACTGT
Ad2.15	TGGATCTG
Ad2.16	CCGTTTGT
Ad2.17	TGCTGGGT
Ad2.18	GAGGGGTT
Ad2.19	AGGTTGGG
Ad2.20	GTGTGGTG
Ad2.21	TGGGTTTC
Ad2.22	TGGTCACA
Ad2.23	TTGACCCT
Ad2.24	CCACTCCT

Table 2.2.6. List of adapters used to tag ATAC-seq samples. Adapter #1 was used in all the samples with adapter #2 tagging individual samples.

2.2.16. ChIP-seq

ChIP-seq libraries were prepared using the BLUEPRINT consortium protocol.

Samples for chromatin immunoprecipitation were fixed with 1% w/v formaldehyde for 10 minut esand quenched using 125mM Glycine before washing with PBS. Cells were centrifuged and lysed in ChIP lysis buffer (50 mM Hepes, pH 7.9, 140 mM NaCl, 1 mM EDTA, pH 8.0, 10% $^{v}/_{v}$ Glycerol, 0.5% $^{v}/_{v}$ NP-40, 0.25% $^{v}/_{v}$ Triton X-100 and protease inhibitors in water). Lysates were washed with ChIP washing buffer (10 mM Tris-HCl, pH 8.0, 200 mM NaCl, 1 mM EDTA, pH 8.0, 0.5 mM EGTA, pH 8.0 in water), before resuspending in shearing buffer 0.1% $^{w}/_{v}$ SDS, 1mM EDTA, 10mM Tris-HCl, pH 8.0 and additional protease inhibitors in water. Lysates were sonicated using a Bioruptor (Diagenode), final SDS concentration of 0.1% w/v for 9 cycles of 30 seconds 'on' and 30 seconds 'off'. Samples were immunoprecipitated in the IP-Star (Diagenode), using the following antibody H3K27ac (Diagenode C15410196). Chromatin was eluted in elution buffer (10mM Tris-HCl, pH 8, 0.3M NaCl, 5mM EDTA, 0.5%SDS, and protease inhibitors) and reverse crosslinked (65^{0} C/4hr), treated with RNase and proteinase K (65^{0} C/30min). Libraries were prepared using the Diagenode MicroPlex Library preparation kit (C05010014), according to manufacturer's instructions. Library quality was evaluated using Bioanalyser and quantified using qPCR library quantification kit (KAPA Biosystems), pooled and sequenced with 50bp single-end protocol on Illumina HiSeq 2500.

2.2.17. RNA-seq

RNA-seq libraries were prepared using the BLUEPRINT consortium protocol.

Cells were cultured as described in previous sections, washed with D-PBS before pelleting by centrifugation. Cell pellets ressuspended in 500µl Trizol reagent (cat. 15596026, Thermo Fisher Scientific) in a fume hood. Samples were kept at -80^{o}C until further processing. RNA was manipulated in a fume hood, limiting environmental nuclease contamination with RNAaseZap (cat. AM9780, Thermo Fisher Scientific) by either myself or Ms Frances Burden, University of Cambridge. RNA was extracted from TRIzol preparations by phase-separation and precipitation. Libraries were synthesized from RNA using the KAPA Stranded RNA-Seq Kit with Riboerase (cat. 07962304001, Roche), using adapters included in the kit, and Agencourt AMPure XP beads (cat. A63880, Beckman Coulter) for purification. Libraries were quantified by RTqPCR using the KAPA Library Quantification Kit (cat. 07960140001, Roche) and 1:6000 final dilution of sample. Sequencing was performed by the Welcome Trust Sanger Institute on the HiSeq2500 using 150bp read length paired-end sequencing.

A001	ATCACG
A002	CGATGT
A003	TTAGGC
A004	TGACCA
A005	ACAGTG
A006	GCCAAT
A007	CAGATC
A008	ACTTGA

Table 2.2.7 Adapters used to prepare RNA-seq libraries.

2.3. Bioinformatics analysis

The bioinformatics analysis described in this section were performed by Dr. Denis Seyres, University of Cambridge.

2.3.1 ATAC-seq and ChIP-seq analysis

Sequence quality control was performed With FastQC from raw fastq files. FastQC runs different modules including:

- Per base sequence quality, shows an overview of the range of quality values across all bases at each position of the FastQ file.
- Per sequence quality scores, allows to identify subsets of sequences with universally low quality values.
- Per base sequence content, plots the proportion of each base position in a file for which one of the 4 DNA bases has been called.
- Per sequence GC content, measures the GC content across the whole length of each sequence, and compares with a modelled normal distribution of GC content.
- Per base N content, plots the percentage of the base calls at each position in which an N has been called (sequencer unable to make a base call with sufficient confidence).
- Sequence length distribution, generates a graphic distribution of fragment sizes in the file.
- Sequence duplication level, calculates the duplication of each sequence.
- Over-represented sequences and adapter contents, lists all sequences that make up more than 0.1% of the total. It also shows a cumulative percentage count of the library proportion with adapter sequences at each position.

Following QC, trimming was processed using Trim Galore to remove Illumina adapters and low quality bases. After trimming, reads under 36 bp length were discarded. Good quality reads were aligned to Human genome (hg38) with Burrows-Wheeler Aligner (recommended for read length shorter than 70bp) with default parameters. Picard MarkDuplicates was used to remove duplicated reads. Duplicated reads, low mapping quality (mapping quality score, q<15) and multi-mapped reads were discarded using samtools. Read enriched regions (peaks) were called using MACS2 (Y. Zhang et al. 2008) for ChIP H3K27ac and FSEQ [http://fureylab.web.unc.edu/software/fseq/] for ATAC samples. Input controls were down sized to ChIP library size prior to MACS2 analysis in matched cell types. No input control was used for the ATAC peak calling as FSEQ is designed to use read density variation in mapped reads to find biologically meaningful sites. A 5% false discovery rate (FDR) cut-off was selected for filtering low confident peaks with MACS2 and a threshold of 6 was applied for FSEQ.

Visualisation and analysis

Bias in read distribution across the genome was analysed with deepTools plotFingerPrint tool. This tool counts the number of reads in each bin of the genome, rank them from low to high count and plot this rank against the cumulative sum of reads. Ideally, sample curves elbow occurs at high x

values, good coverage is shown by low x intercept value and great enrichment by a large area between sample and input curves. Input usually follows the diagonal.

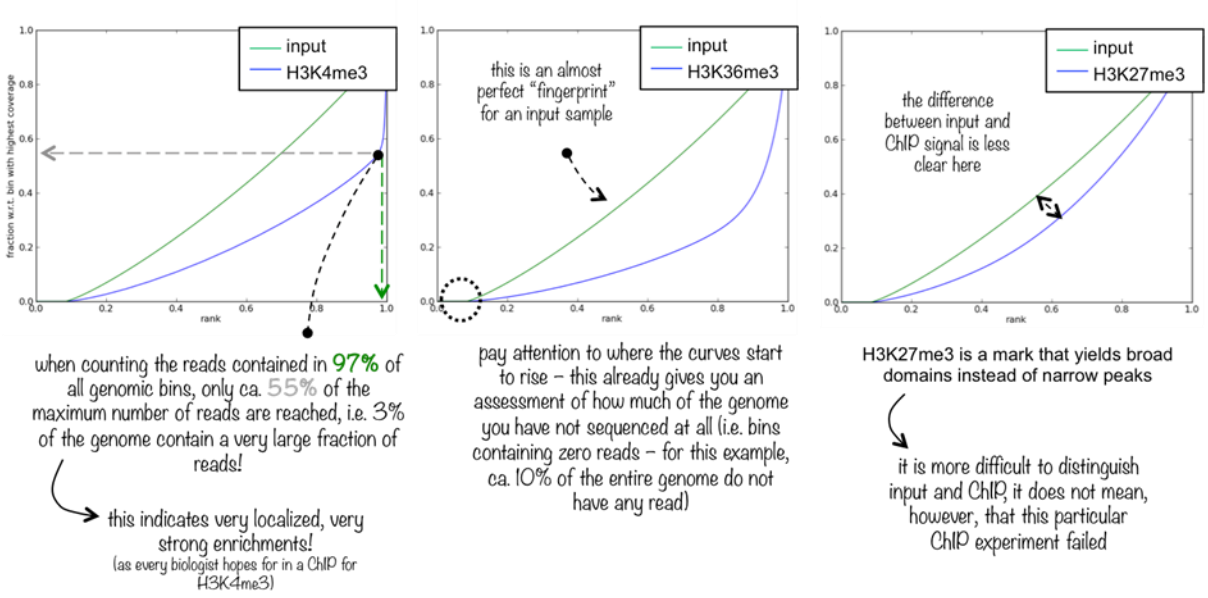

Figure 2.2.1. PlotFingerPrint interpretation for quality analysis of ChIP and ATAC data sets.

Differential analysis was performed by comparing WT and KO in both cell types. Sequencing batches were included as a potential batch effect. We performed differential analysis with two approaches: a peak based method and a binned based method. The peak-based approach, DiffBind (Stark and Brown 2018), starts to build a master set of peaks by making the union of overlapping peaks (at least 1bp) called initially by MACS2 or FSEQ peak caller from all samples. The idea is to assign a read uniquely to a peak and avoid confusion when a read overlap two peaks. We then used the wrapped method DESeq2 to perform differential analysis.

We also tested for differential opened regions or differential acetylation level with bin-based approach, csaw R package (Lun and Smyth 2016). We summarized read counts for each windows of genome. Reads are assigned to each window based on the 5' end without any directional extension. Binned counts were normalised for trended biases with a Loess normalisation. We filtered out low confident region by global enrichment. Csaw computes a threshold based on the fold change over the level of non-specific enrichment (a fold change threshold of 3 was used here). The degree of background enrichment is estimated by counting reads into large bins across the genome (we set 2kb). Binning is necessary here to increase the size of the counts when examining low-density background regions. This ensures that precision is maintained when estimating the

background abundance. Using EdgeR package, a generalized linear mode (GLM) was fitted to the normalized counts for each window using the specified design, dispersions were estimated and p-values are computed using the quasi-likelihood F-test. Putative differentially opened/acetylated bins were then merged to represent regions, a combined p-value was computed and false discovery rate was computed using combined p-values.

2.3.2. Regulatory element detection using patterns of peaks

Open chromatin peaks are called using fseq (Boyle et al. 2008). Additionally, an open chromatin coverage track is generated, which is normalised by dividing by the mean coverage genome-wide, and smoothed by binning consecutive segments of 40bp. Peaks are extended upstream and downstream symmetrically until their length is at least 3.2kb and overlapping segments are subsequently merged. These merged segments are considered separately.

The covariance between the open chromatin track and the H3K27ac track is computed in an 800bp sliding window and subsequently smoothed by replacing each covariance value with the mean of the values in the surrounding 800bp. Local minima of the smoothed covariance are obtained as the positions for which the value is less than the values in the surrounding 160bp. Any local minima with a smoothed covariance less than -1 are recorded.

For each local minimum, the stretch nearest to it and any other stretches within 100bp of it, for which locally normalised open chromatin coverage exceeds the locally normalised H3K27ac coverage are recorded and expanded to 400bp, where locally normalised coverage at a position is given by the coverage divided by the mean coverage in the surrounding 800bp region. These stretches are merged and recorded as the locations of regulatory elements.

2.3.3. RNA-seq data analysis

As for ATAC and ChIP-seq experiments, RNA-seq samples were first checked for sequence quality with FastQC. Then raw data were trimmed to remove Illumina sequencing adapters. Trimmed reads were pseudo-aligned to Ensembl human transcriptome (GRCh38.80) using Kallisto (Bray et al. 2016) with 100 rounds bootstrap in order get high accuracy in transcript abundance estimates. Transcripts abundance were summarized to gene level with tximport R Package (Soneson et al. 2015).

Transcript Per Million (TPM) values (log(TPM+1)) were used to assess sample to sample correlations. R package pheatmap was use to draw heatmap of correlations. Principal component analysis (PCA) analysis was carried out and first two components were plotted.

Prior to differential analysis, genes with 0 count and no variance were filtered out from analysis. Sequencing batch was included into the design analysis to integrate effect of different library preparations. DESeq2 R package (Love et al. 2014) was then used to perform differential analysis. Both Wald and LRT tests were carried out, a FDR threshold of 5% was applied and the intersection of differentially expressed genes (DEG) identified by each test was retained as list of DEG for each comparison. Lists were split according to fold change directions and EnrichR web-server (E. Y. Chen et al. 2013b) was used to perform gene annotation enrichment.

Chapter 3

Results

3.1 Generation of an iPSC BRD3 KO model

3.1.1 Introduction

Platelets activity in thrombus formation is a determinant factor in myocardial infarction (Chu et al. 2010; Klovaite et al. 2011b). This fact highlights the importance of studying the mechanisms that regulate platelet differentiation. As mentioned in chapter 1, Astle *et al.* have performed a large-scale GWAS on platelet traits, and identified BRD3 as a regulator of platelet volume (MPV) and volume distribution width (PDW) (Astle et al. 2016). GWAS are critical for the identification of novel genes in disease, but validation studies are required to understand the mechanistic pathways involved in the regulatory processes. Functional studies have revealed that BRD3 plays a role in formation of thrombocytes in zebrafish (Bielczyk-Maczyńska et al. 2014a), although its regulatory molecular mechanisms in haematopoiesis are largely unknown.

The study of the biological role of proteins often relies on gene inactivation in model organisms. In particular, mouse knockout models became a common tool to study the role of proteins from a whole organism perspective (Vandamme 2014). In collaboration with the Wellcome Trust Sanger Institute, I tried to generate a BRD3 KO mouse model using Clustered Regularly Interspaced Short Palindromic Repeats (CRISPR/Cas9) technology (W. Qin et al. 2016), but BRD3 KO mice were not viable. Several chimeras (animals originating from the injection of KO ES cells in the WT Embryo) (Eckardt, McLaughlin, and Willenbring 2011) were obtained, however no offspring carried the BRD3 KO alleles, indicating that there was no germline contribution from these ES cells. This is in agreement with reported attempts to generate other BET KO mouse models, where embryonic lethality was observed due to defects associated with low proliferation rates (Shang et al. 2009). The embryonic lethality of BRD3 KO mouse model motivated the search for an alternative BRD3 KO model. Upon evaluation of the models available for studying megakaryopoiesis, I have designed and generated an induced pluripotent stem cell (iPSC) model carrying a BRD3 KO mutation.

iPSCs are broadly used in research due to stem cell-like characteristics such as self-renewal and differentiation capabilities (section 1.2.2.3). Self-renewal can be measured by proliferation assays, and the potential for differentiation is often characterised by high pluripotency levels and ability to form somatic-like cells. Alterations in these characteristics should be monitored when genetically

manipulating cells. This is particularly important when studying factors associated with cell cycle and regulatory function, such as BET proteins.

Our understanding of regulatory mechanisms in gene transcription has benefited from advances in genetic engineering techniques. In recent years CRISPR/Cas9 became a ubiquitous method to genetically manipulate cell lines with applications ranging from basic biology research to clinical applications, as reviewed in (Z. Zhang et al. 2017). CRISPR/Cas9 system owes its success to its low cost, precision and simplicity. Although, this system presents disadvantages that need to be considered when selecting a technology to create genetic mutations. 1) The requirement for PAM sequences in the target sequence. 2) The possibility of off-targets occurrence, due to sequence homology with other genomic regions (Zhang et al. 2015). The current alternatives to CRISPR for generation of KO cell lines are Zinc Finger Nucleases (ZFNs) and TALENs, but both are less efficient and more laborious (Gaj et al. 2013). Altogether, these techniques present valuable options to genetically manipulate disease models. CRISPR/Cas9 was the system I used to generate BRD3 KOs cell lines.

In order to study the role of BRD3 in regulation of platelets formation, and due to the lack of reliable models for generation of *in vitro* platelets, the experiments in my thesis were conducted using a megakaryopoiesis forward programming (FoP) protocol. This protocol has already been used in the laboratory and it yields a high number of MK cells in a relatively short period of time (20 days). The choice of this system was further reinforced by the availability of in-house expertise in FoP (Dr Cedric Ghevaert's lab). However, one of the drawbacks of this system is that the generated MKs are low ploidy (2N/4N), indicating low maturation when compared with bone marrow MKs. In fact, the polyploidisation levels, and high proliferative capability are phenotypic characteristics of fetal MKs (De Alarcon et al. 1996; Sola-Visner et al. 2007; Mattia et al. 2002). Despite the low ploidy level, the protocol has been reported to produce pro-platelet, but this is yet an unreliable, cell line-dependent process, hence why I studied BRD3 in MK formation only. Additionally, the protocol rely on the use of viruses containing transcription factors (TFs), including GATA-1. This could introduce artefactual results in my experiments as this TF is a direct BRD3 interactor. The alternative protocols for the generation of MKs have been described in more detail in section 1.2.2.4, but some of the disadvantages associated with these protocols include expensive complex cytokine cocktails, low MK yield and time consuming procedures for direct differentiation of cells. In the quest to avoid overexpression of GATA-1, the protocol developed by *Feng et al*. was tested (Q. Feng et al. 2014), but with no success in generating MKs, and therefore, this second protocol was abandoned.

MKs successful forward programming was evaluated by the expression of characteristic cell surface markers. In my experiments I monitored the expression of CD235a, CD41a and CD42b as these correspond to surface proteins found in MKs at different stages of differentiation. Anti-CD235a antibodies recognise glycophorin A, a sialoglycoprotein present in the cell membrane of erythroid-MK precursors and erythroid mature cells (Dahr et al. 1987; Tomita et al. 1978). CD41a antibodies detect integrin-αIIb surface membrane protein, found on megakaryocytes and platelets (Phillips et al. 1988). This protein is part of the glycoprotein IIb-IIIa receptor complex, which is activated upon triggering of the hemostatic cascade and binds to fibrinogen, vWF and vitronectin (Shattil et al. 1998). The co-expression of CD41a and CD235a has previously been demonstrated on MK progenitor cells differentiated from human ESCs (Moreau et al. 2016). It has also been shown that $CD235a^{+}/CD41a^{+}$ progenitor cells are able to give rise to both erythroid and MK lineages (Klimchenko et al. 2009). Lastly, CD42b is a glycoprotein Ib (GPIb) which is a component of the GPIb-V-IX complex, expressed at late stage of MK differentiation (Du et al. 1987; Nishikii et al. 2015). The GPIb-V-IX complex is present on the surface of platelets and it functions as the receptor for vWF (A. K. Rao and Songdej 2017). In FoP of MKs, CD42b represents the last stage of MK maturity achieved with this protocol (Moreau et al. 2016).

In order to investigate whether BRD3 is essential in megakaryopoiesis, I initiated my studies with the generation and characterisation of two BRD3 KO iPSC lines, containing deletions in the BRD3 open reading frame. The transcripts expressed in MKs were identified and the gene targeted using CRISPR/Cas9. As BET proteins have been previously associated with cell cycle progression, I characterised BRD3 KO cells and compared with WT cells, based on proliferation and pluripotency assays. Ultimately, my aim for this section was to determine whether BRD3 was required for the differentiation of IPSC into MK

3.1.2 Results

3.1.2.1 Generation of BRD3 KO using CRISPR Cas9 nickase

In order to generate BRD3 KO cell lines, I used the CRISPR/Cas9 technology with the Cas9 nickase (Cas9n) variant. The Cas9n was directed to the target site by two sgRNAs complementary to opposite DNA strands. The double targeting strategy has a higher specificity than single sgRNA targeting, and it mitigates off-target activity up to 1,500 fold in cell lines (Mali et al. 2013; F. A. Ran, Hsu, Lin, et al. 2013). This strategy relies on non-homologous end joining (NHEJ) to create mutations (insertions or

deletions) in the gene sequence. Gene knockout strategies often target the downstream region of the ATG (first translated codon) in order to completely disrupt protein synthesis or to create out-of-frame sequences. Otherwise, in frame deletions can produce a truncated protein with partial or complete functional activity.

3.1.2.1.2 Target sequence identification

I initiated this experiment with the identification of the CRISPR/Cas9 target site and the design of the sgRNAs at the BRD3 locus. The BRD3 sequence, and transcript details, were analysed using Ensembl genome browser. The transcripts present in MK cells were identified in the Blueprint database (https://blueprint.haem.cam.ac.uk/bloodatlas/). Conveniently, BRD3 has four protein-coding transcripts with the same start coding site, located on the second exon of the gene locus. To maximise the chances of creating an out of frame mutation, the sgRNAs were designed to target a 200 bp region directly downstream of the ATG site (figure 3.1.1). Potential sgRNA sequences were designed using Wellcome Trust Sanger Institute CRISPR online tool (https://www.sanger.ac.uk/htgt/wge/) and only the 25% best matches (3 sgRNAs) were considered. Each sgRNA must be upstream of a Protospacer Adjacent Motif (PAM) sequence (NGG), although the PAM sequence was not included in the sgRNA.

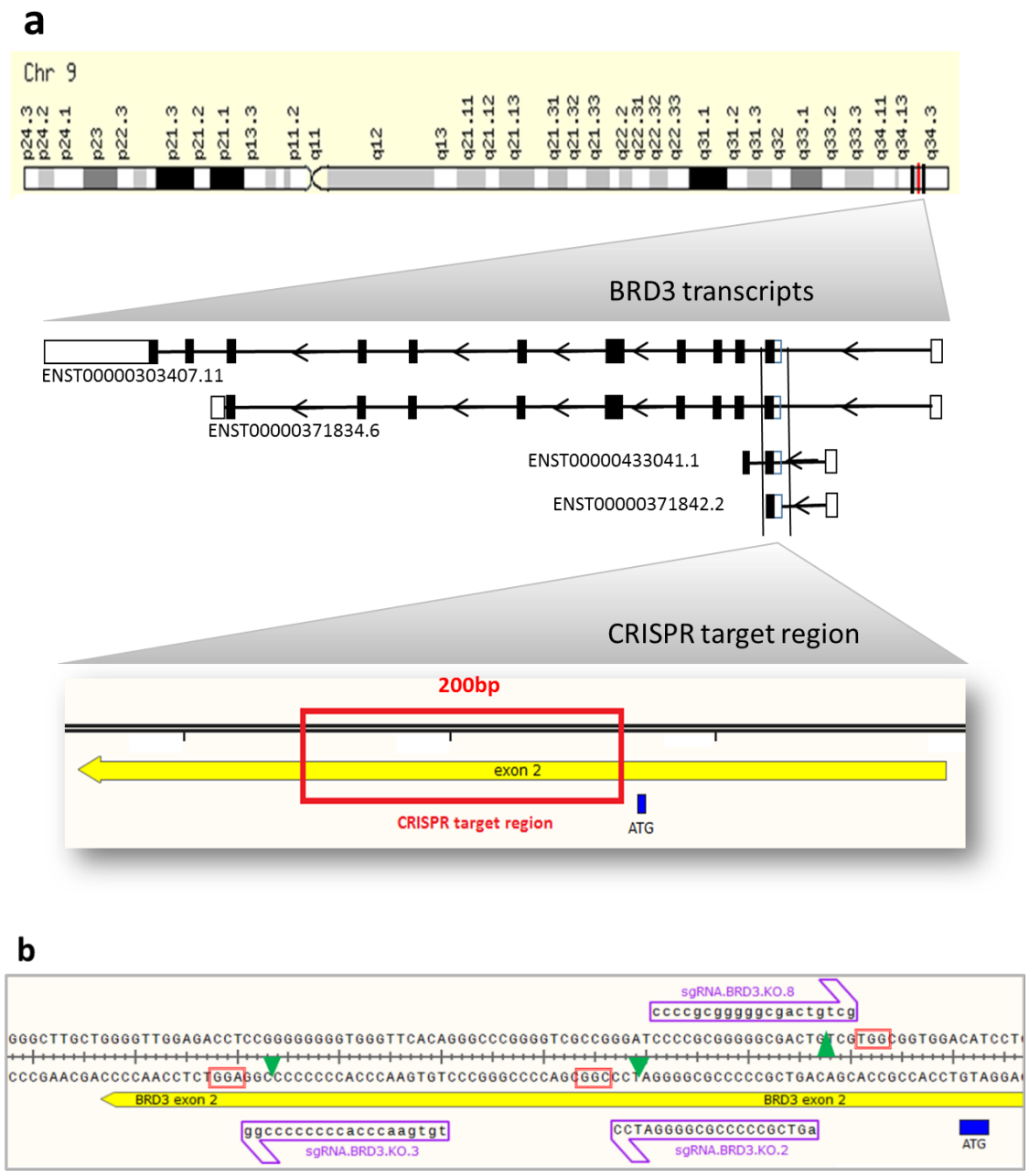

Figure 3.1.1 BRD3 targeting strategy and sgRNA design for generation of BRD3 knockout using double Cas9 nickase. (a) Schematics of BRD3 target region. BRD3 coding sequence is located in the long arm of chromosome 9. The starting site (ATG) for all BRD3 protein-coding transcripts is found on exon 2. The target site was designed to include 200 bp downstream of the ATG codon. This strategy allows complete ablation of the protein by either disrupting the beginning of protein synthesis or creating a functionally inactive out-of-frame protein. **(b)** sgRNAs were designed using WTSI CRISPR online tool with the target sequence as input. Only the 25% best hits were selected (3 sgRNAs represented). The sgRNA sequences are required to be directly upstream of a protospacer adjacent motif (PAM) sequence (red squares). PAM sequences are recognised by Cas9 enzymes, but are not included in the sgRNAs sequences. Cas9 enzymes were expected to target 3 nucleotides upstream of the PAM (green arrows).

3.1.2.1.2 sgRNA targeting test

sgRNAs represented in figure 3.1.1 were cloned (section 2.2.10) into vector pSpCas9(BB)-2A-PURO (appendix 6.1.1.1). The validation of sgRNAs insertion was performed by restriction digestion, followed by Sanger sequencing (using U6 primer for sequencing) to ensure in-frame positioning of the sgRNAs inserts (appendix 6.2.1). Each validated plasmid was then expanded (section 2.2.10.2).

T7 endonuclease assay was performed to verify sgRNAs targeting. gRNA-containing plasmids (sgRNA2, sgRNA 3, sgRNA8) were transfected into HEK293T cells along with Cas9(WT). HEK293T cells were chosen for sgRNA testing due to their high transfection efficiency at population level, leading to lower variability in the population, higher signal without the requirement for sub-cloning and expansion, resulting in a significantly decrease in test timescale. However, I am aware that using HEK293T, instead of the target iPSC, could become redundant if the target sequence was different in both lines. If the iPSC transfections had proven unsuccessful, I would have sequenced the target region in both cell lines to validate this hypothesis. After transfection, the HEK293T genomic DNA was extracted and a PCR of the target region was performed (figure 3.1.2.a). A hybridization step was carried out where PCR products were randomly hybridised to form duplex DNA fragments containing nucleotide mismatches (resulting from sgRNA successful targeting). The assay was completed by digestion of the hybridised PCR products with T7 endonuclease, which recognises and digests DNA mismatches (section 2.2.10.5). The T7 endonuclease assay is expected to reveal smaller product bands, indicating the digestion by T7 endonuclease at mismatched nucleotides near the disrupted region (figure 3.1.2).

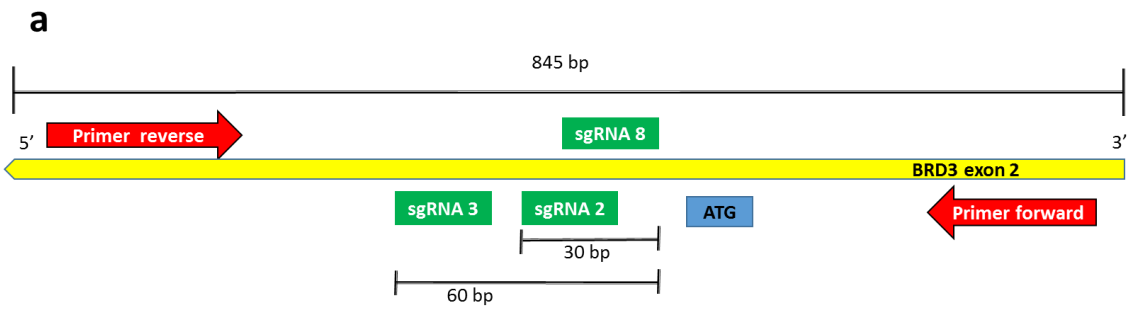

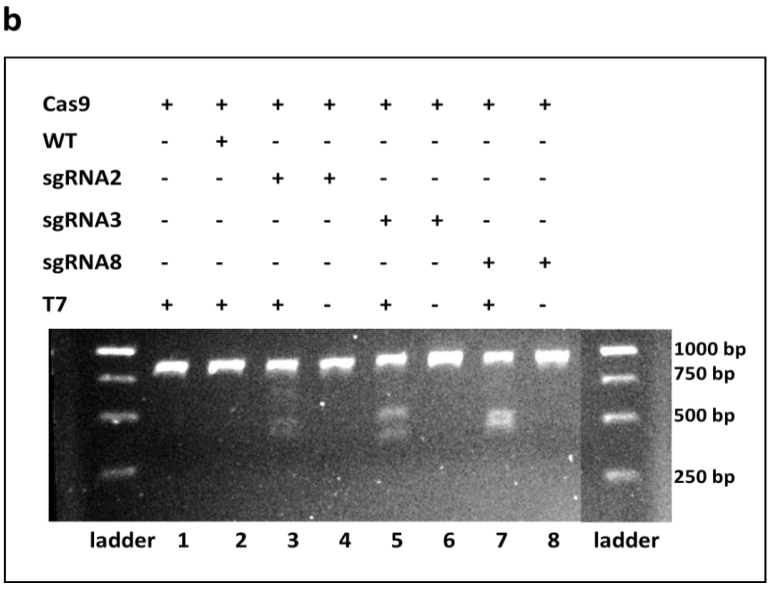

Figure 3.1.2 PCR for confirmation of sgRNA targeting efficiency at BRD3 locus. (a) Schematics of PCR to confirm sgRNAs targeting. Three sgRNAs (2, 3 and 8, green boxes) located downstream of the ATG site (blue) were tested in the assay. PCR primers (red) were designed outside of the targeted region (845 bp). **(b)** Gel showing T7 endonuclease assay results. HEK293T cells were transfected with sgRNAs 2, 3 and 8 targeting BRD3 locus and Cas9. gDNA extracted and PCR performed, before T7 endonudease assay was complete. Results for individual sgRNAs transfections are shown in lanes 3 (sgRNA2), 5 (sgRNA3) and 7 (sgRNA8). All of these sgRNAs successfully created indels at the BRD3 locus. WT and Cas9 only, as well as non-T7 digested transfected conditions were loaded on a gel as controls.

Figure 3.1.2.b shows that sgRNAs 2, 3 and 8 successfully create mismatches in the targeted region. Both 2+8 and 3+8 sgRNA pairs could have been selected to generate BRD3 KO in iPSC lines. Although sgRNA pair 3+8 was selected, due to the spacing between the two sgRNAs.

3.1.2.1.3 Generation of BRD3 KO iPSC

After testing the sgRNAs targeting efficiency, I generated BRD3 KO in two distinct iPSC lines, S4-SF5 and A1ATD1-c. These KOs were generated at different stages, and the targeting strategy was similar, using the same sgRNAs, yet different plasmids and selection method were used. The sgRNAs targeting test was not repeated as the homology between sgRNAs and target region remaining unaltered.

*S4-SF5 cell line- BRD3 KO generated using vector pSpCas9n(BB)-2A-**PURO***

To target BRD3 gene in iPSC S4-SF5, the sgRNAs were cloned into vector *pSpCas9 (BB)-2A-**PURO*** containing a puromycin gene which confers puromycin resistance to successful nucleofected cells. This vector also contains a Cas9n cassette. This allows the expression of the Cas9n enzyme with the ability to create single strand cuts (nicks) in the targeted DNA.

S4-SF5 cells were nucleofected (section 2.2.10.4) with vectors *pSpCas9 (BB)-2A-PURO* containing sgRNA3 and sgRNA8. The experiment included two control conditions: cells nucleofected without plasmids to monitor the effect of nucleofection on cells; and non-nucleofected cells to monitor cell death after puromycin treatment. Puromycin treatment was initiated 2 days post-nucleofection. The treatment lasted until control cells (not nucleofected) were no longer observed (2 days). Twelve puromycin-resistant colonies were observed (from $1x10^6$ nucleofected cells). These were fed 6 times per week and each individual colony passaged separately when large enough to handle and establish robust clonal lines. This method eventually required culture sub-cloning into single cells to ensure culture homogeneity.

*A1ATD1-c cell line- BRD3 KO generated using vector pSpCas9n(BB)-2A-**GFP** and pSpCas9n(BB)-2A-**tomato***

To target BRD3 gene in iPSC A1ATD1-c, sgRNAs 3 and 8 were cloned into vectors pSpCas9n(BB)-2A-**GFP** and pSpCas9n(BB)-2A-**tomato**, respectively. The plasmid containing tomato fluorescent marker was derived from the plasmid containing GFP by removing the GFP gene and replacing it with tomato gene (work done by Dr Annette Muller, Dr Cedric Ghevaert's lab, University of Cambridge). The plasmids also contain the ORF for Cas9 nickase. Plasmids were nucleofected into A1ATD1-c cells. This strategy allowed the sorting of cells containing both sgRNAs based on double labelling ($GFP^+/tomato^+$). The sorted clones were plated individually onto three 96 well plates pre-coated with vitronectin (288 sorted single cells); fed 6 times per week, and passaged when large enough to handle. One hundred and nine (109) sorted cells formed colonies which were expanded. Only four clones were genotyped as a KO was promptly found. This method presents an improvement from the strategy previously used as it select cells successfully nucleofected based on double fluorescence labelling, increasing the probability of success; and it did not require culture subcloning because the clones formed were generated from sorted single cells.

3.1.2.2 Confirmation of BRD3 KO clones

The individual clones of both S4-SF5 and A1ATD1-c nucleofected cells were expanded, and genomic DNA extracted for genotyping by Sanger sequencing using primers BRD3.E2.REV and FWR (table 2.2.1). For clones containing deletions, PCR products were cloned into pGEM-T vector and sequenced to confirm the presence of disrupting mutations on both alleles (section 2.2.10.3). If the tested clone was heterozygous, the PCRs sequenced would present 2 different sequences, and PCRs from a homozygous clone would only present one sequence. Primer T7F, with homology to promoter T7 present in pGEM-

T was used to perform Sanger sequencing. Two successful BRD3 KO clones (S4-SF5 and A1ATD1-c) were confirmed as shown in figure 3.1.3.a.

Protein knockout was confirmed by western blotting in S4-SF5 BRD3 KO and A1ATD1-c BRD3 KO. Western blot membrane was stained with BRD3 antibody and β-actin as a loading control (figure 3.1.3.b).

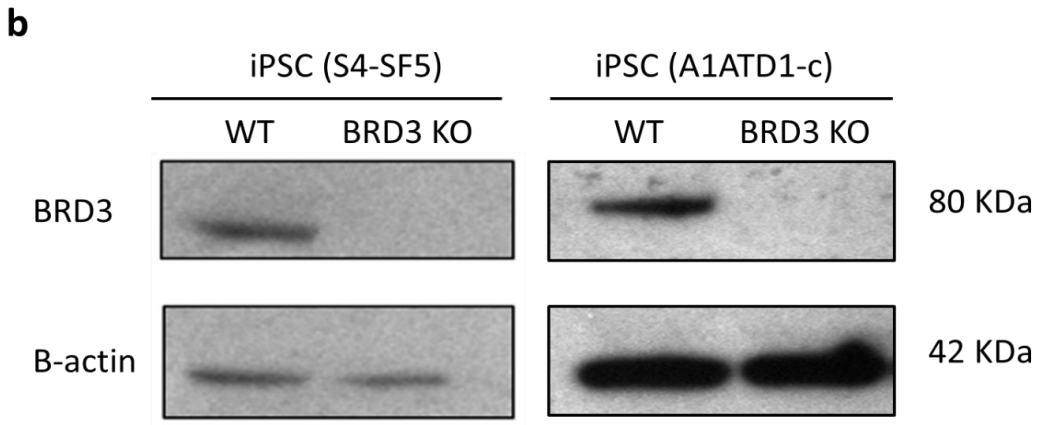

c

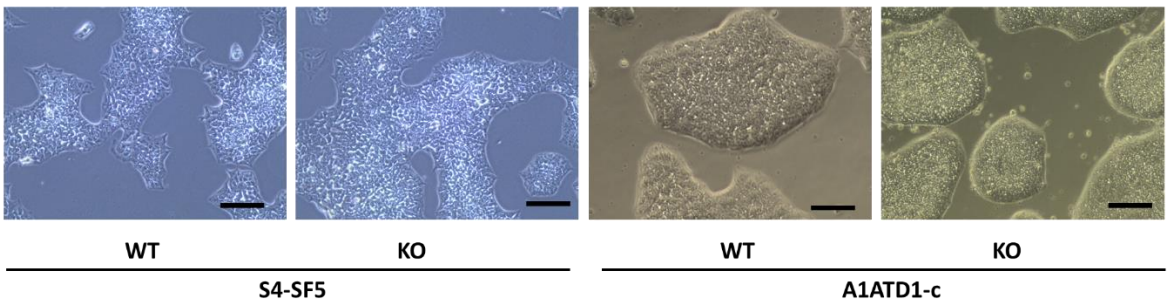

Figure 3.1.3 Confirmation of BRD3 KOs in S4-SF5 and A1ATD1-c iPSc. (a) Sequence alignment of BRD3 KOs to reference WT. PCR products from clonal cultures (generated from single cells) were inserted into PGEM-T and sequenced to confirm present deletions. S4-SF5 BRD3 KO shown is a heterozygous clone for 2 deletions (70 bp and 55 bp) and A1ATD1-c BRD3 KO is homozygous for a 58 bp deletion **(b)** Western blot analysis of BRD3 in WT and KO generated clones. Purified protein extracts from both S4-SF5 BRD3 KO and A1ATD1-c BRD3 KO, as well as WT cells, were collected and fractionated using SDS-PAGE conditions. Subsequently, the protein level of BRD3 and β-actin were analysed using polyclonal antibodies rabbit anti-human BRD3 and mouse anti-human β-actin. BRD3 was not detected in neither S4-SF5 BRD3 KO nor A1ATD1-c BRD3 KO proving complete knockout of BRD3 protein in both clones. **(c)** Transmitted light images of live cultures show no morphological differences between KOs and respective WT. Scale bars, 250 µm.

Figure 3.1.3 shows the confirmation of S4-SF5 BRD3 KO and A1ATD1-c BRD3 KO. Sequencing results of PCR products cloned into pGEM-T confirmed that S4-SF5 BRD3 KO is heterozygous with 2 deletions (70 bp and 55 bp) and A1ATD1-c BRD3 KO is homozygous for a 58 bp deletion (figure 3.1.3.a). To confirm that these deletions generated an out-of-frame protein, a western blot was performed on purified protein extracts from both clones. The membranes were stained with primary BRD3 and β-actin antibodies. Figure 3.1.3.b shows that BRD3 KOs clones did not express BRD3 protein. Morphological observations confirm similarity between KOs and the corresponding WT cells (figure 3.1.3.c).

3.1.2.3 Characterisation of BRD3 KOs

3.1.2.3.1 Proliferation assay

As BET proteins have been associated with proliferation and cell cycle, I investigated whether BRD3 knockout affects proliferation of iPSCs. There are several methods to study cell proliferation, such as DNA synthesis labelling, biomarker concentration measurements or cell staining followed by colorimetric measurement. One of the well-established staining methods used to compare proliferation between cell lines is the crystal violet assay. This assay relies on staining of the DNA and

proteins present in the cells (Sanford et al. 1951; Feoktistova, Geserick, and Leverkus 2016). This method does not distinguish between cell division stages nor does it take into account cells with different protein cargo. However, as crystal violet staining was to be used at iPSC stage only, the method was chosen as it is simple to set up, and it can also be used for cell morphology characterisation (section 2.2.14). In this experiment, iPSC WT and BRD3 KOs were seeded at incremental densities. Cells were fixed at days 4 and 6 post-seeding with glutaraldehyde to cross-link all proteins and preserve morphological structure. Crystal violet assay was performed. Figure 3.1.4 shows results of this proliferation experiment.

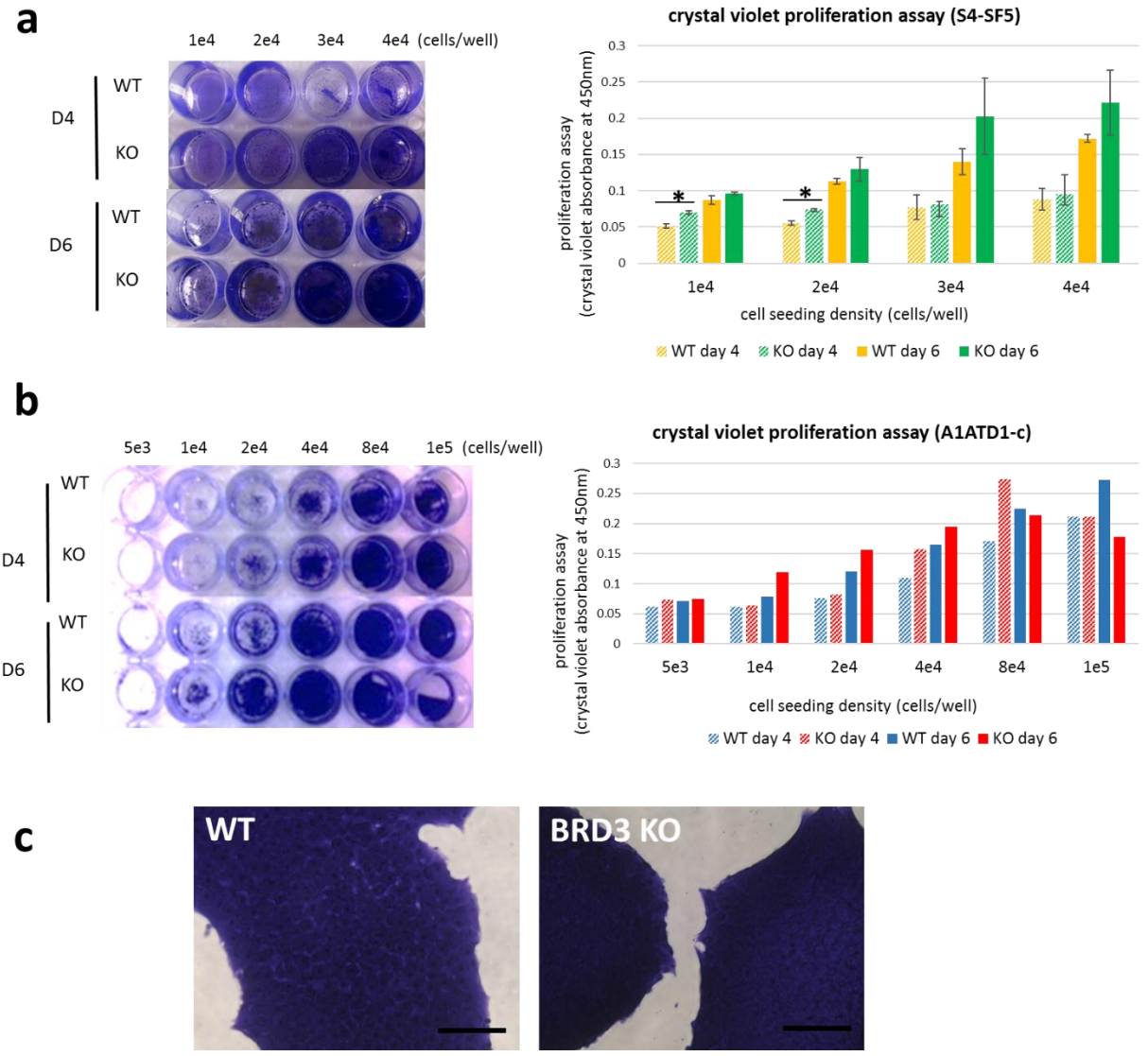

Figure 3.1.4 Proliferation analysis of BRD3 KO on iPSC. WT and KO cells were seeded at incremental densities and fixed at days 4 and 6 post-seeding. Crystal violet staining was performed and dye absorbance measured at 450 nm. **a)** Proliferation assay with S4-SF5 clones. Left panel shows the image of crystal violet stained S4-SF5 cultures at days 4 and 6. The absorbance measurements are plotted on the right panel. Mean absorbance ± standard deviation (SD), n=3, *p<0.05 two-tail t-test against WT

in similar condition. **b)** Proliferation assay for A1ATD1-c clones. Left image shows the stained cultures at days 4 and 6. The absorbance measurements are plotted on the right panel. Same proliferation trend was followed by A1ATD1-c WT and A1ATD1-c BRD3 KO (n=1). **c)** Images of stained WT and BRD3 KO cultures. Scale bars, 250 µm.

The proliferative activity of WT and BRD3 KO cells was determined after 4 and 6 days in culture, using crystal violet assay (figure 3.1.4). In both cell lines, the staining between the WT and BRD3 KO cells for the same condition (time points and densities) were very similar indicating that these cells had a very similar proliferation rate. This result was reflected on the absorbance readings, as BRD3 KO cells generally showed similar readings to the WT cells at the same time point and densities. Two exceptions were noted for S4-SF5 cells at day 4 (figure 3.1.4, top right panel) where statistical significant differences were found between WT and BRD3 KO. These differences were probably due to differences in seeding density and were not confirmed at day 6. Morphological similarities between WT and BRD3 KO were confirmed with crystal violet staining (figure 3.1.4.c). Together, this data shows similar proliferation rates between BRD3 KO cells and the corresponding WT cells suggests that BRD3 does not play a role in proliferation of iPSCs.

3.1.2.3.2 iPSc pluripotency test

Members of the BET family have been shown to regulate pluripotency by binding to regulatory regions of pluripotency genes; as well as regulating the exit of pluripotency states and driving differentiation networks (Wu et al. 2015; Roberts et al. 2017). To study whether absence of BRD3 affects pluripotency, I compared pluripotency levels between WT and BRD3 KOs. Cells were stained with antibodies against pluripotency surface markers SSEA4 (Stage-specific embryonic antigen 4) and Tra-1-60, and analysed by flow cytometry. Human SSEA4 is a glycolipid expressed in early embryonic development, and it is widely used in the identification of pluripotent cells (Kannagi et al. 1983). Equally, Tra-1-60 is present in human embryonic stem and germ cells (Zhao et al. 2012).

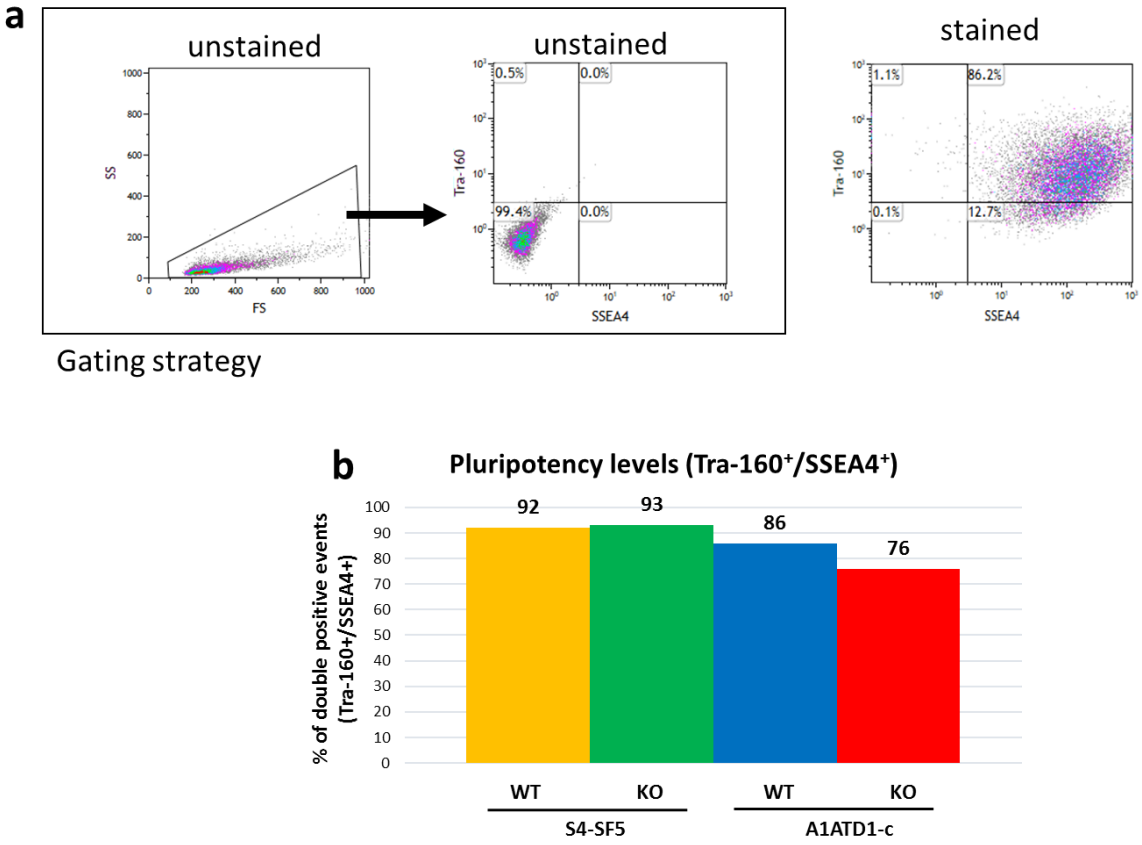

Figure 3.1.5 BRD3 KO does not affect pluripotency of iPSC cultures. Undifferentiated iPSC cells were dissociated and stained with Tra-1-60 and SSEA4 antibodies. These surface markers are commonly found on the surface of undifferentiated and pluripotent cells. Staining intensity was analysed by flow cytometry. **(a)** Gating strategy for identification of pluripotent cells (Tra-1-60$^+$/SSEA4$^+$) using density plots. FS vs SS identifies population of interest. Plot shown with a threshold (discriminator) of 150 applied to reduce the debris visualised. SSEA4 vs Tra-1-60 plot identifies pluripotent cells. **(b)** Comparison of pluripotency levels between cell lines A1ATD1-c and S4-SF5 (WT and KOs). The bar plot shows that all clones tested (WTs and KOs) expressed high levels of Tra-1-60$^+$/SSEA4$^+$ cells, indicating high pluripotency (n=1).

Flow cytometry analysis shows that surface markers Tra-160 and SSEA4 are expressed at high levels, indicating pluripotency of all clones analysed. All clones showed a percentage of double positive cells (Tra-1-60$^+$/SSEA4$^+$) equal or over 75%. This experiment was run at different times for both cell lines (due to KOs being generated at different times). The similarity in pluripotency levels between the WT and KOs clones for both cell lines, suggests that BRD3 does not regulate mechanisms of pluripotency maintenance. The full characterisation of the pluripotency capabilities would only be achieved by differentiation into the 3 germ layers. Although, expression of pluripotency markers is a good indication of the differentiation potential. It was important to verify that pluripotency levels were not

disrupted in BRD3 KO cells, as I aimed to forward programme these cells into MKs and the protocol used is sensitive to the pluripotency levels in the initial population.

3.1.2.4 Forward programming of BRD3 KO into megakaryocytes (MKs)

As confirmed in the section above, BRD3 KO cell lines are viable and phenotypically similar to the corresponding WT. In order to investigate whether BRD3 is essential in megakaryopoiesis, I differentiated iPSC WTs and BRD3 KOs lines into MKs. The differentiation protocol used was the MK forward programming (FoP) protocol, developed by Moreau *et al.* (section 2.1.5). This protocol relies on the overexpression of three transcription factors, critically important in megakaryopoiesis differentiation: TAL1, FLI-1 and GATA-1 (figure 3.1.6). Briefly, the cells are single-cell seeded and infected with the viruses containing the three TFs. For the first 2 days, the differentiating cells are cultured in media containing BMP4 to drive differentiation towards mesoderm. In the following stage, cultures are supplemented with thrombopoietin (TPO) for differentiation towards the megakaryocytic lineage, and stem cell factor (SCF) for supporting cell division. Cell dissociation is performed at day 10 to help selection of suspension MK progenitors based on culture conditions, as adherent cells will not survive suspension culturing.

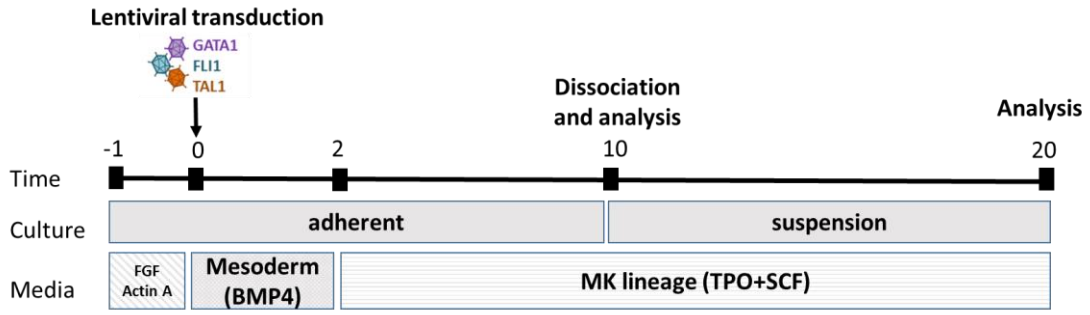

Figure 3.1.6 Schematic representation of FoP protocol. Viral transduction of TAL-1, FLI-1 and GATA-1 along with mesoderm induction initiates the differentiation into mesoderm lineages. This initial stage is followed by culture into MK induction medium (TPO+SCF). Cell dissociation is performed at day 10 and cultures are kept in suspension conditions.

The progression of cells through the differentiation process was tracked by flow cytometry analysis of surface markers. The identification of the differentiating cells was done using a Forward Scatter (FS) versus Side Scatter (SS) plot. FS light is more sensitive to the cell size and SS light is more sensitive to cell homogeneity, therefore the differentiating cells are easily identified using these parameters

(Latimer 1982). The population identified in FS vs SS includes cells at different stages of differentiation, although this analysis gives a good indication to whether the culture is differentiating.

A cell-specific variability in MK generation is characteristic of the FoP protocol. This variability has been observed in several laboratories and it is not currently understood. To investigate whether S4-SF5 and A1ATD1-c iPSC lines are capable to differentiate into MKs using FoP, I initiated 3 different experiments with both lines. In my experiments, S4-SF5 was not able to generate MKs robustly. This cell line only started differentiation in one of the experiments (figure 3.1.7.a), and all of the remaining attempts to form MKs from S4-SF5 cells were unsuccessful. A comparison of the generated MK populations between S4-SF5 clones (WT and BRD3 KO) and A1ATD1-c clones (WT and BRD3 KO) is shown in figure 3.1.7. The data shown is based on FS vs SS analysis (differentiating population).

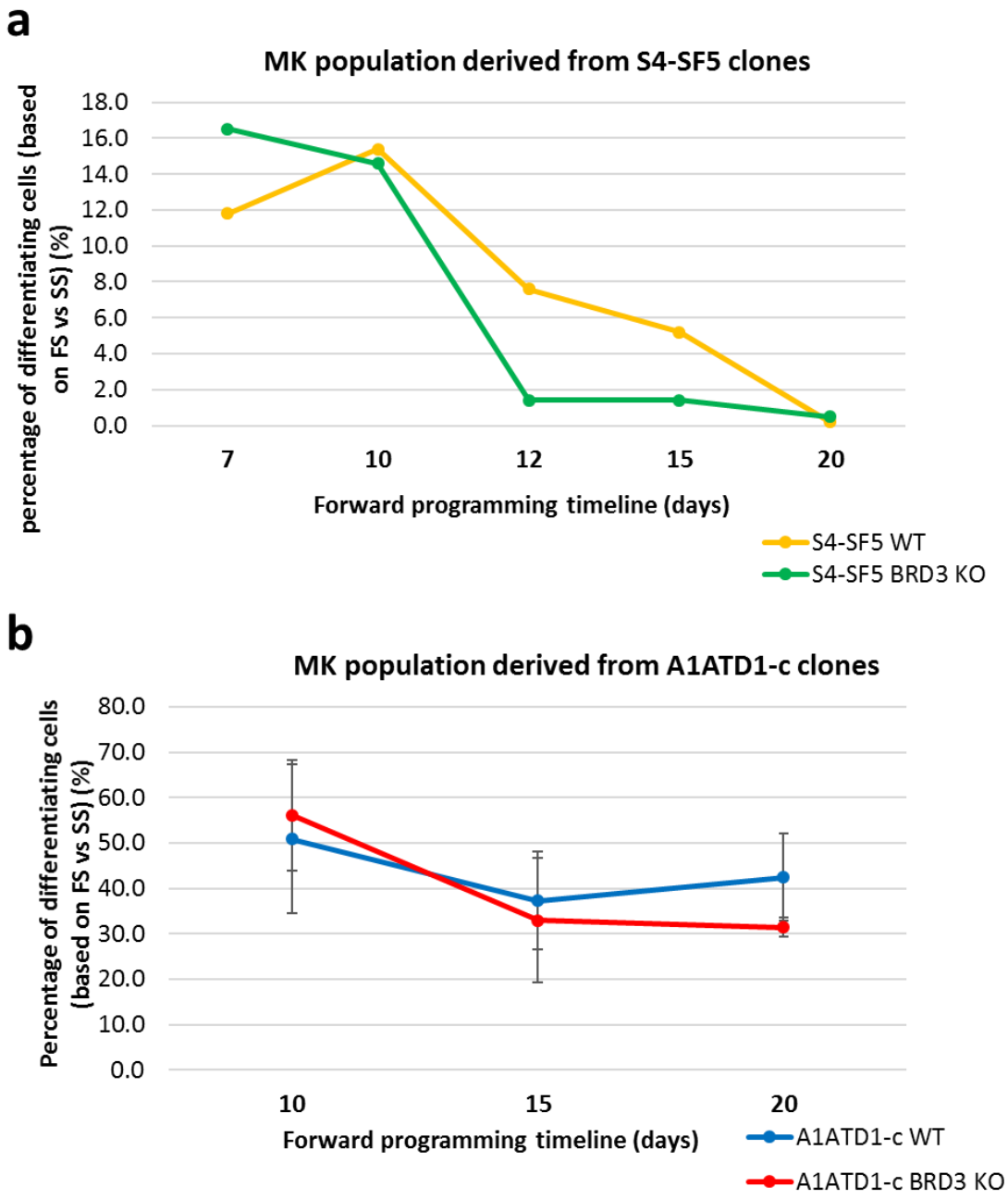

Figure 3.1.7 A1ATD1-c clones (WT and BRD3 KO) generate differentiating populations. Three attempts were made at generating MKs from both S4-SF5 and A1ATD1-c lines using the FoP protocol. Plots show percentage of identified MK populations (FS vs SS, y-axis) along differentiation timeline (x-axis). **a)** S4-SF5 clones (WT and BRD3 KO) do not survive the FoP differentiation. The plotted data represents the only experiment with S4-SF5 where some initial differentiation was observed. The WT (in yellow) and BRD3 KO (in green) followed the same pattern, but eventually the experiment did not succeed at generating MKs. **b)** A1ATD1-c clones (WT and BRD3) are successful at generating MKs. A1ATD1-c BRD3 KO follows the same differentiation pattern as A1ATD1-c WT. Mean of differentiating cells ± SD (n=3).

A1ATD1-c BRD3 KO were capable to generate MKs by forward programming. Figure 3.1.7.b shows the identified MK populations generated from 3 experiments with A1ATD1-c iPSC using FoP protocol

(populations identified by FS vs SS, and include MK progenitors, immature and mature MKs). The data shows that A1ATD1-c BRD3 KO generates MK populations of similar yield to A1ATD1-c WT. This was the model used to study BRD3 requirements in megakaryopoiesis in the rest of my studies. Neither S4-SF5 WT nor S4-SF5 BRD3 KO generated MKs, therefore no further work was carried out on these cells.

The progression of cells through the differentiation process was followed by flow cytometry analysis of cell surface markers. In order to understand whether A1ATD1-c BRD3 KO follow the same differentiation trajectory as A1ATD1-c WT, I analysed the progression of FoP MKs (immature and mature populations) based on cell-surface markers CD235a, CD41a and CD42b. As described above, CD235a identifies glycophorin A, CD41a identifies integrin-αIIb and CD42b identifies glycoprotein Ib (GPIb). The following definitions were used to classify cell populations during forward programming differentiation; $CD235a^{+}/CD41a^{+}$ refers to MK progenitors; $CD41a^{+}/CD235a^{-}$ are lineage committed, immature MK cells; and $CD41a^{+}/CD42b^{+}$ are mature MKs. Cultures were analysed by flow cytometry at day 10 (dissociation day), day 15 and day 20 when generally mature MKs are observed. Cell suspension samples were also cytospinned onto slides, and cells stained using Romanowsky staining to evaluate morphology (section 2.2.12). The gating strategy for population identification and representative images of populations are shown in figure 3.1.8.

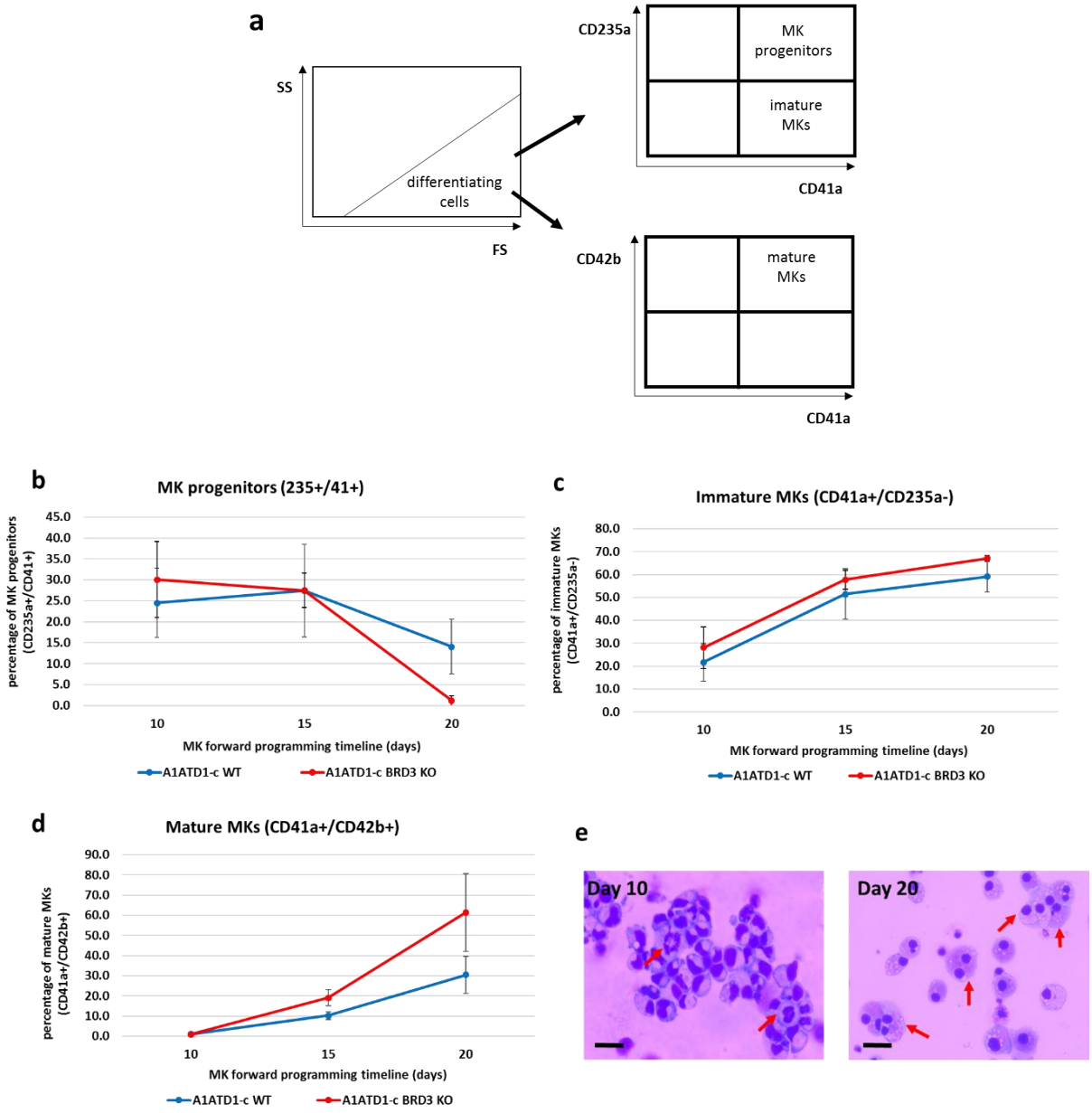

Figure 3.1.8 BRD3 KO generates MKs with similar cell-surface pattern to WT. BRD3 KO and WT iPSCs were differentiated into MKs by FoP. Samples were stained with antibodies against surface markers CD235a, CD41a and CD42b at days 10, 15 and 20. Flow cytometry analysis was performed. **a)** Gating strategy for analysis of MK differentiation. Differentiating populations identified based on forward and side light scatter (FS vs SS). $CD235a^+/CD41a^+$ gates MK progenitors, $CD41a^+/CD235a^-$ gates immature MK cells; and $CD41a^+/CD42b^+$ identify mature MKs. **b)** MK progenitors ($CD235a^+/CD41a^+$) development during FoP process for A1ATD1-c WT and A1ATD1-c BRD3 KO. **c)** Immature MKs ($CD41a^+/CD235a^-$) development. **d)** Mature MKs development ($CD41a^+/CD42b^+$). For a), b) and c) mean of gated population ± SD (n=3). **e)** Representative images of FoP cells at days 10 and 20. Cell suspensions were cytospinned onto slides and stained using Romanowsky staining protocol. Day 10 cultures (left panel) present expanded nucleus and frequent dividing cells (red arrows), indicating a very proliferative, but not highly differentiated culture. Day 20 cultures (right panel) show cells with smaller nucleus and 2N MKs (red arrows), indicating a differentiated MK mature population. Scale bars, 25 µm.

Flow cytometry analysis of cell-surface markers shows that A1ATD1-c BRD3 KO generate MK populations similarly to A1ATD1-c WT. During FoP, cultures generally acquire a MK progenitor cell-surface signature ($CD235a^+/CD41a^+$) prior to day 10 when cultures are still in a high proliferative state (figure 3.1.8.e). MK progenitor cell differentiation was similar to both WT and BRD3 KO cells with 25-30% of differentiating cells identified within the MK progenitor population ($CD235a^+/CD41a^+$) at day 10 (figure 3.1.8.b). Although, the standard deviation between the three experiments (figure 3.1.8.b) is high for the progenitor population, the progression of progenitor cells in culture is very similar between WT and BRD3 KO. MK progenitors gradually lost CD235a and became committed to MK lineage (figure 3.1.8.c), a trend that is expected when using this protocol (Moreau et al. 2016). The differentiation profile for MK committed cells ($CD41a^+/CD235a^-$) was similar between WT and BRD3 KO (figure 3.1.8.c). The loss of CD235a was followed by gain of CD42b (figure 3.1.8.d). This indicates differentiation towards MK maturity where ploidy cells are observed (figure 3.1.8.e). Together this data shows that BRD3 KO did not affect MK differentiation profiles during MK-FoP.

3.1.3 Discussion

BRD3 was previously identified as a regulator of MPV and PDW in a GWAS study, and the attempts to generate a mouse knockout model failed maybe due to lethality at embryonic stage or failure to make gametes, indicating that BRD3 plays critical roles during embryo development. The first section of my thesis describes the generation of an iPSC BRD3 KO model, and the differentiation of these cells into MKs to investigate BRD3 requirements during megakaryopoiesis. These experiments show, for the first time, that BRD3 is not essential for MK differentiation.

The results in this chapter show that BRD3 is not essential for maintenance of undifferentiated cell state. The deletions generated at the BRD3 locus, in both S4-SF5 and A1ATD1-c iPSC cells (figure 3.1.3a), did ablate BRD3 protein production (figure 3.1.3.b). The BRD3 KO clones in both cell lines were viable and phenotypically similar to the corresponding WT cells. This indicates that BRD3 is not essential for iPSC survival. Morphologically, there were no differences observed between WT and KO lines (figure 3.1.3c). The same level of similarity was confirmed in proliferation assays, evaluated by crystal violet absorbance measurements (figure 3.1.4). Figures 3.1.4.a and 3.1.4.b show a proliferation comparison between WT and BRD3 KOs for S4-SF5 and A1ATD1-c, respectively. The results show minimal proliferation difference between the WT and KOs and these differences are maintained for the duration of the study (6 days). Possibly, this reflects a difference in initial cell seeding density rather than in proliferative potential. Overall, both WT and KOs for each line proliferated very similarly. As

well as regulating proliferation, BET proteins have been reported to play a role in pluripotency (Wu et al. 2015; Roberts et al. 2017). For this reason, I investigated the effects of BRD3 on expression of pluripotency markers. Comparison of pluripotency between WT and BRD3 KOs, evaluated by the expression levels of Tra-1-60 and SSEA4 (Figure 3.1.5.b), shows that pluripotency levels were not affected by the absence of BRD3. Together, these results show that BRD3 is not essential for pluripotency maintenance nor proliferation of iPSCs. Considering the failed attempt to generate a BRD3 KO mouse, my results suggest that BRD3 might be essential for regulation of other embryonic differentiation processes, rather than embryonic stem cell maintenance. If the BRD3 KO iPSC clones were not viable I would have designed an inducible knockdown strategy using CRISPR interference (CRISPRi) or shRNA. The inducible knockdowns would not only allow to investigate whether BRD3 is essential during the MK differentiation process, but also to identify the timing when the protein is active, as inducible systems have the convenience to be induced at different stages. With BRD3 KO iPSCs being viable and phenotypically similar to the WT, I investigated whether these cells were able to differentiate into MKs.

BRD3 KO iPSCs were able to generate MKs using a forward programming system. In order to study BRD3 requirements during megakaryopoiesis, I differentiated iPSCs (BRD3 KOs and WTs of both S4-SF5 and A1ATD1-c cell lines) using FoP. The cell lines studied have different MK generation capability. S4-SF5 clones (both WT and BRD3 KO) did not survive the differentiation process, and as a consequence no further work was carried out on S4-SF5 clones (figure 3.1.7.a). The cell line-specific variability in MK generation, using FoP, has been observed by other laboratories, but is currently unexplained. One hypothesis is that different iPSC lines need different amount of lentiviruses for successful infection, and therefore, their outcome in a protocol based on viral infection could be cell-specific. The remaining experiments were conducted in A1ATD1-c clones. A1ATD1-c BRD3 KO clone followed the same differentiation pattern as the corresponding WT for all the MK populations studied (progenitors, immature and mature MKs) (figure 3.1.8). The differentiation of MKs was evaluated by the level of expression of surface markers (CD235a, CD41a and CD42b). The first differentiation stage identified during FOP is MK progenitors ($CD235a^+/CD41a^+$) at day 10. Both WT and BRD3 KO presented cultures with similar levels of MK progenitor cells (figure 3.1.8.b), indicating that BRD3 is not required for early stages of differentiation. The loss of CD235a, and maintenance of CD41a, indicates MK lineage commitment, and the similarities between WT and BRD3 KO (figure 3.1.8.c) suggest that BRD3 is not required during MK lineage commitment. BRD3 KO also differentiated into mature MKs, verified by acquisition of CD42b surface antigen, similarly to the WT. These results indicate that BRD3 is not essential for the establishment of mature MKs.

The results presented in this section were unexpected, particularly following BRD3 identification as a regulator of platelet traits in a GWAS, and the failure in the generation of a mouse BRD3 KO model. As an epigenetic reader, if BRD3 regulated the factors influencing platelet traits, I expected to capture these events at megakaryocyte stage (platelet precursor). However, it is important to remember that GWAS capture very small effects. The absence of BRD3 could cause minimal disruption in MK differentiation that characterisation based on surface markers would not capture. Additionally, the results of my experiments need to be interpreted with caution, due to flaws that could explain the successful generating of MKs from BRD3 KO iPSCs. Firstly, the initial overexpression of GATA-1 in FoP could compensate for the absence of BRD3. GATA-1 and BRD3 are direct interactors, and it has been shown that GATA-1 recruits BRD3 to both active and repressed GATA-1 target genes during erythroid maturation (Janine M Lamonica et al. 2011). In the same study, this association happened independently of histone acetylation, indicating that BRD3 recognises acetylated GATA-1 regardless of chromatin acetylation signatures. If a similar mechanism happened in megakaryopoiesis, the role of BRD3 could become redundant following GATA-1 overexpression. GATA-1 expression levels, as well as the other TFs overexpressed in FoP, have been shown to eventually fall to the normal expression levels found in cord blood (Moreau et al. 2016). However, if BRD3-GATA-1 binding was required for the initial regulatory mechanisms of megakaryopoiesis, this mechanism could have been overcome while GATA-1 was still being overexpressed. A different study looking at the interaction between BET proteins and GATA-1 in erythropoiesis, showed that BRD3 co-occupies a high number of GATA-1-binding sites, but depletion of BRD3 does not affect erythroid transcription (Stonestrom et al. 2015). Together, the above mentioned studies indicate that BRD3 interacts with GATA-1, but is not required for GATA-1-specific gene regulation in erythropoiesis. A similar regulation mechanism could act in megakaryopoiesis, where BRD3 is present at GATA-1 occupied sites, but not actively contributing to GATA-1-mediated transcription. This hypothesis could be tested by comparing chromatin occupancy profiles for BRD3 and GATA-1 during megakaryopoiesis, using a MK differentiation protocol that does not rely on the overexpression of GATA-1. To investigate chromatin co-occupancy between GATA-1 and BRD3, a chromatin immunoprecipitation (ChIP) experiment could be performed using antibodies against GATA-1 and BRD3 on WT MKs. Additionally, a GATA-1-ChIP experiment could be performed on BRD3 KO cells to identify the BRD3 requirement on recruitment of GATA-1. The integration of both experiments would allow to investigate BRD3 requirements on GATA-1-mediated regulation of megakaryopoiesis.

The second reason that could explain the results in this section is that BRD3 might be compensated by a structurally similar protein. The sequence homology between BET proteins has been well studied, and the compensation of BRD3 by BRD2 has been suggested for erythropoiesis (Stonestrom et al. 2015), a process that is evolutionary very close to megakaryopoiesis (Svoboda et al. 2015). One possible experiment to test whether one of the other BET proteins compensates the absence of BRD3 is to generate combinatorial BET KOs on iPSCs, and differentiate these KOs into MKs. A comparison between BRD3 KO and the combinatorial BET KOs would give an indication on potential protein redundancy mechanisms. For example, if BRD2 compensates absence of BRD3, a BRD2+3 KO should form defective MKs or not be able to differentiate into the MK lineage all together.

Finally, BRD3 was identified as a regulator of MPV and PDW, and although megakaryopoiesis is a valid model to study regulation of early platelet formation, conclusions should not be extrapolated lightly. Additionally, the MKs generated by FoP, although comparable to *in vivo* MKs, are still an immature and low ploidy MK cell (Moreau et al. 2016), and the role of BRD3 might be negligible at this stage. If BRD3 is active at a later stage of MK differentiation, or platelet release, that differentiation window might have been missed in my experiments. In order to study BRD3 effects at later stages of MK differentiation, a different protocol would have to be tested; however current *in vitro* differentiated cells do not yet match fully differentiated adult cells.

Importantly, the results presented in this chapter were based only on cell surface markers. Although important in cell characterisation, surface expression signatures do not reveal the molecular mechanisms of differentiation. In order to study the regulatory role of BRD3 in megakaryopoiesis, I have performed further experiments, looking at genome-wide data, which I describe in the section 3.2.

3.2 BRD3 regulation in Megakaryopoiesis

3.2.1 Introduction

Previously, I described the generation of BRD3 KO IPSC lines and their differentiation into MKs. The BRD3 depletion did not affect MK differentiation, evaluated by the expression of well-characterised MK surface markers. Although, these results do not reveal details about the regulatory mechanisms of BRD3 during megakaryopoiesis.

Transcriptional regulation is a well-orchestrated mechanism involving a complex signalling network between chromatin, TFs and cofactors. Transcription machinery locates at active regions characterised by specific features, such as accessible chromatin structure and particular posttranslational chromatin marks (Harrow et al. 2012; Calo and Wysocka 2013). Histone acetylation is a mark present on active promoters and enhancers where cell-specific transcription factors and co-factors bind. Lysine acetylation recruits BET proteins involved in haematopoietic transcription networks, as reviewed in (Stonestrom et al. 2016). However, the role of BRD3 on establishment of acetylation signatures, and consequently on transcriptional regulation during megakaryopoiesis is largely unknown. In this section, I describe the experiments to investigate the regulatory mechanisms of BRD3 during FoP of MKs.

Regulatory elements, such as promoters or enhancers, are often accessible and active in a cell-specific manner (Heintzman et al. 2007a; Thurman et al. 2012; Noh et al. 2015). In order to identify changes in chromatin accessibility resulting from BRD3 absence, I performed assay for transposase-accessible chromatin with sequencing (ATAC-seq) on WT and BRD3 KO cells. ATAC-seq is a simple method that uses efficient enzymatic fragmentation for identification of increased-accessibility regions (Buenrostro et al. 2013). Other methods for assaying chromatin accessibility include DNase-seq (Boyle, Davis, et al. 2008) and formaldehyde assisted isolation of regulatory elements with sequencing (FAIRE-seq) (Giresi et al. 2007), although these alternative methods include laborious protocols and require higher amount of starting material than ATAC-seq. However, ATAC-seq data alone does not provide sufficient high resolution to identify regulatory elements.

A subset of accessible regulatory elements is active in a cell-specific manner, and therefore marked with activation marks, such as H3K27ac (Creyghton et al. 2010). To identify the regions where activation marks change due to BRD3 absence, I performed chromatin immunoprecipitation followed by genome-wide parallel sequencing (ChIP-seq), using antibodies against H3k27ac and BRD3. ChIP-seq is used for genome-wide identification of histone marks and protein-DNA interactions, owing its success to the decreasing cost of next-generation sequencing. ChIP-seq offers advantages such as high resolution, and greater coverage than the predecessor array-based ChIP-chip (Lee et al. 2006; Buck et al. 2004). However, ChIP-seq restricts the identification of regulatory elements to regions that are targeted by specific antibodies, and it is heavily dependent on antibody specificity. The integration of ATAC-seq and ChIP-seq data sets improves the detection of those regions which are both accessible and active. By analysing the differences between WT and BRD3 KO, I aimed at identifying regions directly regulated by BRD3. Therefore, an effect of BRD3 absence would be observed in BRD3 KO cells with possible changes in chromatin activity and/or accessibility.

Changes in regulatory elements generally affect expression of the genes regulated by those elements. In order to evaluate the consequential effects of BRD3 KO, I generated RNA-seq data from WT and BRD3 KO. These datasets were generated to confirm transcription variation as a result of alterations at regulatory regions. Investigation of the changes in chromatin structure and/or active marks (H3K27ac) in regulatory regions, as a result of BRD3 absence, and the study of the transcriptional consequences in MKs would progress our understanding of the BRD3 role in megakaryopoiesis.

3.2.2 Results

In order to study BRD3 regulatory mechanisms during megakaryopoiesis, samples for ATAC-seq, ChIP-seq and RNA-seq were collected from iPSC (WT and BRD3 KO) and MKs (WT and BRD3 KO) cultures. MKs were generated using the FoP protocol in triplicates, and iPSCs samples were collected at the beginning of each FoP experiment. Cells were differentiated for 20 days before sorting based on $CD42b^{+}$ cells (MKs) (section 2.2.9). Other selection methods were tested, such as CD42+-bead selection, but high cell loss was observed. Ficoll separation of cell populations is also routinely performed, although the populations selected are more heterogeneous than sorted populations. Sorted cells were split into 3 aliquots for ChIP-seq, ATAC-seq and RNA-seq, and processed according to respective protocols. Libraries were prepared for all samples. Data analysis was performed by Dr Denis Seyres, University of Cambridge.

3.2.2.1 Changes in accessible chromatin induced by BRD3 KO

To investigate differences in open chromatin between WT and BRD3 KO, I generated ATAC-seq data sets from iPSC and MK samples (WT and KO). ATAC-seq is a method to map chromatin accessibility genome-wide. The method relies on hyperactive T5n transposase to digest the chromatin at accessible regions and insert sequencing adapters compatible with sequencing technologies (Adey et al. 2010). I prepared ATAC-seq libraries from samples containing 100K cells (section 2.2.15). Single-end Illumina sequencing was performed, therefore each fragment was only read by the sequencer in one direction; in contrast to paired-end reading where the sequencer reads each fragment from both ends.

A comparison between the WT and BRD3 KO in iPSC and MK samples was performed. Prior to differential analysis, we assessed quality of ATAC-seq samples by evaluating bias in read distribution over the genome using deepTools plotFingerPrint tool (figure 3.2.1.a). This tool ranks the bins in the genome based on number of reads, and plots this ranking against the cumulative sum of reads. This method is used to evaluate sample enrichment over input. Samples with low enrichment were not considered for analysis. We performed differential analysis with two approaches: a window-based approach (csaw R package) and a peak-based method (diffbind R Package). The former approach does not rely on peak called by another program. The second merges pre-called peaks in order to create a master set of peaks in which reads are counted. None of the methods return differentially opened regions between KO and WT conditions, in both iPSCs and MK at a 5% FDR.

We also analysed the correlation, in terms of read number per peak (log(RPKM+1)), between ATAC-seq replicates in the same cell type. Figure 3.2.1.b shows correlation heatmap for iPSCs (WT and BRD3 KO), and 3.2.1.c shows correlations for MK replicates.

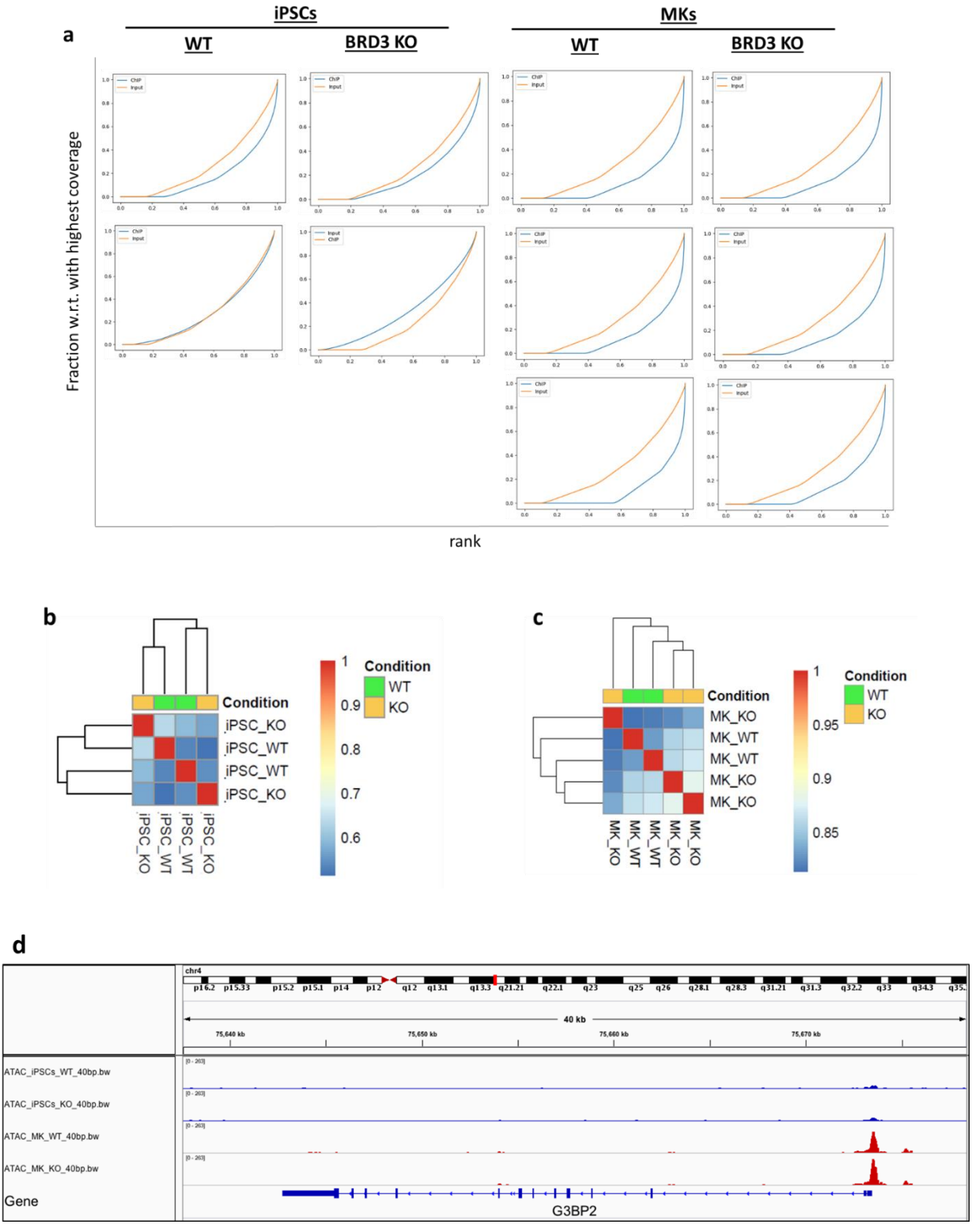

Figure 3.2.1 Quality assessment of ATAC-seq samples. ATAC-seq samples were collected from WT and BRD3 KO cells for both iPSC and MK followed by sequencing. **a)** Enrichment plots of ATAC-seq samples over input for iPSC (left) and MK (right). Enrichment calculated using deepTools plotFingerPrint tool. **b)** Heatmap representing correlation between iPSC replicates (WT and BRD3 KO). **c)** Heatmap representing correlation between MK replicates (WT and BRD3 KO). The correlation values in b) and c) were computed on normalised read count (log(RPKM+1)) over diffbind master set of peaks. **d)** IGV

representation of ATAC-seq peaks called for iPSC and MK over G3BP2 gene promoter. High similarity was observed between WT and BRD3 KO replicates.

All samples presented sufficient enrichment over input. Although, in general MK samples had higher enrichment than iPSC (figure 3.2.1.a). In this analysis, good genome coverage is shown by low X intercept value, and good enrichment by a large area between sample and input curves (diagonal). Heatmaps of sample correlation show no separation by condition (WT and BRD3 KO) (figure 3.2.1.b/c). We noticed a smaller overall correlation in iPSCs (0.55-0.7) compared to MK (0.80-0.85). This difference can be due to a more spread signal in iPSCs. We visually inspected the replicates, using IGV, and confirmed the high similarity of accessible chromatin patterns between WT and BRD3 KO (figure 3.2.1.c).

3.2.2.2 Changes in H3K27ac chromatin signatures due to BRD3 KO

To explore how BRD3 regulates the active chromatin landscape, I performed a ChIP-seq experiment using H3K27ac and BRD3 antibodies in WT and BRD3 KO cells. The ChIP protocol followed is described in section 2.2.16. Essentially, the ChIP-seq protocol relies on the immunoprecipitation step where an antibody is used to enrich the DNA bound to the epitope of interest (in here, H3K27ac and BRD3). Libraries are prepared from the enriched DNA and next-generation sequencing performed to generate ChIP-seq data sets. In my experiments, H3K27ac and BRD3 data sets were generated to analyse any loss of H3K27ac mark in BRD3 KO, and consequently to confirm whether those changes were due to BRD3 absence. To exclude false positives, the ChIP on BRD3 was also done on BRD3 KO cells. Unfortunately, the enrichment above input for BRD3 ChIP-seq on WT data sets was very low and peak calling was not performed (data not shown).

Two of the MK WT samples did not pass quality assessment as the enrichment and signal-to-noise ratio were very low. Therefore, only one MK WT replicate remained, and we were not able to performed differential analysis for MK. For iPSC, and similarly to ATAC, we used diffbind and csaw approaches to identify differences in chromatin acetylation resulting from BRD3 KO. Differentially acetylated regions were not found with a FDR threshold of 5%.

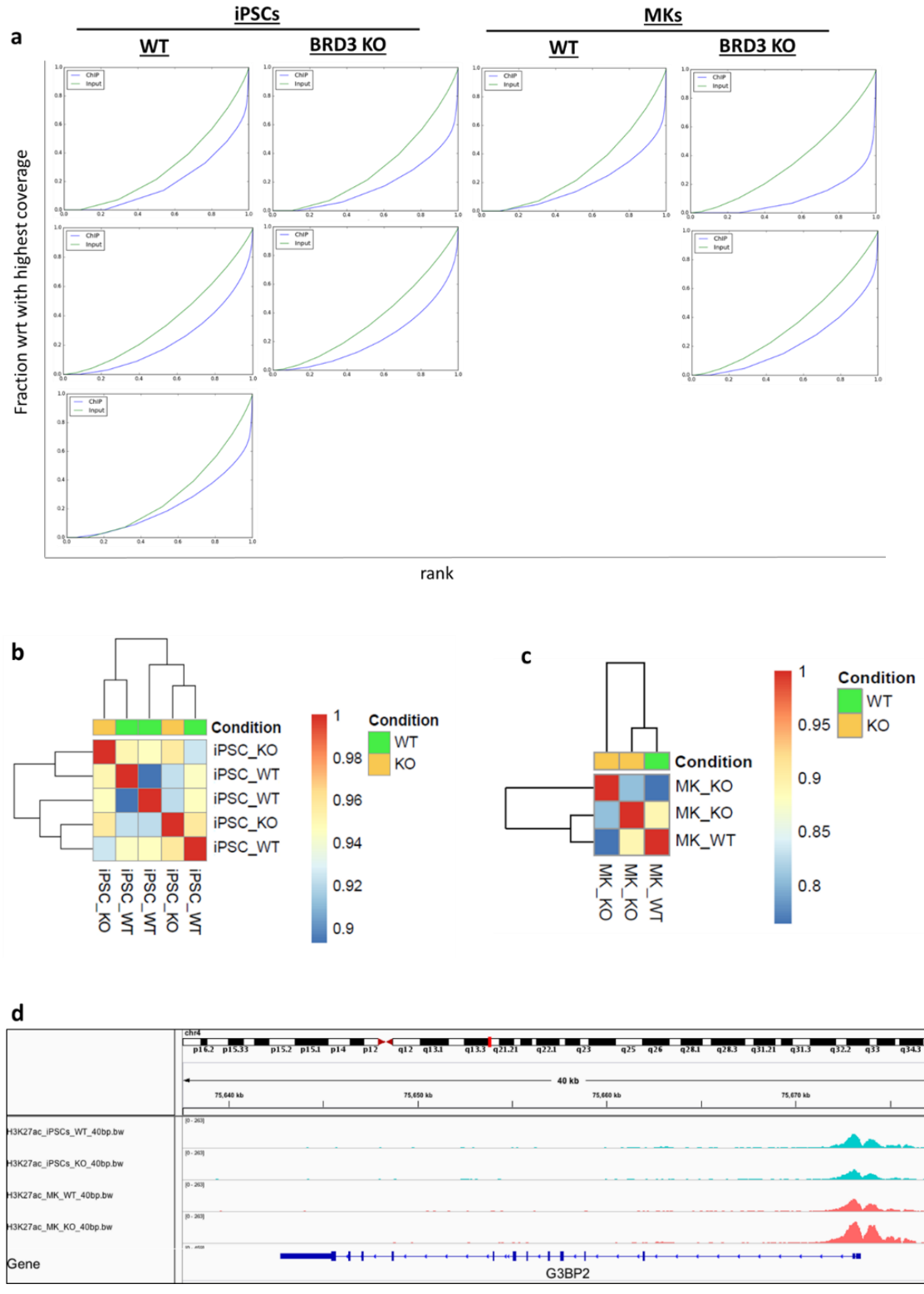

Figure 3.2.1 **Quality assessment of ChIP-seq samples.** ChIP-seq libraries were prepared from WT and BRD3 KO cells for both iPSC and MKs. **a)** Enrichment plots of ChIP-seq samples over input for iPSC (left) and MK (right). Enrichment calculated using deepTools plotFingerPrint tool. **b)** Heatmap representing correlation between iPSC replicates (WT and BRD3 KO). **c)** Heatmap representing correlation between MK replicates (WT and BRD3 KO). The correlation values in b) and c) were computed on normalised read count (log(RPKM+1)) over diffbind master set of peaks . **d)** IGV representation of ChIP-seq peaks

called for iPSC and MK over G3BP2 gene promoter. High similarity was observed between WT and BRD3 KO replicates.

Enrichment analysis shows good enrichment for all ChIP-seq samples (figure 3.2.2.a). Correlation between WT and BRD3 KO replicates, for the same cell type, was confirmed to be high (figures 3.2.2.b/c) (MK: 0.77-0.9 ; iPSCs: 0.9-0.96). Differential analysis on MK was not possible due to the availability of only one WT replicate. However, we manually analysed the ChIP-seq tracks on IGV, and found that WT and BRD3 KO are very similar. As an example, in figure 3.2.2.d, we show ChIP-seq tracks for both iPSC and MK cells (WT vs BRD3 KO). The gene promoter shown is associated to this active histone mark in both cell lines and presents a typical pattern of acetylation with two ChIP-seq H3K27ac peaks (figure 3.2.2.d) and one broader peak for ATAC-seq (figure 3.2.1.d). This combination of patterns can be integrated for the detection of regulatory regions. In here, we used it to evaluate differences in patterns between WT and BRD3 KO.

3.2.2.3 Integration of accessible and active chromatin using patterns of peaks (RedPop)

Due to the striking similarity between WT and BRD3 KO data sets analysed in this section, we investigate whether any differences could be identified in patterns of ATAC-seq and ChIP-seq data integration. Open chromatin around binding sites typically results in a broad, low-resolution peak of elevated ATAC-seq coverage (Ernst et al. 2011; Consortium 2012). The surrounding nucleosomes of a regulatory element are typically acetylated, leaving two peaks in H3K27ac coverage, spaced a few hundred base-pairs apart. By combining the genomic coverage tracks of an open chromatin and an H3K27ac assay, regulatory elements can be detected with high precision. Dr Ernest Turro, University of Cambridge, developed an algorithm for regulatory element detection using patterns of peaks (RedPop) that utilises these patterns. This method for mapping chromatin landscape has not been published yet and it is briefly described in section 2.3.2. Figure 3.2.3 shows results of ATAC-seq and ChIP-seq data integration for iPSCs and MKs, respectively. No differences in patterns was identified between WT and BRD3 KO in both iPSC and MKs.

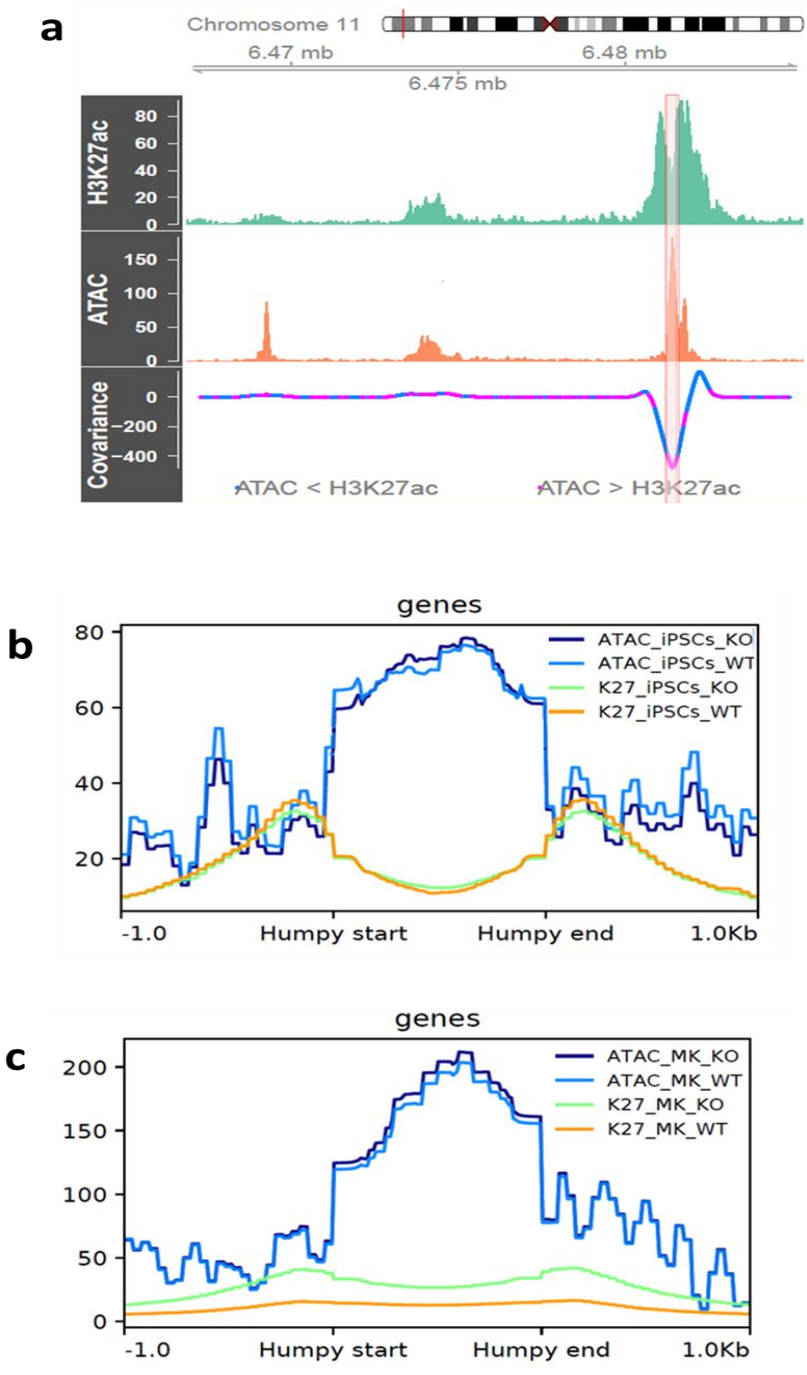

Figure 3.2.3 **Humpy pattern search on ATAC-seq and ChIP-seq data sets shows no difference between WT and BRD3 KO.** a) Covariance analysis principle. Local minimum is identified in regions with high covariance value. These regions reflect a depletion in H3K27ac signal and an enrichment of ATAC signal. b) computeMatrix and plotProfile tools from deepTools were used to plot profile over identified humpy regions. All regions were scaled to the same size ('humpy start' and 'humpy end' on x-axis) and an additional region of 1kb were added for plotting upstream and downstream of the scaled regions. The y-axis represents the number of reads normalized to get a 1x depth of coverage (RPGC). Sequencing depth is defined as: (total number of mapped reads * fragment length) / effective genome size.

3.2.2.4 RNA-seq data sets

To explore the transcriptional regulation function of BRD3, and verify the consequences of the results obtained with ATAC-seq and ChIP-seq, I used RNA-seq to study transcriptome expression of WT and KO samples at iPSC and MK stages. For all samples, three replicates were collected, and libraries prepared according to method described in section 2.2.17. Transcripts abundance were estimated with Kallisto [PMID:27043002] and summarized to gene-level with tximport R package [PMID: 26925227].

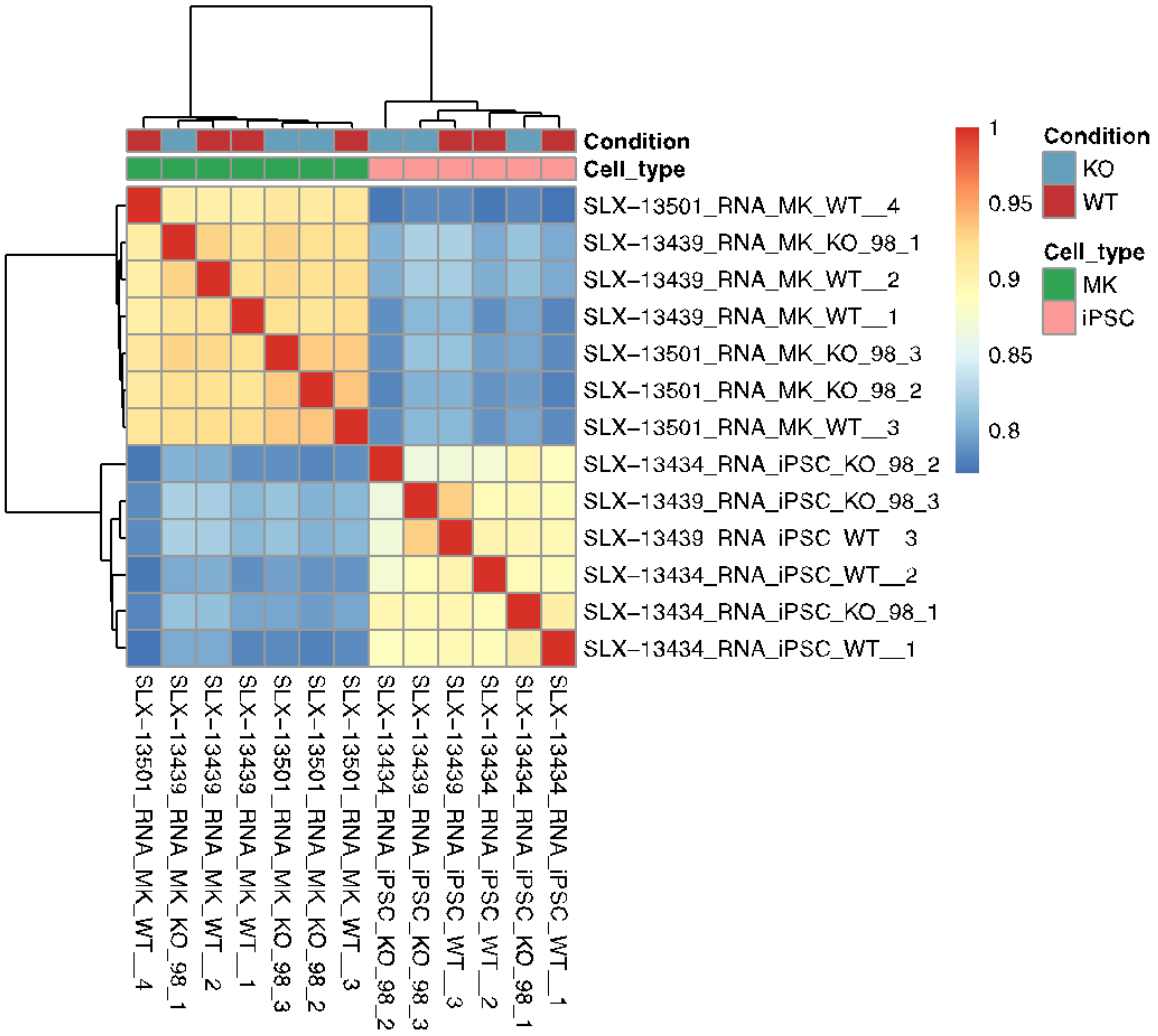

Figure 3.2.4 RNA-seq correlation heatmap shows no differences between WT and KO. Correlation heatmap using log(TPM+1) was computed for RNA-seq experiments. It shows a clear split between cell types but no separation by condition (WT and KO). Within each cell types, overall spearman correlation is very high.

Differential expression analysis between WT and BRD3 KO was performed for iPSC and MK data sets using Deseq2. Results are shown in figure 3.2.5.

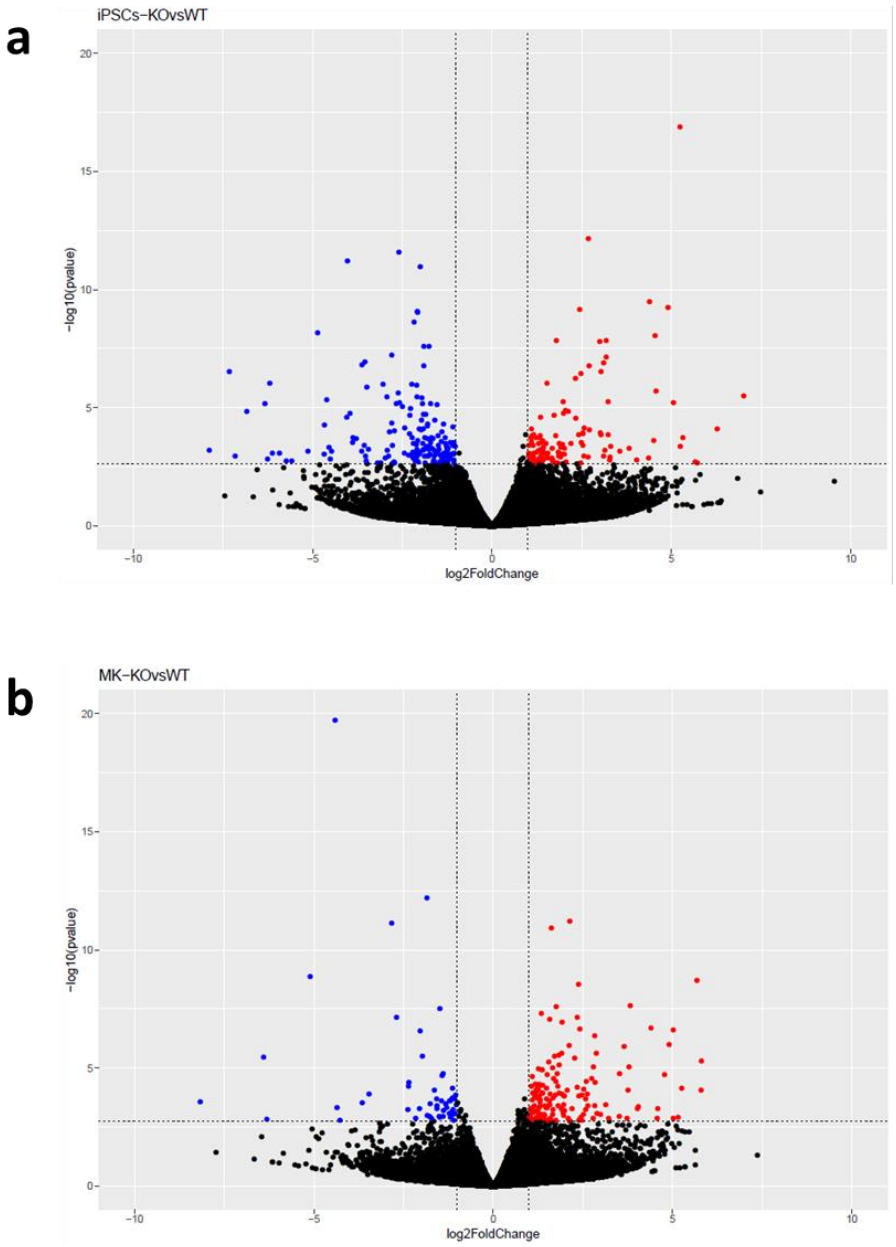

Figure 3.2.5 Volcano plots show differentially expressed genes between WT and BRD3 KO. RNA-seq libraries were prepared from WT and BRD3 KO cells (iPSC and MKs) for pair-end Illumina sequencing. Volcano plots representation of differential gene expression analysis in WT vs BRD3 KO for **a)** iPSC and **b)** MKs. Blue and red dots mark the genes with significantly decreased or increased expression in BRD3 KO compared to WT samples (FDR>0.05). The x-axis shows log2fold-changes in expression and the y-axis –log10 (p-value). Horizontal dashed lines show the log10 of the maximum p-value observed at FDR 5%. A low number of differentially expressed genes between BRD3 KO and WT were identified in both iPSC and MKs.

Differential expression analysis in iPSC and MKs reveals transcriptional differences between BRD3 KO and WT. Only 95 genes in BRD3 KO iPSC and 89 genes in BRD3 KO MKs were differentially expressed when compared to the respective WTs (supplementary tables 1 and 2 for lists of genes). Gene ontology (GO) enrichment analysis was performed using EnrichR (Kuleshov et al. 2016; Chen et al. 2013), but gene enrichment associations were low, e.g. only 4/95 dysregulated genes in iPSC were associated with mineral absorption mechanisms and 2/89 differentially expressed genes in MKs were associated with cAMP metabolic processes. The comparison between differentially expressed genes in iPSC and MKs revealed 8 common genes (DYNLT3, CXCL11, ZNF555, S100A6, ZNF560, HIST1H3C, GRID2 and CYP2E1). GO enrichment analysis did not revealed a particular biological function for this set of common genes.

In order to determine if any correlation between the set of differentially expressed genes in BRD3 KO MKs and transcriptional functions exist, I performed a transcriptional enrichment analysis using EnrichR with ENCODE (Consortium 2012) and CHEA (Lachmann et al. 2010) databases. Transcriptional enrichment identifies TF binding sites at gene promoters, and it is used to infer associations between those genes and the TFs. This analysis can be used to discover the biological function of TFs. Eight genes were identified as being associated with GATA-1 transcription regulation (figure 3.2.6.a).

To explore whether any of the differentially expressed genes in BRD3 KO MKs had been previously associated with MKs or platelet traits, I compared this list with genes previously identified in GWAS and metadata analysis on blood traits (Astle et al. 2016; Gieger et al. 2011; J. Li et al. 2013; Vasquez et al. 2016). Interestingly, only gene ZFPM2 was common between my data and the list of genes previously associated with platelet traits in all of the references above. Figure 3.2.6.b shows the expression levels of this gene in my iPSC and MKs. ZFPM2 encodes for a zinc finger protein known as FOG2. ZFPM2 protein product interacts with elements of the GATA family with important functions in cell fate determination (Chlon and Crispino 2012). This gene is highly expressed in platelets, as shown in Blueprint data (figure 3.2.6.c).

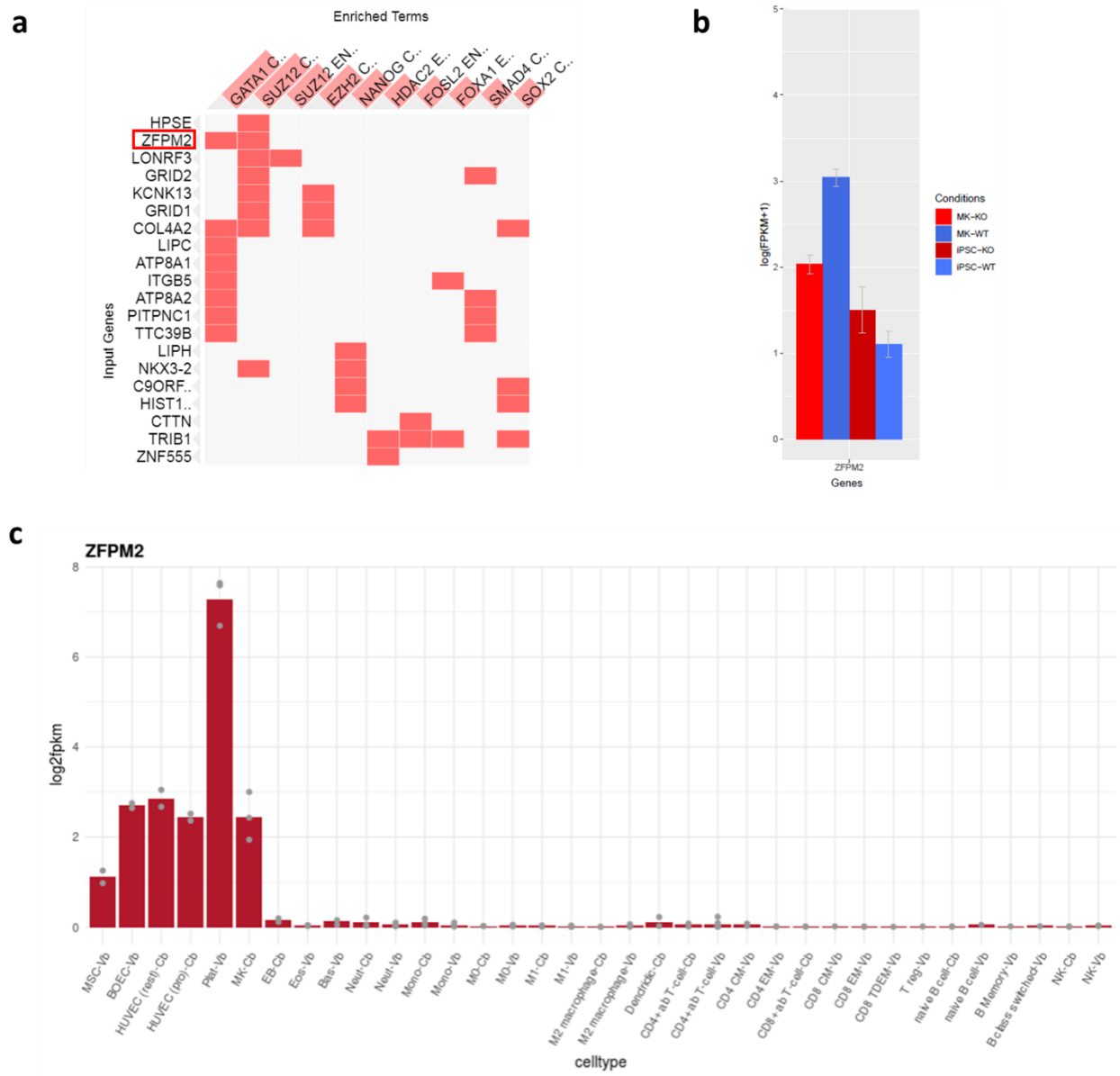

Figure 3.2.6. BRD3 KO disrupts expression of genes previously associated with GATA-1 transcription and platelet traits. a) Transcription enrichment analysis (EnrichR) revealed association of differentially expressed genes in BRD3 KO MKs (y-axis) and GATA-1 (x-axis for enriched terms), including ZFPM2 previously associated with platelet traits **b)** Expression of gene ZFPM2 in my iPSC and MK samples (WT and BRD3 KO). Expression levels represented as log(FPKM). **c)** Expression of gene ZFPM2 in blood cells was analysed in Blueprint data (blueprint.haem.cam.ac.uk/bloodatlas). Axis represent blood cell type (x-axis) and expression levels as log2fpkm (y-axis).

Following the low number of differentially expressed genes in BRD3 KO cells (both iPSC and MKs), and to determine whether a possible compensatory mechanism exists at transcriptional level in megakaryopoiesis, I compared the BRD2 and BRD4 transcript levels between WT and BRD3 KO iPSCs and MKs (figure 3.2.7).

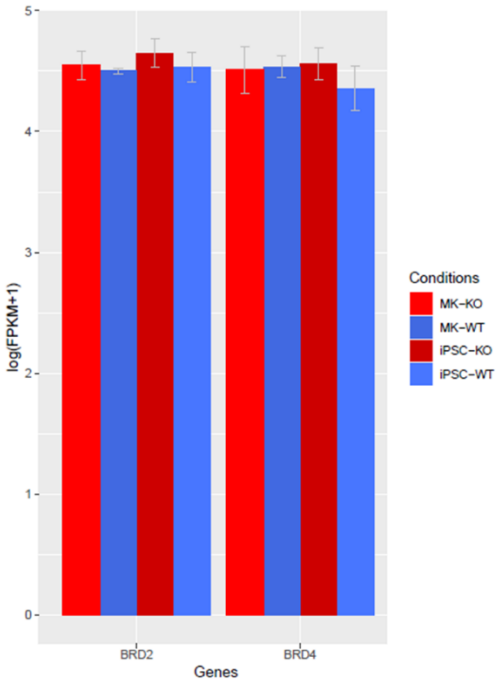

Figure 3.2.7 BRD2 and BRD4 are similarly expressed in WT and BRD3 KO cells. RNA-seq data from iPSC and MKs was analysed for comparison of BRD2 and BRD4 transcripts between WT and BRD3 KO cells. The x-axis shows genes analysed (BRD2 on left, BRD4 on right) and the y-axis shows gene expression levels as log (FPKM).

Comparison of gene transcription levels revealed that BRD2 and BRD4 are similarly expressed between WT and BRD3 KO cells (figure 3.2.7). This similarity was confirmed in both iPSC and MK cells. No major effect was observed on BRD2 and BRD4 transcription associated with BRD3 depletion.

3.2.3 Discussion

Despite being identified in a GWAS study as a regulator of platelet traits, BRD3 is not essential for generation of megakaryocytes (the platelet progenitor cell). Although, the translational mechanisms regulated by BRD3 during megakaryopoiesis remain unknown. In this section, I described experiments that aimed at understanding the BRD3 role at regulatory elements during megakaryopoiesis. In order to achieve this goal, I investigated differences in accessible and active chromatin induced by the

absence of BRD3, and investigated the gene transcriptional differences between WT and BRD3 KO model at two stages of megakaryopoiesis.

I have found that genome-wide chromatin accessibility and H3K27ac marks do not change in absence of BRD3 during FoP of MKs. Comparison of ATAC-seq and ChIP-seq on H3K27ac datasets between WT and BRD3 KO revealed that both chromatin accessibility and H3K27 acetylation levels are very similar (figures 3.2.1 and 3.2.2). This result was confirmed at both iPSC and MK stage of differentiation, and reinforces my results in section 3.1 where BRD3 KO did not fail to generate MKs. However, these results also augment the concerns around the potential artefactual contribution of overexpression of GATA-1 in the FoP protocol. Interestingly, a study looking at the regulation of acetylation on erythroid-specific chromatin domains found that GATA-1 establishes erythroid-specific acetylation signatures on histones H3 and H4 through recruitment of CREB-binding protein (CBP) (Letting et al. 2003). Therefore, it is acceptable to hypothesise that GATA-1 overexpression in FoP could induce MK-specific H3K27ac signatures similarly in WT and BRD3 KO. This would explain why chromatin activation marks were identical in WT and BRD3 KO MKs. To avoid this downfall, a new protocol for generation of MKs should be used to perform these experiments. If differences in accessible and active chromatin between WT and BRD3 KO were identified, it would be interesting to fully characterise these (promoters, enhancers, etc) to investigate BRD3 transcription targets. This data would help understand whether BRD3 regulates gene transcription via enhancer-mediated regulation, or at promoters via recruitment of transcriptional machinery.

A second explanation for the similarity between WT and BRD3 KO acetylation signatures in MKs is that the establishment of H3K27ac could be BRD3-independent. As an epigenetic reader, BRD3 is capable of recognising acetyl lysines and regulate transcription, but the protein might not have an active role in the deposition of the histone mark. In this case, the absence of BRD3 would not be expected to alter chromatin acetylation, and the genome-wide H3K27ac landscape would be equivalent to WT. Interestingly, a study on the role of BRD4 at enhancer regions during differentiation, demonstrates that this BET protein does not regulate H3K27ac enrichment at enhancer regions (Lee et al. 2017). Additionally, the study shows that BRD4 recruitment to acetylation-activated enhancers is facilitated by the cooperation between TFs and CREB-binding protein (CBP). A similar mechanism could regulate the recruitment of BRD3 to active regulatory elements in megakaryopoiesis. As mentioned above, GATA-1 establishes acetylation via interaction with CBP in erythropoiesis, therefore we can hypothesise that if a similar cooperation mechanism regulates BRD3 recruitment in megakaryopoiesis, acetylation signatures would not change in the absence of BRD3. In order to investigate whether MK-specific TFs and HATs recruit BRD3 to regulatory elements during MK formation, a ChIP-seq

experiment against BRD3 and histone marks could be performed on directed differentiated MKs derived from MK-specific TFs-KO cells and HATs-KO cells. This experiment would allow to identify the elements where a particular TF and/or HAT are required for the recruitment of BRD3. The ChIP-seq experiment on histone marks would allow to characterise those regulatory elements, e.g. $H3K4me1^{+}/H3K27ac^{+}$ for active enhancers.

A third hypothesis that could explain the ChIP-seq results of my experiments is that BRD3 might not interact directly with H3K27ac regions. A study on histone recognition by bromodomain modules reported that BRD3 interacts preferentially with H2K36ac and H2K85ac (Filippakopoulos et al. 2012). In this study, the researchers developed a peptide-based array harbouring acetyl lysine sites of N-terminal tails of histones H3 and H4, to screen for interactions with bromodomains. The lack of interaction between H3K27ac on histone tails and BRD3 could explain why H3K27ac signalling is similar between WT and BRD3 KO, despite the differences in gene transcription, as BRD3 could regulate those genes through binding to a different histone mark.

My experiments revealed transcriptional differences between WT and BRD3 KO in both iPSCs and MKs (figure 3.2.5). The differentially expressed genes in BRD3 KO MKs could be regulated in a GATA-1 independent manner, explaining the discrepancy between genome-wide acetylation signatures and gene expression. A study exploring GATA-1 and BET interaction mechanisms in erythropoiesis revealed that, despite the high chromatin co-occupancy between BRD3 and GATA-1, BRD3 KO cells expressed all GATA-1 target genes at normal levels upon GATA-1 induction (Stonestrom et al. 2015). Therefore, in my experiments, GATA-1 could be controlling acetylation levels and transcription of all its related genes, but not transcription of the differentially expressed genes identified.

Although the number of genes differentially expressed was low, the BRD3 role on transcription of those genes could explain the GWAS identification of BRD3 as a regulator of platelet traits. BRD3 could be part of the transcriptional machinery at the gene promoters, or could regulate gene transcription via enhancer occupancy. Interestingly, ZFPM2, was the only differentially expressed gene in BRD3 KO MKs that has been previously identified in several GWAS as being associated with platelet traits (Astle et al. 2016; Gieger et al. 2011; J. Li et al. 2013; Vasquez et al. 2016). ZFPM2 encodes for FOG2, an interactor with members of the GATA family (Chlon and Crispino 2012). If BRD3 regulates ZFPM2, the effects of the gene dysregulation in MK generation could have been overcome by the overexpression of TFs. Alternatively, as expression of ZFPM2 is higher in platelets than in MKs (figure 3.2.6.b), the effects of the gene dysregulation in BRD3 KO cells may only affect platelet formation and not MKs.

The transcriptional differences between WT and BRD3 KO cells could also be an indirect effect of the BRD3 absence in transcriptional complexes regulating those genes. BRD3 is part of transcriptional complexes, including BET proteins and other important proteins (Dawson et al. 2011). The absence of one of the protein elements from the complex is probably compensated, at least partially, by other proteins in the same complex, but it could still have a knockdown effect on transcription. To identify BRD3-interactors, a BRD3-pull down experiment could be performed during MK differentiation. Knocking out those proteins in iPSC and differentiating into MKs would reveal whether the effects on transcriptional were similar to those observed in BRD3 KO, and therefore, whether the results of my experiments were an indirect result of BRD3 KO.

BET proteins are elements of transcriptional complexes, and in order to investigate whether one of the other BET proteins compensated the absence of BRD3, I compared BRD2 and BRD4 RNA expression levels between WT and BRD3 KO cells (figure 3.2.7). Differences in BRD2 and BRD4 expression were not identified, although this does not confirm the absence of a BET compensatory mechanism, as the proteins levels were not investigated. A study on the role of BRD3 and BRD4 in myogenesis has reported that BET protein expressions varied throughout the time course of the experiments without change in mRNA expression (Roberts et al. 2017). In order to further investigate the interactions between BET proteins during megakaryopoiesis, I performed the BET inhibition experiments described in section 3.3.

3.3 BET inhibition in Megakaryopoiesis

3.3.1 Introduction

In the previous chapters I showed that, using a forward programming model for megakaryopoiesis, BRD3 is not essential for MK differentiation. BRD3 KO cells are viable, capable of differentiating into MKs, and no effects on chromatin accessibility nor H3K27ac levels or position were observed when compared with WT cells. Despite these similarities in chromatin architecture, BRD3 KO cells presented a set of differentially expressed genes, probably as the result of BRD3 dysregulation on transcription of those genes.

BRD3 protein has been shown to be present in BET protein-containing complexes with important transcriptional functions (Dawson et al. 2011). In order to identify nuclear complexes associated with BET proteins in leukemia cells, Dawson *et al.* applied a multiple approach including identification of protein complexes that bind to a BET-inhibitor; immunoprecipitation of BET-bound chromatin; and identification of protein complexes bound to chromatin marks previously associated with BET proteins. This complementary approach enabled the identification of the inhibitor targets (BETs) and the proteins associated with those targets. Interestingly, this study revealed that BET proteins associate with transcriptionally relevant complexes PAFc and SEC, and may function to recruit these complexes to chromatin. BET inhibition affected recruitment of BET-containing transcriptional complexes to chromatin, resulting in disruption of gene transcription.

BET inhibitors bind with high affinity to the binding pockets in BETs proteins, thereby resulting in displacement of BET proteins from chromatin. The therapeutic potential of these antagonist molecules has been explored for treatment of various malignancies, but also to dissect the mechanisms of BET regulation in a variety of systems (Junwei Shi and Vakoc 2014). Interestingly, BET inhibition targets gene transcription in a selective and cell-dependent manner which could be caused by BET proteins occupancy at enhancer elements (Lovén et al. 2013a). As an example, BRD4 has been found to bind chromatin at promoters and active enhancers, and its occupancy pattern correlates with that of active histone marks, such as H3K27ac (Lovén et al. 2013a). The ablation of BRD4 from such regulatory elements, by inhibition treatment, leads to dysregulation of nearby genes (Delmore et al. 2011a). However, association of enhancers and genes based on genomic distance is a poor predictor of direct regulation. As enhancer activation is a dynamic process during cell cycle and differentiation, it is

reasonable to speculate that BET inhibition effect is cell stage-dependent as well as cell type-dependent.

BET inhibition targets all BET proteins, and therefore disrupts BET complexes that regulate cell differentiation. My previous results show that iPSCs are capable of differentiating into MKs in the absence of BRD3. Although, the requirements of other BET proteins during megakaryopoiesis, and the timing of their function, are unknown. Additionally, BET proteins present in the complexes could potentially compensate for the absence of BRD3. Therefore, I used BET inhibition to investigate the effects of disrupting BET complexes at different stages of differentiation. The results of these experiments could also help unveil the possible role of BRD3 in BET-containing transcriptional complexes during megakaryopoiesis, by comparison with BRD3 KO experiments previously described. Due to the structure similarities between BETs, protein-specific inhibitors have not yet been developed and all BET inhibitors target BET proteins indiscriminately, although with different affinities. In my experiments I used BET inhibitor PFI-1, a molecule that binds preferentially to BRD2 and BRD4 (Picaud et al. 2013). That study showed that, in a leukemic cell line model, this inhibitor causes G1 cell-cycle arrest and induces apoptosis by displacing BRD4 from the chromatin.

My inhibition experiments were initiated by identifying the maximum inhibitor concentration tolerated by iPSCs. By using a concentration at which iPSC survive, I was able to discriminate between the outcomes of inhibition during FoP and the possible side effects on cell proliferation. This experiment was followed by a series of experiments to evaluate the impact of BET inhibition on MK generation. Finally, I inhibited different stages of MK differentiation and evaluated outcomes based on cell surface stage-specific markers. Thus, blood-committed cells were identified based on expression of transmembrane glycoprotein CD34 (Sidney et al. 2014) and transmembrane leukosialin CD43 (Kessel et al. 2017); MK progenitors and immature MKs were identified based on CD41a and CD235a as described previously in section 3.1.

3.3.2 Results

3.3.2.1 BET inhibition on iPSC proliferation

BET proteins have been shown to play important roles in stem cell cycle and proliferation, and it was important to identify concentrations that would not affect cell proliferation to isolate the real effect

on differentiation from a collateral effect on proliferation. This way, any adverse effects observed during MK differentiation would be due to the BET biological inhibition during differentiation rather than an effect on initial iPSC proliferation. The rationale for this experiment was that the highest concentration with no effect on iPSC would be used in the MK forward programming.

The first experiment to test the effect of BET inhibition on iPSC proliferation was performed at concentrations ranging from 1nM to 0.2µM. These concentrations were based on literature where the same BET inhibitor was used (Picaud et al. 2013). The experiment was initiated by seeding iPSC cells (A1ATD1-c WT) at 2e4 cells/well in 24 well plates pre-coated with vitronectin. BET inhibition was initiated 24 hr post-seeding. The inhibitor was reconstituted in DMSO and further dilutions were completed in media by sequential dilution. Control wells were fed with either regular iPSC media with no DMSO (-DMSO), as a control for normal cell proliferation; or media supplemented with DMSO (+ DMSO), as a control for DMSO effects on proliferation. The concentration of DMSO used in the control was equivalent to the concentration of DMSO present in the highest concentration of inhibitor. Triplicates for each condition were set in each plate and 3 plates were set up to allow timeline analysis. Cultures were fed daily for 5 days. At days 1 (D1), 3 (D3) and 5 (D5) a plate was fixed to perform crystal violet assay (2.2.14). The results of this experiment are shown in figure 3.3.1.

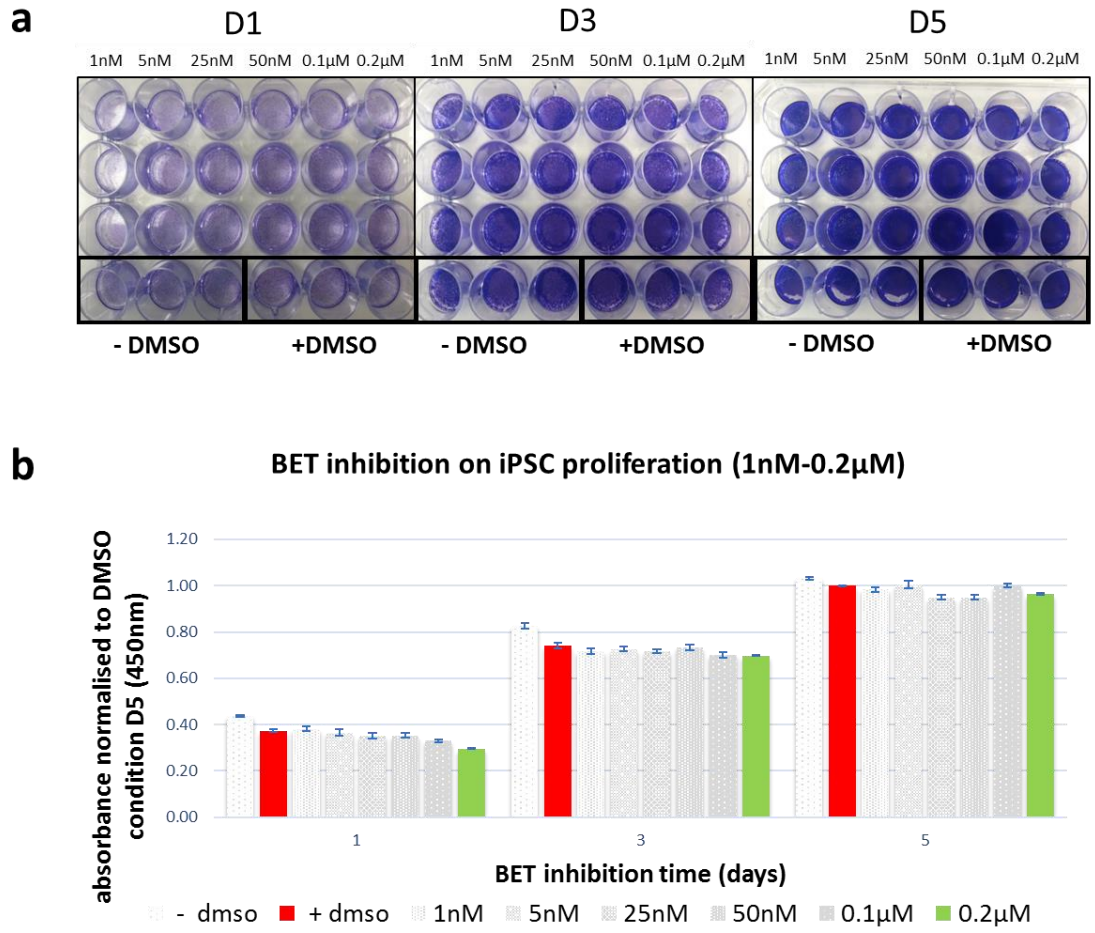

Figure 3.3.1 BET inhibition at 1nM - 0.2µM does not affect iPSC proliferation. iPSC WT were seeded on vitronectin coated 24 well plates. 24hr later, inhibition treatment was initiated with media containing BET inhibitor in concentrations ranging from 1nM to 0.2µM. Control conditions included iPSC routine media (-DMSO) to monitor against iPSC normal growing conditions, and media with DMSO (+DMSO) as DMSO was used to reconstitute the inhibitor. **(a)** Images of cultures stained with crystal violet. Cultures were fixed at 3 time points (D1, D3 and D5) and crystal violet proliferation assay performed. At each time point, the staining was very similar among all the conditions tested. **(b)** Normalised absorbance readings. Readings were recorded at 450nm and normalised to the highest absorbance reading of DMSO control on D5. All concentrations tested (including the highest = 0.2µM, in green) showed similar absorbance readings to control conditions (+DMSO in red), pair end t-test vs DMSO at each time point, n=3.

BET inhibition at concentrations between 1nM and 0.2µM did not affect iPSC proliferation. For each time point, crystal violet staining was homogenous throughout the plates, indicating no difference in proliferation among all conditions (figure 3.3.1.a). The staining was more intense for older cultures indicating that cultures were proliferating along the timeline of the experiment. Both control conditions (- DMSO and + DMSO) stained similarly, suggesting that DMSO did not affect cell proliferation. Similarly, none of the inhibitor concentrations tested decrease proliferation. This result was confirmed by absorbance readings, as all the conditions tested were similar to the controls at the

same time point. Absorbance readings were normalised to the +DMSO control condition at D5. Figure 3.3.1.b clearly shows the increase in absorbance as a result of increased cell numbers, and independent of culture condition. The tested inhibitor concentrations did not cause an effect on proliferation, as even the highest concentration tested (0.2µM) showed similar absorbance to both control conditions. Therefore, I hypothesised that the tested concentrations might have been too low, and the experiment described below was performed to test a higher range of inhibitor concentrations.

In the second experiment, in addition to identify the inhibitor concentration that affects iPSC proliferation, I also wanted to investigate whether BRD3 KO cells respond differently to BET inhibition than WT cells. Therefore, the experiment was performed with WT and KO cells. The experiment was performed with inhibitor concentrations ranging from 0.2µM to 10µM. The lowest concentration (0.2µM) was the highest concentration tested in the previous experiment. The experiment was initiated by seeding iPSC cells (A1ATD1-c WT and BRD3 KO) at 2e4 cells/well in 24 well plates. The inhibition initiation and culturing conditions were similar to the previous experiment. The same set of controls as in the previous experiment were used. Triplicates for each condition were set up and cultures were maintained for 4 days (3 inhibition days). The cultures were stopped earlier than on the previous experiment, as severe differences were observed and some of the cultures did not survive for longer than 4 days. Results are shown in figure 3.3.2.

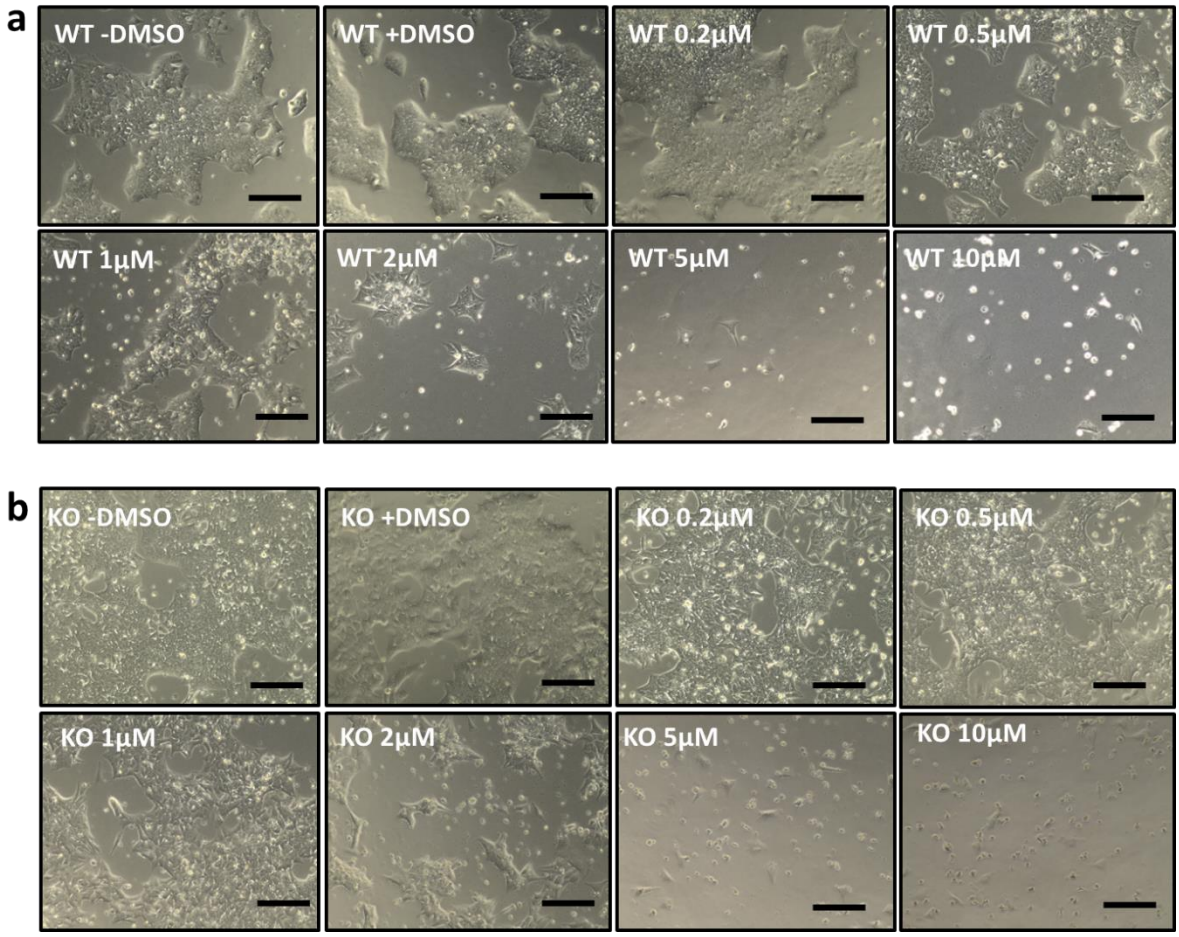

Figure 3.3.2 Morphological analysis show effect of BET inhibition on iPSC proliferation. WT and BRD3 KO cells were seeded at 2e4 cells/well and treated with concentrations of BET inhibitor ranging from 0.2µM-10µM. Control conditions included media-only (-DMSO) and media supplemented with the highest DMSO concentration used to reconstitute the inhibitor (+DMSO). Representative images show that the effect of BET inhibition on iPSC proliferation is concentration-dependent. Scale bars, 250 µm.

Representative microscopy pictures show a concentration-dependent effect of BET inhibition on iPSC proliferation (figure 3.3.2). For both WT (figure 3.3.2.a) and BRD3 KO (figure 3.3.2.b), the control conditions, and the lower concentration of inhibitor (0.2 µM), presented a high cell monolayer coverage as a result of high proliferation. These cells formed large colonies with defined edges, characteristic of iPSC. Morphological changes were observed at concentrations higher than 0.2 µM with colonies presenting a fibroblastic appearance (spindle appearance). The severity of this phenotype was directly associated with inhibitor concentration (figure 3.3.2.a and b). A decrease in cell numbers (based on visual observation) was also directly correlated with increase in inhibitor concentration. Complete cell death was observed at 5µM and 10µM (figure 3.3.2.a and b, bottom right). The effect of BET inhibition on iPSC proliferation was similar between WT and BRD3 KO cells.

In order to quantify the inhibitor effects observed on iPSC proliferation, I performed a crystal violet proliferation assay. At day 4, the cultures were fixed and stained with crystal violet. The dye was dissolved and absorbance readings of the solubilised dye were recorded (section 2.2.14). Darker staining, and consequently higher absorbance values, are directly associated with higher cell numbers. The results of this proliferation assay are represented in figure 3.3.3.

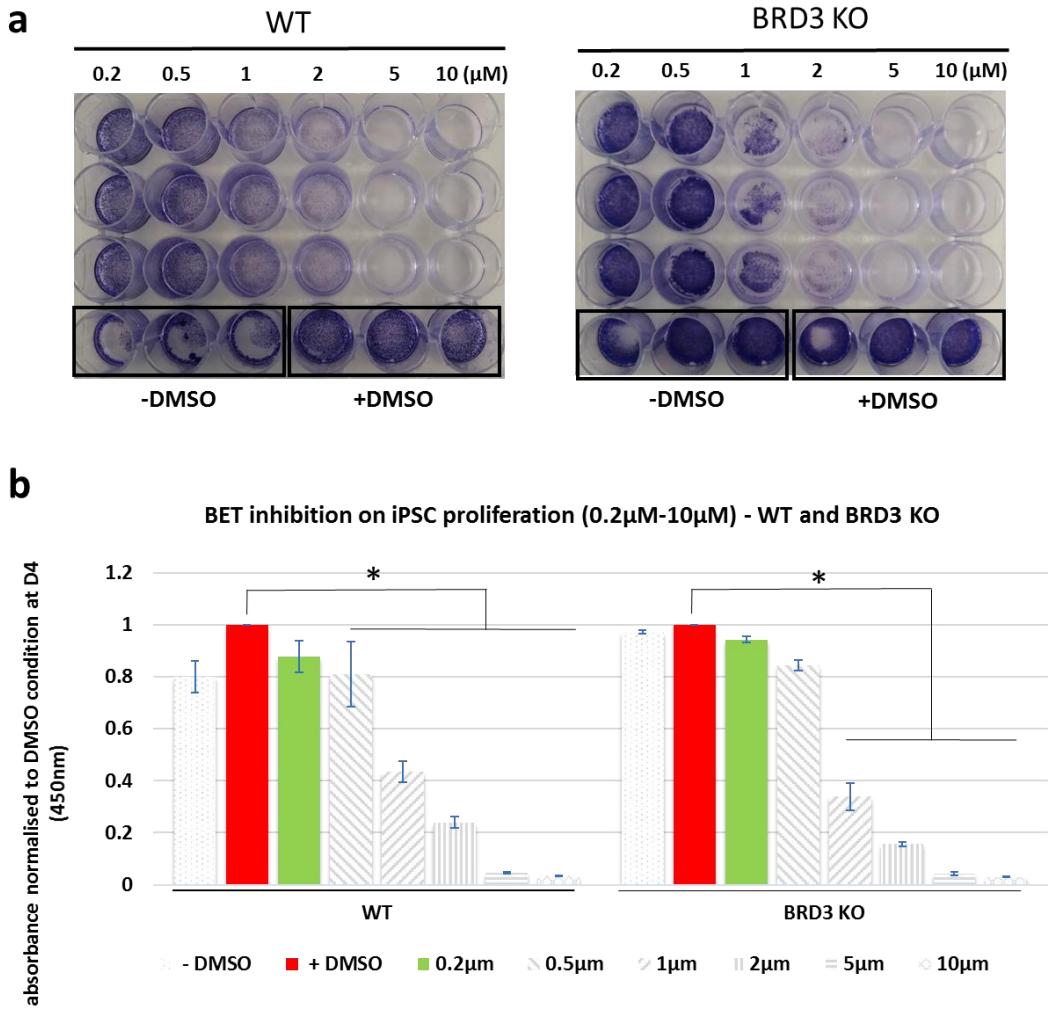

Figure 3.3.3 Crystal violet assay confirms BET inhibition effects on iPSC proliferation for inhibitor concentrations higher than 0.2µM. Cultures pictured in figure 3.3.2 were fixed with glutaraldehyde and stained with crystal violet. **(a)** Images of culture plates stained with crystal violet solution. WT and KO cells present similar levels of stain for similar conditions. Controls and lower inhibitor concentrations resulted in darker staining, confirming higher cell proliferation. A decrease in colour intensity was observed with the increase in inhibitor concentration. **(b)** Normalised absorbance reading of crystal violet. The crystal violet dye was extracted from the cells monolayer and the solution collected for reading absorbance at 450nm wavelength. Mean of normalised values to DMSO ± SD, n=3, *p<0.05 two-tail t-test against DMSO.

Crystal violet stained cultures (WT and BRD3 KO) confirmed the concentration-dependent effect of inhibition on iPSC proliferation. Image 3.3.3.a shows the culture plates stained with crystal violet. Each plate contains triplicates of all experimental conditions. Staining confirmed the inhibitor concentration effect observed with microscopy for both WT and BRD3 KO cells. Control conditions show intense staining similarly to conditions with lower inhibitor concentrations. For conditions with high density of cells, some of the cell monolayer lifted during the assay processing, hence some missing staining is seen in figure 3.3.3.a. Higher concentrations (5 µM and 10 µM) presented clear wells, as a result of cell death.

Figure 3.3.3.b shows the absorbance readings for both WT and BRD3KO. The values were normalised to +DMSO condition for two reasons: firstly, as in the previous experiment, this condition represents a more accurate control as it contains the DMSO present in the inhibitor conditions, which could potentially have an effect on proliferation independently from the inhibitor effect; secondly, the stained cell monolayer in the -DMSO control condition was significantly affected by processing, particularly in the WT plate, introducing an error in the absorbance readings. Absorbance readings confirmed the BET inhibitor concentration effect on iPSC proliferation. Lower concentration tested (0.2 µM in green) showed significantly similar readings to control (+DMSO in red) as in the previous experiment (figure 3.3.1) where this was the highest concentration tested. Absorbance readings between WT and KO were very similar for each condition. Statistically significant differences in absorbance were recorded for concentrations higher than 0.2 µM (for WT) and 0.5 µM (for BRD3 KO). For both clones, the normalised readings steadily decrease with the increase of inhibitor concentration. This correlation suggests a direct association between proliferation of cells and the BET proteins function.

3.3.2.2 BET inhibition on MK FoP – inhibitor concentration test

The results shown above demonstrate that BET inhibition severely affected iPSC proliferation at concentrations higher than 0.2µM. That experiment also showed that low concentrations of BET inhibitor used (< 0.2 µM) are tolerable by iPSCs. Following these results, I interrogated whether BET inhibition affects MK formation. In order to study BET inhibition on MK generation, 3 concentrations were tested: 2nM, 20nM, 200nM. These concentrations are within the concentration range that did not affect iPSC proliferation (lower and equal to 0.2µM). These concentrations were chosen in order to separate the inhibitor effects on proliferation from the effects on differentiation.

BET inhibition was administered from day 1 (1i) during the forward programming protocol (figure 3.3.4). The choice of inhibition starting day was based on the FoP timeline (figure 3.3.4.a). On day 0, cells were infected with viruses containing the TFs, and in order to keep this step undisrupted, inhibition was initiated on day 1 (day after infection). A +DMSO control condition was included as this was the vehicle used to dissolve the inhibitor. DMSO was used at the equivalent amount present in the highest inhibitor concentration (200nM). Cells were cultured as an adherent monolayer, and fed with media supplemented with inhibitors until day 10. At day 10, cultures were dissociated and stained with surface markers CD235a and CD41a. Population analysis was performed by flow cytometry. Day 10 cultures normally present a major population of $CD235a^+$ cells, and a secondary population of $CD235a^+/CD41a^+$ cells, indicating the presence of MK progenitors.

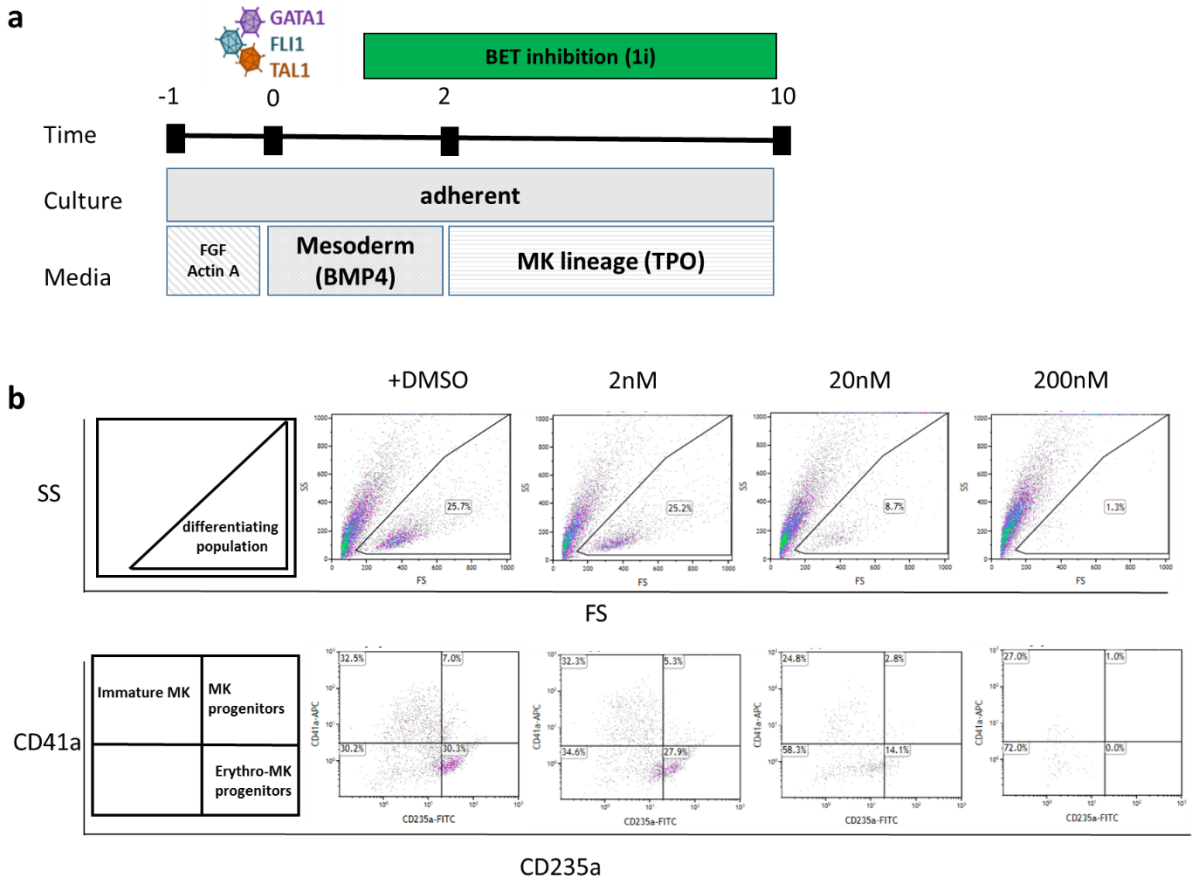

Figure 3.3.4 BET inhibition at Fop-day 1 (1i) affects MK progenitor differentiation. (a) Schematics of the experiment. Single-cell culture seeded for infection with virus containing 3 MK-specific TFs. Cultures were fed according to the FoP MK protocol. Inhibition was started at day 1 (1i) with BET inhibitor supplemented in the media at 2nM, 20nM and 200nM. +DMSO control condition was included. Cultures were kept adherent until day 10 before dissociation and analysis. **(b)** Day 10 dissociated cells were stained with CD235a and CD41a antibodies and analysed by flow cytometry. FS

vs SS plots show gated differentiating population. CD235a vs CD41a plots show the stained populations within the differentiating population. BET inhibition severely affects formation of MK progenitors at concentrations equal and higher than 20nM.

Results in figure 3.3.4 show that BET inhibition affects MK progenitor formation when initiated at day 1. Flow cytometry analysis of cultures at day 10 are shown in figure 3.3.4.b. The number of events identified in the differentiating population (in 3.3.3.b, top panel) was significantly affected at concentrations equal and higher than 20nM. The inhibition at the highest concentration tested (200nM) resulted in complete cell death. This inhibition effect was also observed in the generation of bi-potent (erythroid-MK) progenitor cells ($CD235a^+$) where concentrations ≥ 20nM severely reduced progenitor numbers (figure 3.3.4.b, bottom panel).

3.3.2.3 BET inhibition in MK FOP - day 1 vs day 10 inhibition (1i vs 10i)

The inhibition experiments described above show that BET inhibition at concentrations ≥ 20nM affects generation of MK progenitors (figure 3.3.4), but not iPSC proliferation (figure 3.3.1). The results on generation of MK progenitor were observed with inhibition initiated at an early stage of differentiation. However, the experiments described do not explore the effect on BET inhibition at later stages of MK differentiation. In order to study BET requirement at later stage of MK differentiation, the following experiment was designed with inhibition initiated when cells are already committed to the MK lineage ($CD235a^+/CD41a^+$). The MK-lineage committed population is generally observed at day 10 of the FoP MK protocol, hence this was the time point selected to start inhibition at later stage (10i). In addition, early inhibition (1i) was also included in this experiment to confirm the results obtained in the previous experiment. The same concentrations of inhibitor were tested (2nM, 20nM and 200nM).

The experiment was initiated by setting up a FoP MK run. Three replicates were subjected to BET inhibition on day 1 (1i) at three different concentrations: 2nM, 20nM and 200nM. Controls included +DMSO (DMSO 1) and –DMSO (figure 3.3.5). Cultures were kept adherent until day 10, when all cells were dissociated and stained with CD235a and CD41a antibodies for flow cytometry analysis. From day 10 onwards, three replicates cultures were subjected to BET inhibition (10i) at the same concentrations as 1i, and three +DMSO controls were included (DMSO 10). Cultures were kept in suspension until day 20 with regular feeds, following the FoP MK feeding schedule. Flow cytometry

analysis for CD235a, CD41a and CD42b was performed at days 10 and 20 for 1i and 10i cultures. Day 10 results (for 1i cultures) were similar to the previous experiment (Appendix 6.2). Figure 3.3.5.b shows results for this experiment at day 20 (1i and 10i, respectively).

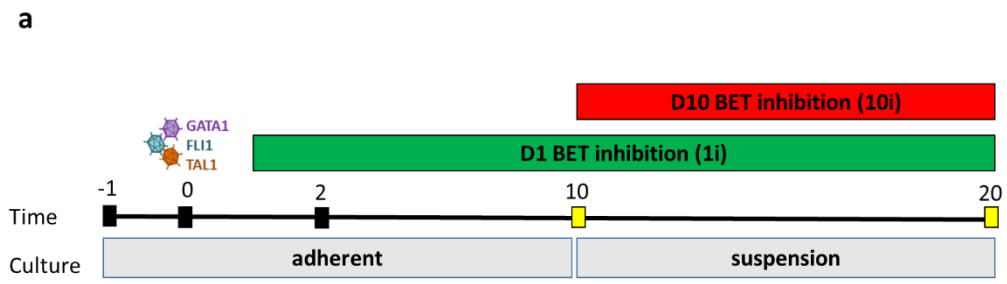

Figure 3.3.5 BET inhibition affects early stage of MK differentiation (1i), but not late differentiation (10i). (a) Experiment schematics. iPSC WT were single-cell seeded and infected with viruses containing the ORF for 3 TFs. BET inhibition was initiated either at day 1 (1i in green) or day 10 (10i in red). Three concentrations were used: 2nM, 20nM and 200nM. DMSO control included at equivalent amount used to resuspend the highest concentration of inhibitor (200nM). Samples were stained with antibodies against CD235a, CD41a and CD42b and analysed by flow cytometry at day 10 and day 20 (yellow time points).

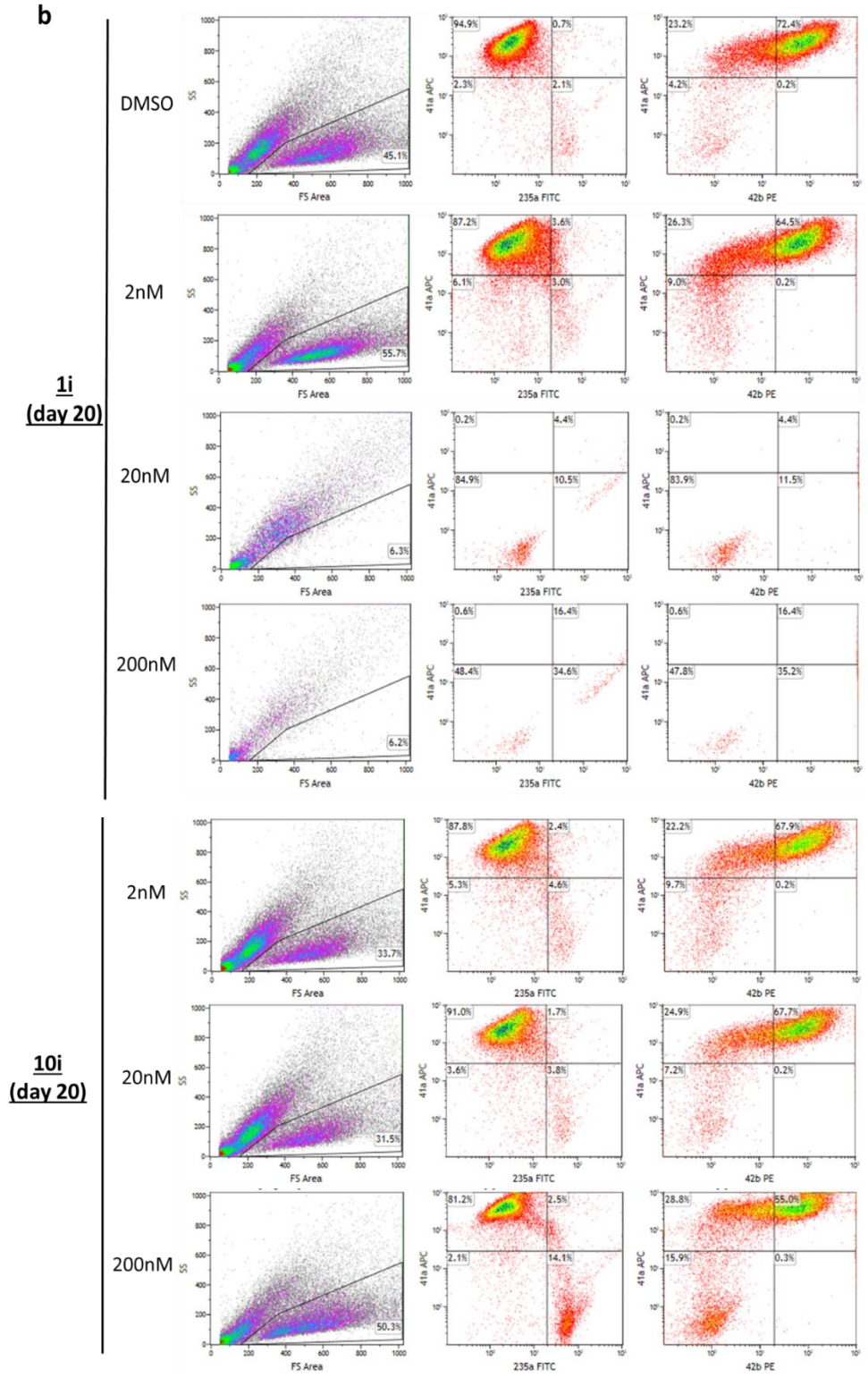

(b) Flow cytometry results at day 20 for 1i cultures (same cultures as in (b)) and 10i cultures. Cells stained with antibodies against CD235a, CD41a and CD42b to analyse MK progenitor population ($CD3235^{+}/CD41a^{+}$) and mature MK population ($CD41a^{+}/CD42b^{+}$).

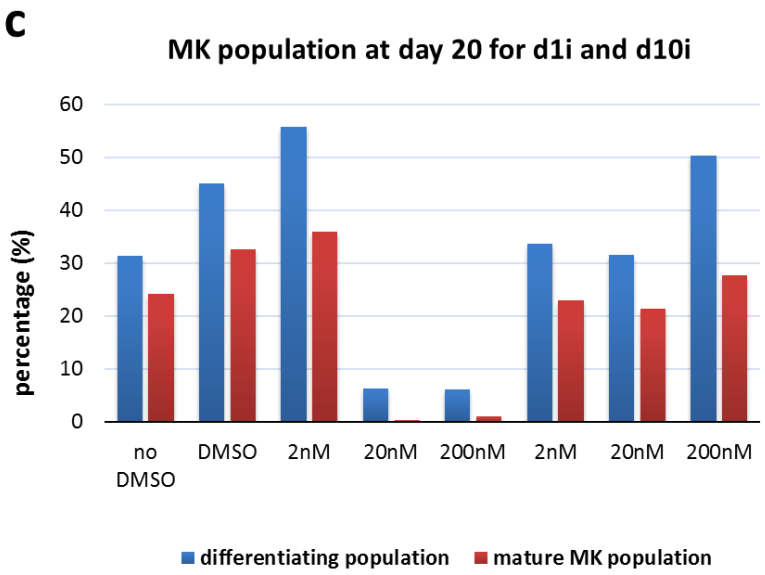

d) Comparison of differentiating population (FS vs SS) and MK mature population ($CD41a^+/CD42b^+$) at day 20 for all inhibition conditions (n=1). MK generation was observed in all conditions, except in 1i at concentrations 20nM and 200nM.

BET inhibition affects early stages of MK differentiation. Flow cytometry results demonstrate that early BET inhibition (1i) affects megakaryopoiesis prior to MK progenitors ($CD235^+/CD41a^+$) differentiation (figure 3.3.5.b). At day 10, differentiating population (identified in FS vs SS plot) was not observed for inhibitor concentrations higher than 2nM (i.e. 20nM and 200nM). At the lowest concentration used (2nM), a lower number of events was observed, but the differentiation pattern of the progenitors was similar to DMSO control. The affected cultures (20 nM, 200nM) did not recover from the effects of early inhibition (figure 3.3.5.c). Day 20 analysis of these cultures (20nM and 200nM) show an absence of differentiated population. Cultures inhibited with 2nM recovered after day 10, and the population profile was similar to DMSO control with progenitors loosing CD235a ($CD41a^+/CD235a^-$) and gaining CD42b ($CD41a^+/CD42b^+$) indicating MK maturation (figure 3.3.3.c, top panel).

BET inhibition from day 10 did not affect megakaryopoiesis. At day 10, when 10i cultures were treated with the inhibitor, MK progenitors ($CD235a^+/CD41a^+$) represented 50% of the live population of cells (fig 3.3.5.b). These cultures were not affected by inhibition, at any of the tested concentrations, as day 20 results show mature MKs in culture (figure 3.3.5.c, 10i). Interestingly, the 10i cultures at the highest concentration, 200nM, show a slight delay in MK maturation in comparison with the other conditions. Flow cytometry analysis of this culture (10i at 200nM) at day 20 shows that 15% of the differentiating population did not acquire CD41a, remaining only $CD235a^+$. This differentiation delay could be the result of inhibition on cells that at day 10 were at an early differentiation stage than rest of the

population. Altogether, the results of this experiment show that early megakaryopoiesis stages, but not late stages, are affected by BET inhibition at concentrations that do not cause an effect on iPSC proliferation (≥20nM) (figure 3.3.5.d).

3.3.2.4 Defining the megakaryopoiesis stage affected by BET inhibition

The effect of BET inhibition on early megakaryopoiesis was confirmed in the experiments described above. However, the mechanism by which BET proteins regulate early megakaryopoiesis has not been previously studied. The experiment described below aimed at identifying the megakaryopoiesis stage affected by BET inhibition. To do so, samples from inhibited cultures (and corresponding DMSO controls) were characterised at different time points, based on surface markers characteristic of early MK differentiation stages: haemogenic endothelium (CD144 and CD309), blood-lineage commitment ($CD43^+/CD34^+$), MK progenitors ($CD41a^+/CD235a^+$) and immature MKs ($CD41^+/CD235^-$). Inhibition was initiated at days 1, 5 or 10 (1i, 5i and 10i) and samples were stained with antibodies for flow cytometry analysis at days 5, 10, 15 and 20. Haemogenic endothelium staining is not shown as at day 5 cultures were no longer staining positive, either because the timeframe for expression of these markers had been missed, or this stage is non-existent in FoP cells. Figure 3.3.6 shows the results for 2 experiments performed: experiment 1 only included one replicate, and experiment 2 was performed in triplicate.

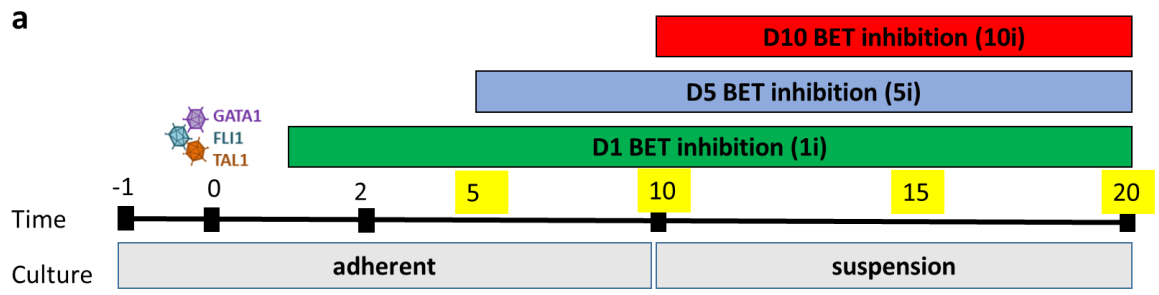

Figure 3.3.6 BET inhibition affects early differentiation and MK-lineage commitment. iPSC cells were differentiated into MKs using FoP. BET inhibition was initiated at days 1, 5 and 10 (i1 (green), 5i (blue) and 10i (red)) and samples analysed at days 5, 10, 15 and 18/20 (yellow). Results of flow cytometry analysis for blood-commitment ($CD34^+/CD43^+$) and MK lineage commitment ($CD41a^+/CD235a^+$) overtime are shown in b) c) and d). Photos of cultures at day 10 are shown on e).

b

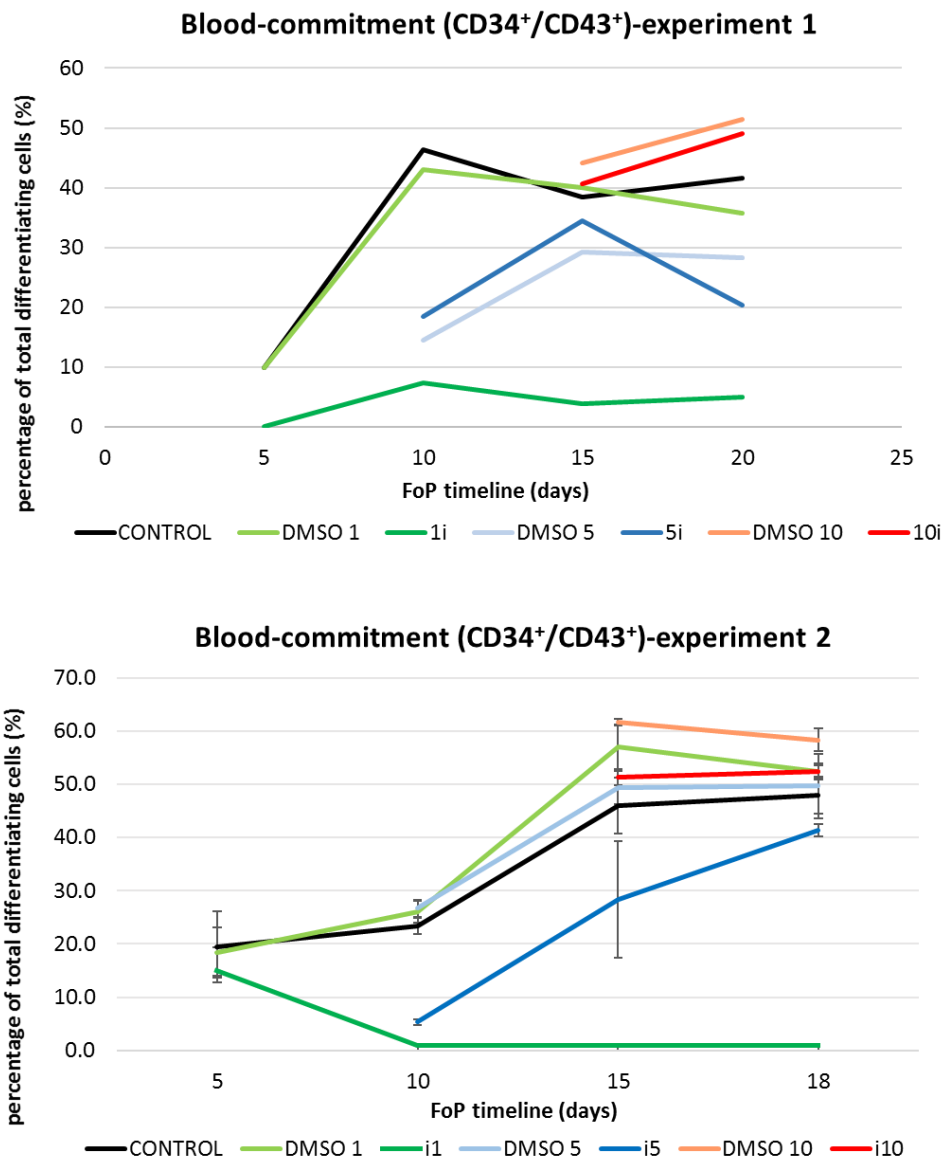

b) Development of blood-committed cells in BET inhibited cultures over time. Samples were stained with antibodies against CD34 and CD43 markers. Control cultures shown in black. Inhibition conditions (1i, 5i and 10i are shown in dark colours) and corresponding DMSO controls (DMSO 1, DMSO 5 and DMSO 10) are shown in light colours. Top plot shows results for experiment 1 (n=1) and bottom plot shows results for experiment 2 as mean percentage of ($CD34^+/CD43^+$) cells ± SD (n=3). Blood-commitment was impaired with BET inhibition from day 1, and significantly affected with BET inhibition from day 5.

c

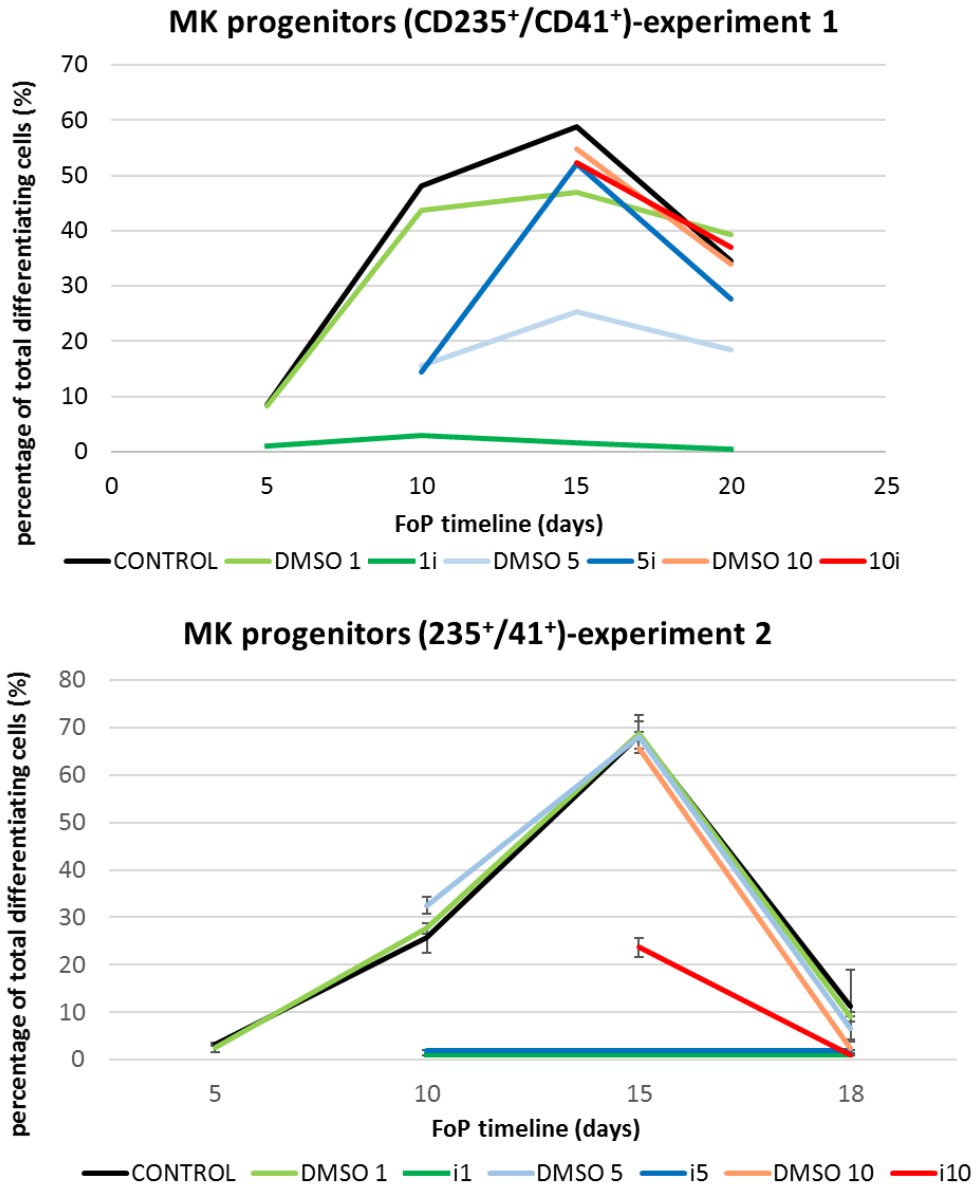

c) Development of MK progenitor ($CD235a^+/CD41a^+$) cells in BET inhibited cultures over time. Differentiation of MK progenitors was impaired with BET inhibition from day 1 (dark green) in both experiments. In experiment 2 (bottom) 5i also impaired MK progenitor generation and 10i was significantly affected. Top plot shows experiment 1 (n=1) and bottom plot shows results for experiment 2 as mean percentage of ($CD235a^+/CD41a^+$) cells ± SD (n=3).

d

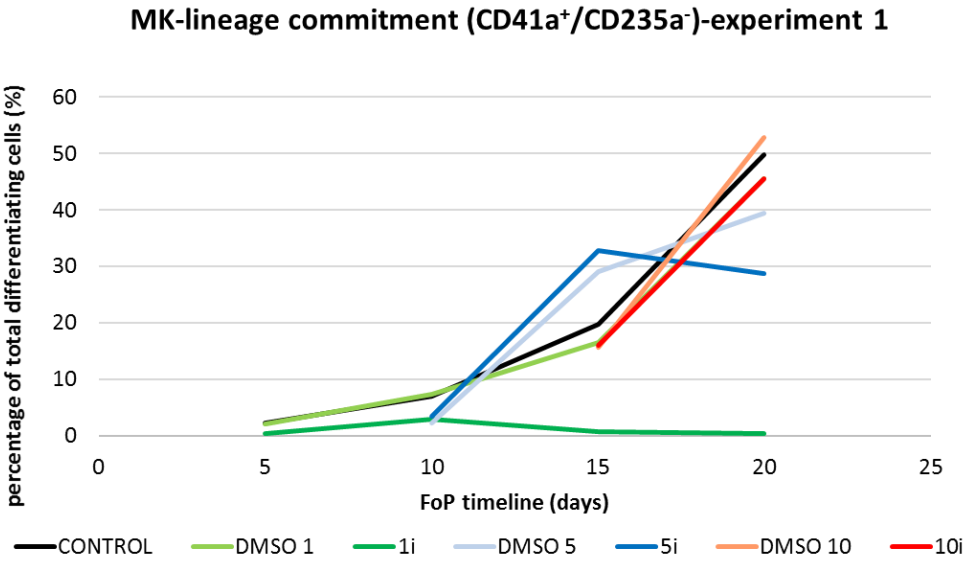

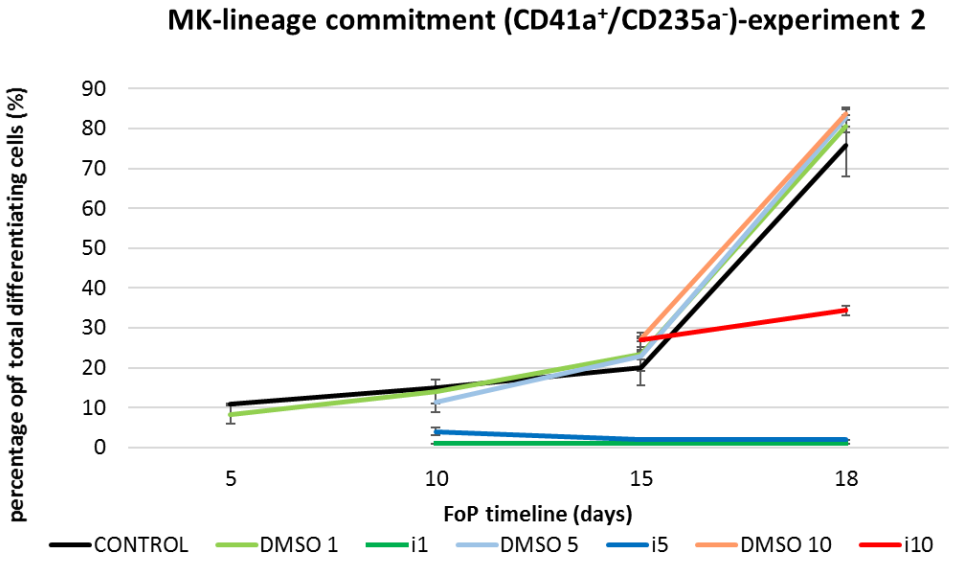

d) Development of MK-lineage committed cells in BET inhibited cultures over time. Samples stained with antibodies against CD235a and CD41a. Populations shown have lost CD235a and retained CD41, prior to expression of CD42b. In both experiments, 1i cultures did not form immature MKs. In experiment 2, 5i also failed to generate MKs and 10i cultures were significant affected with a decreased percentage of immature MK in culture. Top plot shows experiment 1 (n=1) and bottom plot shows results for experiment 2 as mean percentage of ($CD41a^+/CD235a^+$) cells ± SD (n=3).

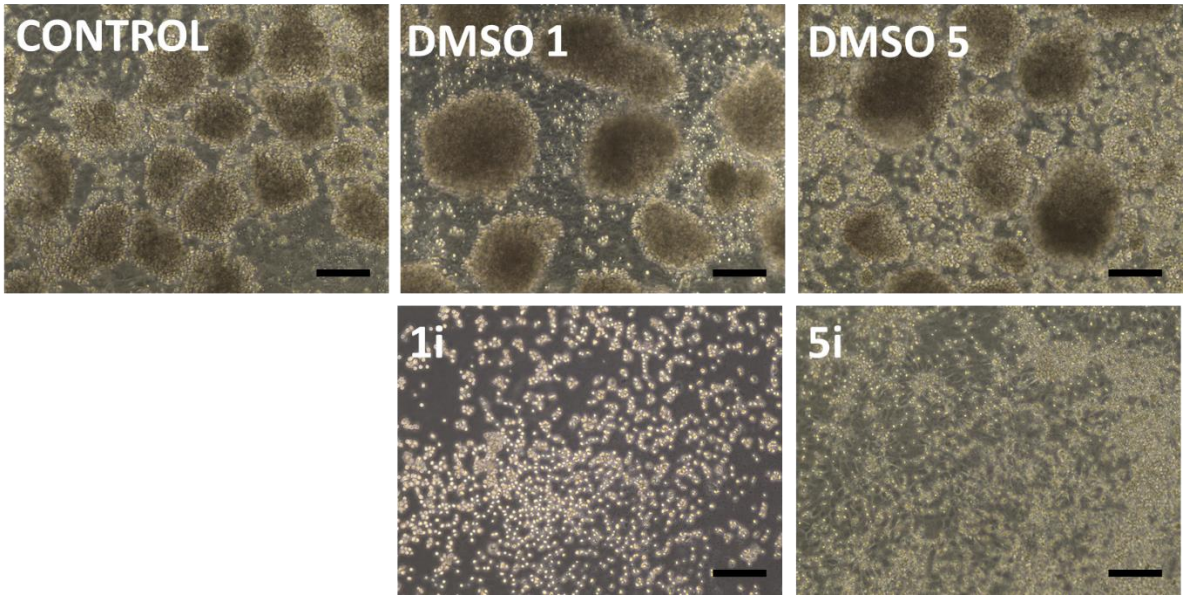

e) Light transmission images of cultures at day 10 prior to dissociation (experiment 2). All control conditions presented cell clumps in suspension, characteristic of differentiating FoP cells (generally $CD235a^+/CD41a^+$). Inhibited cultures at day 1 (1i) and day 5 (5i) presented undifferentiated single-cells in suspension. Scale bars, 250 µm.

BET inhibition impaired MK differentiation prior to blood-commitment as well as MK progenitor commitment. In experiments shown in figure 3.3.6, condition 1i did not differentiate and eventually died. In both experiments, generation of blood-committed cells ($CD34^+/CD43^+$) was severely impaired in 5i cultures (figure 3.3.6.b, dark blue). When inhibition was initiated (day 5), control cultures were equally around 10%-20% $CD34^+/CD43^+$ in both experiments. The development of these cells over time was very similar in both experiments. Interestingly, the development of MK progenitor cells ($CD235a^+/CD41a^+$) was very different for 5i conditions in both experiments (figure 3.3.6.c dark blue). In experiment 1, 5i cells developed MK progenitors to a similar level to the control conditions, whilst in experiment 2 the cells in 5i condition did not survive. The same result was observed at the next stage of differentiation ($CD41^+/CD235a^-$ immature MKs) with 5i cells in experiment 1 forming immature MKs and 5i cells in experiment 2 not surviving. This difference in results is probably due to the disparity in differentiation pattern observed in both experiments. At day 10, control cultures in experiment 1 were 50% $CD235a^+/CD41a^+$ while in experiment 2 cultures were only 20% $CD235a^+/CD41a^+$ (figure 3.3.6.c, black). Differentiation of 10i cells was not affected in experiment 1, but differentiation was severely impaired in experiment 2. This suggests that BET proteins are required prior to MK progenitor generation.

3.3.3 Discussion

BET proteins have been shown to be part of multiprotein complexes playing important roles in transcription (Dawson et al. 2011). The role of these complexes, and individual BET proteins, in megakaryopoiesis has never been investigated. In this chapter, I described a series of experiments designed to study the effects of inhibiting BET proteins (BRD2, BRD3 and BRD4) during MK differentiation, in order to understand the requirements of these proteins during FoP of MKs. BET inhibitors have a high affinity to the BET family, and therefore are an important tool to study the roles of BET proteins in cell biology. Several BET inhibitors are currently being tested for the treatment of haematopoietic cancers and inflammatory diseases (Prinjha, Witherington, and Lee 2012). Understanding the functions of BET proteins in megakaryopoiesis will allow a better prediction of BET inhibition effects on MKs and platelets in patients undertaking the treatments.

BET proteins are required for iPSC maintenance as BET inhibition affects proliferation. The FoP protocol is established on iPSC, therefore this study was initiated with the determination of the inhibitor concentration range tolerated by iPSC. This allowed the uncoupling of the inhibition effects on cell proliferation from the effects on cell differentiation during FoP. Using proliferation assays, I determined that iPSC are resistant to the inhibitor used (PFI-1) at concentrations below 200nM (fig. 3.3.1, 3.3.2 and 3.3.3). In agreement with these results, the inhibitor has been shown to have a high affinity to all BET proteins at IC_{50} values ranging from 98nM-220nM for BRD4 (BD1, BD2) and 111nM for BRD2 (Picaud et al. 2013). In the same study, PFI-1 inhibitor was shown to affect cell survival of sensitive cells at concentrations higher than 100nM, and resistant cells did not respond to inhibition concentrations below 5-10µM. In my experiments, if the tested concentrations had no effect on iPSC proliferation, I would have further increased the inhibitor concentrations. If the iPSCs were insensitive to the inhibitor, this would suggest that BET proteins have no function on iPSC proliferation. However, the role of BET proteins on cell cycle progression has been extensively reported in human cell line models (LeRoy, Rickards, and Flint 2008a; Maruyama et al. 2002; Dey et al. 2000). In particular, BRD4 has been shown to stimulate G2/M transition (Dey et al. 2000) and regulate cell cycle progression (Dey et al. 2003). Therefore, my results on BET inhibition of iPSCs are aligned with previous reports. After determining the inhibitor concentration at which iPSCs were insensitive, I designed inhibition experiments to evaluate effects of BET proteins ablation on MK differentiation.

BET inhibition impaired early (1i), but not late (10i), MK differentiation, suggesting that BET proteins have a stage-dependent function in early megakaryopoiesis. At day 1 of FoP, cells are still very

immature and are cultured in mesoderm media (BMP4 supplementation), whilst at day 10 the presence of MK progenitors ($CD235a^+/CD41a^+$) is normally observed. In my experiments, a significant difference was observed in differentiation of progenitors and mature MKs following inhibition at different stages of FoP. Using flow cytometry analysis of cell surface markers, I observed that BET inhibition severely impaired megakaryopoiesis prior to MK progenitor stage (figure 3.3.6.b, c and d). These results suggest that BET proteins regulate early haematopoietic differentiation, but are dispensable after the generation of MK progenitors. If no significant differences had been found upon inhibition at neither stage, this would suggest that BET proteins do not regulate megakaryopoiesis. On the other hand, if inhibition affected several stages, it would suggest that BET proteins were essential throughout megakaryopoiesis.

These findings are consistent with earlier research on the effects of BET inhibition in early haematopoietic differentiation. It has been reported that BRD4 interacts with haematopoietic TFs, and BET inhibition suppresses the functional outcome of the haematopoietic TFs (Roe et al. 2015). Furthermore, BRD4 has been shown to interact with TWIST, a TF that controls mesodermal development, and this interaction is disrupted by BET inhibition (Jian Shi et al. 2014). In a different study, BRD4 knockdown affected mesodermal gene expression, indicating a BRD4 regulatory role in mesodermal differentiation (Rodriguez et al. 2014a). Thus, it can be hypothesised that the disruption of BRD4-TFs interactions could have affected mesoderm differentiation in 1i cultures. Interestingly, a study exploring the effects of BRD4 at different stages of thymocytes differentiation found that BRD4 deletion results in reduced proliferation rates and impaired early cell development (Gegonne et al. 2018). That study also showed that BRD4 deletion did not affect late stage of thymocytes differentiation, despite the protein normally being expressed at that stage. That report is in agreement with the hypothesis that BET proteins are required for the recruitment of cell-specific TFs and transcriptional regulatory complexes to chromatin during gene activation (Bhagwat et al. 2016b), but have a seemingly redundant function after cell-identity acquisition. In order to study which BET protein regulates early megakaryopoiesis, a ChIP experiment on BET proteins (especially BRD4 and BRD2) could be performed to investigate these proteins occupancy at genes whose transcription is affected by BET inhibition. Thus, if a gene promoter or enhancer was occupied by a BET protein, and its expression changed following BET inhibition, we could infer that the BET protein identified had an active role in regulation of those genes.

One significant flaw in my experiments, as mentioned in earlier sections, is the overexpression of TFs in the chosen differentiation model. In the context of BET inhibition, Lamonica *et al.* showed that BET inhibition displaces both BRD3 and GATA-1 from chromatin with inhibitory consequences in erythroid-

specific gene expression (Lamonica et al. 2011). However, this study only focused on the interactions between BRD3 and GATA-1, neglecting the possible contribution of other BET proteins in the regulation of GATA-1 target genes. In fact, a different study in erythropoiesis, showed that depletion of BRD2 fails to promote expression of GATA-1 target genes, similarly to the effect of BET inhibition (Stonestrom et al. 2015). Together, these studies show that BET inhibition affects GATA-1-dependent gene signatures in erythropoiesis, as BETs are required for stabilisation of GATA-1 under normal conditions. In my experiments, the failed differentiation of 1i cultures could be explained if BET proteins were required for GATA-1 recruitment only at early stages.

The discrepancy between the BRD3 KO results (section 3.1) and the inhibition results (section 3.3) on MK generation suggests distinct roles for BET proteins in megakaryopoiesis. Firstly, the BRD3 deficiency could be compensated by one of the other BET proteins. This, at least partially, compensation of protein functions has been previously suggested within the BET family as BRD2 compensates BRD3 during erythropoiesis (Stonestrom et al. 2015). This compensation would have been prevented in the inhibition experiments, explaining the discrepancy in results between BRD3 KO and inhibition experiments. Secondly, BET proteins BRD4 and/or BRD2 might be critical for MK differentiation either individually or as part of transcriptional complexes that are disrupted by BET inhibition. In order to clarify these hypothesis, I designed an experiment where BET proteins were ablated in iPSCs and differentiated into MKs. The BET KOs were designed either individually or in combination (e.g. BRD2 KO, BRD2+3 KO, etc) to understand individual, as well as compensatory functions between BET proteins during megakaryopoiesis. This experiment is described in section 3.4.

3.4 BET regulation in Megakaryopoiesis

3.4.1 Introduction

The results shown above led to the hypothesis that either BRD3 is not essential in megakaryopoiesis or its functions are compensated by one of the other BET proteins. If the compensation hypothesis was correct, it would explain the discrepancy between the inhibition and the BRD3 KO results, as the surrogate BET protein would be inactivated by inhibition. On the other hand, if BRD3 KO results are due to BRD3 simply being redundant, the inhibition experiments revealed the critical role of other BET proteins. Therefore, this section describes the experiments designed to investigate the role of individual BET proteins, and understand the possible compensatory effects among BET proteins during MK differentiation.

To investigate whether BET proteins compensate BRD3 absence, and/or which BET protein is essential for megakaryopoiesis, a knockdown experiment was initially designed. CRISPRi or RNAi are commonly used systems to generate selective knockdowns, and these methods differ mainly on their targets, as CRISPRi targets DNA while RNAi targets mRNA. CRISPRi offers lower off-target effects, and a cleaner depletion of the target gene than RNAi (Stojic et al. 2018). To perform the experiments in this section, I initially designed a system comprising stably expressed dCAS9 fused to a transcription repressor domain KRAB. Being an rTetR (reverse tetracycline repressor) inducible system, it would be induced in the presence of tetracycline, and this feature could be exploited at different stages of differentiation. This is an important feature, as it would be interesting not only to identify the essential BET(s) protein(s) in megakaryopoiesis, but also the timing when the protein is active. The system also contained sgRNAs targeting individual BET proteins promoters that, upon induction, lead the dCas9-KRAB to the target sequence. The plasmids containing dCas9-KRAB and BET-targeted sgRNA inserts were stably integrated into iPSCs by viral infection (plasmid maps in appendix 6.1.3). Unfortunately, the system failed to induce dCas9 once it had been induced once. This presented a challenge as upon the induction to verify integration, the system became unusable. Due to time constraints, the dCas9-KRAB system was not optimised, and this study plan was replaced by the generation of individual and combinations of BET KOs using CRISPR/Cas9n.

The aim of this experiment was to generate iPSCs deficient in individual or combinations of BET proteins (BET KOs), and differentiate these cells into MKs. The BET KOs included individual (BRD2 KO, BRD3 KO and BRD4 KO) and a combination of KOs (BRD2+3, BRD2+4, BRD3+4 and BRD2+3+4). This approach allows to evaluate the effects of each individual BET protein, as well as the possible redundancy in BET protein function, during the differentiation of MKs. Thus, for example if BRD2 compensates the absence of BRD3 in megakaryopoiesis as it does in erythropoiesis, the BRD2+3 KO would not be able to generate MKs, while the BRD2 KO could or not be successful. Equally, this experiment would help to reveal if one of the BET proteins was absolutely essential for MK differentiation, as all of the lines with a KO of the protein would not generate MKs.

3.4.2 Results

3.4.2.1 Design and synthesis of CRISPR/Cas9 system to target BRD2 and BRD4

The aim of this work was to generate BET KO cell lines using CRISPR technology. The strategy used was similar to the generation of BRD3 KO (section 3.1) with 2 sgRNAs and Cas9 nickase directed at the target region. The target regions for BRD2 and BRD4 were identified by evaluation of the protein-coding transcripts using Ensembl, followed by the selection of the transcripts significantly expressed in MKs using Blueprint data (transcripts with FPKM ≥1). The BRD2 and BRD4 targeted transcripts are listed in table 3.4.1.

PROTEIN	TRANSCRIPT	LOG2 FPKM IN MKS
BRD2	ENST00000374825	1.726150138
	ENST00000607833	3.567799186
	ENST00000449085	2.71428508
BRD4	ENST00000263377	1.681969935
	ENST00000371835	1.919117427

Table 3.4.1 **Targeted transcripts for BRD2 and BRD4 KO generation.** Transcripts significantly expressed in MKs, according to Blueprint data. Transcript information extracted from Ensembl.

The target sites were established based on the first common exon between the transcripts for each gene (figures 3.4.1 for BRD2 and 3.4.2 for BRD4). sgRNA sequences were designed using Wellcome

Trust Sanger Institute CRISPR online tool (https://www.sanger.ac.uk/htgt/wge/) with selection of the 25% best targets, based on sequence homology prediction (off-targets prediction).

3.4.2.1.1 BRD2 targeting

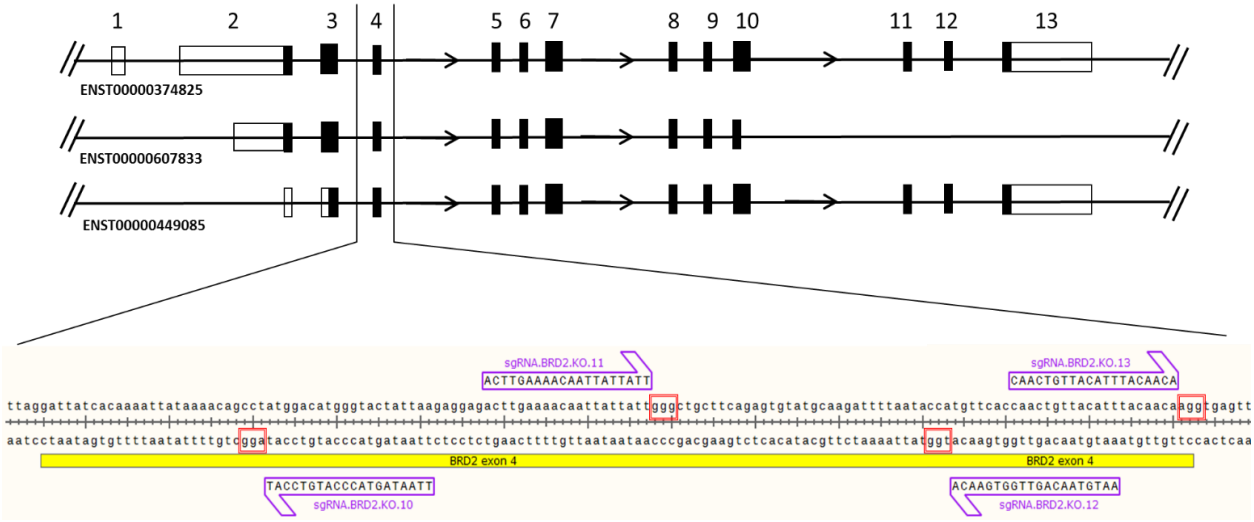

Figure 3.4.1 Schematics of BRD2 targeted transcripts. BRD2 transcripts expressed in MKs were identified from Blueprint data. First common exon (4) was selected to knockout all the protein variations in MKs. Within exon 4, sgRNA sequences were determined and sequence homology verified (BLAST) in order to minimize off-target effects. sgRNA sequences (purple) and PAM sequences (red boxes) shown.

Exon 4 of the BRD2 longer transcript is the first common exon among the BRD2 transcripts expressed in MKs, and therefore it was selected as the target region. Despite being a small exon (138 bp), four sgRNAs were identified with low sequence homology to other regions in the genome (verified by BLAST).

3.4.2.1.2 BRD4 targeting

The first common exon in both BRD4 transcripts expressed in MKs corresponds to exon 10 of the longer transcript, and therefore the BRD4 was targeted in 2 regions to avoid partial expression of transcript ENST00000263377 that could lead to a partially or completely active protein. Exons 10 and 11 were not targeted, despite being common exons between both transcripts, because the sgRNA sequences found in that region presented high homology with distant genomic regions (off-targets).

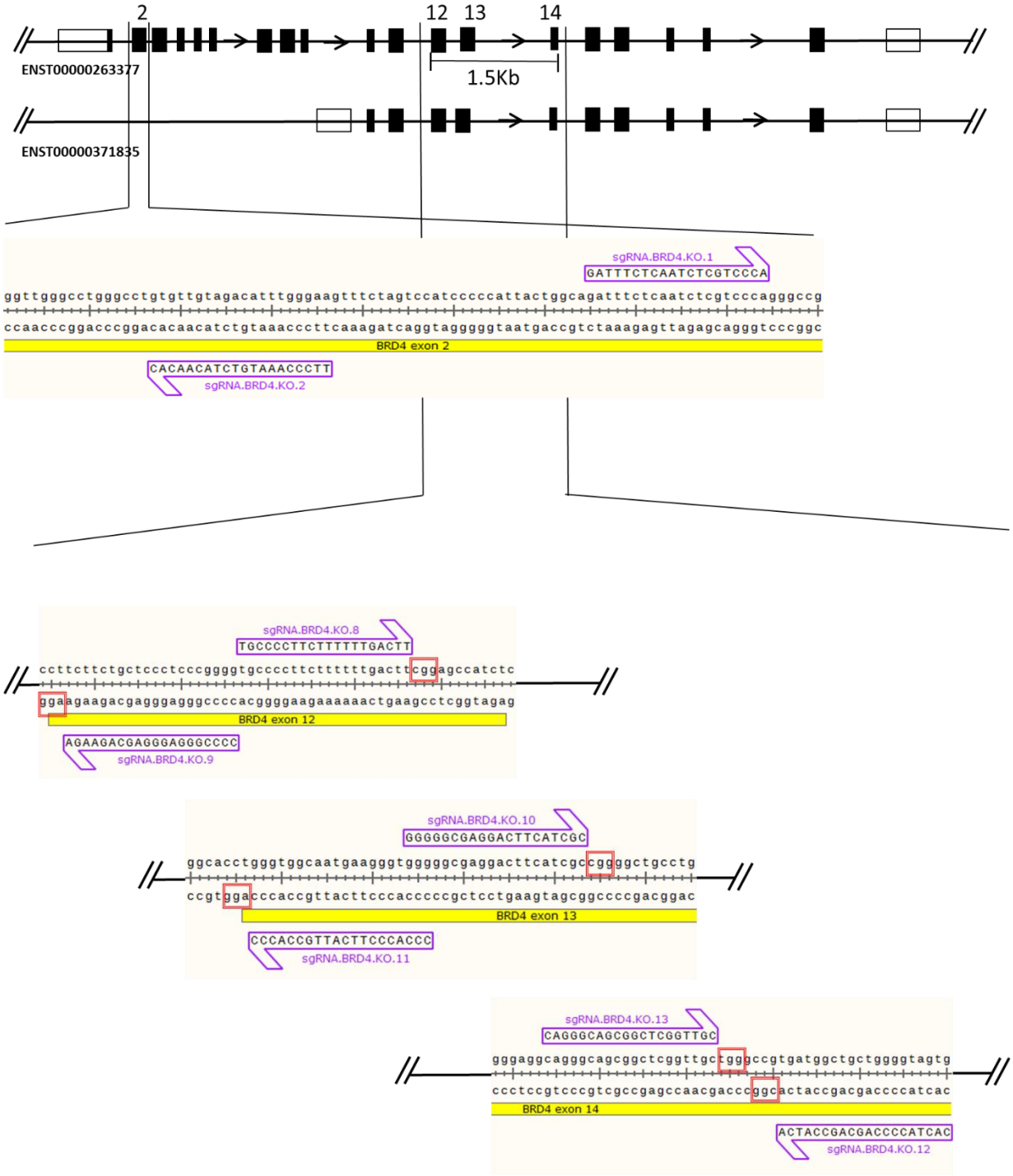

Figure 3.4.2 Schematics of BRD4 targeted transcripts. Two BRD4 transcripts expressed in MKs were identified from Blueprint data. Due to the transcripts significant length difference, two regions were targeted. sgRNA sequences were identified and sequence homology verified (BLAST) in order to minimize off-target effects. Exons 10 and 11 were not targeted due to high sequence homology with other regions that can lead to off-target effects. Exons 12, 13 and 14 are short exons, and therefore were all targeted to maximize success. sgRNA sequences (purple) and PAM sequences (red boxes) shown.

The selected sgRNAs were cloned into vectors *pSpCas9n(BB)-2A-**GFP*** (for BRD2 sgRNAs) and *pSpCas9n(BB)-2A-**tomato*** (for BRD4 sgRNAs) (section 2.2.10.2). The cloning success was confirmed by restriction digestion and Sanger sequencing (appendix 6.2.2 and 6.2.3), before the plasmids were expanded. T7 endonuclease (section 2.2.10.5) was performed to test target efficiency of the sgRNAs (figure 3.4.3). Primer sequences are listed in table 2.2.1.

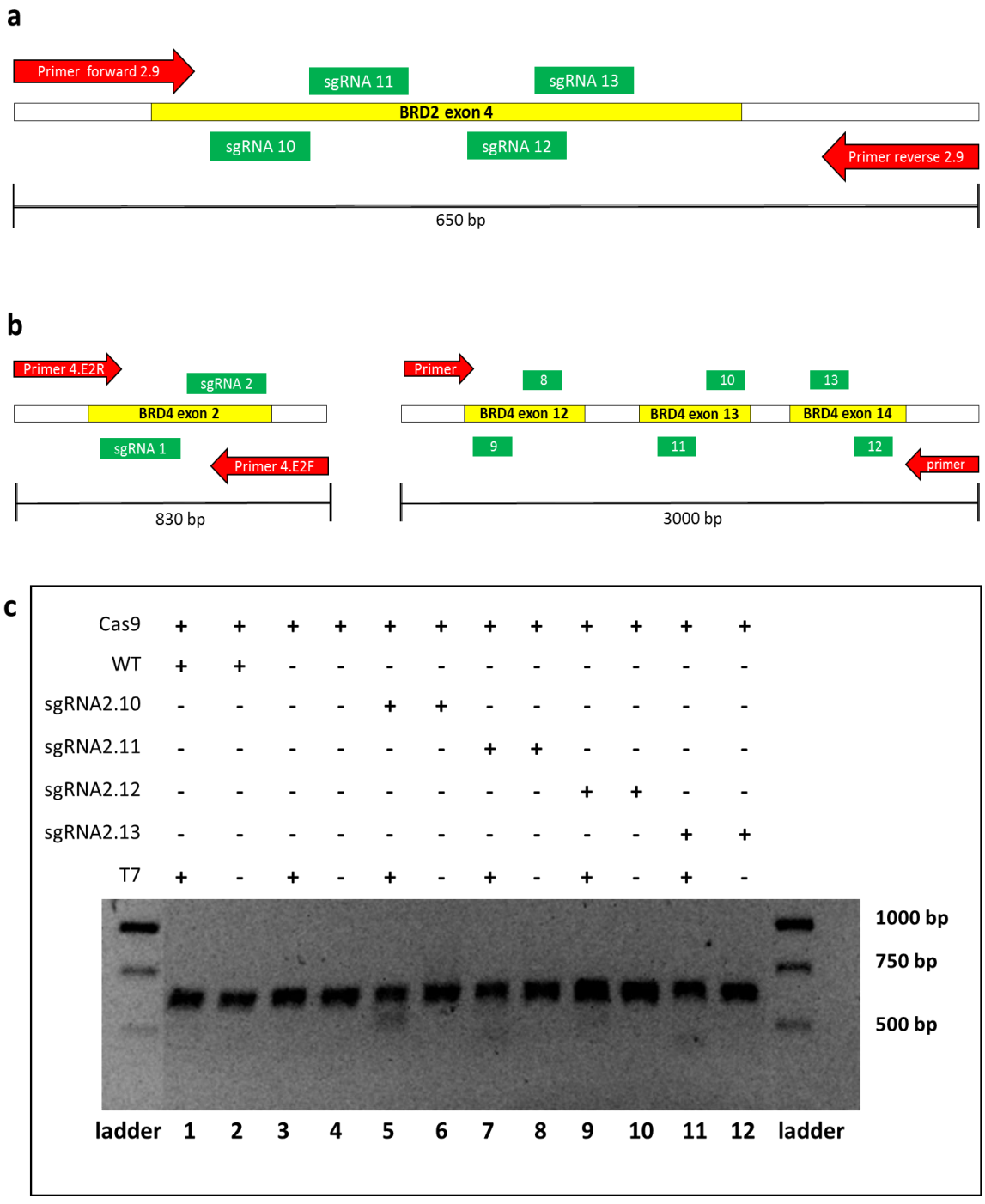

Figure 3.4.3 T7 endonuclease assay confirms BRD2 sgRNAs target efficiency. PCR strategy for T7 endonuclease for **a)** BRD2 and **b)** BRD4. **c)** BRD2 sgRNAs (10, 11, 12 and 13) located on exon 4 were

tested in the T7 assay. Gel showing T7 endonuclease assay results. HEK293T cells were transfected with sgRNAs targeting BRD2 locus and Cas9. gDNA extracted and PCR performed, before T7 endonuclease assay was complete. Results for individual sgRNAs transfections are shown in lanes 5 (sgRNA10), 7 (sgRNA11), 9 (sgRNA12) and 11 (sgRNA13). All of these sgRNAs successfully created indels at the BRD2 locus. WT (lane 1) and Cas9 only (lane 3), as well as non-T7 digested transfected conditions (lanes 2, 4, 6, 8, 10, 12) were loaded on a gel as controls for the T7 digestion.

All selected sgRNAs were successful as smaller bands than the WT band were observed. This indicates T7 endonuclease digestion at mismatches near the disrupted region. sgRNAs targeting BRD4 were not tested by T7 endonuclease as primers for the region had not been optimised. Although, the nucleofection for generation of the BET KOs was performed with BRD2 and BRD4 targeting sgRNAs.

3.4.2.2 Generation and confirmation of BET KO clones

Plasmids containing sgRNAs were nucleofected either into WT cells (for all BRD2 and BRD4 KO combinations) or into BRD3 KO cells (for all the combinations including BRD3 KO) (section 2.2.10.4). Combinations of sgRNAs nucleofected are listed in table 3.4.2.

TARGET KO	SGRNAS NUCLEOFECTED	IPSC LINE
BRD2	sgRNA.BRD2.KO_10,11,12,13	A1ATD1-c WT
BRD4	sgRNA.BRD4.KO_1,2,8,9,10,11,12,13	A1ATD1-c WT
BRD2+BRD4	sgRNA.BRD2.KO_10,11,12,13 sgRNA.BRD4.KO_1,2,8,9,10,11,12,13	A1ATD1-c WT
BRD2+BRD3	sgRNA.BRD2.KO_10,11,12,13	A1ATD1-c BRD3 KO
BRD4+BRD3	sgRNA.BRD4.KO_1,2,8,9,10,11,12,13	A1ATD1-c BRD3 KO
BRD2+BRD3+BRD4	sgRNA.BRD2.KO_10,11,12,13 sgRNA.BRD4.KO_1,2,8,9,10,11,12,13	A1ATD1-c BRD3 KO

Table 3.4.2 **sgRNAs nucleofected into iPSC for generation of BET KOs.**

Nucleofected cells were individually sorted into 96 well plates coated with vitronectin. Using a different fluorescent protein per gene facilitated sorting of clones containing sgRNAs targeting different genes (GFP for BRD2, and tomato for BRD4). Individual clones (36 in total) were expanded until stable lines were obtained. gDNA was extracted from each clone for PCR amplification across the target region (same primers as represented in figure 3.4.3.a and b). The PCR products sizes were

compared with WT PCR product. Clones with smaller product sizes, indicating deletions in the target sequence, were selected for Sanger sequencing. From a total of 36 unconfirmed KO clones, the following were sequenced: 8 BRD2 KOs, 6 BRD2+3 KOs, 9 BRD4 KOs, 8 BRD3+4 KOs, 4 BRD2+4 KOs and only 1 was a BRD2+3+4 KO. PCR products from BRD2+3 revealed WT for BRD2. Similarly, sequencing of BRD4 exon 2, in unconfirmed BRD4 KOs, revealed that none of the clones was a BRD4 KO and PCRs of exons 12, 13 and 14 were not successful despite several attempts. Due to the limited amount of time left, the study of BRD4 KOs was abandoned for the scope of this thesis, including BRD4 KO, BRD2+4 KO, BRD3+4 KO and BRD2+3+4 KO. Therefore, work was carried out on BRD2.

PCR products from one promising BRD2 KO clone (following sequencing) were inserted into pGEM-T easy vector to confirm the deletions. pGEM-T was transformed into E.coli and blue-white recombination screening performed by using X-gal in the agar plate (section 2.2.10.3). Six white colonies from each clone were expanded and mini preps sent for sequencing. Figure 3.4.4 shows confirmation of the BRD2 KO.

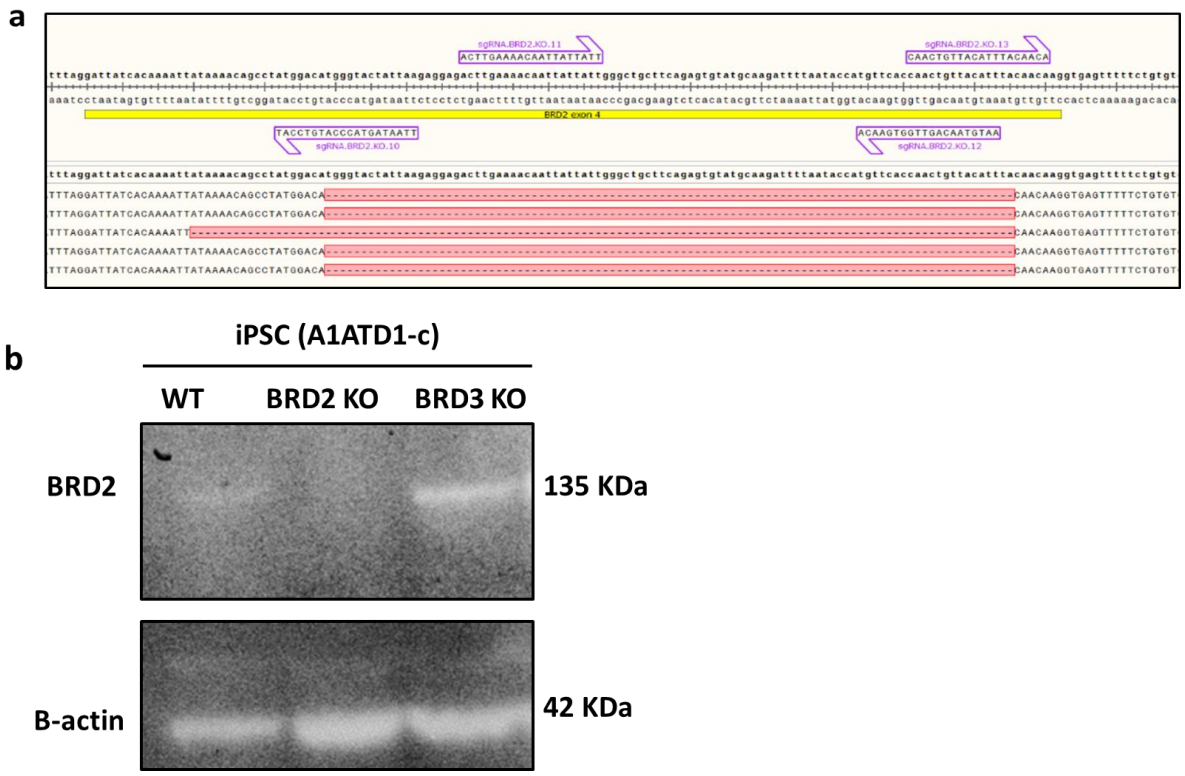

c

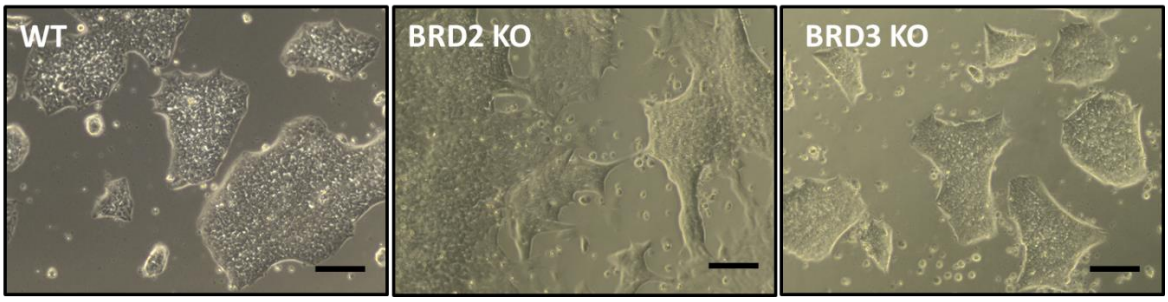

Figure 3.4.4 Confirmation of BRD2 KO clone. (a) Alignment of sequenced PCR products from the successful BRD2 KO to the BRD2 gene sequence. **(b)** Western blot confirmation of BRD2 protein KO. **(c)** Morphological comparison between WT, BRD2 KO and BRD3 KO (studied in sections 3.1 and 3.2). Scale bars, 250 µm.

Sanger sequencing revealed deletions in exon 4 of BRD2, and the absence of protein was confirmed by western blotting. Morphological assessment of BRD2 KO reveals differences to the WT and BRD3 KO. Transmitted light images (figure 3.4.4.c) show that BRD2 KO presents an uncharacteristic iPSC morphology, as colonies have less defined edges than both WT and BRD3 KO. Also, the cell morphology of BRD2 KO is more stretched than the typical iPSCs round cell morphology.

3.4.2.3 Characterisation of BRD2 KO - proliferation and pluripotency

A proliferation assay was performed motivated by an observed difference in growth between WT and BRD2 KO cells. iPSCs (WT and BRD2 KO) were dissociated into single cell suspensions and seeded onto vitronectin coated 48 well plates. Cells were cultured with standard iPSC media for 6 days. Crystal violet assay was performed at days 4 and 6 (section 2.2.14). The results of the proliferation assay are shown in figure 3.4.5.

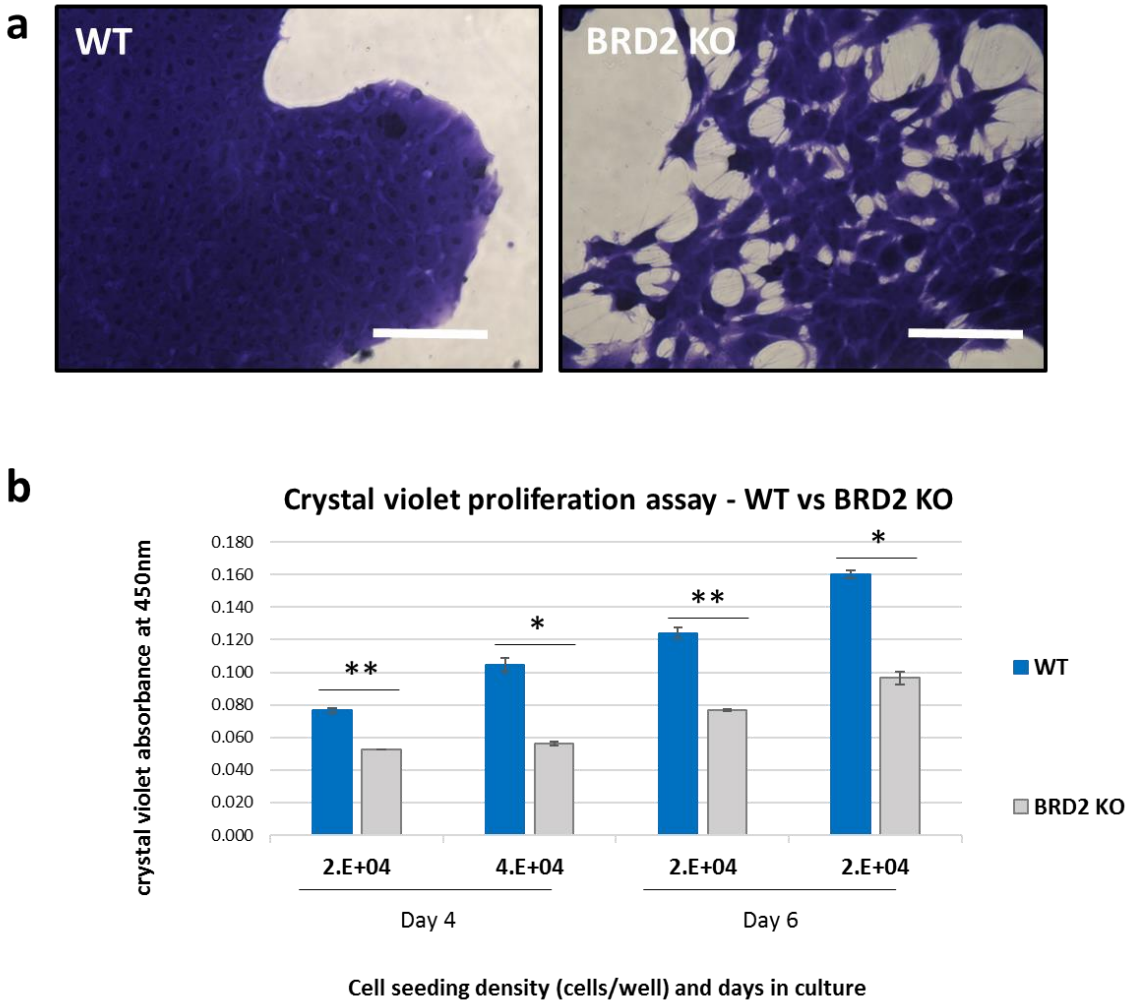

Figure 3.4.5 Proliferation assay reveals decreased growth phenotype for BRD2 KO. Single cell cultures were seeded at 2e4 and 4e4 cells/well in 48 well plates, and cultured for 6 days. Cultures were fixed with glutaraldehyde at days 4 and 6 and crystal violet assay performed. Experiment included triplicates for each condition. **(a)** Microscopic images (40x) of crystal violet stained cultures show atypical cell morphology of BRD2 KO in comparison with WT. Scale bars, 250 µm. **(b)** Absorbance readings at 450 nm. Dye was dissolved and absorbance read at 450 nm. Represented are the mean absorbance ± SD, n=3, *p<0.05, **p<0.001 two-tail t-test against WT in similar condition.

Proliferation assay confirms growth and morphology phenotypes observed for BRD2 KO. Crystal violet staining revealed differences in colony growth with the BRD2 KO clone staining more sparingly than WT. Microscopic images confirm the spindle morphology of BRD2 KO (figure 3.4.5.a). These cultures present a differentiated morphology that is completely atypical of iPSCs. Absorbance readings revealed that BRD2 KO proliferates significantly slower than WT.

The morphological phenotype observed in BRD2 KO motivated a pluripotency test to analyse whether this is a real phenotype, or whether these cells were differentiated. The flow cytometry antibodies for

pluripotency markers (Tra-1-60 and SSEA4) used for characterisation of BRD3 KO (section 3.1) were used in this test. Cells from WT and BRD2 KO iPSC cultures were dissociated and stained with antibodies against Tra-1-60 and SSEA4 (section 2.2.8). Results of the BRD2 KO pluripotency test are shown in (figure 3.4.6).

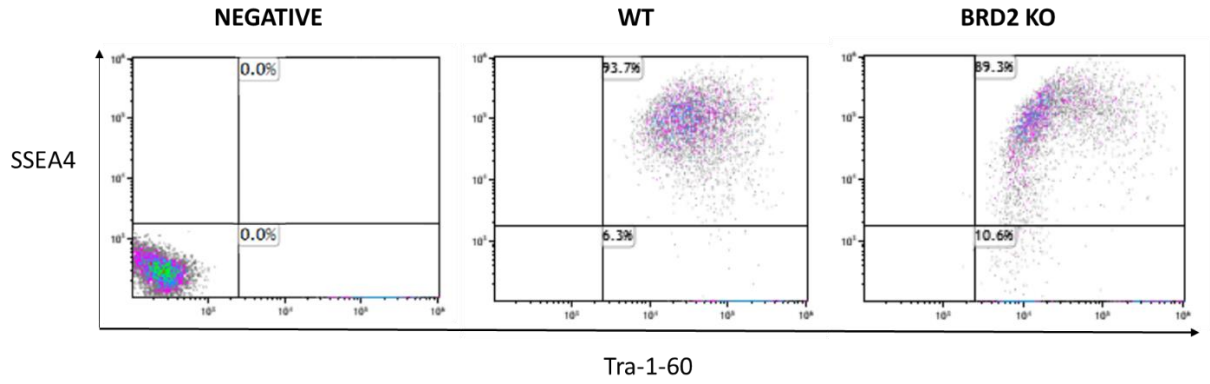

Figure 3.4.6 Pluripotency analysis reveals BRD2 KO population heterogeneity. Single cells were stained with antibodies against SSEA4 and Tra-1-60. Unstained single cells were used as negative control. BRD2 KO cells analysed (right) presented heterogeneously expressed SSEA4 and Tra-1-60. The WT cells (left) presented high levels of expression for both markers tested.

Flow cytometry analysis revealed heterogeneity in expression of pluripotency markers on the surface of BRD2 KO cells (figure 3.4.6). These cultures contained cells with a range of SSEA4 and Tra-1-60 expression, including a small percentage of cells not expressing SSEA4 (right panel). This could reflect BRD2 functions in cell cycle. However, the majority of the BRD2 KO population sustained a high level of pluripotency, indicating that BRD2 is not essential for pluripotency maintenance. WT cells presented a homogeneous population with high expression of both SSEA4 and Tra-1-60 (figure 3.4.6, middle).

3.4.2.4 Forward programming of BET KOs into MKs

In order to investigate whether BRD2 is essential in megakaryopoiesis, I differentiated BRD2 KO into MKs using the FoP protocol. WT and BRD3 KO were also included to compare differentiation efficiency in the same FoP experiment. Triplicates experiments were performed for each clone. The FoP protocol was followed as described previously and at day 10 (dissociation day), samples were stained with antibodies against CD34, CD43, CD235a and CD41a for identification of blood-commitment and MK progenitors differentiation potential, expected at day 10. Results are shown in figure 3.4.7.

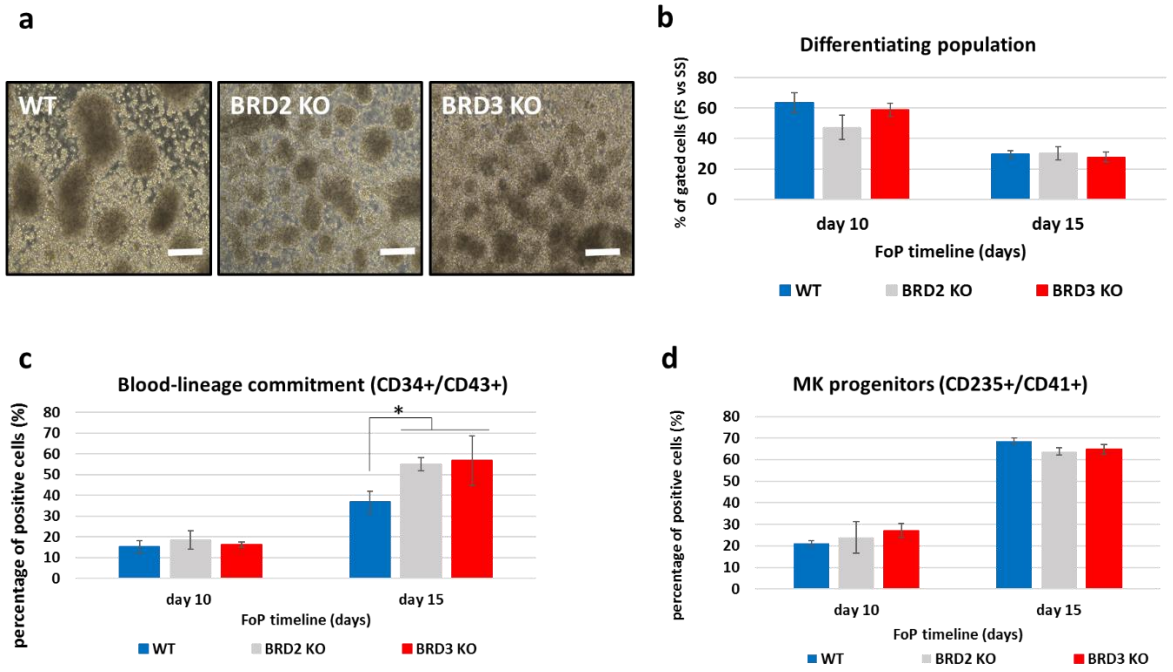

Figure 3.4.7 BRD2 KO differentiates into MK lineage. BRD2 KO was differentiated into MKs in a FoP experiment, alongside with WT and BRD3 KO. At days 10 and 15, cultures were stained with surface marker antibodies to study the cultures differentiation potential. **a)** Microscopy images of WT, BRD2 KO and BRD3 KO cultures in suspension at day 10. The clumps observed are characteristic of day 10 cultures and represent MK progenitor cells. Scale bars, 250 µm. **b)** Percentage of differentiating cells in culture, identified by flow cytometry using FS vs SS gating strategy. **c)** Percentage of blood-committed cells ($CD34^+/CD43^+$) in culture. **d)** Percentages of MK progenitors ($CD235a^+/CD41a^+$) present in culture. Mean % of positive stained populations ± SD, n=3, *p<0.05 two-tail t-test against WT in the same condition (b,c and d).

BRD2 KO are capable of differentiating into MK lineage cells. At day 10 of FoP differentiation, BRD2 KO cells were morphologically similar to both WT and BRD3 KO with agglomerates of cells in suspension, typical of day 10 differentiating cultures (figure 3.4.7.a). Flow cytometry analysis confirmed the differential potential of BRD2 KO, as over 40% of cells in culture were differentiating at day 10 and 30% at day 15 (figure 3.4.7.b). This population is identified through FS vs SS gating. Comparatively, the amount of differentiating cells in WT and BRD3 KO cultures was slightly higher at day 10 (60%), but similar to BRD2 KO at day 15 (figure 3.4.7.b). Surface markers staining at day 10 shows that 15-20% of differentiating cells in the 3 cultures were similarly expressing CD34 and CD43 (figure 3.4.7.c), and around 25% of differentiating cells were MK progenitors ($CD235^+/CD41a^+$) (figure 3.4.7.d). This indicates that the potential to differentiate into blood-committed and MK-committed lineage is not disrupted by the absence of neither BRD2 nor BRD3. The same result was observed at day 15 with BRD2 KO differentiating similarly to BRD3 KO and WT (figures 3.4.7.c and 3.4.7.d).

3.4.3. Discussion

The previous results described in my thesis raised the hypothesis that BRD3 could be compensated by another BET protein. Additionally, I reported that a BET antagonist inhibits the differentiation of early stages of MK generation. This second result suggests that one of the BET proteins, or a combination of them, is essential for the formation of MKs. However, it remains unknown which BET protein plays a critical role in megakaryopoiesis. The identification of the critical BET protein, and their function in megakaryopoiesis, would allow further understanding of the process regulating MKs and platelets differentiation. This would lead to better prediction of the consequences on MKs and platelets resulting from BET inhibitor treatments.

In order to investigate which BET protein is required for differentiation of MKs, I designed a set of experiments to KO BET proteins individually and in combination. These experiments would allow to study individual BET protein requirements for the process of MK formation, but also to investigate any potential redundancies in protein functions. Due to time constraints, I was only able to generate and characterise the BRD2 KO. The morphology of BRD2 KO iPSCs is dissimilar to that of WT and BRD3 KO, suggesting that BRD2 could have a role in regulation of genes important for the determination of the cytoskeleton structure. Despite this difference in morphology, BRD2 KO cells are pluripotent and are capable of generating MK progenitors. The results of my experiments show that BRD2 is not required for the differentiation of blood-committed cells (figure 3.4.7.c) nor for the formation of MK progenitors (figure 3.4.7.d). Together the differentiation of BRD2 KO experiment shows that BRD2 is not essential for the differentiation of pluripotent cells into the MK-lineage, using the FoP system.

However, the redundancy hypothesis among BET proteins could also apply to the BRD2 KO. If BRD2 is being compensated by other BETs, the generation and differentiation of combinatorial KOs would allow to identify which of the BET proteins has compensatory functions. Once identified the redundancy, and in order to confirm it, an overexpression experiment could be performed, where both proteins would be singularly overexpressed in the combinatorial KO. For example, if BRD3 compensates BRD2 during megakaryopoiesis, BRD2+3 KO would not generate MKs, and the overexpression of BRD3 or BRD2 in BRD2+3 KO would potentially recover the MK formation ability observed in BRD2 KO and BRD3 KO.

In my experiments, both BRD2 KO and BRD3 KO were capable of forming MK progenitors, suggesting that individually BRD3 and BRD2 are not essential during early stages of megakaryopoiesis.

Considering that BET inhibition impaired differentiation of MKs, I hypothesise that BRD4 might play a major role in early MK differentiation. The differentiation of BRD4 KO into MKs would answer this question, because if BRD4 was essential, BRD4 KO would not form MKs. This hypothesis is supported by previous studies where BRD4 was reported to coactivate lineage-specific TF TWIST during normal mesoderm differentiation (Shi et al. 2014). Mesoderm is the first stage in FoP MK differentiation, and the inhibition of BRD4 could be the cause for the impairment of early MK differentiation. Together the results reported in this section show that BRD2 is not essential for generation of MK progenitors using the FoP protocol.

Chapter 4

Conclusion and future work

The association of BRD3 as a regulator of PMV and PDW in a GWAS for platelet traits (Astle et al. 2016), and the current testing of BET inhibitors in clinical trials for haematological cancers (Abedin et al. 2016; Doroshow et al. 2017) are driving motives to understand the role of BRD3 in platelet differentiation. The aim of my project was to study the role of BRD3 in megakaryopoiesis, the process that generates platelet progenitors. In order to do so, I conducted my experiments using a megakaryopoiesis model, forward programming (FoP), developed by Dr Thomas Moreau (Moreau et al. 2016).

Despite being a GATA-1 direct interactor, BRD3 is dispensable for MK differentiation using the MK-FoP protocol. The generation of a BRD3 KO iPSC model proved that BRD3 is not required for the maintenance of pluripotent cells (figures 3.1.3.c and 3.1.5). BRD3 KO cells are also capable of differentiating into MKs, indicating that BRD3 is not essential during megakaryopoiesis (figure 3.1.8). In fact, my experiments show that BRD3 does not play a role in regulating chromatin architecture (figure 3.2.1) nor H3K27 acetylation signatures (figure 3.2.2) in megakaryopoiesis. These results align with previously reported studies showing that BRD3 is dispensable for GATA-1-induced transcription, despite the direct BRD3-GATA-1 interaction (Stonestrom et al. 2015). I suggest three possible hypothesis for the lack of detectable phenotype upon BRD3 ablation. Firstly, BRD3 could simply be redundant, or have little regulatory functions in the differentiation of MKs. Secondly, GATA-1 overexpression in FoP could overcome the role of BRD3 in TFs recruitment and MK-specific gene activation. Lastly, BRD3 absence could be compensated by other BET protein. A BET protein compensation mechanism has been shown in erythropoiesis (Stonestrom et al. 2015). The high gene expression correlation between erythroblasts and MKs has been reported (Watkins et al. 2009), and this could be reflected on protein function to a certain extent. Therefore, it is acceptable to speculate that one of the other BETs could replace BRD3. Interestingly, in this thesis I show that BRD2 is also dispensable in megakaryopoiesis, using a FoP system. The differentiation of BRD2+3 KO is required to verify whether there is compensation between BRD2 and BRD3 in megakaryopoiesis.

BET inhibition impairs MK progenitor generation, but not late megakaryopoiesis. Inhibition of BET proteins at early stages of megakaryopoiesis severely impaired the differentiation of iPSCs into MK progenitors, indicating that BET proteins are required for early differentiation (figure 3.3.6). This result is supported by previous studies showing that BET proteins regulate cell-specific TF recruitment (Stonestrom et al. 2015), and BET inhibition dysregulates TF-regulated gene signatures (Roe et al. 2015), impeding differentiation. Moreover, given that BRD2 KO and BRD3 KO were successful at

generating MK progenitors, it is acceptable to hypothesise that BRD4 could be the essential BET protein in early megakaryopoiesis. The BRD4 depletion in the inhibition experiments would explain why the iPSCs did not differentiate into MKs. Previous studies demonstrated that BRD4 is a major regulator of mesoderm differentiation, the first differentiation stage in megakaryopoiesis (Rodriguez et al. 2014b; Jian Shi et al. 2014). Also, BET inhibition has an effect on lineage-specific networks due to the disruption of BRD4 from cell-specific enhancers (J.-E. Lee et al. 2017; Chapuy et al. 2013). My inhibition experiments were subjected to the same study flaws that I identified in my other experiments: the overexpression of GATA-1, and the possibility for a BET compensatory effects. However, if GATA-1 overexpression overcame the BRD3 requirement for MK differentiation; the same artefactual influence could not overcome the absence of all the BET proteins. Additionally, if there was a BET compensatory mechanism, it would have been impaired with inhibition, hence why differentiation failed at early stages, probably when BRD4 is essential. This hypothesis will require further validation with experiments suggested below.

In order to overcome some of the possible flaws in my experiments and progress the study of BET proteins regulation in megakaryopoiesis, I suggest the following experiments. Firstly, the TFs overexpression in the MK-FoP presents an impediment to explore the transcriptional mechanisms regulated by BET proteins, as these are direct TFs interactors. To perform future experiments, an alternative directed differentiation protocol for generation of MKs could be tested. Secondly, in order to dissect whether there is a BET compensation in megakaryopoiesis, the BET KOs experiment described in section 3.4 would require completion. To get insights into the transcriptional pathways regulated by BET proteins, a transcriptome analysis of the BET KO combinations at MK stage would be performed. If one of the BET proteins is essential (BETe) in megakaryopoiesis, it is expected that the BETe KO clones will not generate MKs. In that case, a knockdown of BETe could be generated and differentiated into MKs. To identify the transcriptional pathways regulated by the BETe, RNA-seq data from WT and BETe KD would allow the analysis of differentially expressed genes and the assessment of pathway enrichment. It would be interesting to compare BETe KD transcriptome with RNA-seq data from BET inhibition of MKs to verify whether the affected pathways are similar. Lastly, to characterise the BETe regulatory mechanisms in megakaryopoiesis, a MK ChIP-seq experiment, using BETe and MK-specific TFs antibodies on MKs, would allow to identify genome-wide regions co-occupied by both BETe and TFs in WT and BETe KD. Additionally, in order to establish the chromatin landscape for differentiated MKs, the same ChIP-seq experiment would include antibodies against H3K4me3 (for promoter identification) and H3K27ac (for active promoter and enhancer identification). The correlation between co-binding of BETe and TFs at identified regulatory regions (promoters and

enhancers) and the pathways affected by BETe KD (and/or inhibition) would provide insights on the BET regulation in megakaryopoiesis.

This thesis presents the first reported experiments to study the role of BRD3 in chromatin architecture and H3K27ac signature during megakaryopoiesis. Additionally, BET regulatory mechanisms in generation of MKs have never been explored. Here, I show that BRD3 ablation does not significantly affect MK generation, as opposed to BET inhibition that impairs early megakaryopoiesis. Therefore, my studies progress the available knowledge on regulatory circuits in megakaryopoiesis, and consequently, platelets generation. These, and suggested future studies, will help inform the mechanisms behind the occurrence of side effects, such as thrombocytopenia, in current clinical trials testing BET inhibitors, and guide the development and application of future BET antagonist drugs.

Chapter 5

References

Abedin, Sameem M, Craig S Boddy, and Hidayatullah G Munshi. 2016. "BET Inhibitors in the Treatment of Hematologic Malignancies: Current Insights and Future Prospe cts." *OncoTargets and Therapy* 9. Dove Press: 5943–53. doi:10.2147/OTT.S100515.

Adey, Andrew, Hilary G Morrison, Asan (no last name), Xu Xun, Jacob O Kitzman, Emily H Turner, Bethany Stackhouse, et al. 2010. "Rapid, Low-Input, Low-Bias Construction of Shotgun Fragment Libraries by High-Density in Vitro Transposition." *Genome Biology* 11 (12). BioMed Central: R119. doi:10.1186/gb-2010-11-12-r119.

Akashi, K., Xi He, Jie Chen, Hiromi Iwasaki, Chao Niu, Brooke Steenhard, Jiwang Zhang, Jeff Haug, and Linheng Li. 2003. "Transcriptional Accessibility for Genes of Multiple Tissues and Hematopoietic Lineages Is Hierarchically Controlled during Early Hematopoiesis." *Blood* 101 (2): 383–89. doi:10.1182/blood-2002-06-1780.

Akashi, Koichi, David Traver, Toshihiro Miyamoto, and Irving L. Weissman. 2000. "A Clonogenic Common Myeloid Progenitor That Gives Rise to All Myeloid Lineages." *Nature* 404 (6774): 193–97. doi:10.1038/35004599.

Alexander, W S, A W Roberts, N A Nicola, R Li, and D Metcalf. 1996. "Deficiencies in Progenitor Cells of Multiple Hematopoietic Lineages and Defective Megakaryocytopoiesis in Mice Lacking the Thrombopoietic Receptor C-Mpl." *Blood* 87 (6): 2162–70. http://www.ncbi.nlm.nih.gov/pubmed/8630375.

Amorim, Sandy, Anastasios Stathis, Mary Gleeson, Sunil Iyengar, Valeria Magarotto, Xavier Leleu, Franck Morschhauser, et al. 2016. "Bromodomain Inhibitor OTX015 in Patients with Lymphoma or Multiple Myeloma: A Dose-Escalation, Open-Label, Pharmacokinetic, Phase 1 Study." *The Lancet Haematology* 3 (4). Elsevier: e196–204. doi:10.1016/S2352-3026(16)00021-1.

Anand, Priti, Jonathan D. Brown, Charles Y. Lin, Jun Qi, Rongli Zhang, Pedro Calderon Artero, M. Amer Alaiti, et al. 2013. "BET Bromodomains Mediate Transcriptional Pause Release in Heart Failure." *Cell* 154 (3): 569–82. doi:10.1016/j.cell.2013.07.013.

Antoniani, Chiara, Oriana Romano, and Annarita Miccio. 2017. "Concise Review: Epigenetic Regulation of Hematopoiesis: Biological Insights and Therapeutic Applications." *STEM CELLS Translational Medicine* 6 (12): 2106–14. doi:10.1002/sctm.17-0192.

Arany, Z, W R Sellers, D M Livingston, and R Eckner. 1994. "E1A-Associated P300 and CREB-Associated CBP Belong to a Conserved Family of Coactivators." *Cell* 77 (6): 799–800. http://www.ncbi.nlm.nih.gov/pubmed/8004670.

Arnaudo, Anna M, and Benjamin A Garcia. 2013. "Proteomic Characterization of Novel Histone Post-Translational Modifications." *Epigenetics & Chromatin* 6 (1): 24. doi:10.1186/1756-8935-6-24.

Astle, William J, Heather Elding, Tao Jiang, and Willem H Ouwehand. 2016. "The Allelic Landscape of Human Blood Cell Trait Variation and Links to Common Complex Disease." *Cell* 167: 1415–29. doi:10.1016/j.cell.2016.10.042.

Barrangou, R., C. Fremaux, H. Deveau, M. Richards, P. Boyaval, S. Moineau, D. A. Romero, and P. Horvath. 2007. "CRISPR Provides Acquired Resistance Against Viruses in Prokaryotes." *Science* 315 (5819): 1709–12. doi:10.1126/science.1138140.

Barski, Artem, Suresh Cuddapah, Kairong Cui, Tae-Young Roh, Dustin E. Schones, Zhibin Wang, Gang

Wei, Iouri Chepelev, and Keji Zhao. 2007. “High-Resolution Profiling of Histone Methylations in the Human Genome.” *Cell* 129 (4): 823–37. doi:10.1016/j.cell.2007.05.009.

Bartley, T D, J Bogenberger, P Hunt, Y S Li, H S Lu, F Martin, M S Chang, B Samal, J L Nichol, and S Swift. 1994. “Identification and Cloning of a Megakaryocyte Growth and Development Factor That Is a Ligand for the Cytokine Receptor Mpl.” *Cell* 77 (7): 1117–24. http://www.ncbi.nlm.nih.gov/pubmed/8020099.

Bastian, L S, B A Kwiatkowski, J Breininger, S Danner, and G Roth. 1999. “Regulation of the Megakaryocytic Glycoprotein IX Promoter by the Oncogenic Ets Transcription Factor Fli-1.” *Blood* 93 (8): 2637–44. http://www.ncbi.nlm.nih.gov/pubmed/10194443.

Berthon, Céline, Emmanuel Raffoux, Xavier Thomas, Norbert Vey, Carlos Gomez-Roca, Karen Yee, David Christopher Taussig, et al. 2016. “Bromodomain Inhibitor OTX015 in Patients with Acute Leukaemia: A Dose-Escalation, Phase 1 Study.” *The Lancet Haematology* 3 (4). Elsevier: e186–95. doi:10.1016/S2352-3026(15)00247-1.

Bessman, J D. 1984. “The Relation of Megakaryocyte Ploidy to Platelet Volume.” *American Journal of Hematology* 16 (2): 161–70. http://www.ncbi.nlm.nih.gov/pubmed/6538064.

Bhagwat, Anand S, Jae-Seok Roe, Beverly Y L Mok, Anja F Hohmann, Junwei Shi, and Christopher R Vakoc. 2016a. “BET Bromodomain Inhibition Releases the Mediator Complex from Select Cis-Regulatory Elements.” *Cell Reports* 15 (3). NIH Public Access: 519–30. doi:10.1016/j.celrep.2016.03.054.

———. 2016b. “BET Bromodomain Inhibition Releases the Mediator Complex from Select Cis-Regulatory Elements.” *Cell Reports* 15 (3). NIH Public Access: 519–30. doi:10.1016/j.celrep.2016.03.054.

Bielczyk-Maczyńska, Ewa, Jovana Serbanovic-Canic, Lauren Ferreira, Nicole Soranzo, Derek L. Stemple, Willem H. Ouwehand, and Ana Cvejic. 2014a. “A Loss of Function Screen of Identified Genome-Wide Association Study Loci Reveals New Genes Controlling Hematopoiesis.” *PLoS Genetics* 10 (7). doi:10.1371/journal.pgen.1004450.

———. 2014b. “A Loss of Function Screen of Identified Genome-Wide Association Study Loci Reveals New Genes Controlling Hematopoiesis.” Edited by Leonard I. Zon. *PLoS Genetics* 10 (7). Public Library of Science: e1004450. doi:10.1371/journal.pgen.1004450.

Bluteau, O., T. Langlois, P. Rivera-Munoz, F. Favale, P. Rameau, G. Meurice, P. Dessen, et al. 2013. “Developmental Changes in Human Megakaryopoiesis.” *Journal of Thrombosis and Haemostasis* 11 (9). Wiley/Blackwell (10.1111): 1730–41. doi:10.1111/jth.12326.

Bondy-Denomy, Joe, April Pawluk, Karen L Maxwell, and Alan R Davidson. 2013. “Bacteriophage Genes That Inactivate the CRISPR/Cas Bacterial Immune System.” *Nature* 493 (7432). Nature Publishing Group: 429–32. doi:10.1038/nature11723.

Botstein, David, and Neil Risch. 2003. “Discovering Genotypes Underlying Human Phenotypes: Past Successes for Mendelian Disease, Future Approaches for Complex Disease.” *Nature Genetics* 33 (3s). Nature Publishing Group: 228–37. doi:10.1038/ng1090.

Bowie, M. B., D. G. Kent, M. R. Copley, and C. J. Eaves. 2007. “Steel Factor Responsiveness Regulates the High Self-Renewal Phenotype of Fetal Hematopoietic Stem Cells.” *Blood* 109 (11): 5043–48. doi:10.1182/blood-2006-08-037770.

Boyes, Joan, Peter Byfield, Yoshihiro Nakatani, and Vasily Ogryzko. 1998. “Regulation of Activity of the Transcription Factor GATA-1 by Acetylation.” *Nature* 396 (6711). Nature Publishing Group:

594–98. doi:10.1038/25166.

Boyle, Alan P, Sean Davis, Hennady P Shulha, Paul Meltzer, Elliott H Margulies, Zhiping Weng, Terrence S Furey, and Gregory E Crawford. 2008. "High-Resolution Mapping and Characterization of Open Chromatin across the Genome." *Cell* 132 (2). NIH Public Access: 311–22. doi:10.1016/j.cell.2007.12.014.

Boyle, Alan P, Justin Guinney, Gregory E Crawford, and Terrence S Furey. 2008. "F-Seq: A Feature Density Estimator for High-Throughput Sequence Tags." *Bioinformatics (Oxford, England)* 24 (21): 2537–38. doi:10.1093/bioinformatics/btn480.

Bray, Nicolas L, Harold Pimentel, Páll Melsted, and Lior Pachter. 2016. "Near-Optimal Probabilistic RNA-Seq Quantification." *Nature Biotechnology* 34 (5): 525–27. doi:10.1038/nbt.3519.

Buck, Michael J, and Jason D Lieb. 2004. "ChIP-Chip: Considerations for the Design, Analysis, and Application of Genome-Wide Chromatin Immunoprecipitation Experiments." *Genomics* 83 (3). Academic Press: 349–60. doi:10.1016/J.YGENO.2003.11.004.

Buenrostro, Jason D, Paul G Giresi, Lisa C Zaba, Howard Y Chang, and William J Greenleaf. 2013. "Transposition of Native Chromatin for Fast and Sensitive Epigenomic Profiling of Open Chromatin, DNA-Binding Proteins and Nucleosome Position." *Nature Methods* 10 (12): 1213–18. doi:10.1038/nmeth.2688.

Buenrostro, Jason D, Beijing Wu, Howard Y Chang, and William J Greenleaf. 2015. "ATAC-Seq: A Method for Assaying Chromatin Accessibility Genome-Wide." *Current Protocols in Molecular Biology* 109 (January). NIH Public Access: 21.29.1-9. doi:10.1002/0471142727.mb2129s109.

Buta, Christiane, Robert David, Ralf Dressel, Mia Emgård, Christiane Fuchs, Ulrike Gross, Lyn Healy, et al. 2013. "Reconsidering Pluripotency Tests: Do We Still Need Teratoma Assays?" *Stem Cell Research* 11 (1): 552–62. doi:10.1016/j.scr.2013.03.001.

Butler, Joe M, Neil Hall, Niro Narendran, Yit C Yang, and Luminita Paraoan. 2017. "Identification of Candidate Protective Variants for Common Diseases and Evaluation of Their Protective Potential." *BMC Genomics* 18 (1). BioMed Central: 575. doi:10.1186/s12864-017-3964-3.

Calo, Eliezer, and Joanna Wysocka. 2013. "Modification of Enhancer Chromatin: What, How, and Why?" *Molecular Cell* 49 (5). NIH Public Access: 825–37. doi:10.1016/j.molcel.2013.01.038.

Cecchetti, Luca, Neal D Tolley, Noemi Michetti, Loredana Bury, Andrew S Weyrich, and Paolo Gresele. 2011. "Megakaryocytes Differentially Sort MRNAs for Matrix Metalloproteinases and Their Inhibitors into Platelets: A Mechanism for Regulating Synthetic Events." *Blood* 118 (7). American Society of Hematology: 1903–11. doi:10.1182/blood-2010-12-324517.

Celic, Ivana, Hiroshi Masumoto, Wendell P Griffith, Pamela Meluh, Robert J Cotter, Jef D Boeke, and Alain Verreault. 2006. "The Sirtuins Hst3 and Hst4p Preserve Genome Integrity by Controlling Histone H3 Lysine 56 Deacetylation." *Current Biology : CB* 16 (13). Elsevier: 1280–89. doi:10.1016/j.cub.2006.06.023.

Chagraoui, H., M. Kassouf, S. Banerjee, N. Goardon, K. Clark, A. Atzberger, A. C. Pearce, et al. 2011. "SCL-Mediated Regulation of the Cell-Cycle Regulator P21 Is Critical for Murine Megakaryopoiesis." *Blood* 118 (3): 723–35. doi:10.1182/blood-2011-01-328765.

Chagraoui, Hedia, Mira Kassouf, Sreemoti Banerjee, Nicolas Goardon, Kevin Clark, Ann Atzberger, Andrew C. Pearce, et al. 2011. "SCL-Mediated Regulation of the Cell-Cycle Regulator P21 Is Critical for Murine Megakaryopoiesis." *Blood* 118: 723–35. doi:10.1182/blood-2011-01-328765.

Chang, Aaron N, Alan B Cantor, Yuko Fujiwara, Maya B Lodish, Steven Droho, John D Crispino, and Stuart H Orkin. 2002. "GATA-Factor Dependence of the Multitype Zinc-Finger Protein FOG-1 for Its Essential Role in Megakaryopoiesis." *Proceedings of the National Academy of Sciences of the United States of America* 99 (14). National Academy of Sciences: 9237–42. doi:10.1073/pnas.142302099.

Chapuy, Bjoern, Michael R. McKeown, Charles Y. Lin, Stefano Monti, Margaretha G.M. Roemer, Jun Qi, Peter B. Rahl, et al. 2013. "Discovery and Characterization of Super-Enhancer-Associated Dependencies in Diffuse Large B Cell Lymphoma." *Cancer Cell* 24 (6): 777–90. doi:10.1016/j.ccr.2013.11.003.

Chen, Baohui, Luke A Gilbert, Beth A Cimini, Joerg Schnitzbauer, Wei Zhang, Gene-Wei Li, Jason Park, et al. 2013. "Dynamic Imaging of Genomic Loci in Living Human Cells by an Optimized CRISPR/Cas System." *Cell* 155 (7). Elsevier: 1479–91. doi:10.1016/j.cell.2013.12.001.

Chen, Edward Y, Christopher M Tan, Yan Kou, Qiaonan Duan, Zichen Wang, Gabriela Meirelles, Neil R Clark, and Avi Ma'ayan. 2013a. "Enrichr: Interactive and Collaborative HTML5 Gene List Enrichment Analysis Tool." *BMC Bioinformatics* 14 (1): 128. doi:10.1186/1471-2105-14-128.

Chen, Edward Y, Christopher M Tan, Yan Kou, Qiaonan Duan, Zichen Wang, Gabriela Vaz Meirelles, Neil R Clark, and Avi Ma'ayan. 2013b. "Enrichr: Interactive and Collaborative HTML5 Gene List Enrichment Analysis Tool." *BMC Bioinformatics* 14 (1): 128. doi:10.1186/1471-2105-14-128.

Chen, Lu, Myrto Kostadima, Joost H A Martens, Giovanni Canu, Sara P Garcia, Ernest Turro, Kate Downes, et al. 2014. "Transcriptional Diversity during Lineage Commitment of Human Blood Progenitors." *Science (New York, N.Y.)* 345 (6204). Europe PMC Funders: 1251033. doi:10.1126/science.1251033.

Chen, Xiaoyong, and James J Bieker. 2004. "Stage-Specific Repression by the EKLF Transcriptional Activator." *Molecular and Cellular Biology* 24 (23). American Society for Microbiology (ASM): 10416–24. doi:10.1128/MCB.24.23.10416-10424.2004.

Cheung, Ka Lung, Fan Zhang, Anbalagan Jaganathan, Rajal Sharma, Qiang Zhang, Tsuyoshi Konuma, Tong Shen, et al. 2017. "Distinct Roles of Brd2 and Brd4 in Potentiating the Transcriptional Program for Th17 Cell Differentiation." *Molecular Cell* 65 (6): 1068–1080.e5. doi:10.1016/j.molcel.2016.12.022.

Chlon, Timothy M, and John D Crispino. 2012. "Combinatorial Regulation of Tissue Specification by GATA and FOG Factors." *Development (Cambridge, England)* 139 (21). Oxford University Press for The Company of Biologists Limited: 3905–16. doi:10.1242/dev.080440.

Choudhary, Chunaram, Chanchal Kumar, Florian Gnad, Michael L Nielsen, Michael Rehman, Tobias C Walther, Jesper V Olsen, and Matthias Mann. 2009. "Lysine Acetylation Targets Protein Complexes and Co-Regulates Major Cellular Functions." *Science (New York, N.Y.)* 325 (5942). American Association for the Advancement of Science: 834–40. doi:10.1126/science.1175371.

Chu, S G, R C Becker, P B Berger, D L Bhatt, J W Eikelboom, B Konkle, E R Mohler, M P Reilly, and J S Berger. 2010. "Mean Platelet Volume as a Predictor of Cardiovascular Risk: A Systematic Review and Meta-Analysis." *Journal of Thrombosis and Haemostasis : JTH* 8 (1). NIH Public Access: 148–56. doi:10.1111/j.1538-7836.2009.03584.x.

Cianfrocco, Michael A, George A Kassavetis, Patricia Grob, Jie Fang, Tamar Juven-Gershon, James T Kadonaga, and Eva Nogales. 2013. "Human TFIID Binds to Core Promoter DNA in a Reorganized Structural State." *Cell* 152 (1–2). NIH Public Access: 120–31. doi:10.1016/j.cell.2012.12.005.

Clapier, Cedric R., and Bradley R. Cairns. 2009. "The Biology of Chromatin Remodeling Complexes." *Annual Review of Biochemistry* 78 (1): 273–304. doi:10.1146/annurev.biochem.77.062706.153223.

Clayton, Alison L., Catherine A. Hazzalin, and Louis C. Mahadevan. 2006. "Enhanced Histone Acetylation and Transcription: A Dynamic Perspective." *Molecular Cell* 23 (3): 289–96. doi:10.1016/j.molcel.2006.06.017.

Consortium, The ENCODE Project. 2012. "An Integrated Encyclopedia of DNA Elements in the Human Genome." *Nature* 489 (7414). Nature Publishing Group: 57–74. doi:10.1038/nature11247.

Creyghton, Menno P, Albert W Cheng, G Grant Welstead, Tristan Kooistra, Bryce W Carey, Eveline J Steine, Jacob Hanna, et al. 2010. "Histone H3K27ac Separates Active from Poised Enhancers and Predicts Developmental State." *Proceedings of the National Academy of Sciences of the United States of America* 107 (50). National Academy of Sciences: 21931–36. doi:10.1073/pnas.1016071107.

Crowley, Thomas E., Emily M. Kaine, Manabu Yoshida, Anindita Nandi, and Debra J. Wolgemuth. 2002. "Reproductive Cycle Regulation of Nuclear Import, Euchromatic Localization, and Association with Components of Pol II Mediator of a Mammalian Double-Bromodomain Protein." *Molecular Endocrinology* 16 (8): 1727–37. doi:10.1210/me.2001-0353.

Cubeñas-Potts, Caelin, and Michael J Matunis. 2013. "SUMO: A Multifaceted Modifier of Chromatin Structure and Function." *Developmental Cell* 24 (1). NIH Public Access: 1–12. doi:10.1016/j.devcel.2012.11.020.

D'Souza, Sunita L, Andrew G Elefanty, and Gordon Keller. 2005. "SCL/Tal-1 Is Essential for Hematopoietic Commitment of the Hemangioblast but Not for Its Development." *Blood* 105 (10). American Society of Hematology: 3862–70. doi:10.1182/blood-2004-09-3611.

DAHR, Wolfgang, Konrad BEYREUTHER, and John J. MOULDS. 1987. "Structural Analysis of the Major Human Erythrocyte Membrane Sialoglycoprotein from Miltenberger Class VII Cells." *European Journal of Biochemistry* 166 (1). Wiley/Blackwell (10.1111): 27–30. doi:10.1111/j.1432-1033.1987.tb13478.x.

Dawson, Mark A., Rab K. Prinjha, Antje Dittmann, George Giotopoulos, Marcus Bantscheff, Wai-In Chan, Samuel C. Robson, et al. 2011. "Inhibition of BET Recruitment to Chromatin as an Effective Treatment for MLL-Fusion Leukaemia." *Nature* 478 (7370): 529–33. doi:10.1038/nature10509.

De Alarcon, Pedro A, and Janet L A Graeve. 1996. "Analysis of Megakaryocyte Ploidy in Fetal Bone Marrow Biopsies Using a New Adaptation of the Feulgen Technique to Measure DNA Content and Estimate Megakaryocyte Ploidy from Biopsy Specimens." *Pediatric Research* 39 (1). Nature Publishing Group: 166–70. doi:10.1203/00006450-199601000-00026.

de Sauvage, F J, K Carver-Moore, S M Luoh, A Ryan, M Dowd, D L Eaton, and M W Moore. 1996. "Physiological Regulation of Early and Late Stages of Megakaryocytopoiesis by Thrombopoietin." *The Journal of Experimental Medicine* 183 (2): 651–56. http://www.ncbi.nlm.nih.gov/pubmed/8627177.

de Sauvage, Frederic J., Philip E. Hass, Susan D. Spencer, Beth E. Malloy, Austin L. Gurney, Steven A. Spencer, Walter C. Darbonne, et al. 1994. "Stimulation of Megakaryocytopoiesis and Thrombopoiesis by the C-Mpl Ligand." *Nature* 369 (6481): 533–38. doi:10.1038/369533a0.

Delmore, Jake E., Ghayas C. Issa, Madeleine E. Lemieux, Peter B. Rahl, Junwei Shi, Hannah M. Jacobs,

Efstathios Kastritis, et al. 2011a. "BET Bromodomain Inhibition as a Therapeutic Strategy to Target C-Myc." *Cell* 146 (6). Elsevier Inc.: 904–17. doi:10.1016/j.cell.2011.08.017.

Delmore, Jake E, Ghayas C Issa, Madeleine E Lemieux, Peter B Rahl, Junwei Shi, Hannah M Jacobs, Efstathios Kastritis, et al. 2011b. "BET Bromodomain Inhibition as a Therapeutic Strategy to Target C-Myc." *Cell* 146 (6). Elsevier: 904–17. doi:10.1016/j.cell.2011.08.017.

Denis, Gerald V., Mark E. McComb, Douglas V. Faller, Anupama Sinha, Paul B. Romesser, and Catherine E. Costello. 2006. "Identification of Transcription Complexes That Contain the Double Bromodomain Protein Brd2 and Chromatin Remodeling Machines." *Journal of Proteome Research* 5 (3): 502–11. doi:10.1021/pr050430u.

Deutsch, Varda R., and Aaron Tomer. 2013. "Advances in Megakaryocytopoiesis and Thrombopoiesis: From Bench to Bedside." *British Journal of Haematology* 161 (6): 778–93. doi:10.1111/bjh.12328.

Devaiah, B. N., B. A. Lewis, N. Cherman, M. C. Hewitt, B. K. Albrecht, P. G. Robey, K. Ozato, R. J. Sims, and D. S. Singer. 2012. "BRD4 Is an Atypical Kinase That Phosphorylates Serine2 of the RNA Polymerase II Carboxy-Terminal Domain." *Proceedings of the National Academy of Sciences* 109 (18): 6927–32. doi:10.1073/pnas.1120422109.

Dey, A., F. Chitsaz, A. Abbasi, T. Misteli, and K. Ozato. 2003. "The Double Bromodomain Protein Brd4 Binds to Acetylated Chromatin during Interphase and Mitosis." *Proceedings of the National Academy of Sciences* 100 (15): 8758–63. doi:10.1073/pnas.1433065100.

Dey, A, J Ellenberg, A Farina, A E Coleman, T Maruyama, S Sciortino, J Lippincott-Schwartz, and K Ozato. 2000. "A Bromodomain Protein, MCAP, Associates with Mitotic Chromosomes and Affects G(2)-to-M Transition." *Molecular and Cellular Biology* 20 (17). American Society for Microbiology (ASM): 6537–49. http://www.ncbi.nlm.nih.gov/pubmed/10938129.

Di Paola, Jorge. 2015. "Paris-Trousseau: Evidence Keeps Pointing to FLI1." *Blood* 126 (17). American Society of Hematology: 1973–74. doi:10.1182/blood-2015-09-667634.

Doench, John G. 2017. "Am I Ready for CRISPR? A User's Guide to Genetic Screens." *Nature Reviews Genetics* 19 (2). Nature Publishing Group: 67–80. doi:10.1038/nrg.2017.97.

Doré, Louis C, and John D Crispino. 2011. "Transcription Factor Networks in Erythroid Cell and Megakaryocyte Development." *Blood* 118 (2). American Society of Hematology: 231–39. doi:10.1182/blood-2011-04-285981.

Doroshow, D. B., J. P. Eder, and P. M. LoRusso. 2017. "BET Inhibitors: A Novel Epigenetic Approach." *Annals of Oncology* 28 (8). Oxford University Press: 1776–87. doi:10.1093/annonc/mdx157.

Drachman, J G, J D Griffin, and K Kaushansky. 1995. "The C-Mpl Ligand (Thrombopoietin) Stimulates Tyrosine Phosphorylation of Jak2, Shc, and c-Mpl." *The Journal of Biological Chemistry* 270 (10): 4979–82. http://www.ncbi.nlm.nih.gov/pubmed/7534285.

Du, X, L Beutler, C Ruan, PA Castaldi, and MC Berndt. 1987. "Glycoprotein Ib and Glycoprotein IX Are Fully Complexed in the Intact Platelet Membrane." *Blood* 69 (5). http://www.bloodjournal.org/content/69/5/1524?sso-checked=true.

Dzierzak, Elaine, and Nancy A Speck. 2008. "Of Lineage and Legacy: The Development of Mammalian Hematopoietic Stem Cells." *Nature Immunology* 9 (2). Nature Publishing Group: 129–36. doi:10.1038/ni1560.

Eberharter, Anton, and Peter B Becker. 2002. "Histone Acetylation: A Switch between Repressive and

Permissive Chromatin. Second in Review Series on Chromatin Dynamics." *EMBO Reports* 3 (3). European Molecular Biology Organization: 224–29. doi:10.1093/embo-reports/kvf053.

Eckardt, Sigrid, K John McLaughlin, and Holger Willenbring. 2011. "Mouse Chimeras as a System to Investigate Development, Cell and Tissue Function, Disease Mechanisms and Organ Regeneration." *Cell Cycle (Georgetown, Tex.)* 10 (13). Taylor & Francis: 2091–99. doi:10.4161/cc.10.13.16360.

Eisbacher, Michael, Melissa L Holmes, Anthea Newton, Philip J Hogg, Levon M Khachigian, Merlin Crossley, and Beng H Chong. 2003. "Protein-Protein Interaction between Fli-1 and GATA-1 Mediates Synergistic Expression of Megakaryocyte-Specific Genes through Cooperative DNA Binding." *Molecular and Cellular Biology* 23 (10): 3427–41. http://www.ncbi.nlm.nih.gov/pubmed/12724402.

Elagib, K. E., Frederick K Racke, Michael Mogass, Rina Khetawat, Lorrie L Delehanty, and Adam N Goldfarb. 2003. "RUNX1 and GATA-1 Coexpression and Cooperation in Megakaryocytic Differentiation." *Blood* 101 (11): 4333–41. doi:10.1182/blood-2002-09-2708.

Ernst, Jason, Pouya Kheradpour, Tarjei S Mikkelsen, Noam Shoresh, Lucas D Ward, Charles B Epstein, Xiaolan Zhang, et al. 2011. "Mapping and Analysis of Chromatin State Dynamics in Nine Human Cell Types." *Nature* 473 (7345). NIH Public Access: 43–49. doi:10.1038/nature09906.

Evans, M. J., and M. H. Kaufman. 1981. "Establishment in Culture of Pluripotential Cells from Mouse Embryos." *Nature* 292 (5819). Nature Publishing Group: 154–56. doi:10.1038/292154a0.

Feng, Qiang, Namrata Shabrani, Jonathan N Thon, Hongguang Huo, Austin Thiel, Kellie R Machlus, Kyungho Kim, et al. 2014. "Scalable Generation of Universal Platelets from Human Induced Pluripotent Stem Cells." *Stem Cell Reports* 3 (5). Elsevier: 817–31. doi:10.1016/j.stemcr.2014.09.010.

Feng, Weiyi, Maria Madajka, Bethany A Kerr, Ganapati H Mahabeleshwar, Sidney W Whiteheart, and Tatiana V Byzova. 2011. "A Novel Role for Platelet Secretion in Angiogenesis: Mediating Bone Marrow-Derived Cell Mobilization and Homing." *Blood* 117 (14): 3893–3902. http://www.ncbi.nlm.nih.gov/pubmed/21224474.

Feoktistova, Maria, Peter Geserick, and Martin Leverkus. 2016. "Crystal Violet Assay for Determining Viability of Cultured Cells." *Cold Spring Harbor Protocols* 2016 (4): pdb.prot087379. doi:10.1101/pdb.prot087379.

Ferkowicz, Michael J, and Mervin C Yoder. 2005. "Blood Island Formation: Longstanding Observations and Modern Interpretations." *Experimental Hematology* 33 (9): 1041–47. doi:10.1016/j.exphem.2005.06.006.

Filippakopoulos, Panagis, and Stefan Knapp. 2012a. "The Bromodomain Interaction Module." *FEBS Letters*. doi:10.1016/j.febslet.2012.04.045.

———. 2012b. "The Bromodomain Interaction Module." *FEBS Letters* 586 (17): 2692–2704. doi:10.1016/j.febslet.2012.04.045.

Filippakopoulos, Panagis, Sarah Picaud, Maria Mangos, Tracy Keates, Jean Philippe Lambert, Dalia Barsyte-Lovejoy, Ildiko Felletar, et al. 2012. "Histone Recognition and Large-Scale Structural Analysis of the Human Bromodomain Family." *Cell* 149 (1): 214–31. doi:10.1016/j.cell.2012.02.013.

Filippakopoulos, Panagis, Jun Qi, Sarah Picaud, Yao Shen, William B. Smith, Oleg Fedorov, Elizabeth M. Morse, et al. 2010. "Selective Inhibition of BET Bromodomains." *Nature* 468 (7327). Nature

Publishing Group: 1067–73. doi:10.1038/nature09504.

Fourel, Genevieve, Frederique Magdinier, and Eric Gilson. 2004. "Insulator Dynamics and the Setting of Chromatin Domains." *BioEssays* 26 (5): 523–32. doi:10.1002/bies.20028.

Freson, Kathleen, Koen Devriendt, Gert Matthijs, Achiel Van Hoof, Rita De Vos, Chantal Thys, Kristien Minner, Marc F Hoylaerts, Jos Vermylen, and Chris Van Geet. 2001. "Platelet Characteristics in Patients with X-Linked Macrothrombocytopenia Because of a Novel GATA1 Mutation." www.bloodjournal.org.

Fugman, Douglas A, David P Witte, Cindy L A Jones, Bruce J Aronow, and Michael A Lieberman. 2018. "In Vitro Establishment and Characterization of a Human Megakaryoblastic Cell Line." Accessed September 14. www.bloodjournal.org.

Fukazawa, Hidesuke, and Atsuko Masumi. 2012. "The Conserved 12-Amino Acid Stretch in the Inter-Bromodomain Region of BET Family Proteins Functions as a Nuclear Localization Signal." *Biological & Pharmaceutical Bulletin* 35 (11): 2064–68. http://www.ncbi.nlm.nih.gov/pubmed/22971749.

Gaj, Thomas, Charles A Gersbach, Carlos F Barbas, and III. 2013. "ZFN, TALEN, and CRISPR/Cas-Based Methods for Genome Engineering." *Trends in Biotechnology* 31 (7). NIH Public Access: 397–405. doi:10.1016/j.tibtech.2013.04.004.

Gallagher, Michael D, and Alice S Chen-Plotkin. 2018. "The Post-GWAS Era: From Association to Function." *The American Journal of Human Genetics* 102: 717–30. doi:10.1016/j.ajhg.2018.04.002.

Gamsjaeger, Roland, Sarah R Webb, Janine M Lamonica, Andrew Billin, Gerd A Blobel, and Joel P Mackay. 2011. "Structural Basis and Specificity of Acetylated Transcription Factor GATA1 Recognition by BET Family Bromodomain Protein Brd3." *Molecular and Cellular Biology* 31 (13). American Society for Microbiology (ASM): 2632–40. doi:10.1128/MCB.05413-11.

Garcia-Gutierrez, P., M. Mundi, and M. Garcia-Dominguez. 2012. "Association of Bromodomain BET Proteins with Chromatin Requires Dimerization through the Conserved Motif B." *Journal of Cell Science* 125 (15): 3671–80. doi:10.1242/jcs.105841.

Garcia-Gutierrez, Pablo, and Mario Garcia-Dominguez. 2015. "Pleiotrophin Fights Brd2 for Neuronal Differentiation." *Neural Regeneration Research* 10 (4). Medknow Publications and Media Pvt. Ltd.: 544–46. doi:10.4103/1673-5374.155416.

Garcia-Martinez, Virginio, and Gary C. Schoenwolf. 1993. "Primitive-Streak Origin of the Cardiovascular System in Avian Embryos." *Developmental Biology* 159 (2). Academic Press: 706–19. doi:10.1006/DBIO.1993.1276.

Gardner, Kathryn E, C David Allis, and Brian D Strahl. 2011. "Operating on Chromatin, a Colorful Language Where Context Matters." *Journal of Molecular Biology* 409 (1). NIH Public Access: 36–46. doi:10.1016/j.jmb.2011.01.040.

GAUR, M., T. KAMATA, S. WANG, B. MORAN, S. J. SHATTIL, and A. D. LEAVITT. 2006. "Megakaryocytes Derived from Human Embryonic Stem Cells: A Genetically Tractable System to Study Megakaryocytopoiesis and Integrin Function." *Journal of Thrombosis and Haemostasis* 4 (2): 436–42. doi:10.1111/j.1538-7836.2006.01744.x.

Geddis, Amy E., Norma E. Fox, Eugene Tkachenko, and Kenneth Kaushansky. 2007. "Endomitotic Megakaryocytes That Form a Bipolar Spindle Exhibit Cleavage Furrow Ingression Followed by Furrow Regression." *Cell Cycle* 6 (4). Taylor & Francis: 455–60. doi:10.4161/cc.6.4.3836.

Geddis, Amy E, Hannah M Linden, and Kenneth Kaushansky. 2002. "Thrombopoietin: A Pan-Hematopoietic Cytokine." *Cytokine & Growth Factor Reviews* 13 (1): 61–73. http://www.ncbi.nlm.nih.gov/pubmed/11750880.

Gegonne, Anne, Qing-Rong Chen, Anup Dey, Ruth Etzensperger, Xuguang Tai, Alfred Singer, Daoud Meerzaman, Keiko Ozato, and Dinah S Singer. 2018. "Immature CD8 Single-Positive Thymocytes Are a Molecularly Distinct Subpopulation, Selectively Dependent on BRD4 for Their Differentiation." *Cell Reports* 24 (1). Elsevier: 117–29. doi:10.1016/j.celrep.2018.06.007.

Gekas, Christos, Thomas Graf, and N Pampori. 2013. "CD41 Expression Marks Myeloid-Biased Adult Hematopoietic Stem Cells and Increases with Age." *Blood* 121 (22). American Society of Hematology: 4463–72. doi:10.1182/blood-2012-09-457929.

Geyer, P K, M M Green, and V G Corces. 1990. "Tissue-Specific Transcriptional Enhancers May Act in Trans on the Gene Located in the Homologous Chromosome: The Molecular Basis of Transvection in Drosophila." *The EMBO Journal* 9 (7): 2247–56. http://www.ncbi.nlm.nih.gov/pubmed/2162766.

Gieger, C, B Kühnel, a Radhakrishnan, a Cvejic, J Serbanovic-Canic, S Meacham, K Voss, et al. 2011. "New Gene Functions in Megakaryopoiesis and Platelet Formation." *Nature* 480 (7376). Nature Publishing Group: 201–8. doi:10.1038/nature10659.

Giresi, Paul G., Jonghwan Kim, Ryan M. McDaniell, Vishwanath R. Iyer, and Jason D. Lieb. 2007. "FAIRE (Formaldehyde-Assisted Isolation of Regulatory Elements) Isolates Active Regulatory Elements from Human Chromatin." *Genome Research* 17 (6). Cold Spring Harbor Laboratory Press: 877. doi:10.1101/GR.5533506.

Glozak, M A, and E Seto. 2007. "Histone Deacetylases and Cancer." *Oncogene* 26 (37): 5420–32. doi:10.1038/sj.onc.1210610.

Godin, I, F Dieterlen-Lièvre, and A Cumano. 1995. "Emergence of Multipotent Hemopoietic Cells in the Yolk Sac and Paraaortic Splanchnopleura in Mouse Embryos, Beginning at 8.5 Days Postcoitus." *Proceedings of the National Academy of Sciences of the United States of America* 92 (3). National Academy of Sciences: 773–77. http://www.ncbi.nlm.nih.gov/pubmed/7846049.

González, Federico, Stéphanie Boué, and Juan Carlos Izpisúa Belmonte. 2011. "Methods for Making Induced Pluripotent Stem Cells: Reprogramming à La Carte." *Nature Reviews Genetics* 12 (4). Nature Publishing Group: 231–42. doi:10.1038/nrg2937.

Greenberg, S M, D S Rosenthal, T A Greeley, R Tantravahi, and R I Handin. 1988. "Characterization of a New Megakaryocytic Cell Line: The Dami Cell." *Blood* 72 (6): 1968–77. http://www.ncbi.nlm.nih.gov/pubmed/3196874.

Greene, Marianne E, Gina Mundschau, Joshua Wechsler, Michael Mcdevitt, Alan Gamis, Judith Karp, Sandeep Gurbuxani, Robert Arceci, and John D Crispino. 2003. "Mutations in GATA1 in Both Transient Myeloproliferative Disorder and Acute Megakaryoblastic Leukemia of Down Syndrome." doi:10.1016/j.bcmd.2003.08.001.

Greer, Eric L., and Yang Shi. 2012. "Histone Methylation: A Dynamic Mark in Health, Disease and Inheritance." *Nature Reviews Genetics* 13 (5). Nature Publishing Group: 343–57. doi:10.1038/nrg3173.

Grover, Amit, Alejandra Sanjuan-Pla, Supat Thongjuea, Joana Carrelha, Alice Giustacchini, Adriana Gambardella, Iain Macaulay, et al. 2016. "Single-Cell RNA Sequencing Reveals Molecular and Functional Platelet Bias of Aged Haematopoietic Stem Cells." *Nature Communications* 7

(March). Nature Publishing Group: 11075. doi:10.1038/ncomms11075.

Growney, Joseph D, Hirokazu Shigematsu, Zhe Li, Benjamin H Lee, Jennifer Adelsperger, Rebecca Rowan, David P Curley, et al. 2005. "Loss of Runx1 Perturbs Adult Hematopoiesis and Is Associated with a Myeloproliferative Phenotype." *Blood* 106 (2). American Society of Hematology: 494–504. doi:10.1182/blood-2004-08-3280.

Grozovsky, Renata, Antonija Jurak Begonja, Kaifeng Liu, Gary Visner, John H Hartwig, Hervé Falet, and Karin M Hoffmeister. 2015. "The Ashwell-Morell Receptor Regulates Hepatic Thrombopoietin Production via JAK2-STAT3 Signaling." *Nature Medicine* 21 (1). NIH Public Access: 47–54. doi:10.1038/nm.3770.

Guo, Guoji, Sidinh Luc, Eugenio Marco, Ta-Wei Lin, Cong Peng, Marc A. Kerenyi, Semir Beyaz, et al. 2013. "Mapping Cellular Hierarchy by Single-Cell Analysis of the Cell Surface Repertoire." *Cell Stem Cell* 13 (4): 492–505. doi:10.1016/j.stem.2013.07.017.

Haberland, Michael, Rusty L Montgomery, and Eric N Olson. 2009. "The Many Roles of Histone Deacetylases in Development and Physiology: Implications for Disease and Therapy." *Nature Reviews. Genetics* 10 (1). NIH Public Access: 32–42. doi:10.1038/nrg2485.

Harrow, J., A. Frankish, J. M. Gonzalez, E. Tapanari, M. Diekhans, F. Kokocinski, B. L. Aken, et al. 2012. "GENCODE: The Reference Human Genome Annotation for The ENCODE Project." *Genome Research* 22 (9): 1760–74. doi:10.1101/gr.135350.111.

Haynes, S R, C Dollard, F Winston, S Beck, J Trowsdale, and I B Dawid. 1992. "The Bromodomain: A Conserved Sequence Found in Human, Drosophila and Yeast Proteins." *Nucleic Acids Research* 20 (10). Oxford University Press: 2603. http://www.ncbi.nlm.nih.gov/pubmed/1350857.

He, Meian, Min Xu, Ben Zhang, Jun Liang, Peng Chen, Jong-Young Lee, Todd A Johnson, et al. 2015. "Meta-Analysis of Genome-Wide Association Studies of Adult Height in East Asians Identifies 17 Novel Loci." *Human Molecular Genetics* 24 (6). Oxford University Press: 1791–1800. doi:10.1093/hmg/ddu583.

Hebbes, T R, A W Thorne, and C Crane-Robinson. 1988. "A Direct Link between Core Histone Acetylation and Transcriptionally Active Chromatin." *The EMBO Journal* 7 (5). European Molecular Biology Organization: 1395–1402. http://www.ncbi.nlm.nih.gov/pubmed/3409869.

Heemskerk, Johan W M, Edouard M Bevers, and Theo Lindhout. 2002. "Platelet Activation and Blood Coagulation." *Thromb Haemost*. Vol. 88. https://pdfs.semanticscholar.org/5b28/480153d055208becd22c3651ffa000a70e73.pdf.

Heintzman, Nathaniel D., Gary C. Hon, R. David Hawkins, Pouya Kheradpour, Alexander Stark, Lindsey F. Harp, Zhen Ye, et al. 2009. "Histone Modifications at Human Enhancers Reflect Global Cell-Type-Specific Gene Expression." *Nature* 459 (7243): 108–12. doi:10.1038/nature07829.

Heintzman, Nathaniel D, Rhona K Stuart, Gary Hon, Yutao Fu, Christina W Ching, R David Hawkins, Leah O Barrera, et al. 2007a. "Distinct and Predictive Chromatin Signatures of Transcriptional Promoters and Enhancers in the Human Genome." *Nature Genetics* 39 (3): 311–18. doi:10.1038/ng1966.

———. 2007b. "Distinct and Predictive Chromatin Signatures of Transcriptional Promoters and Enhancers in the Human Genome." *Nature Genetics* 39 (3): 311–18. doi:10.1038/ng1966.

Heller, P. G., Ana C Glembotsky, Manish J Gandhi, Carrie L Cummings, Carlos J Pirola, Rosana F Marta, Laura I Kornblihtt, Jonathan G Drachman, and Felisa C Molinas. 2005. "Low Mpl Receptor Expression in a Pedigree with Familial Platelet Disorder with Predisposition to Acute

Myelogenous Leukemia and a Novel AML1 Mutation." *Blood* 105 (12): 4664–70. doi:10.1182/blood-2005-01-0050.

Hihara, Saera, Chan-Gi Pack, Kazunari Kaizu, Tomomi Tani, Tomo Hanafusa, Tadasu Nozaki, Satoko Takemoto, et al. 2012. "Local Nucleosome Dynamics Facilitate Chromatin Accessibility in Living Mammalian Cells." *Cell Reports* 2 (6). Elsevier: 1645–56. doi:10.1016/j.celrep.2012.11.008.

Hill, W G, and Alan Robertson'. 2018. "THE EFF'ECTS OF INBREEDING AT LOCI WITH HETEROZYGOTE ADVANTAGE." Accessed September 20. https://www.ncbi.nlm.nih.gov/pmc/articles/PMC1212065/pdf/615.pdf.

Hilton, Isaac B, Anthony M D'Ippolito, Christopher M Vockley, Pratiksha I Thakore, Gregory E Crawford, Timothy E Reddy, and Charles A Gersbach. 2015. "Epigenome Editing by a CRISPR-Cas9-Based Acetyltransferase Activates Genes from Promoters and Enhancers." *Nature Biotechnology* 33 (5): 510–17. doi:10.1038/nbt.3199.

Hirsch, Emilio, Antonio Iglesias, Alexandra J. Potocnik, Ursula Hartmann, and Reinhard Fässler. 1996. "Impaired Migration but Not Differentiation of Haematopoietic Stem Cells in the Absence of B1 Integrins." *Nature* 380 (6570): 171–75. doi:10.1038/380171a0.

Hon, Gary C, R David Hawkins, and Bing Ren. 2009. "Predictive Chromatin Signatures in the Mammalian Genome." *Human Molecular Genetics* 18 (R2). Oxford University Press: R195-201. doi:10.1093/hmg/ddp409.

Hsu, H L, L Huang, J T Tsan, W Funk, W E Wright, J S Hu, R E Kingston, and R Baer. 1994. "Preferred Sequences for DNA Recognition by the TAL1 Helix-Loop-Helix Proteins." *Molecular and Cellular Biology* 14 (2): 1256–65. http://www.ncbi.nlm.nih.gov/pubmed/8289805.

Hu, M, D Krause, M Greaves, S Sharkis, M Dexter, C Heyworth, and T Enver. 1997. "Multilineage Gene Expression Precedes Commitment in the Hemopoietic System." *Genes & Development* 11 (6): 774–85. http://www.ncbi.nlm.nih.gov/pubmed/9087431.

Hu, Zhenhua, and Wee-Wei Tee. 2017. "Enhancers and Chromatin Structures: Regulatory Hubs in Gene Expression and Diseases." *Bioscience Reports* 37 (2). Portland Press Ltd. doi:10.1042/BSR20160183.

Huber, Tara L., Valerie Kouskoff, H. Joerg Fehling, James Palis, and Gordon Keller. 2004. "Haemangioblast Commitment Is Initiated in the Primitive Streak of the Mouse Embryo." *Nature* 432 (7017). Nature Publishing Group: 625–30. doi:10.1038/nature03122.

Iwasaki, Hiromi, Shin-ichi Mizuno, Richard A Wells, Alan B Cantor, Sumiko Watanabe, and Koichi Akashi. 2003. "GATA-1 Converts Lymphoid and Myelomonocytic Progenitors into the Megakaryocyte/Erythrocyte Lineages." *Immunity* 19 (3): 451–62. http://www.ncbi.nlm.nih.gov/pubmed/14499119.

Izzo, Annalisa, Kinga Kamieniarz, and Robert Schneider. 2008. "The Histone H1 Family: Specific Members, Specific Functions?" *Biological Chemistry* 389 (4): 333–43. doi:10.1515/BC.2008.037.

Jacobson, R H, A G Ladurner, D S King, and R Tjian. 2000. "Structure and Function of a Human TAFII250 Double Bromodomain Module." *Science (New York, N.Y.)* 288 (5470): 1422–25. http://www.ncbi.nlm.nih.gov/pubmed/10827952.

Jagannathan-Bogdan, Madhumita, and Leonard I Zon. 2013. "Hematopoiesis." *Development (Cambridge, England)* 140 (12). Company of Biologists: 2463–67. doi:10.1242/dev.083147.

Jang, Moon Kyoo, Kazuki Mochizuki, Meisheng Zhou, Ho-Sang Jeong, John N. Brady, and Keiko Ozato.

2005a. "The Bromodomain Protein Brd4 Is a Positive Regulatory Component of P-TEFb and Stimulates RNA Polymerase II-Dependent Transcription." *Molecular Cell* 19 (4): 523–34. doi:10.1016/j.molcel.2005.06.027.

Jang, Moon Kyoo, Kazuki Mochizuki, Meisheng Zhou, Ho-Sang Jeong, John N Brady, and Keiko Ozato. 2005b. "The Bromodomain Protein Brd4 Is a Positive Regulatory Component of P-TEFb and Stimulates RNA Polymerase II-Dependent Transcription." *Molecular Cell* 19 (4). Elsevier: 523–34. doi:10.1016/j.molcel.2005.06.027.

Jeppesen, P, and B M Turner. 1993. "The Inactive X Chromosome in Female Mammals Is Distinguished by a Lack of Histone H4 Acetylation, a Cytogenetic Marker for Gene Expression." *Cell* 74 (2): 281–89. http://www.ncbi.nlm.nih.gov/pubmed/8343956.

Josling, Gabrielle A, Shamista A Selvarajah, Michaela Petter, and Michael F Duffy. 2012. "The Role of Bromodomain Proteins in Regulating Gene Expression." *Genes* 3 (2). Multidisciplinary Digital Publishing Institute (MDPI): 320–43. doi:10.3390/genes3020320.

Junt, T., H. Schulze, Z. Chen, S. Massberg, T. Goerge, A. Krueger, D. D. Wagner, et al. 2007. "Dynamic Visualization of Thrombopoiesis Within Bone Marrow." *Science* 317 (5845): 1767–70. doi:10.1126/science.1146304.

Kagey, Michael H., Jamie J. Newman, Steve Bilodeau, Ye Zhan, David A. Orlando, Nynke L. van Berkum, Christopher C. Ebmeier, et al. 2010. "Mediator and Cohesin Connect Gene Expression and Chromatin Architecture." *Nature* 467 (7314). Nature Publishing Group: 430–35. doi:10.1038/nature09380.

Kaneko, Hiroshi, Eri Kobayashi, Masayuki Yamamoto, and Ritsuko Shimizu. 2012. "N- and C-Terminal Transactivation Domains of GATA1 Protein Coordinate Hematopoietic Program." *Journal of Biological Chemistry* 287 (25): 21439–49. doi:10.1074/jbc.M112.370437.

Kanno, Tomohiko, Yuka Kanno, Gary LeRoy, Eric Campos, Hong-Wei Sun, Stephen R Brooks, Golnaz Vahedi, et al. 2014. "BRD4 Assists Elongation of Both Coding and Enhancer RNAs by Interacting with Acetylated Histones." *Nature Structural & Molecular Biology* 21 (12). Nature Publishing Group: 1047–57. doi:10.1038/nsmb.2912.

Kanno, Tomohiko, Yuka Kanno, Richard M Siegel, Moon Kyoo Jang, Michael J Lenardo, and Keiko Ozato. 2004. "Selective Recognition of Acetylated Histones by Bromodomain Proteins Visualized in Living Cells." *Molecular Cell* 13 (1). Elsevier: 33–43. doi:10.1016/S1097-2765(03)00482-9.

Karim, F D, L D Urness, C S Thummel, M J Klemsz, S R McKercher, A Celada, C Van Beveren, R A Maki, C V Gunther, and J A Nye. 1990. "The ETS-Domain: A New DNA-Binding Motif That Recognizes a Purine-Rich Core DNA Sequence." *Genes & Development* 4 (9): 1451–53. http://www.ncbi.nlm.nih.gov/pubmed/2253872.

Kaser, A, G Brandacher, W Steurer, S Kaser, F A Offner, H Zoller, I Theurl, et al. 2001. "Interleukin-6 Stimulates Thrombopoiesis through Thrombopoietin: Role in Inflammatory Thrombocytosis." *Blood* 98 (9). American Society of Hematology: 2720–25. doi:10.1182/BLOOD.V98.9.2720.

Kassouf, Mira T, Jim R Hughes, Stephen Taylor, Simon J McGowan, Shamit Soneji, Angela L Green, Paresh Vyas, and Catherine Porcher. 2010. "Genome-Wide Identification of TAL1's Functional Targets: Insights into Its Mechanisms of Action in Primary Erythroid Cells." *Genome Research* 20 (8). Cold Spring Harbor Laboratory Press: 1064–83. doi:10.1101/gr.104935.110.

Kaushansky, K, V C Broudy, N Lin, M J Jorgensen, J McCarty, N Fox, D Zucker-Franklin, and C Lofton-

Day. 1995. “Thrombopoietin, the Mp1 Ligand, Is Essential for Full Megakaryocyte Development.” *Proceedings of the National Academy of Sciences of the United States of America* 92 (8): 3234–38. http://www.ncbi.nlm.nih.gov/pubmed/7536928.

Kaushansky, Kenneth. 2005. “The Molecular Mechanisms That Control Thrombopoiesis.” *The Journal of Clinical Investigation* 115 (12). American Society for Clinical Investigation: 3339–47. doi:10.1172/JCI26674.

Kawada, Hiroshi, Tatsuya Ito, Pamela N. Pharr, Demetri D. Spyropoulos, Dennis K. Watson, and Makio Ogawa. 2001. “Defective Megakaryopoiesis and Abnormal Erythroid Development in Fli-1 Gene-Targeted Mice.” *International Journal of Hematology* 73 (4): 463–68. doi:10.1007/BF02994008.

Kent, D. G., M. R. Copley, C. Benz, S. Wohrer, B. J. Dykstra, E. Ma, J. Cheyne, et al. 2009. “Prospective Isolation and Molecular Characterization of Hematopoietic Stem Cells with Durable Self-Renewal Potential.” *Blood* 113 (25): 6342–50. doi:10.1182/blood-2008-12-192054.

Kerem, B, J M Rommens, J A Buchanan, D Markiewicz, T K Cox, A Chakravarti, M Buchwald, and L C Tsui. 1989. “Identification of the Cystic Fibrosis Gene: Genetic Analysis.” *Science (New York, N.Y.)* 245 (4922): 1073–80. http://www.ncbi.nlm.nih.gov/pubmed/2570460.

Kessel, Katharina U, Anika Bluemke, Hans R Schöler, Holm Zaehres, Peter Schlenke, and Isabel Dorn. 2017. “Emergence of CD43-Expressing Hematopoietic Progenitors from Human Induced Pluripotent Stem Cells.” *Transfusion Medicine and Hemotherapy : Offizielles Organ Der Deutschen Gesellschaft Fur Transfusionsmedizin Und Immunhamatologie* 44 (3). Karger Publishers: 143–50. doi:10.1159/000477357.

Khavari, Paul A., Craig L. Peterson, John W. Tamkun, Dirk B. Mendel, and Gerald R. Crabtree. 1993. “BRG1 Contains a Conserved Domain of the SWI2/SNF2 Family Necessary for Normal Mitotic Growth and Transcription.” *Nature* 366 (6451): 170–74. doi:10.1038/366170a0.

Kie, Jeong-Hae, Woo-Ick Yang, Mi-Kyung Lee, Tae-Jung Kwon, Yoo-Hong Min, Hyun-Ok Kim, Hyo-Seop Ahn, et al. 2002. “Decrease in Apoptosis and Increase in Polyploidization of Megakaryocytes by Stem Cell Factor During Ex Vivo Expansion of Human Cord Blood CD34 $^{+}$ Cells Using Thrombopoietin.” *Stem Cells* 20 (1): 73–79. doi:10.1634/stemcells.20-1-73.

Kim, K., E. Hahm, J. Li, L.-M. Holbrook, P. Sasikumar, R. G. Stanley, M. Ushio-Fukai, J. M. Gibbins, and J. Cho. 2013. “Platelet Protein Disulfide Isomerase Is Required for Thrombus Formation but Not for Hemostasis in Mice.” *Blood* 122 (6): 1052–61. doi:10.1182/blood-2013-03-492504.

Kimura, Shinya, Andrew W. Roberts, Donald Metcalf, and Warren S. Alexander. 1998. “Hematopoietic Stem Cell Deficiencies in Mice Lacking C-Mpl, the Receptor for Thrombopoietin.” *Proceedings of the National Academy of Sciences* 95 (3).

Kissa, Karima, and Philippe Herbomel. 2010. “Blood Stem Cells Emerge from Aortic Endothelium by a Novel Type of Cell Transition.” *Nature* 464 (7285). Nature Publishing Group: 112–15. doi:10.1038/nature08761.

Klimchenko, O., M. Mori, A. DiStefano, T. Langlois, F. Larbret, Y. Lecluse, O. Feraud, W. Vainchenker, F. Norol, and N. Debili. 2009. “A Common Bipotent Progenitor Generates the Erythroid and Megakaryocyte Lineages in Embryonic Stem Cell-Derived Primitive Hematopoiesis.” *Blood* 114 (8): 1506–17. doi:10.1182/blood-2008-09-178863.

KLOVAITE, J., M. BENN, S. YAZDANYAR, and B. G. NORDESTGAARD. 2011a. “High Platelet Volume and Increased Risk of Myocardial Infarction: 39 531 Participants from the General Population.”

Journal of Thrombosis and Haemostasis 9 (1): 49–56. doi:10.1111/j.1538-7836.2010.04110.x.

———. 2011b. "High Platelet Volume and Increased Risk of Myocardial Infarction: 39 531 Participants from the General Population." *Journal of Thrombosis and Haemostasis* 9 (1): 49–56. doi:10.1111/j.1538-7836.2010.04110.x.

Koenig, M, E P Hoffman, C J Bertelson, A P Monaco, C Feener, and L M Kunkel. 1987. "Complete Cloning of the Duchenne Muscular Dystrophy (DMD) CDNA and Preliminary Genomic Organization of the DMD Gene in Normal and Affected Individuals." *Cell* 50 (3): 509–17. http://www.ncbi.nlm.nih.gov/pubmed/3607877.

Kondo, M, I L Weissman, and K Akashi. 1997. "Identification of Clonogenic Common Lymphoid Progenitors in Mouse Bone Marrow." *Cell* 91 (5): 661–72. http://www.ncbi.nlm.nih.gov/pubmed/9393859.

Kori, Yekaterina, Simone Sidoli, Zuo-Fei Yuan, Peder J. Lund, Xiaolu Zhao, and Benjamin A. Garcia. 2017. "Proteome-Wide Acetylation Dynamics in Human Cells." *Scientific Reports* 7 (1). Nature Publishing Group: 10296. doi:10.1038/s41598-017-09918-3.

Kouzarides, Tony. 2007. "Chromatin Modifications and Their Function." *Cell* 128 (4): 693–705. doi:10.1016/j.cell.2007.02.005.

Kuleshov, Maxim V., Matthew R. Jones, Andrew D. Rouillard, Nicolas F. Fernandez, Qiaonan Duan, Zichen Wang, Simon Koplev, et al. 2016. "Enrichr: A Comprehensive Gene Set Enrichment Analysis Web Server 2016 Update." *Nucleic Acids Research* 44 (W1): W90–97. doi:10.1093/nar/gkw377.

Kuter, D J, and R D Rosenberg. 1995. "The Reciprocal Relationship of Thrombopoietin (c-Mpl Ligand) to Changes in the Platelet Mass during Busulfan-Induced Thrombocytopenia in the Rabbit." *Blood* 85 (10): 2720–30. http://www.ncbi.nlm.nih.gov/pubmed/7742532.

Lacaud, Georges, and Valerie Kouskoff. 2017. "Hemangioblast, Hemogenic Endothelium, and Primitive versus Definitive Hematopoiesis." *Experimental Hematology* 49 (May). Elsevier: 19–24. doi:10.1016/J.EXPHEM.2016.12.009.

Lachmann, Alexander, Huilei Xu, Jayanth Krishnan, Seth I. Berger, Amin R. Mazloom, and Avi Ma'ayan. 2010. "ChEA: Transcription Factor Regulation Inferred from Integrating Genome-Wide ChIP-X Experiments." *Bioinformatics* 26 (19): 2438–44. doi:10.1093/bioinformatics/btq466.

Lamonica, J. M., C. R. Vakoc, and G. A. Blobel. 2006. "Acetylation of GATA-1 Is Required for Chromatin Occupancy." *Blood* 108 (12): 3736–38. doi:10.1182/blood-2006-07-032847.

Lamonica, Janine M, Wulan Deng, Stephan Kadauke, Amy E Campbell, Roland Gamsjaeger, Hongxin Wang, Yong Cheng, et al. 2011. "Bromodomain Protein Brd3 Associates with Acetylated GATA1 to Promote Its Chromatin Occupancy at Erythroid Target Genes." *Proceedings of the National Academy of Sciences of the United States of America* 108 (22): E159–68. doi:10.1073/pnas.1102140108.

Lancrin, Christophe, Patrycja Sroczynska, Catherine Stephenson, Terry Allen, Valerie Kouskoff, and Georges Lacaud. 2009. "The Haemangioblast Generates Haematopoietic Cells through a Haemogenic Endothelium Stage." *Nature* 457 (7231). Nature Publishing Group: 892–95. doi:10.1038/nature07679.

Lander, E S, and N J Schork. 1994. "Genetic Dissection of Complex Traits." *Science (New York, N.Y.)* 265 (5181). American Association for the Advancement of Science: 2037–48. doi:10.1126/science.8091226.

Latimer, P. 1982. "Light Scattering and Absorption as Methods of Studying Cell Population Parameters." *Annual Review of Biophysics and Bioengineering* 11 (1). Annual Reviews 4139 El Camino Way, P.O. Box 10139, Palo Alto, CA 94303-0139, USA : 129–50. doi:10.1146/annurev.bb.11.060182.001021.

Lee, Ji-Eun, Young-Kwon Park, Sarah Park, Younghoon Jang, Nicholas Waring, Anup Dey, Keiko Ozato, Binbin Lai, Weiqun Peng, and Kai Ge. 2017. "Brd4 Binds to Active Enhancers to Control Cell Identity Gene Induction in Adipogenesis and Myogenesis." *Nature Communications* 8 (1). Nature Publishing Group: 2217. doi:10.1038/s41467-017-02403-5.

Lee, Kenneth K., and Jerry L. Workman. 2007. "Histone Acetyltransferase Complexes: One Size Doesn't Fit All." *Nature Reviews Molecular Cell Biology* 8 (4). Nature Publishing Group: 284–95. doi:10.1038/nrm2145.

Lee, Tong Ihn, Sarah E Johnstone, and Richard A Young. 2006. "Chromatin Immunoprecipitation and Microarray-Based Analysis of Protein Location." *Nature Protocols* 1 (2): 729–48. doi:10.1038/nprot.2006.98.

Lefrançais, Emma, Guadalupe Ortiz-Muñoz, Axelle Caudrillier, Beñat Mallavia, Fengchun Liu, David M. Sayah, Emily E. Thornton, et al. 2017. "The Lung Is a Site of Platelet Biogenesis and a Reservoir for Haematopoietic Progenitors." *Nature* 544 (7648). Nature Publishing Group: 105–9. doi:10.1038/nature21706.

Lei, Yong, Xiaotian Zhang, Jianzhong Su, Mira Jeong, Michael C. Gundry, Yung-Hsin Huang, Yubin Zhou, Wei Li, and Margaret A. Goodell. 2017. "Targeted DNA Methylation in Vivo Using an Engineered DCas9-MQ1 Fusion Protein." *Nature Communications* 8 (July). Nature Publishing Group: 16026. doi:10.1038/ncomms16026.

Lenhard, Boris, Albin Sandelin, and Piero Carninci. 2012. "Metazoan Promoters: Emerging Characteristics and Insights into Transcriptional Regulation." *Nature Reviews Genetics* 13 (4): 233–45. doi:10.1038/nrg3163.

LeRoy, Gary, Brenden Rickards, and S J Flint. 2008a. "The Double Bromodomain Proteins Brd2 and Brd3 Couple Histone Acetylation to Transcription." *Molecular Cell* 30 (1). NIH Public Access: 51–60. doi:10.1016/j.molcel.2008.01.018.

———. 2008b. "The Double Bromodomain Proteins Brd2 and Brd3 Couple Histone Acetylation to Transcription." *Molecular Cell* 30 (1). Elsevier: 51–60. doi:10.1016/j.molcel.2008.01.018.

Letting, Danielle L, Carrie Rakowski, Mitchell J Weiss, and Gerd A Blobel. 2003. "Formation of a Tissue-Specific Histone Acetylation Pattern by the Hematopoietic Transcription Factor GATA-1." *Molecular and Cellular Biology* 23 (4). American Society for Microbiology (ASM): 1334–40. doi:10.1128/MCB.23.4.1334-1340.2003.

Li, Jin, Joseph T. Glessner, Haitao Zhang, Cuiping Hou, Zhi Wei, Jonathan P. Bradfield, Frank D. Mentch, et al. 2013. "GWAS of Blood Cell Traits Identifies Novel Associated Loci and Epistatic Interactions in Caucasian and African-American Children." *Human Molecular Genetics* 22 (7): 1457–64. doi:10.1093/hmg/dds534.

Li, Mulin Jun, Zipeng Liu, Panwen Wang, Maria P. Wong, Matthew R. Nelson, Jean-Pierre A. Kocher, Meredith Yeager, et al. 2016. "GWASdb v2: An Update Database for Human Genetic Variants Identified by Genome-Wide Association Studies." *Nucleic Acids Research* 44 (D1): D869–76. doi:10.1093/nar/gkv1317.

Lin, Yin C, Suchit Jhunjhunwala, Christopher Benner, Sven Heinz, Eva Welinder, Robert Mansson,

Mikael Sigvardsson, et al. 2010. "A Global Network of Transcription Factors, Involving E2A, EBF1 and Foxo1, That Orchestrates B Cell Fate." *Nature Immunology* 11 (7): 635–43. doi:10.1038/ni.1891.

Ling, Kam-Wing, Katrin Ottersbach, Jan Piet van Hamburg, Aneta Oziemlak, Fong-Ying Tsai, Stuart H. Orkin, Rob Ploemacher, Rudi W. Hendriks, and Elaine Dzierzak. 2004. "GATA-2 Plays Two Functionally Distinct Roles during the Ontogeny of Hematopoietic Stem Cells." *The Journal of Experimental Medicine* 200 (7): 871–82. doi:10.1084/jem.20031556.

Liu, Feng, Maggie Walmsley, Adam Rodaway, and Roger Patient. 2008. "Fli1 Acts at the Top of the Transcriptional Network Driving Blood and Endothelial Development." *Current Biology* 18 (16): 1234–40. doi:10.1016/j.cub.2008.07.048.

Liu, X. Shawn, Hao Wu, Xiong Ji, Yonatan Stelzer, Xuebing Wu, Szymon Czauderna, Jian Shu, Daniel Dadon, Richard A. Young, and Rudolf Jaenisch. 2016. "Editing DNA Methylation in the Mammalian Genome." *Cell* 167 (1): 233–247.e17. doi:10.1016/j.cell.2016.08.056.

Lok, Si, Kenneth Kaushansky, Richard D. Holly, Joseph L. Kuijper, Catherine E. Lofton-Day, Pieter J. Oort, Francis J. Grant, et al. 1994. "Cloning and Expression of Murine Thrombopoietin CDNA and Stimulation of Platelet Production in Vivo." *Nature* 369 (6481). Nature Publishing Group: 565–68. doi:10.1038/369565a0.

López, J A. 1994. "The Platelet Glycoprotein Ib-IX Complex." *Blood Coagulation & Fibrinolysis : An International Journal in Haemostasis and Thrombosis* 5 (1): 97–119. http://www.ncbi.nlm.nih.gov/pubmed/8180344.

Lordier, L., A. Jalil, F. Aurade, F. Larbret, J. Larghero, N. Debili, W. Vainchenker, and Y. Chang. 2008. "Megakaryocyte Endomitosis Is a Failure of Late Cytokinesis Related to Defects in the Contractile Ring and Rho/Rock Signaling." *Blood* 112 (8): 3164–74. doi:10.1182/blood-2008-03-144956.

Lordier, Larissa, Dominique Bluteau, Abdelali Jalil, Céline Legrand, Jiajia Pan, Philippe Rameau, Dima Jouni, et al. 2012. "RUNX1-Induced Silencing of Non-Muscle Myosin Heavy Chain IIB Contributes to Megakaryocyte Polyploidization." *Nature Communications* 3 (1): 717. doi:10.1038/ncomms1704.

Lorsbach, R. B., Jennifer Moore, Sonny O Ang, Weili Sun, Noel Lenny, and James R Downing. 2004. "Role of RUNX1 in Adult Hematopoiesis: Analysis of RUNX1-IRES-GFP Knock-in Mice Reveals Differential Lineage Expression." *Blood* 103 (7): 2522–29. doi:10.1182/blood-2003-07-2439.

Love, Michael I, Wolfgang Huber, and Simon Anders. 2014. "Moderated Estimation of Fold Change and Dispersion for RNA-Seq Data with DESeq2." *Genome Biology* 15 (12): 550. doi:10.1186/s13059-014-0550-8.

Lovén, Jakob, Heather A Hoke, Charles Y Lin, Ashley Lau, David A Orlando, Christopher R Vakoc, James E Bradner, Tong Ihn Lee, and Richard A Young. 2013a. "Selective Inhibition of Tumor Oncogenes by Disruption of Super-Enhancers." *Cell* 153 (2). Elsevier: 320–34. doi:10.1016/j.cell.2013.03.036.

———. 2013b. "Selective Inhibition of Tumor Oncogenes by Disruption of Super-Enhancers." *Cell* 153 (2). Elsevier: 320–34. doi:10.1016/j.cell.2013.03.036.

Lu, Shi-Jiang, Feng Li, Hong Yin, Qiang Feng, Erin a Kimbrel, Eunsil Hahm, Jonathan N Thon, et al. 2011. "Platelets Generated from Human Embryonic Stem Cells Are Functional in Vitro and in the Microcirculation of Living Mice." *Cell Research* 21 (3). Nature Publishing Group: 530–45.

doi:10.1038/cr.2011.8.

Lugus, Jesse J, Changwon Park, Yunglin D Ma, and Kyunghee Choi. 2009. "Both Primitive and Definitive Blood Cells Are Derived from Flk-1+ Mesoderm." *Blood* 113 (3). American Society of Hematology: 563–66. doi:10.1182/blood-2008-06-162750.

Lun, Aaron T L, and Gordon K Smyth. 2016. "Csaw: A Bioconductor Package for Differential Binding Analysis of ChIP-Seq Data Using Sliding Windows." *Nucleic Acids Research* 44 (5): e45. doi:10.1093/nar/gkv1191.

Lux, Christopher T, Momoko Yoshimoto, Kathleen McGrath, Simon J Conway, James Palis, and Mervin C Yoder. 2008. "All Primitive and Definitive Hematopoietic Progenitor Cells Emerging before E10 in the Mouse Embryo Are Products of the Yolk Sac." *Blood* 111 (7). American Society of Hematology: 3435–38. doi:10.1182/blood-2007-08-107086.

MacArthur, Jacqueline, Emily Bowler, Maria Cerezo, Laurent Gil, Peggy Hall, Emma Hastings, Heather Junkins, et al. 2017. "The New NHGRI-EBI Catalog of Published Genome-Wide Association Studies (GWAS Catalog)." *Nucleic Acids Research* 45 (D1). Oxford University Press: D896–901. doi:10.1093/nar/gkw1133.

Machlus, Kellie R., Jonathan N. Thon, and Joseph E. Italiano. 2014. "Interpreting the Developmental Dance of the Megakaryocyte: A Review of the Cellular and Molecular Processes Mediating Platelet Formation." *British Journal of Haematology* 165 (2): 227–36. doi:10.1111/bjh.12758.

Mali, Prashant, John Aach, P Benjamin Stranges, Kevin M Esvelt, Mark Moosburner, Sriram Kosuri, Luhan Yang, and George M Church. 2013. "CAS9 Transcriptional Activators for Target Specificity Screening and Paired Nickases for Cooperative Genome Engineering." *Nature Biotechnology* 31 (9). NIH Public Access: 833–38. doi:10.1038/nbt.2675.

Martin, G R. 1981. "Isolation of a Pluripotent Cell Line from Early Mouse Embryos Cultured in Medium Conditioned by Teratocarcinoma Stem Cells." *Proceedings of the National Academy of Sciences of the United States of America* 78 (12): 7634–38. http://www.ncbi.nlm.nih.gov/pubmed/6950406.

Marushige, K. 1976. "Activation of Chromatin by Acetylation of Histone Side Chains." *Proceedings of the National Academy of Sciences of the United States of America* 73 (11). National Academy of Sciences: 3937–41. http://www.ncbi.nlm.nih.gov/pubmed/1069278.

Maruyama, Tetsuo, Andrea Farina, Anup Dey, JaeHun Cheong, Vladimir P Bermudez, Tomohiko Tamura, Selvaggia Sciortino, Jon Shuman, Jerard Hurwitz, and Keiko Ozato. 2002. "A Mammalian Bromodomain Protein, Brd4, Interacts with Replication Factor C and Inhibits Progression to S Phase." *Molecular and Cellular Biology* 22 (18): 6509–20. http://www.ncbi.nlm.nih.gov/pubmed/12192049.

Mattia, Gianfranco, Francesca Vulcano, Luisa Milazzo, Alessandra Barca, Giampiero Macioce, Adele Giampaolo, and H Jane Hassan. 2002. "Different Ploidy Levels of Megakaryocytes Generated from Peripheral or Cord Blood CD34+ Cells Are Correlated with Different Levels of Platelet Release." *Blood* 99 (3): 888–97. http://www.ncbi.nlm.nih.gov/pubmed/11806991.

Maurano, Matthew T, Richard Humbert, Eric Rynes, Robert E Thurman, Eric Haugen, Hao Wang, Alex P Reynolds, et al. 2018. "Systematic Localization of Common Disease-Associated Variation in Regulatory DNA Downloaded From." Accessed September 12. http://science.sciencemag.org/.

Mazur, E M, D L Lindquist, P A de Alarcon, and J L Cohen. 1988. "Evaluation of Bone Marrow Megakaryocyte Ploidy Distributions in Persons with Normal and Abnormal Platelet Counts." *The*

Journal of Laboratory and Clinical Medicine 111: 194–202.

McGrath, Kathleen E, Jenna M Frame, Katherine H Fegan, James R Bowen, Simon J Conway, Seana C Catherman, Paul D Kingsley, Anne D Koniski, and James Palis. 2015. "Distinct Sources of Hematopoietic Progenitors Emerge before HSCs and Provide Functional Blood Cells in the Mammalian Embryo." *Cell Reports* 11 (12). Elsevier: 1892–1904. doi:10.1016/j.celrep.2015.05.036.

Meas, Rithy, and Peng Mao. 2015. "Histone Ubiquitylation and Its Roles in Transcription and DNA Damage Response." *DNA Repair* 36 (December). NIH Public Access: 36–42. doi:10.1016/j.dnarep.2015.09.016.

Medvinsky, A, and E Dzierzak. 1996. "Definitive Hematopoiesis Is Autonomously Initiated by the AGM Region." *Cell* 86 (6): 897–906. http://www.ncbi.nlm.nih.gov/pubmed/8808625.

Medvinsky, Alexander, Stanislav Rybtsov, and Samir Taoudi. 2011. "Embryonic Origin of the Adult Hematopoietic System: Advances and Questions." *Development (Cambridge, England)* 138 (6). Oxford University Press for The Company of Biologists Limited: 1017–31. doi:10.1242/dev.040998.

Meinders, Marjolein, Mark Hoogenboezem, Maaike R Scheenstra, Iris M De Cuyper, Petros Papadopoulos, Tamás Németh, Attila Mócsai, Timo K van den Berg, Taco W Kuijpers, and Laura Gutiérrez. 2016. "Repercussion of Megakaryocyte-Specific Gata1 Loss on Megakaryopoiesis and the Hematopoietic Precursor Compartment." *PloS One* 11 (5). Public Library of Science: e0154342. doi:10.1371/journal.pone.0154342.

Miyamoto, Toshihiro, Hiromi Iwasaki, Boris Reizis, Min Ye, Thomas Graf, Irving L Weissman, and Koichi Akashi. 2002. "Myeloid or Lymphoid Promiscuity as a Critical Step in Hematopoietic Lineage Commitment." *Developmental Cell* 3 (1). Elsevier: 137–47. doi:10.1016/S1534-5807(02)00201-0.

Mochizuki, Kazuki, Akira Nishiyama, Moon Kyoo Jang, Anup Dey, Anu Ghosh, Tomohiko Tamura, Hiroko Natsume, Hongjie Yao, and Keiko Ozato. 2008. "The Bromodomain Protein Brd4 Stimulates G1 Gene Transcription and Promotes Progression to S Phase." *The Journal of Biological Chemistry* 283 (14). American Society for Biochemistry and Molecular Biology: 9040–48. doi:10.1074/jbc.M707603200.

Moignard, Victoria, Iain C. Macaulay, Gemma Swiers, Florian Buettner, Judith Schütte, Fernando J. Calero-Nieto, Sarah Kinston, et al. 2013. "Characterization of Transcriptional Networks in Blood Stem and Progenitor Cells Using High-Throughput Single-Cell Gene Expression Analysis." *Nature Cell Biology* 15 (4): 363–72. doi:10.1038/ncb2709.

Moore, Carmel, Jennifer Sambrook, Matthew Walker, Zoe Tolkien, Stephen Kaptoge, David Allen, Susan Mehenny, et al. 2014. "The INTERVAL Trial to Determine Whether Intervals between Blood Donations Can Be Safely and Acceptably Decreased to Optimise Blood Supply: Study Protocol for a Randomised Controlled Trial." *Trials* 15 (1). BioMed Central: 363. doi:10.1186/1745-6215-15-363.

Moore, Malcolm A. S., and Donald Metcalf. 1970. "Ontogeny of the Haemopoietic System: Yolk Sac Origin of In Vivo and In Vitro Colony Forming Cells in the Developing Mouse Embryo." *British Journal of Haematology* 18 (3). Blackwell Publishing Ltd: 279–96. doi:10.1111/j.1365-2141.1970.tb01443.x.

Mora, Antonio, Geir Kjetil Sandve, Odd Stokke Gabrielsen, and Ragnhild Eskeland. 2016. "In the Loop: Promoter-Enhancer Interactions and Bioinformatics." *Briefings in Bioinformatics* 17 (6). Oxford

University Press: 980–95. doi:10.1093/bib/bbv097.

Moreau, Thomas, Amanda L. Evans, Louella Vasquez, Marloes R. Tijssen, Ying Yan, Matthew W. Trotter, Daniel Howard, et al. 2016. "Large-Scale Production of Megakaryocytes from Human Pluripotent Stem Cells by Chemically Defined Forward Programming." *Nature Communications* 7 (April). Nature Publishing Group: 11208. doi:10.1038/ncomms11208.

Morrison, S J, and I L Weissman. 1994. "The Long-Term Repopulating Subset of Hematopoietic Stem Cells Is Deterministic and Isolatable by Phenotype." *Immunity* 1 (8): 661–73. http://www.ncbi.nlm.nih.gov/pubmed/7541305.

Mujtaba, Shiraz, Yan He, Lei Zeng, Sherry Yan, Olga Plotnikova, Sachchidanand, Roberto Sanchez, Nancy J Zeleznik-Le, Ze'ev Ronai, and Ming-Ming Zhou. 2004. "Structural Mechanism of the Bromodomain of the Coactivator CBP in P53 Transcriptional Activation." *Molecular Cell* 13 (2): 251–63. http://www.ncbi.nlm.nih.gov/pubmed/14759370.

Muller-Sieburg, C. E., Rebecca H Cho, Lars Karlsson, Jing-F Huang, and Hans B Sieburg. 2004a. "Myeloid-Biased Hematopoietic Stem Cells Have Extensive Self-Renewal Capacity but Generate Diminished Lymphoid Progeny with Impaired IL-7 Responsiveness." *Blood* 103 (11): 4111–18. doi:10.1182/blood-2003-10-3448.

———. 2004b. "Myeloid-Biased Hematopoietic Stem Cells Have Extensive Self-Renewal Capacity but Generate Diminished Lymphoid Progeny with Impaired IL-7 Responsiveness." *Blood* 103 (11): 4111–18. doi:10.1182/blood-2003-10-3448.

Müller-Sieburg, Christa E, Rebecca H Cho, Marilyn Thoman, Becky Adkins, and Hans B Sieburg. 2002. "Deterministic Regulation of Hematopoietic Stem Cell Self-Renewal and Differentiation." *Blood* 100 (4): 1302–9. http://www.ncbi.nlm.nih.gov/pubmed/12149211.

Muller-Sieburg, Christa E, Hans B Sieburg, Jeff M Bernitz, and Giulio Cattarossi. 2012. "Stem Cell Heterogeneity: Implications for Aging and Regenerative Medicine." *Blood* 119 (17). American Society of Hematology: 3900–3907. doi:10.1182/blood-2011-12-376749.

Muntean, Andrew G., Liyan Pang, Mortimer Poncz, Steven F. Dowdy, Gerd A. Blobel, and John D. Crispino. 2007. "Cyclin D-Cdk4 Is Regulated by GATA-1 and Required for Megakaryocyte Growth and Polyploidization." *Blood* 109: 5199–5207. doi:10.1182/blood-2006-11-059378.

Nagy, Z, and L Tora. 2007. "Distinct GCN5/PCAF-Containing Complexes Function as Co-Activators and Are Involved in Transcription Factor and Global Histone Acetylation." *Oncogene* 26 (37). Nature Publishing Group: 5341–57. doi:10.1038/sj.onc.1210604.

Nakagawa, Masato, Michiyo Koyanagi, Koji Tanabe, Kazutoshi Takahashi, Tomoko Ichisaka, Takashi Aoi, Keisuke Okita, Yuji Mochiduki, Nanako Takizawa, and Shinya Yamanaka. 2008. "Generation of Induced Pluripotent Stem Cells without Myc from Mouse and Human Fibroblasts." *Nature Biotechnology* 26 (1): 101–6. doi:10.1038/nbt1374.

Nakamura, Sou, Naoya Takayama, Shinji Hirata, Hideya Seo, Hiroshi Endo, Kiyosumi Ochi, Ken-ichi Fujita, et al. 2014. "Expandable Megakaryocyte Cell Lines Enable Clinically Applicable Generation of Platelets from Human Induced Pluripotent Stem Cells." *Cell Stem Cell* 14 (4): 535–48. doi:10.1016/j.stem.2014.01.011.

Nichols, Kim E., John D. Crispino, Mortimer Poncz, James G. White, Stuart H. Orkin, John M. Maris, and Mitchell J. Weiss. 2000. "Familial Dyserythropoietic Anaemia and Thrombocytopenia Due to an Inherited Mutation in GATA1." *Nature Genetics* 24 (3). Nature Publishing Group: 266–70. doi:10.1038/73480.

Nicodeme, Edwige, Kate L. Jeffrey, Uwe Schaefer, Soren Beinke, Scott Dewell, Chun-wa Chung, Rohit Chandwani, et al. 2010. "Suppression of Inflammation by a Synthetic Histone Mimic." *Nature* 468 (7327): 1119–23. doi:10.1038/nature09589.

Nieswandt, B., and Steve P Watson. 2003. "Platelet-Collagen Interaction: Is GPVI the Central Receptor?" *Blood* 102 (2): 449–61. doi:10.1182/blood-2002-12-3882.

Nishikii, Hidekazu, Yosuke Kanazawa, Terumasa Umemoto, Yury Goltsev, Yu Matsuzaki, Kenji Matsushita, Masayuki Yamato, Garry P. Nolan, Robert Negrin, and Shigeru Chiba. 2015. "Unipotent Megakaryopoietic Pathway Bridging Hematopoietic Stem Cells and Mature Megakaryocytes." *STEM CELLS* 33 (7): 2196–2207. doi:10.1002/stem.1985.

Noh, Ji-yoon, Shilpa Gandre-babbe, Yuhuan Wang, Vincent Hayes, Yu Yao, Paul Gadue, Spencer K Sullivan, et al. 2015. "Inducible Gata1 Suppression Expands Megakaryocyte-Erythroid Progenitors from Embryonic Stem Cells." *Journal of Clinical Investigation* 125 (6): 2369–74. doi:10.1172/JCI77670DS1.

North, Trista E., Wolfram Goessling, Marian Peeters, Pulin Li, Craig Ceol, Allegra M. Lord, Gerhard J. Weber, et al. 2009. "Hematopoietic Stem Cell Development Is Dependent on Blood Flow." *Cell* 137 (4): 736–48. doi:10.1016/j.cell.2009.04.023.

Notta, F., S. Doulatov, E. Laurenti, A. Poeppl, I. Jurisica, and J. E. Dick. 2011. "Isolation of Single Human Hematopoietic Stem Cells Capable of Long-Term Multilineage Engraftment." *Science* 333 (6039): 218–21. doi:10.1126/science.1201219.

Notta, Faiyaz, Sasan Zandi, Naoya Takayama, Stephanie Dobson, Olga I Gan, Gavin Wilson, Kerstin B Kaufmann, et al. 2016. "Distinct Routes of Lineage Development Reshape the Human Blood Hierarchy across Ontogeny." *Science (New York, N.Y.)* 351 (6269). American Association for the Advancement of Science: aab2116. doi:10.1126/science.aab2116.

Ogbourne, S, and T M Antalis. 1998. "Transcriptional Control and the Role of Silencers in Transcriptional Regulation in Eukaryotes." *The Biochemical Journal* 331 (Pt 1) (April): 1–14. http://www.ncbi.nlm.nih.gov/pubmed/9512455.

Oh, Ji Hee, Yun Kyoung Kim, Sanghoon Moon, Young Jin Kim, and Bong-Jo Kim. 2014. "Genome-Wide Association Study Identifies Candidate Loci Associated with Platelet Count in Koreans." *Genomics & Informatics* 12 (4). Korea Genome Organization: 225. doi:10.5808/GI.2014.12.4.225.

Orkin, S H, R a Shivdasani, Y Fujiwara, and M a McDevitt. 1998. "Transcription Factor GATA-1 in Megakaryocyte Development." *Stem Cells (Dayton, Ohio)* 16 Suppl 2 (suppl 2): 79–83. doi:10.1002/stem.5530160710.

Orkin, Stuart H., and Leonard I. Zon. 2008. "Hematopoiesis: An Evolving Paradigm for Stem Cell Biology." *Cell* 132 (4). Cell Press: 631–44. doi:10.1016/J.CELL.2008.01.025.

Osawa, M, K Hanada, H Hamada, and H Nakauchi. 1996. "Long-Term Lymphohematopoietic Reconstitution by a Single CD34-Low/Negative Hematopoietic Stem Cell." *Science (New York, N.Y.)* 273 (5272): 242–45. http://www.ncbi.nlm.nih.gov/pubmed/8662508.

Owen, D J, P Ornaghi, J C Yang, N Lowe, P R Evans, P Ballario, D Neuhaus, P Filetici, and A A Travers. 2000. "The Structural Basis for the Recognition of Acetylated Histone H4 by the Bromodomain of Histone Acetyltransferase Gcn5p." *The EMBO Journal* 19 (22). European Molecular Biology Organization: 6141–49. doi:10.1093/emboj/19.22.6141.

Palii, Carmen G, Carolina Perez-Iratxeta, Zizhen Yao, Yi Cao, Fengtao Dai, Jerry Davison, Harold

Atkins, et al. 2011. "Differential Genomic Targeting of the Transcription Factor TAL1 in Alternate Haematopoietic Lineages." *The EMBO Journal* 30 (3). European Molecular Biology Organization: 494–509. doi:10.1038/emboj.2010.342.

Palis, J, S Robertson, M Kennedy, C Wall, and G Keller. 1999. "Development of Erythroid and Myeloid Progenitors in the Yolk Sac and Embryo Proper of the Mouse." *Development (Cambridge, England)* 126 (22): 5073–84. http://www.ncbi.nlm.nih.gov/pubmed/10529424.

Pang, Liyan, Hai Hui Xue, Gabor Szalai, Xun Wang, Yuhuan Wang, Dennis K. Watson, Warren J. Leonard, Gerd A. Blobel, and Mortimer Poncz. 2006. "Maturation Stage-Specific Regulation of Megakaryopoiesis by Pointed-Domain Ets Proteins." *Blood* 108: 2198–2206. doi:10.1182/blood-2006-04-019760.

Pang, Wendy W., Stanley L. Schrier, and Irving L. Weissman. 2017. "Age-Associated Changes in Human Hematopoietic Stem Cells." *Seminars in Hematology* 54 (1). W.B. Saunders: 39–42. doi:10.1053/J.SEMINHEMATOL.2016.10.004.

Pang, Wendy W, Elizabeth A Price, Debashis Sahoo, Isabel Beerman, William J Maloney, Derrick J Rossi, Stanley L Schrier, and Irving L Weissman. 2011. "Human Bone Marrow Hematopoietic Stem Cells Are Increased in Frequency and Myeloid-Biased with Age." *Proceedings of the National Academy of Sciences of the United States of America* 108 (50). National Academy of Sciences: 20012–17. doi:10.1073/pnas.1116110108.

Paul, Franziska, Ya'ara Arkin, Amir Giladi, Diego Adhemar Jaitin, Ephraim Kenigsberg, Hadas Keren-Shaul, Deborah Winter, et al. 2015. "Transcriptional Heterogeneity and Lineage Commitment in Myeloid Progenitors." *Cell* 163 (7). Cell Press: 1663–77. doi:10.1016/J.CELL.2015.11.013.

Phillips, DR, IF Charo, LV Parise, and LA Fitzgerald. 1988. "The Platelet Membrane Glycoprotein IIb-IIIa Complex." *Blood* 71 (4). http://www.bloodjournal.org/content/71/4/831.long?sso-checked=true.

Picaud, Sarah, David Da Costa, Angeliki Thanasopoulou, Panagis Filippakopoulos, Paul V Fish, Martin Philpott, Oleg Fedorov, et al. 2013. "PFI-1, a Highly Selective Protein Interaction Inhibitor, Targeting BET Bromodomains." *Cancer Research* 73 (11). American Association for Cancer Research: 3336–46. doi:10.1158/0008-5472.CAN-12-3292.

Pope, Nathaniel J, and Emery H Bresnick. 2010. "Differential Coregulator Requirements for Function of the Hematopoietic Transcription Factor GATA-1 at Endogenous Loci." *Nucleic Acids Research* 38 (7). Oxford University Press: 2190–2200. doi:10.1093/nar/gkp1159.

Potocnik, A J, C Brakebusch, and R Fässler. 2000. "Fetal and Adult Hematopoietic Stem Cells Require Beta1 Integrin Function for Colonizing Fetal Liver, Spleen, and Bone Marrow." *Immunity* 12 (6): 653–63. http://www.ncbi.nlm.nih.gov/pubmed/10894165.

Prinjha, R K, J Witherington, and K Lee. 2012. "Place Your BETs: The Therapeutic Potential of Bromodomains." *Trends in Pharmacological Sciences* 33 (3). Elsevier: 146–53. doi:10.1016/j.tips.2011.12.002.

Psaila, Bethan, Nikolaos Barkas, Deena Iskander, Anindita Roy, Stacie Anderson, Neil Ashley, Valentina S. Caputo, et al. 2016. "Single-Cell Profiling of Human Megakaryocyte-Erythroid Progenitors Identifies Distinct Megakaryocyte and Erythroid Differentiation Pathways." *Genome Biology* 17 (1). BioMed Central: 83. doi:10.1186/s13059-016-0939-7.

Qayyum, Rehan, Lewis C Becker, Diane M Becker, Nauder Faraday, Lisa R Yanek, Suzanne M Leal, Chad Shaw, Rasika Mathias, Bhoom Suktitipat, and Paul F Bray. 2015. "Genome-Wide

Association Study of Platelet Aggregation in African Americans." *BMC Genetics* 16 (May). BioMed Central: 58. doi:10.1186/s12863-015-0217-9.

Qayyum, Rehan, Beverly M Snively, Elad Ziv, Michael A Nalls, Yongmei Liu, Weihong Tang, Lisa R Yanek, et al. 2012. "A Meta-Analysis and Genome-Wide Association Study of Platelet Count and Mean Platelet Volume in African Americans." *PLoS Genetics* 8 (3). Public Library of Science: e1002491. doi:10.1371/journal.pgen.1002491.

Qi, Lei S., Matthew H. Larson, Luke A. Gilbert, Jennifer A. Doudna, Jonathan S. Weissman, Adam P. Arkin, and Wendell A. Lim. 2013. "Repurposing CRISPR as an RNA-Guided Platform for Sequence-Specific Control of Gene Expression." *Cell* 152 (5): 1173–83. doi:10.1016/j.cell.2013.02.022.

Qin, Peiwu, Mahmut Parlak, Cem Kuscu, Jigar Bandaria, Mustafa Mir, Karol Szlachta, Ritambhara Singh, Xavier Darzacq, Ahmet Yildiz, and Mazhar Adli. 2017. "Live Cell Imaging of Low- and Non-Repetitive Chromosome Loci Using CRISPR-Cas9." *Nature Communications* 8 (March). Nature Publishing Group: 14725. doi:10.1038/ncomms14725.

Qin, Wenning, Peter M Kutny, Richard S Maser, Stephanie L Dion, Jeffrey D Lamont, Yingfan Zhang, Greggory A Perry, and Haoyi Wang. 2016. "Generating Mouse Models Using CRISPR-Cas9-Mediated Genome Editing." *Current Protocols in Mouse Biology* 6 (1). NIH Public Access: 39–66. doi:10.1002/9780470942390.mo150178.

Rahman, S., M. E. Sowa, M. Ottinger, J. A. Smith, Y. Shi, J. W. Harper, and P. M. Howley. 2011. "The Brd4 Extraterminal Domain Confers Transcription Activation Independent of PTEFb by Recruiting Multiple Proteins, Including NSD3." *Molecular and Cellular Biology* 31 (13): 2641–52. doi:10.1128/MCB.01341-10.

Ran, F. Ann, Patrick D. Hsu, Chie-Yu Lin, Jonathan S. Gootenberg, Silvana Konermann, Alexandro E. Trevino, David A. Scott, et al. 2013. "Double Nicking by RNA-Guided CRISPR Cas9 for Enhanced Genome Editing Specificity." *Cell* 154 (6): 1380–89. doi:10.1016/j.cell.2013.08.021.

Ran, F Ann, Patrick D Hsu, Jason Wright, Vineeta Agarwala, David A Scott, and Feng Zhang. 2013. "Genome Engineering Using the CRISPR-Cas9 System." *Nature Protocols* 8 (11). Nature Publishing Group: 2281–2308. doi:10.1038/nprot.2013.143.

Ran, Fa, Pd Hsu, Jason Wright, and Vineeta Agarwala. 2013. "Genome Engineering Using the CRISPR-Cas9 System." *Nature Protocols* 8 (11): 2281–2308. doi:10.1038/nprot.2013.143.

Rao, A Koneti, and Natthapol Songdej. 2017. "Parsing the Repertoire of GPIb-IX-V Disorders." *Blood* 129 (4). American Society of Hematology: 403–4. doi:10.1182/blood-2016-12-753186.

Rao, Suhas S.P., Miriam H. Huntley, Neva C. Durand, Elena K. Stamenova, Ivan D. Bochkov, James T. Robinson, Adrian L. Sanborn, et al. 2014. "A 3D Map of the Human Genome at Kilobase Resolution Reveals Principles of Chromatin Looping." *Cell* 159 (7): 1665–80. doi:10.1016/j.cell.2014.11.021.

Raslova, Hana, Emiko Komura, Jean Pierre Le Couédic, Frederic Larbret, Najet Debili, Jean Feunteun, Olivier Danos, Olivier Albagli, William Vainchenker, and Rémi Favier. 2004. "FLI1 Monoallelic Expression Combined with Its Hemizygous Loss Underlies Paris-Trousseau/Jacobsen Thrombopenia." *The Journal of Clinical Investigation* 114 (1). American Society for Clinical Investigation: 77–84. doi:10.1172/JCI21197.

Reith, A D, R Rottapel, E Giddens, C Brady, L Forrester, and A Bernstein. 1990. "W Mutant Mice with Mild or Severe Developmental Defects Contain Distinct Point Mutations in the Kinase Domain

of the C-Kit Receptor." *Genes & Development* 4 (3): 390–400. http://www.ncbi.nlm.nih.gov/pubmed/1692559.

Reya, Tannishtha, Sean J. Morrison, Michael F. Clarke, and Irving L. Weissman. 2001. "Stem Cells, Cancer and Cancer Stem Cells." *Nature* 414 (6859): 105–11. doi:10.1038/35102167.

Risitano, Antonina, Lea M Beaulieu, Olga Vitseva, and Jane E Freedman. 2012. "Platelets and Platelet-like Particles Mediate Intercellular RNA Transfer." *Blood* 119 (26). American Society of Hematology: 6288–95. doi:10.1182/blood-2011-12-396440.

Roberts, Thomas C., Usue Etxaniz, Alessandra Dall'Agnese, Shwu-Yuan Wu, Cheng-Ming Chiang, Paul E. Brennan, Matthew J. A. Wood, and Pier Lorenzo Puri. 2017. "BRD3 and BRD4 BET Bromodomain Proteins Differentially Regulate Skeletal Myogenesis." *Scientific Reports* 7 (1). Nature Publishing Group: 6153. doi:10.1038/s41598-017-06483-7.

Robinson, Philip C., Hyon K. Choi, Ron Do, and Tony R. Merriman. 2016. "Insight into Rheumatological Cause and Effect through the Use of Mendelian Randomization." *Nature Reviews Rheumatology* 12 (8): 486–96. doi:10.1038/nrrheum.2016.102.

Rodriguez, Ramon M, Beatriz Suarez-Alvarez, Ruben Salvanés, Covadonga Huidobro, Estela G Toraño, Jose L Garcia-Perez, Carlos Lopez-Larrea, et al. 2014a. "Role of BRD4 in Hematopoietic Differentiation of Embryonic Stem Cells." *Epigenetics* 9 (4). Taylor & Francis: 566–78. doi:10.4161/epi.27711.

———. 2014b. "Role of BRD4 in Hematopoietic Differentiation of Embryonic Stem Cells." *Epigenetics* 9 (4). Taylor & Francis: 566–78. doi:10.4161/epi.27711.

Roe, Jae-Seok, Fatih Mercan, Keith Rivera, Darryl J. Pappin, and Christopher R. Vakoc. 2015. "BET Bromodomain Inhibition Suppresses the Function of Hematopoietic Transcription Factors in Acute Myeloid Leukemia." *Molecular Cell* 58 (6). Elsevier Inc.: 1028–39. doi:10.1016/j.molcel.2015.04.011.

Rossetto, Dorine, Nikita Avvakumov, and Jacques Côté. 2012. "Histone Phosphorylation: A Chromatin Modification Involved in Diverse Nuclear Events." *Epigenetics* 7 (10). Taylor & Francis: 1098–1108. doi:10.4161/epi.21975.

Roth, S Y, and C D Allis. 1992. "Chromatin Condensation: Does Histone H1 Dephosphorylation Play a Role?" *Trends in Biochemical Sciences* 17 (3): 93–98. http://www.ncbi.nlm.nih.gov/pubmed/1412698.

Rouhani, Foad, Natsuhiko Kumasaka, Miguel Cardoso de Brito, Allan Bradley, Ludovic Vallier, and Daniel Gaffney. 2014. "Genetic Background Drives Transcriptional Variation in Human Induced Pluripotent Stem Cells." *PLoS Genetics* 10 (6): e1004432. doi:10.1371/journal.pgen.1004432.

Ruthenburg, Alexander J., Haitao Li, Thomas A. Milne, Scott Dewell, Robert K. McGinty, Melanie Yuen, Beatrix Ueberheide, et al. 2011. "Recognition of a Mononucleosomal Histone Modification Pattern by BPTF via Multivalent Interactions." *Cell* 145 (5): 692–706. doi:10.1016/j.cell.2011.03.053.

Ryu, K H, S Chun, S Carbonierre, S A Im, H L Kim, M H Shin, H Y Shin, et al. 2001. "Apoptosis and Megakaryocytic Differentiation during Ex Vivo Expansion of Human Cord Blood CD34+ Cells Using Thrombopoietin." *British Journal of Haematology* 113 (2): 470–78. http://www.ncbi.nlm.nih.gov/pubmed/11380418.

Sambrook, Joseph. n.d. *Molecular Cloning : A Laboratory Manual*. Third edition. Cold Spring Harbor, N.Y. : Cold Spring Harbor Laboratory Press, [2001] ©2001.

https://search.library.wisc.edu/catalog/999897924602121.

Sander, Jeffry D, and J Keith Joung. 2014. "CRISPR-Cas Systems for Editing, Regulating and Targeting Genomes." *Nature Biotechnology* 32 (4). Nature Research: 347–55. doi:10.1038/nbt.2842.

Sandmann, Thomas, Charles Girardot, Marc Brehme, Waraporn Tongprasit, Viktor Stolc, and Eileen E M Furlong. 2007. "A Core Transcriptional Network for Early Mesoderm Development in Drosophila Melanogaster." *Genes & Development* 21 (4). Cold Spring Harbor Laboratory Press: 436–49. doi:10.1101/gad.1509007.

Sandmann, Thomas, Lars J. Jensen, Janus S. Jakobsen, Michal M. Karzynski, Michael P. Eichenlaub, Peer Bork, and Eileen E.M. Furlong. 2006. "A Temporal Map of Transcription Factor Activity: Mef2 Directly Regulates Target Genes at All Stages of Muscle Development." *Developmental Cell* 10 (6): 797–807. doi:10.1016/j.devcel.2006.04.009.

Sanford, Katherine K., Wilton R. Earle, Virginia J. Evans, Helen K. Waltz, and John E. Shannon. 1951. "The Measurement of Proliferation in Tissue Cultures by Enumeration of Cell Nuclei." *JNCI: Journal of the National Cancer Institute* 11 (4). Oxford University Press: 773–95. doi:10.1093/jnci/11.4.773.

Sanjuan-Pla, Alejandra, Iain C. Macaulay, Christina T. Jensen, Petter S. Woll, Tiago C. Luis, Adam Mead, Susan Moore, et al. 2013. "Platelet-Biased Stem Cells Reside at the Apex of the Haematopoietic Stem-Cell Hierarchy." *Nature* 502 (7470). Nature Publishing Group: 232–36. doi:10.1038/nature12495.

Schachtner, H., S. D. J. Calaminus, A. Sinclair, J. Monypenny, M. P. Blundell, C. Leon, T. L. Holyoake, et al. 2013. "Megakaryocytes Assemble Podosomes That Degrade Matrix and Protrude through Basement Membrane." *Blood* 121 (13): 2542–52. doi:10.1182/blood-2012-07-443457.

Schick, Ursula M., Deepti Jain, Chani J. Hodonsky, Jean V. Morrison, James P. Davis, Lisa Brown, Tamar Sofer, et al. 2016. "Genome-Wide Association Study of Platelet Count Identifies Ancestry-Specific Loci in Hispanic/Latino Americans." *The American Journal of Human Genetics* 98 (2): 229–42. doi:10.1016/j.ajhg.2015.12.003.

Schlaeger, T. M., Hanna K A Mikkola, Christos Gekas, Hildur B Helgadottir, and Stuart H Orkin. 2005. "Tie2Cre-Mediated Gene Ablation Defines the Stem-Cell Leukemia Gene (SCL/Tal1)-Dependent Window during Hematopoietic Stem-Cell Development." *Blood* 105 (10): 3871–74. doi:10.1182/blood-2004-11-4467.

Schmitt, Christopher E., Carlos O. Lizama, and Ann C. Zovein. 2014. "From Transplantation to Transgenics: Mouse Models of Developmental Hematopoiesis." *Experimental Hematology* 42 (8). Elsevier: 707–16. doi:10.1016/J.EXPHEM.2014.06.008.

Schreiber, Stuart L, and Bradley E Bernstein. 2002. "Signaling Network Model of Chromatin." *Cell* 111 (6): 771–78. http://www.ncbi.nlm.nih.gov/pubmed/12526804.

Schröder, Sebastian, Sungyoo Cho, Lei Zeng, Qiang Zhang, Katrin Kaehlcke, Lily Mak, Joann Lau, et al. 2012. "Two-Pronged Binding with Bromodomain-Containing Protein 4 Liberates Positive Transcription Elongation Factor b from Inactive Ribonucleoprotein Complexes." *The Journal of Biological Chemistry* 287 (2). American Society for Biochemistry and Molecular Biology: 1090–99. doi:10.1074/jbc.M111.282855.

Schulze, H., Manav Korpal, Jonathan Hurov, Sang-We Kim, Jinghang Zhang, Lewis C Cantley, Thomas Graf, and Ramesh A Shivdasani. 2006. "Characterization of the Megakaryocyte Demarcation Membrane System and Its Role in Thrombopoiesis." *Blood* 107 (10): 3868–75.

doi:10.1182/blood-2005-07-2755.

Semple, John W., Joseph E. Italiano, and John Freedman. 2011. "Platelets and the Immune Continuum." *Nature Reviews Immunology* 11 (4). Nature Publishing Group: 264–74. doi:10.1038/nri2956.

Seok, Junhee, H Shaw Warren, Alex G Cuenca, Michael N Mindrinos, Henry V Baker, Weihong Xu, Daniel R Richards, et al. 2013. "Genomic Responses in Mouse Models Poorly Mimic Human Inflammatory Diseases." *Proceedings of the National Academy of Sciences of the United States of America* 110 (9). National Academy of Sciences: 3507–12. doi:10.1073/pnas.1222878110.

Shang, Enyuan, Xiangyuan Wang, Duancheng Wen, David A. Greenberg, and Debra J. Wolgemuth. 2009. "Double Bromodomain-Containing Gene Brd2 Is Essential for Embryonic Development in Mouse." *Developmental Dynamics* 238 (4): 908–17. doi:10.1002/dvdy.21911.

Shattil, Sanford J, Hirokazu Kashiwagi, and Nisar Pampori. 2018. "Integrin Signaling: The Platelet Paradigm." Accessed September 16. www.bloodjournal.org.

Shi, Jian, Yifan Wang, Lei Zeng, Yadi Wu, Jiong Deng, Qiang Zhang, Yiwei Lin, et al. 2014. "Disrupting the Interaction of BRD4 with Diacetylated Twist Suppresses Tumorigenesis in Basal-like Breast Cancer." *Cancer Cell* 25 (2). Cell Press: 210–25. doi:10.1016/J.CCR.2014.01.028.

Shi, Junwei, and Christopher R Vakoc. 2014. "The Mechanisms behind the Therapeutic Activity of BET Bromodomain Inhibition." *Molecular Cell* 54 (5). Elsevier: 728–36. doi:10.1016/j.molcel.2014.05.016.

Shin, Eun-Kyung, Hanseul Park, Ji-Yoon Noh, Kyung-Min Lim, and Jin-Ho Chung. 2017. "Platelet Shape Changes and Cytoskeleton Dynamics as Novel Therapeutic Targets for Anti-Thrombotic Drugs." *Biomolecules & Therapeutics* 25 (3). Korean Society of Applied Pharmacology: 223–30. doi:10.4062/biomolther.2016.138.

Shivdasani, Ramesh A., Erica L. Mayer, and Stuart H. Orkin. 1995. "Absence of Blood Formation in Mice Lacking the T-Cell Leukaemia Oncoprotein Tal-1/SCL." *Nature* 373 (6513): 432–34. doi:10.1038/373432a0.

Shogren-Knaak, Michael, Haruhiko Ishii, Jian-Min Sun, Michael J Pazin, James R Davie, and Craig L Peterson. 2006. "Histone H4-K16 Acetylation Controls Chromatin Structure and Protein Interactions." *Science (New York, N.Y.)* 311 (5762). American Association for the Advancement of Science: 844–47. doi:10.1126/science.1124000.

Sidney, Laura E., Matthew J. Branch, Siobhán E. Dunphy, Harminder S. Dua, and Andrew Hopkinson. 2014. "Concise Review: Evidence for CD34 as a Common Marker for Diverse Progenitors." *STEM CELLS* 32 (6): 1380–89. doi:10.1002/stem.1661.

Sieburg, H. B., Rebecca H Cho, Brad Dykstra, Naoyuki Uchida, Connie J Eaves, and Christa E Muller-Sieburg. 2006. "The Hematopoietic Stem Compartment Consists of a Limited Number of Discrete Stem Cell Subsets." *Blood* 107 (6): 2311–16. doi:10.1182/blood-2005-07-2970.

Slater, D N, E A Trowbridge, and J F Martin. 1983. "The Megakaryocyte in Thrombocytopenia: A Microscopic Study Which Supports the Theory That Platelets Are Produced in the Pulmonary Circulation." *Thrombosis Research* 31 (1): 163–76. http://www.ncbi.nlm.nih.gov/pubmed/6612695.

Slayton, William B., David A. Wainman, Xiao Miao Li, Zhongbo Hu, Anil Jotwani, Christopher R. Cogle, Danielle Walker, et al. 2005. "Developmental Differences in Megakaryocyte Maturation Are Determined by the Microenvironment." *Stem Cells* 23 (9): 1400–1408.

doi:10.1634/stemcells.2004-0373.

Sledge, G W, M Glant, J Jansen, N A Heerema, B J Roth, M Goheen, and R Hoffman. 1986. "Establishment in Long Term Culture of Megakaryocytic Leukemia Cells (EST-IU) from the Marrow of a Patient with Leukemia and a Mediastinal Germ Cell Neoplasm." *Cancer Research* 46 (4 Pt 2): 2155–59. http://www.ncbi.nlm.nih.gov/pubmed/3004722.

Smale, Stephen T., and James T. Kadonaga. 2003. "The RNA Polymerase II Core Promoter." *Annual Review of Biochemistry* 72 (1): 449–79. doi:10.1146/annurev.biochem.72.121801.161520.

Smith, Jennifer N, Jenna M Negrelli, Megha B Manek, Emily M Hawes, and Anthony J Viera. 2015. "Diagnosis and Management of Acute Coronary Syndrome: An Evidence-Based Update." *Journal of the American Board of Family Medicine : JABFM* 28 (2). American Board of Family Medicine: 283–93. doi:10.3122/jabfm.2015.02.140189.

Smock, K. J., and S. L. Perkins. 2014. "Thrombocytopenia: An Update." *International Journal of Laboratory Hematology* 36 (3): 269–78. doi:10.1111/ijlh.12214.

Sola-Visner, Martha C, Robert D Christensen, Alan D Hutson, and Lisa M Rimsza. 2007. "Megakaryocyte Size and Concentration in the Bone Marrow of Thrombocytopenic and Nonthrombocytopenic Neonates." *Pediatric Research* 61 (4): 479–84. doi:10.1203/pdr.0b013e3180332c18.

Soneson, Charlotte, Michael I Love, and Mark D Robinson. 2015. "Differential Analyses for RNA-Seq: Transcript-Level Estimates Improve Gene-Level Inferences." *F1000Research* 4 (February): 1521. doi:10.12688/f1000research.7563.2.

Spain, Sarah L., and Jeffrey C. Barrett. 2015. "Strategies for Fine-Mapping Complex Traits." *Human Molecular Genetics* 24 (R1). Oxford University Press: R111–19. doi:10.1093/hmg/ddv260.

Spitz, François, and Eileen E. M. Furlong. 2012. "Transcription Factors: From Enhancer Binding to Developmental Control." *Nature Reviews Genetics* 13 (9). Nature Publishing Group: 613–26. doi:10.1038/nrg3207.

Stachura, D. L., Stella T Chou, and Mitchell J Weiss. 2006. "Early Block to Erythromegakaryocytic Development Conferred by Loss of Transcription Factor GATA-1." *Blood* 107 (1): 87–97. doi:10.1182/blood-2005-07-2740.

Starck, J., M. Weiss-Gayet, C. Gonnet, B. Guyot, J.-M. Vicat, and F. Morle. 2010. "Inducible Fli-1 Gene Deletion in Adult Mice Modifies Several Myeloid Lineage Commitment Decisions and Accelerates Proliferation Arrest and Terminal Erythrocytic Differentiation." *Blood* 116 (23): 4795–4805. doi:10.1182/blood-2010-02-270405.

Stark, Rory, and Gord Brown. 2018. "DiffBind: Differential Binding Analysis of ChIP-Seq Peak Data." Accessed September 28. http://bioconductor.org/packages/release/bioc/vignettes/DiffBind/inst/doc/DiffBind.pdf.

Stenberg, Paula E., Jack Levin, Georgiann Baker, Yuen Mok, and Laurence Corash. 1991. "Neuraminidase-Induced Thrombocytopenia in Mice: Effects on Thrombopoiesis." *Journal of Cellular Physiology* 147 (1): 7–16. doi:10.1002/jcp.1041470103.

Stevenson, William S, David J Rabbolini, Lucinda Beutler, Qiang Chen, Sara Gabrielli, Joel P Mackay, Timothy A Brighton, Christopher M Ward, and Marie-Christine Morel-Kopp. 2015. "Paris-Trousseau Thrombocytopenia Is Phenocopied by the Autosomal Recessive Inheritance of a DNA-Binding Domain Mutation in FLI1." *Blood* 126 (17). American Society of Hematology: 2027–30. doi:10.1182/blood-2015-06-650887.

Stojic, Lovorka, Aaron T L Lun, Jasmin Mangei, Patrice Mascalchi, Valentina Quarantotti, Alexis R Barr, Chris Bakal, John C Marioni, Fanni Gergely, and Duncan T Odom. 2018. "Specificity of RNAi, LNA and CRISPRi as Loss-of-Function Methods in Transcriptional Analysis." *Nucleic Acids Research* 46 (12). Oxford University Press: 5950–66. doi:10.1093/nar/gky437.

Stonestrom, Aaron J, Sarah C Hsu, Kristen S Jahn, Peng Huang, Cheryl A Keller, Belinda M Giardine, Stephan Kadauke, et al. 2015. "Functions of BET Proteins in Erythroid Gene Expression." *Blood* 125 (18). American Society of Hematology: 2825–34. doi:10.1182/blood-2014-10-607309.

Stonestrom, Aaron J, Sarah C Hsu, Michael T Werner, and Gerd A Blobel. 2016. "Erythropoiesis Provides a BRD's Eye View of BET Protein Function." *Drug Discovery Today. Technologies* 19 (March). NIH Public Access: 23–28. doi:10.1016/j.ddtec.2016.05.004.

Strahl, Brian D., and C. David Allis. 2000. "The Language of Covalent Histone Modifications." *Nature* 403 (6765): 41–45. doi:10.1038/47412.

Sudlow, Cathie, John Gallacher, Naomi Allen, Valerie Beral, Paul Burton, John Danesh, Paul Downey, et al. 2015. "UK Biobank: An Open Access Resource for Identifying the Causes of a Wide Range of Complex Diseases of Middle and Old Age." *PLOS Medicine* 12 (3). Public Library of Science: e1001779. doi:10.1371/journal.pmed.1001779.

Sudo, K, H Ema, Y Morita, and H Nakauchi. 2000. "Age-Associated Characteristics of Murine Hematopoietic Stem Cells." *The Journal of Experimental Medicine* 192 (9): 1273–80. http://www.ncbi.nlm.nih.gov/pubmed/11067876.

Svoboda, Ondrej, and Petr Bartunek. 2015. "Origins of the Vertebrate Erythro/Megakaryocytic System." *BioMed Research International* 2015 (October). Hindawi: 1–10. doi:10.1155/2015/632171.

Sylman, Joanna L., Hunter B. Boyce, Annachiara Mitrugno, Garth W. Tormoen, I-Chun Thomas, Todd H. Wagner, Jennifer S. Lee, John T. Leppert, Owen J. T. McCarty, and Parag Mallick. 2018. "A Temporal Examination of Platelet Counts as a Predictor of Prognosis in Lung, Prostate, and Colon Cancer Patients." *Scientific Reports* 8 (1). Nature Publishing Group: 6564. doi:10.1038/s41598-018-25019-1.

Takahashi, Kazutoshi, and Shinya Yamanaka. 2006. "Induction of Pluripotent Stem Cells from Mouse Embryonic and Adult Fibroblast Cultures by Defined Factors." *Cell* 126 (4). Elsevier: 663–76. doi:10.1016/j.cell.2006.07.024.

Takayama, N., H. Nishikii, J. Usui, H. Tsukui, A. Sawaguchi, T. Hiroyama, K. Eto, and H. Nakauchi. 2008. "Generation of Functional Platelets from Human Embryonic Stem Cells in Vitro via ES-Sacs, VEGF-Promoted Structures That Concentrate Hematopoietic Progenitors." *Blood* 111 (11): 5298–5306. doi:10.1182/blood-2007-10-117622.

Taoudi, Samir, Christèle Gonneau, Kate Moore, Julie M Sheridan, C Clare Blackburn, Erin Taylor, and Alexander Medvinsky. 2008. "Extensive Hematopoietic Stem Cell Generation in the AGM Region via Maturation of VE-Cadherin+CD45+ Pre-Definitive HSCs." *Cell Stem Cell* 3 (1). Elsevier: 99–108. doi:10.1016/j.stem.2008.06.004.

Tavian, Manuela, and Bruno Peault. 2005. "Embryonic Development of the Human Hematopoietic System." *The International Journal of Developmental Biology* 49 (2–3). UPV/EHU Press: 243–50. doi:10.1387/ijdb.041957mt.

Thakore, Pratiksha I, Anthony M D'Ippolito, Lingyun Song, Alexias Safi, Nishkala K Shivakumar, Ami M Kabadi, Timothy E Reddy, Gregory E Crawford, and Charles A Gersbach. 2015. "Highly Specific

Epigenome Editing by CRISPR-Cas9 Repressors for Silencing of Distal Regulatory Elements." *Nature Methods* 12 (12): 1143–49. doi:10.1038/nmeth.3630.

Thomas, Mark, and Robert Storey. 2015. "The Role of Platelets in Inflammation." *Thrombosis and Haemostasis* 114 (09): 449–58. doi:10.1160/TH14-12-1067.

Thon, Jonathan N, Hannah Macleod, Antonija Jurak Begonja, Jie Zhu, Kun-Chun Lee, Alex Mogilner, John H. Hartwig, and Joseph E. Italiano. 2012. "Microtubule and Cortical Forces Determine Platelet Size during Vascular Platelet Production." *Nature Communications* 3 (1): 852. doi:10.1038/ncomms1838.

Thon, Jonathan N, Alejandro Montalvo, Sunita Patel-Hett, Matthew T Devine, Jennifer L Richardson, Allen Ehrlicher, Mark K Larson, Karin Hoffmeister, John H Hartwig, and Joseph E Italiano. 2010. "Cytoskeletal Mechanics of Proplatelet Maturation and Platelet Release." *The Journal of Cell Biology* 191 (4): 861–74. doi:10.1083/jcb.201006102.

Thurman, Robert E., Eric Rynes, Richard Humbert, Jeff Vierstra, Matthew T. Maurano, Eric Haugen, Nathan C. Sheffield, et al. 2012. "The Accessible Chromatin Landscape of the Human Genome." *Nature* 489 (7414): 75–82. doi:10.1038/nature11232.

Tober, Joanna, Anne Koniski, Kathleen E McGrath, Radhika Vemishetti, Rachael Emerson, Karen K L de Mesy-Bentley, Richard Waugh, James Palis, and A R Migliaccio. 2007. "The Megakaryocyte Lineage Originates from Hemangioblast Precursors and Is an Integral Component Both of Primitive and of Definitive Hematopoiesis." *Blood* 109 (4). American Society of Hematology: 1433–41. doi:10.1182/blood-2006-06-031898.

Tomita, M, H Furthmayr, and V T Marchesi. 1978. "Primary Structure of Human Erythrocyte Glycophorin A. Isolation and Characterization of Peptides and Complete Amino Acid Sequence." *Biochemistry* 17 (22): 4756–70. http://www.ncbi.nlm.nih.gov/pubmed/728384.

Trojer, Patrick, and Danny Reinberg. 2007. "Facultative Heterochromatin: Is There a Distinctive Molecular Signature?" *Molecular Cell* 28 (1): 1–13. doi:10.1016/j.molcel.2007.09.011.

Tsai, Fong-Ying, Gordon Keller, Frank C. Kuo, Mitchell Weiss, Jianzhou Chen, Margery Rosenblatt, Frederick W. Alt, and Stuart H. Orkin. 1994. "An Early Haematopoietic Defect in Mice Lacking the Transcription Factor GATA-2." *Nature* 371 (6494): 221–26. doi:10.1038/371221a0.

Tsang, Alice P, Jane E Visvader, C.Alexander Turner, Yuko Fujiwara, Channing Yu, Mitchell J Weiss, Merlin Crossley, and Stuart H Orkin. 1997. "FOG, a Multitype Zinc Finger Protein, Acts as a Cofactor for Transcription Factor GATA-1 in Erythroid and Megakaryocytic Differentiation." *Cell* 90 (1). Elsevier: 109–19. doi:10.1016/S0092-8674(00)80318-9.

Vallier, Ludovic, and Roger Pedersen. 2008. "Differentiation of Human Embryonic Stem Cells in Adherent and in Chemically Defined Culture Conditions." In *Current Protocols in Stem Cell Biology*, 4:1D.4.1-1D.4.7. Hoboken, NJ, USA: John Wiley & Sons, Inc. doi:10.1002/9780470151808.sc01d04s4.

Vandamme, Thierry F. 2014. "Use of Rodents as Models of Human Diseases." *Journal of Pharmacy & Bioallied Sciences* 6 (1). Wolters Kluwer -- Medknow Publications: 2–9. doi:10.4103/0975-7406.124301.

Vasquez, LJ, A L Mann, L Chen, and N Soranzo. 2016. "From GWAS to Function: Lessons from Blood Cells." *ISBT Science Series* 11 (Suppl Suppl 1). Wiley-Blackwell: 211–19. doi:10.1111/voxs.12217.

Velten, Lars, Simon F. Haas, Simon Raffel, Sandra Blaszkiewicz, Saiful Islam, Bianca P. Hennig, Christoph Hirche, et al. 2017. "Human Haematopoietic Stem Cell Lineage Commitment Is a

Continuous Process." *Nature Cell Biology* 19 (4): 271–81. doi:10.1038/ncb3493.

Verdin, Eric, and Melanie Ott. 2015a. "50 Years of Protein Acetylation: From Gene Regulation to Epigenetics, Metabolism and Beyond." *Nature Reviews Molecular Cell Biology* 16 (4). Nature Publishing Group: 258–64. doi:10.1038/nrm3931.

———. 2015b. "50 Years of Protein Acetylation: From Gene Regulation to Epigenetics, Metabolism and Beyond." *Nature Reviews Molecular Cell Biology* 16 (4). Nature Publishing Group: 258–64. doi:10.1038/nrm3931.

Voigt, Philipp, Gary LeRoy, William J Drury, Barry M Zee, Jinsook Son, David B Beck, Nicolas L Young, Benjamin A Garcia, and Danny Reinberg. 2012. "Asymmetrically Modified Nucleosomes." *Cell* 151 (1). Elsevier: 181–93. doi:10.1016/j.cell.2012.09.002.

Volarevic, Vladislav, Bojana Simovic Markovic, Marina Gazdic, Ana Volarevic, Nemanja Jovicic, Nebojsa Arsenijevic, Lyle Armstrong, Valentin Djonov, Majlinda Lako, and Miodrag Stojkovic. 2018. "Ethical and Safety Issues of Stem Cell-Based Therapy." *International Journal of Medical Sciences* 15 (1). Ivyspring International Publisher: 36–45. doi:10.7150/ijms.21666.

Vyas, P, K Ault, C W Jackson, S H Orkin, and R A Shivdasani. 1999. "Consequences of GATA-1 Deficiency in Megakaryocytes and Platelets." *Blood* 93 (9): 2867–75. http://www.ncbi.nlm.nih.gov/pubmed/10216081.

Wang, W, J Côté, Y Xue, S Zhou, P A Khavari, S R Biggar, C Muchardt, et al. 1996. "Purification and Biochemical Heterogeneity of the Mammalian SWI-SNF Complex." *The EMBO Journal* 15 (19): 5370–82. http://www.ncbi.nlm.nih.gov/pubmed/8895581.

Wang, Zhibin, Chongzhi Zang, Jeffrey A Rosenfeld, Dustin E Schones, Artem Barski, Suresh Cuddapah, Kairong Cui, et al. 2008. "Combinatorial Patterns of Histone Acetylations and Methylations in the Human Genome." *Nature Genetics* 40 (7). NIH Public Access: 897–903. doi:10.1038/ng.154.

Watkins, Nicholas A, Arief Gusnanto, Bernard de Bono, Subhajyoti De, Diego Miranda-Saavedra, Debbie L Hardie, Will G J Angenent, et al. 2009. "A HaemAtlas: Characterizing Gene Expression in Differentiated Human Blood Cells." *Blood* 113 (19). American Society of Hematology: e1-9. doi:10.1182/blood-2008-06-162958.

Weissman, Irving L., David J. Anderson, and Fred Gage. 2001. "Stem and Progenitor Cells: Origins, Phenotypes, Lineage Commitments, and Transdifferentiations." *Annual Review of Cell and Developmental Biology* 17 (1): 387–403. doi:10.1146/annurev.cellbio.17.1.387.

Weksberg, D. C., S. M. Chambers, N. C. Boles, and M. A. Goodell. 2008. "CD150- Side Population Cells Represent a Functionally Distinct Population of Long-Term Hematopoietic Stem Cells." *Blood* 111 (4): 2444–51. doi:10.1182/blood-2007-09-115006.

Whyte, Warren A, David A Orlando, Denes Hnisz, Brian J Abraham, Charles Y Lin, Michael H Kagey, Peter B Rahl, Tong Ihn Lee, and Richard A Young. 2013. "Master Transcription Factors and Mediator Establish Super-Enhancers at Key Cell Identity Genes." *Cell* 153 (2). Elsevier: 307–19. doi:10.1016/j.cell.2013.03.035.

Willer, Cristen J, Ellen M Schmidt, Sebanti Sengupta, Gina M Peloso, Stefan Gustafsson, Stavroula Kanoni, Andrea Ganna, et al. 2013. "Discovery and Refinement of Loci Associated with Lipid Levels." *Nature Genetics* 45 (11). Nature Publishing Group: 1274–83. doi:10.1038/ng.2797.

Wood, Andrew R, Tonu Esko, Jian Yang, Sailaja Vedantam, Tune H Pers, Stefan Gustafsson, Audrey Y Chu, et al. 2014a. "Defining the Role of Common Variation in the Genomic and Biological Architecture of Adult Human Height." *Nature Genetics* 46 (11). Nature Publishing Group: 1173–

86. doi:10.1038/ng.3097.

———. 2014b. “Defining the Role of Common Variation in the Genomic and Biological Architecture of Adult Human Height.” *Nature Genetics* 46 (11): 1173–86. doi:10.1038/ng.3097.

Wu, Tao, Hugo Borges Pinto, Yasunao F Kamikawa, and Mary E Donohoe. 2015. “The BET Family Member BRD4 Interacts with OCT4 and Regulates Pluripotency Gene Expression.” *Stem Cell Reports* 4 (3). Elsevier: 390–403. doi:10.1016/j.stemcr.2015.01.012.

Xu, G, R Kanezaki, T Toki, S Watanabe, Y Takahashi, K Terui, I Kitabayashi, and E Ito. 2006. “Physical Association of the Patient-Specific GATA1 Mutants with RUNX1 in Acute Megakaryoblastic Leukemia Accompanying Down Syndrome.” *Leukemia* 20 (6): 1002–8. doi:10.1038/sj.leu.2404223.

Yoshimoto, Momoko, Encarnacion Montecino-Rodriguez, Michael J Ferkowicz, Prashanth Porayette, W Christopher Shelley, Simon J Conway, Kenneth Dorshkind, and Mervin C Yoder. 2011. “Embryonic Day 9 Yolk Sac and Intra-Embryonic Hemogenic Endothelium Independently Generate a B-1 and Marginal Zone Progenitor Lacking B-2 Potential.” *Proceedings of the National Academy of Sciences of the United States of America* 108 (4). National Academy of Sciences: 1468–73. doi:10.1073/pnas.1015841108.

Yoshimoto, Momoko, Prashanth Porayette, Nicole L Glosson, Simon J Conway, Nadia Carlesso, Angelo A Cardoso, Mark H Kaplan, and Mervin C Yoder. 2012. “Autonomous Murine T-Cell Progenitor Production in the Extra-Embryonic Yolk Sac before HSC Emergence.” *Blood* 119 (24). American Society of Hematology: 5706–14. doi:10.1182/blood-2011-12-397489.

Yung, Sun, Maria Ledran, Inmaculada Moreno-Gimeno, Ana Conesa, David Montaner, Joaquín Dopazo, Ian Dimmick, et al. 2011. “Large-Scale Transcriptional Profiling and Functional Assays Reveal Important Roles for Rho-GTPase Signalling and SCL during Haematopoietic Differentiation of Human Embryonic Stem Cells.” *Human Molecular Genetics* 20 (24): 4932–46. doi:10.1093/hmg/ddr431.

Yusa, Kosuke, S. Tamir Rashid, Helene Strick-Marchand, Ignacio Varela, Pei-Qi Liu, David E. Paschon, Elena Miranda, et al. 2011. “Targeted Gene Correction of A1-Antitrypsin Deficiency in Induced Pluripotent Stem Cells.” *Nature* 478 (7369): 391–94. doi:10.1038/nature10424.

Zeng, Lei, and Ming Ming Zhou. 2002. “Bromodomain: An Acetyl-Lysine Binding Domain.” *FEBS Letters*. doi:10.1016/S0014-5793(01)03309-9.

Zhang, Wendy. 2014. “Teratoma Formation: A Tool for Monitoring Pluripotency in Stem Cell Research.” *StemBook*. doi:10.3824/stembook.1.53.1.

Zhang, Yong, Tao Liu, Clifford A Meyer, Jérôme Eeckhoute, David S Johnson, Bradley E Bernstein, Chad Nusbaum, et al. 2008. “Model-Based Analysis of ChIP-Seq (MACS).” *Genome Biology* 9 (9): R137. doi:10.1186/gb-2008-9-9-r137.

Zhang, Zhao, Yuelin Zhang, Fei Gao, Shuo Han, Kathryn S. Cheah, Hung-Fat Tse, and Qizhou Lian. 2017. “CRISPR/Cas9 Genome-Editing System in Human Stem Cells: Current Status and Future Prospects.” *Molecular Therapy - Nucleic Acids* 9 (December). Cell Press: 230–41. doi:10.1016/J.OMTN.2017.09.009.

Zhou, Ming-Ming, Christophe Dhalluin, Justin E. Carlson, Lei Zeng, Cheng He, Aneel K. Aggarwal, and Ming-Ming Zhou. 1999. “Structure and Ligand of a Histone Acetyltransferase Bromodomain.” *Nature* 399 (6735): 491–96. doi:10.1038/20974.

Zovein, Ann C., Jennifer J. Hofmann, Maureen Lynch, Wendy J. French, Kirsten A. Turlo, Yanan Yang,

Michael S. Becker, et al. 2008. "Fate Tracing Reveals the Endothelial Origin of Hematopoietic Stem Cells." *Cell Stem Cell* 3 (6). Cell Press: 625–36. doi:10.1016/J.STEM.2008.09.018.

Zsebo, K M, D A Williams, E N Geissler, V C Broudy, F H Martin, H L Atkins, R Y Hsu, et al. 1990. "Stem Cell Factor Is Encoded at the Sl Locus of the Mouse and Is the Ligand for the C-Kit Tyrosine Kinase Receptor." *Cell* 63 (1). Elsevier: 213–24. doi:10.1016/0092-8674(90)90302-U.

Chapter 6

Appendix

6.1. Plasmids

6.1.1 Plasmids used for generation of Knockouts

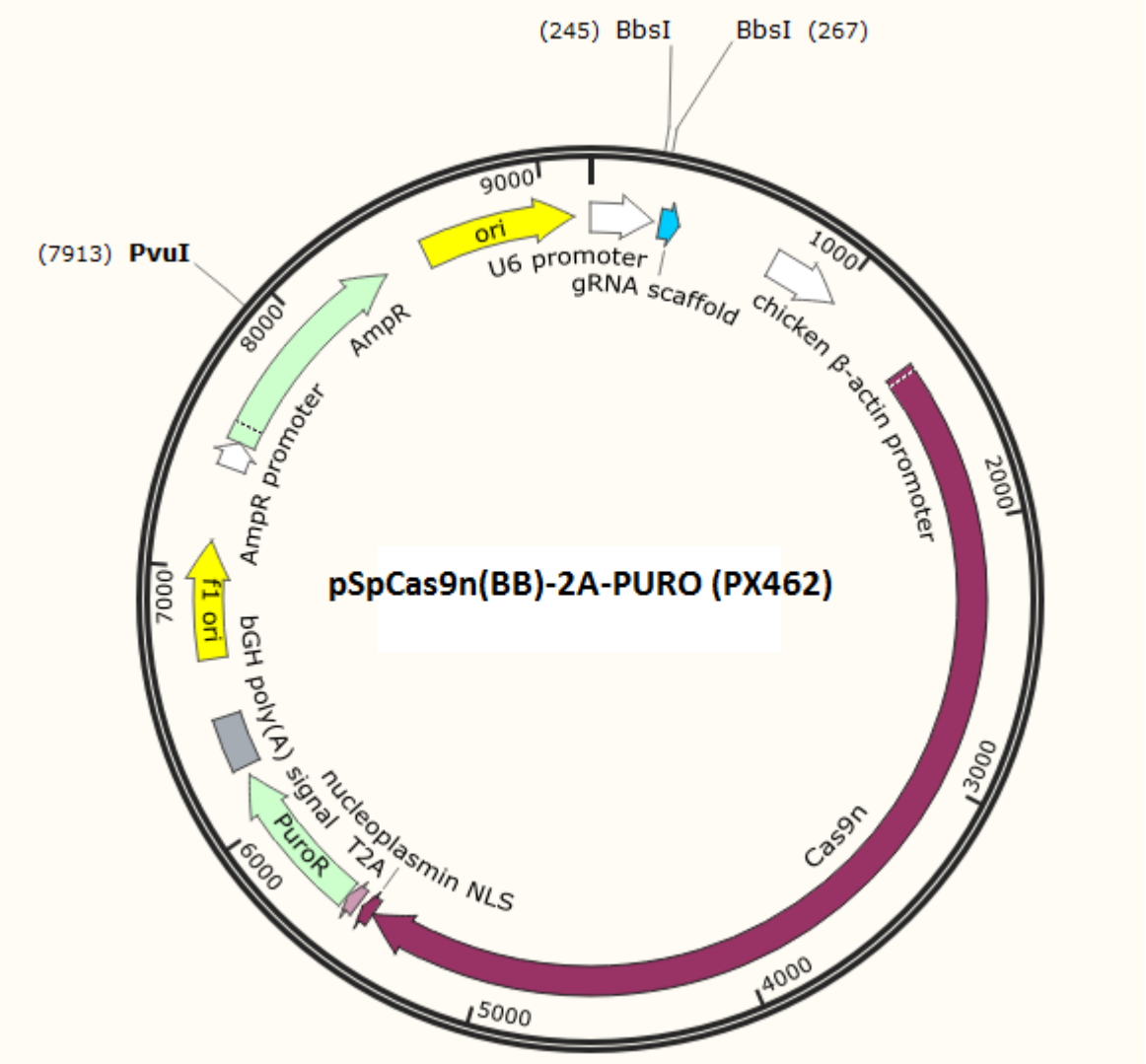

Figure 6.1.1.1 pSpCas9n(BB)-2A-PURO (PX462, Addgene). This vector contains two expression cassettes, Cas9n and the gRNA scaffold. The vector also contain a puromycin sequence for selection based on puromycin treatment. The vector was digested using BbsI enzyme for insertion of the annealed oligos into the sgRNA scaffold. PvuI enzyme was used to check sgRNA insertion before sequencing. Plasmid used for generation of BRD3 KO in S4-SF5 cells.

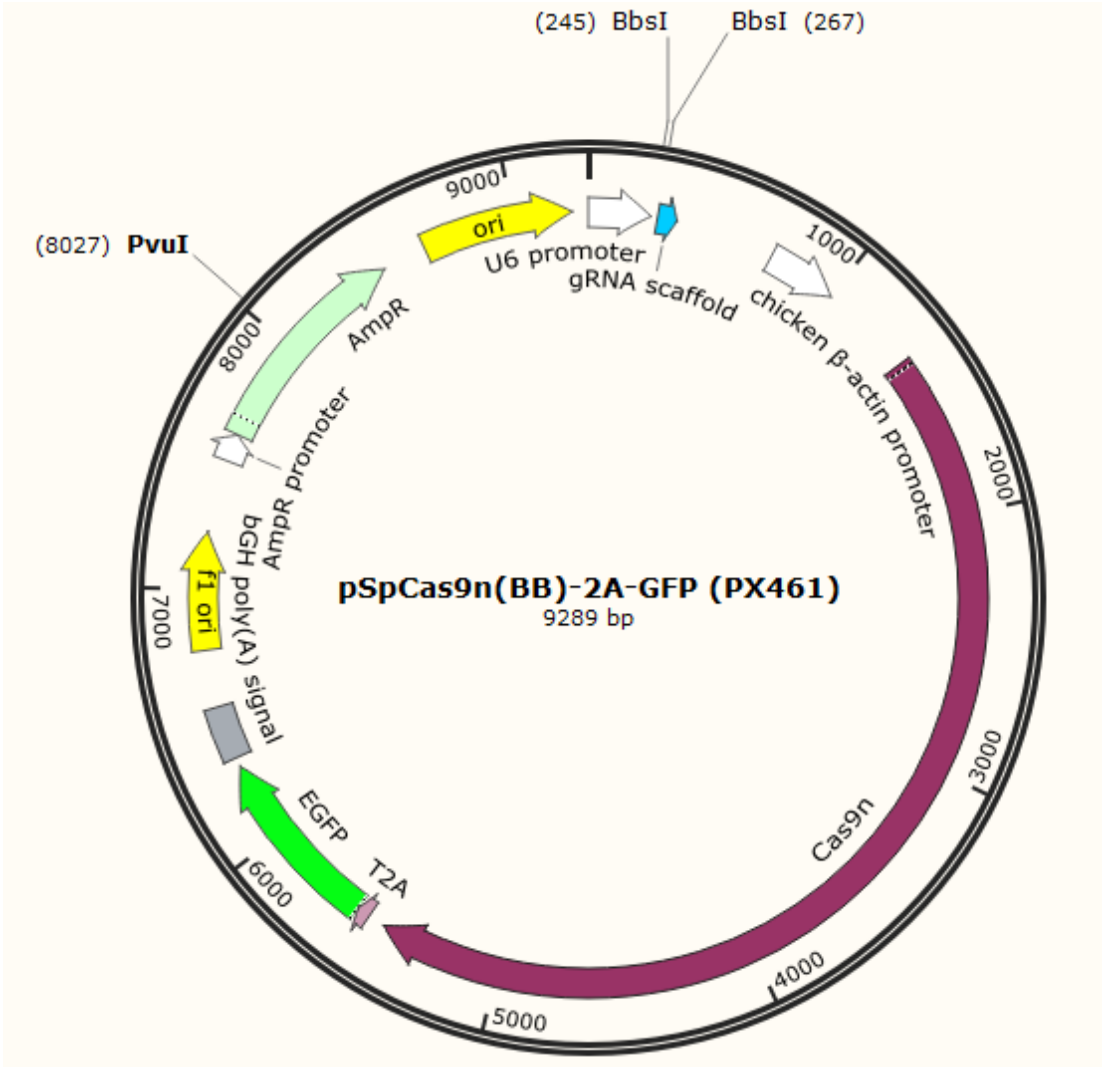

Figure 6.1.1.2 pSpCas9n(BB)-2A-GFP (PX461, Addgene). This vector contains two expression cassettes, Cas9n and the gRNA scaffold. The vector also contain a green fluorescence protein (GFP) sequence for visualisation. The vector was digested using BbsI enzyme for insertion of the annealed oligos into the sgRNA scaffold. PvuI enzyme was used to check sgRNA insertion before sequencing. Plasmid used for generation of BRD3 KO and BRD2 KO in A1ATD1-c cells.

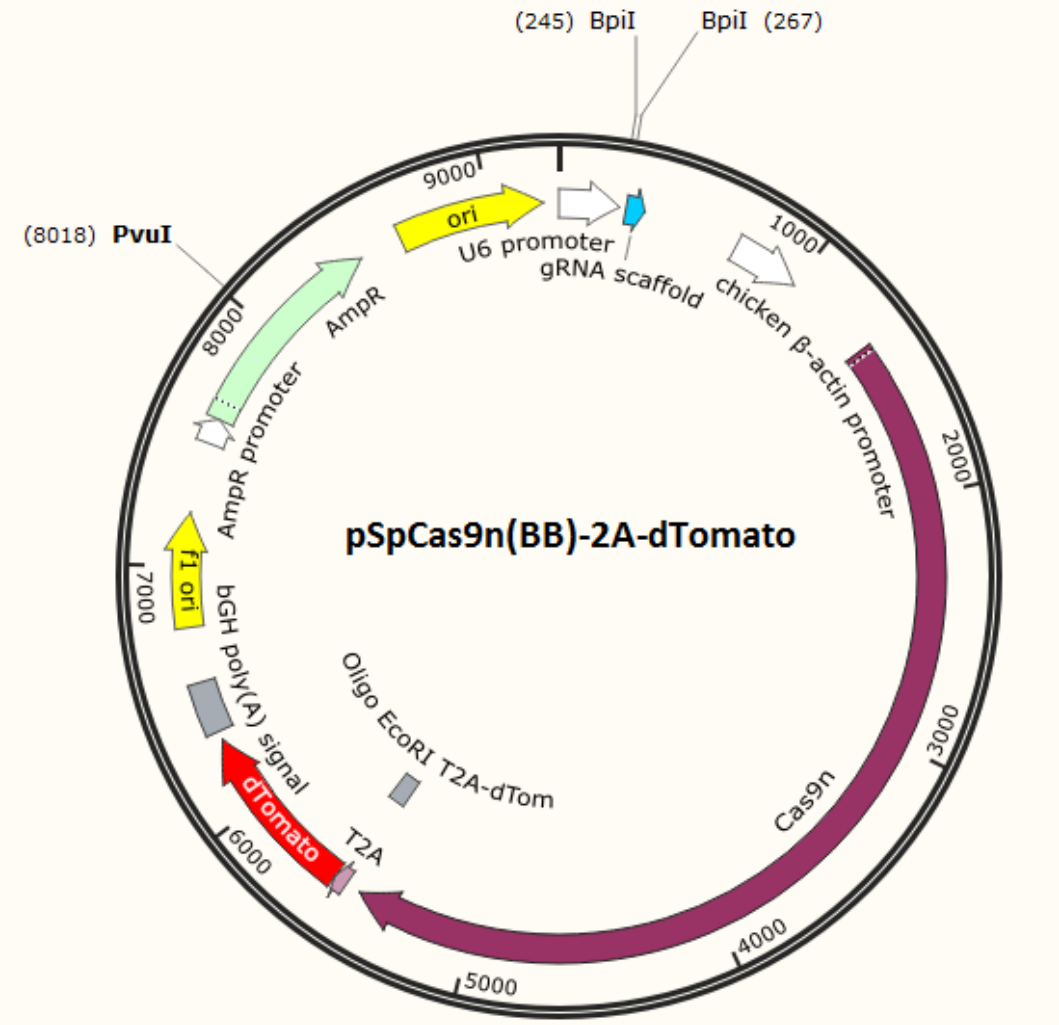

Figure 6.1.1.3 pSpCas9n(BB)-2A-tomato. This vector contains two expression cassettes, Cas9n and the gRNA scaffold. The vector also contain a tomato sequence for visualisation. The vector was digested using BbsI enzyme for insertion of the annealed oligos into the sgRNA scaffold. PvuI enzyme was used to check sgRNA insertion before sequencing. Plasmid used for generation of BRD4 KO in A1ATD1-c cells.

6.1.2 Plasmids used for generation viral particles containing TFs for FoP protocol

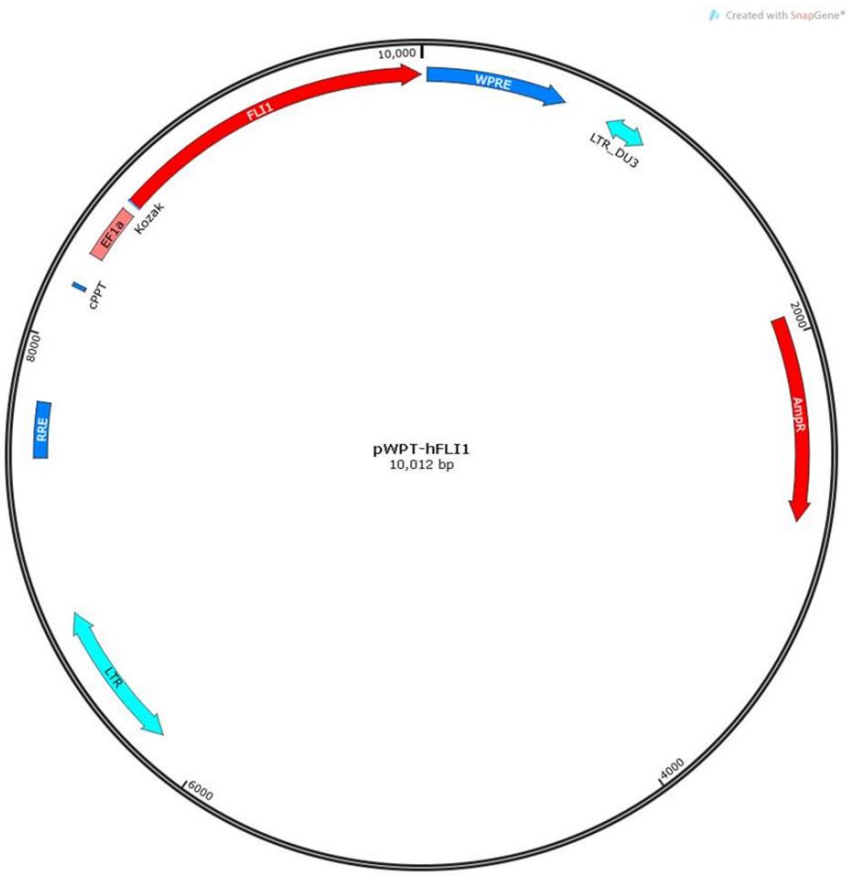

Figure 6.1.2.1 pWPT-FLI-1. Plasmid containing ORF for FLI-1. This plasmid was used to produced viruses used in FoP for differentiation of MKs.

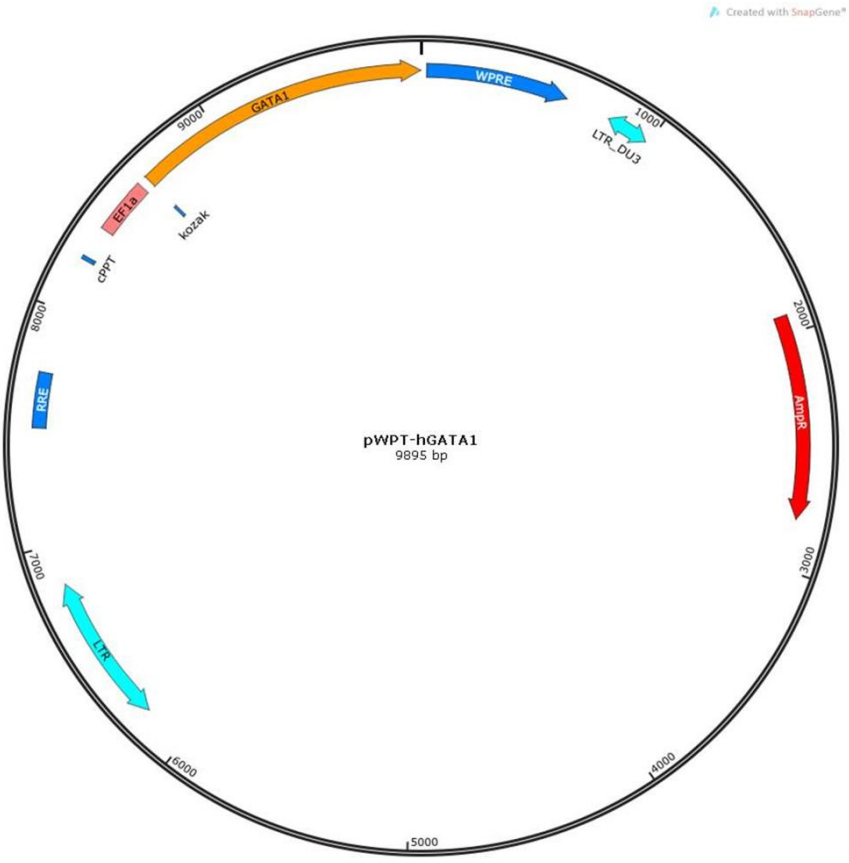

Figure 6.1.2.2 pWPT-GATA1. Plasmid containing ORF for GATA-1. This plasmid was used to produced viruses used in FoP for differentiation of MKs.

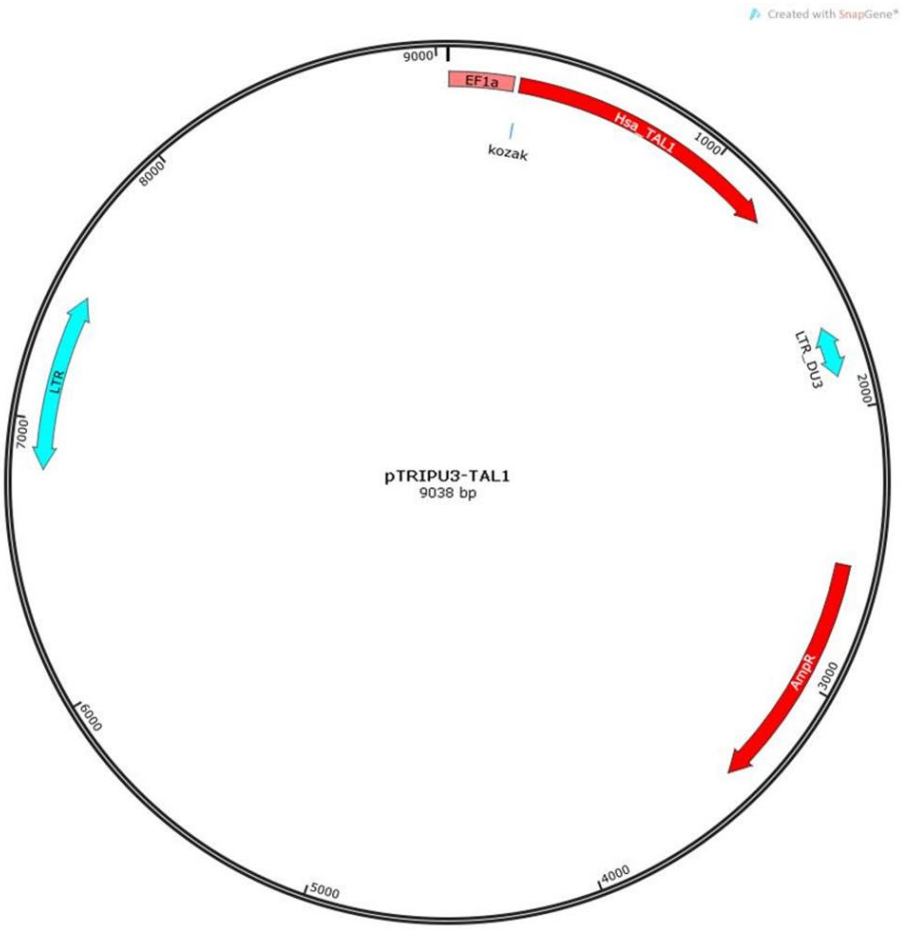

Figure 6.1.2.3 pTRIP-TAL1. Plasmid containing ORF for GATA-1. This plasmid was used to produced viruses used in FoP for differentiation of MKs.

6.1.3 Plasmids used for generation of Knockdowns

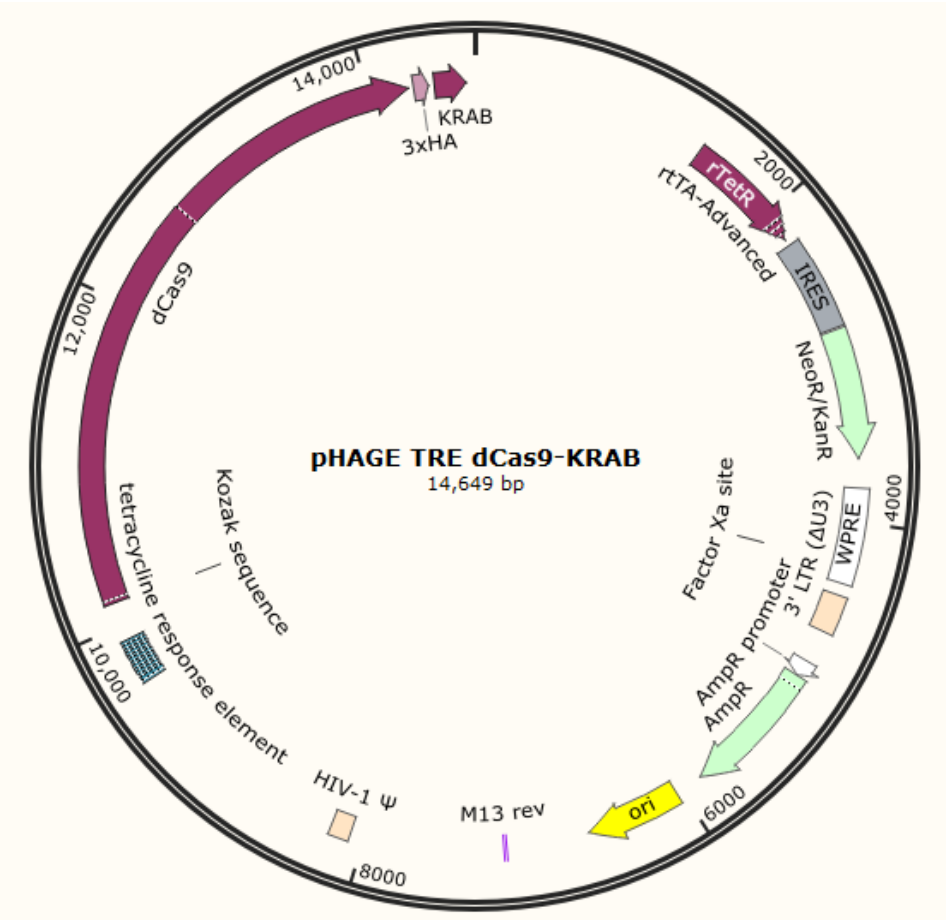

Figure 6.1.3.1 dCas9-KRAB plasmid (Addgene# 50917). Tet-inducible dCas9 lentiviral expression vector. The neomycin cassette confers resistance to the infected cells. This plasmid is TRE-promoter regulated, a 3rd generation plasmid. Therefore, infections with this plasmid also require a packaging plasmid, encoding for GAG, POL, TAT and REV genes, and an envelope plasmid, containing the VSV-G gene. Plasmid-containing virus were produced and cells infected along with lentiGuide Puro (figure 6.1.5). This plasmid was used for the attempts to generate BET knockdowns.

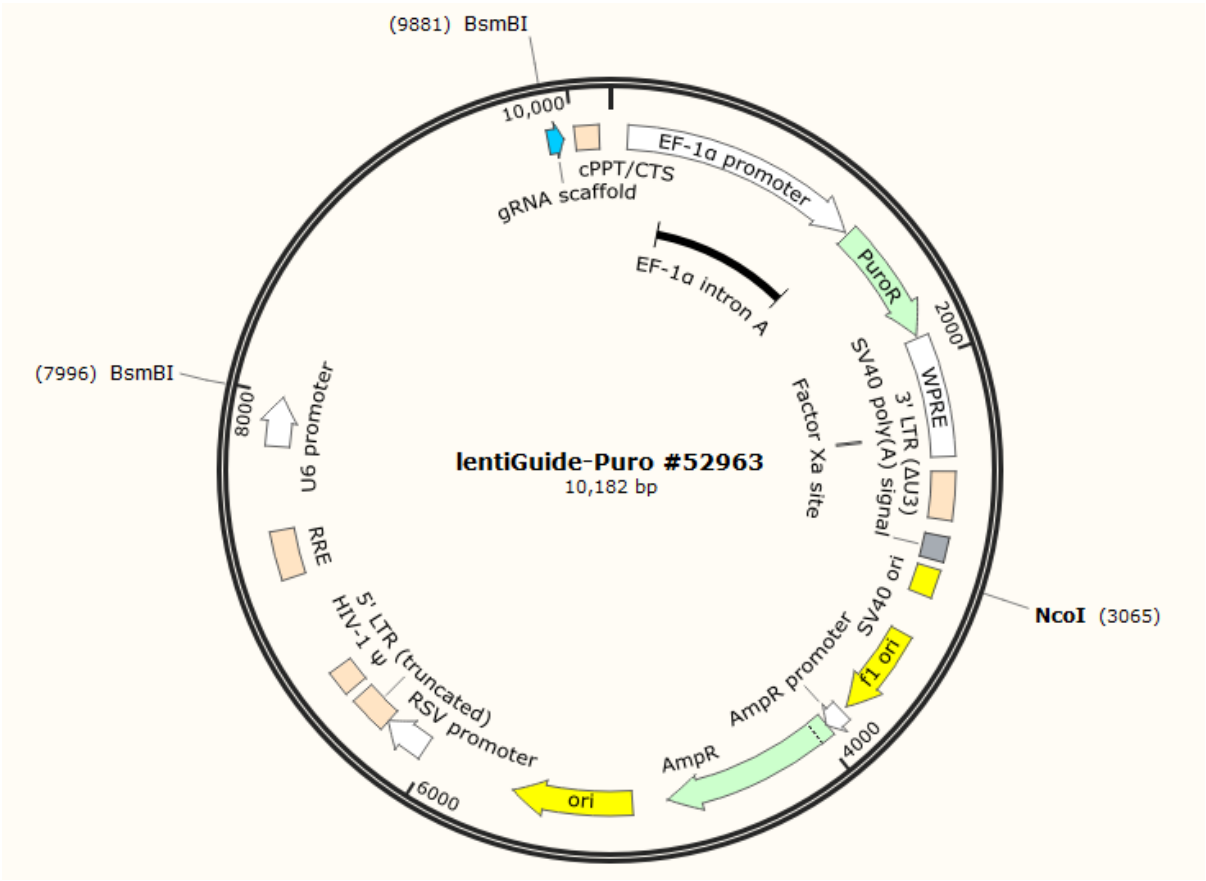

Figure 6.1.3.2 lentiGuide-PURO plasmid (Addgene # 52963). This lentiviral backbone expression vector contains a RNA scaffold element for insertion of customisable RNAs. The puromycin cassette confers resistance to the infected cells. Plasmid was cloned with respective sgRNAs duplexes by restriction digestion (BsmbI). Plasmid-containing virus were produced and cells infected along with dCas9-KRAB (figure 6.1.4). This plasmid was used for the attempts to generate BET knockdowns.

6.2 Alignment of Sanger sequences to confirm sgRNAs insertions

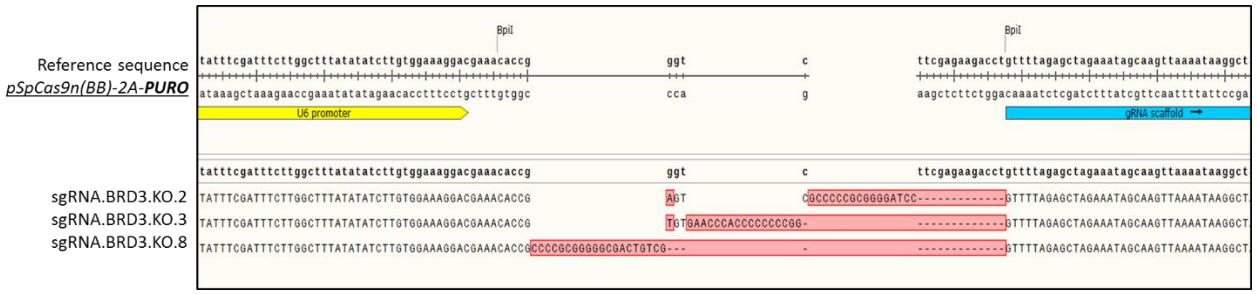

Figure 6.2.1 Sequence alignment for confirmation of BRD3 sgRNAs insertion into *pSpCas9n(BB)-2A-PURO* (for generation of *BRD3 KO in S4-SF5 cells).* Sanger sequencing was performed using U6 forward primer (GGGCAGGAAGAGGGCCTAT). sgRNAs cloned: sgRNA.BRD3.KO.2 (AGTCGCCCCCGCGGGG), sgRNA.BRD3.KO.3 (TGTGAACCCACCCCCCCCGG) and sgRNA.BRD3.KO.8 (CCCCGCGGGGGCGACTGTCG).

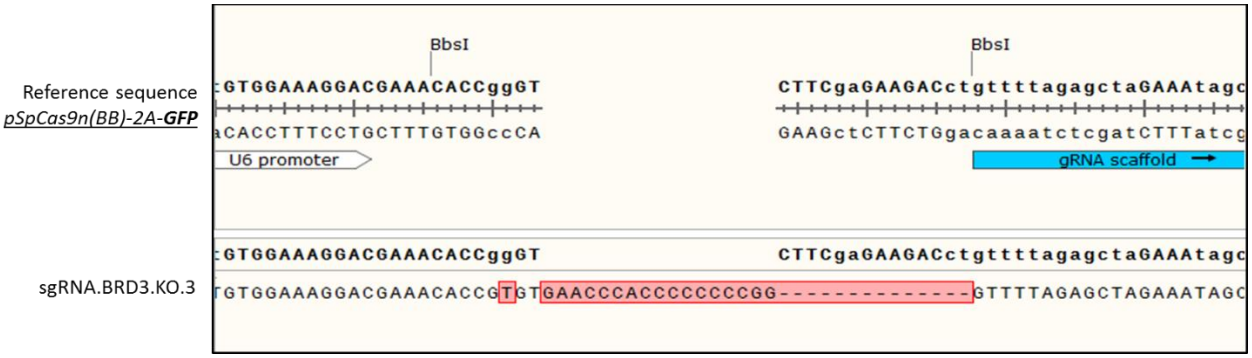

Figure 6.2.2 Sequence alignment for confirmation of BRD3 sgRNA 3 insertion into *pSpCas9n(BB)-2A-GFP* (generation of *BRD3 KO in A1ATD1-c cells).* Sanger sequencing was performed using U6 forward primer (GGGCAGGAAGAGGGCCTAT). sgRNAs cloned: sgRNA.BRD3.KO.3 (TGTGAACCCACCCCCCCCGG).

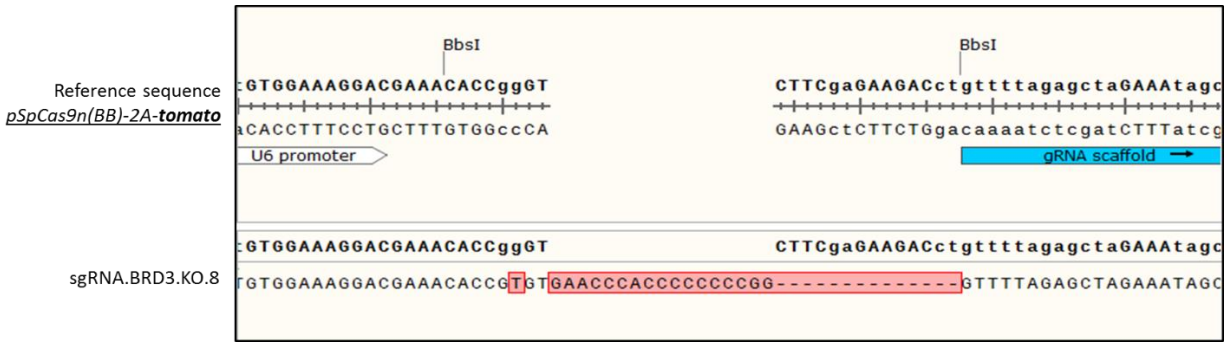

Figure 6.2.3 Sequence alignment for confirmation of BRD3 sgRNA 3 insertion into *pSpCas9n(BB)-2A-tomato (generation of BRD3 KO in A1ATD1-c cells).* Sanger sequencing was performed using U6 forward primer (GGGCAGGAAGAGGGCCTAT). sgRNAs cloned: sgRNA.BRD3.KO.8 (CCCCGCGGGGGCGACTGTCG).

Figure 6.2.4 Sequence alignment for confirmation of BRD2 sgRNAs insertion into *pSpCas9n(BB)-2A-GFP (for generation of BRD2 KO in A1ATD1-c cells).* Sanger sequencing was performed using U6 forward primer (GGGCAGGAAGAGGGCCTAT). sgRNAs cloned: sgRNA.BRD2.KO.10 (TTAATAGTACCCATGTCCAT), sgRNA.BRD2.KO.11 (ACTTGAAAACAATTATTATT), sgRNA.BRD2.KO.12(AATGTAACAGTTGGTGAACA) and sgRNA.BRD2.KO.13 (CAACTGTTACATTTACAACA).

Figure 6.2.5 Sequence alignment for confirmation of BRD4 sgRNAs insertion into *pSpCas9n(BB)-2A-tomato (for generation of BRD4 KO in A1ATD1-c cells).* Sanger sequencing was performed using U6 forward primer (GGGCAGGAAGAGGGCCTAT). sgRNAs inserted: sgRNA.BRD4.KO.1 (GATTTCTCAATCTCGTCCCA), sgRNA.BRD4.KO.2 (TTCCCAAATGTCTACAACAC), sgRNA.BRD4.KO.8 (TGCCCCTTCTTTTTTGACTT), sgRNA.BRD4.KO.9 (CCCCGGGAGGGAGCAGAAGA), sgRNA.BRD4.KO.10 (GGGGGCGAGGACTTCATCGC), sgRNA.BRD4.KO.11 (ACCCTTCATTGCCACCCAGG), sgRNA.BRD4.KO.12 (CACTACCCCAGCAGCCATCA) and sgRNA.BRD4.KO.13 (CAGGGCAGCGGCTCGGTTGC).

6.2. Differentially expressed genes in BRD3 KO

6.2.1 BRD3 KO iPSC

Ensembl ID	gene name	log2FoldChange	pvalue	FDR
ENSG00000005381	MPO	3.044	1.38E-03	3.35E-02
ENSG00000007129	CEACAM21	-6.192	1.05E-07	3.35E-05
ENSG00000015153	YAF2	-1.794	4.50E-04	1.65E-02
ENSG00000018280	SLC11A1	1.983	2.29E-08	1.06E-05
ENSG00000038295	TLL1	3.025	1.21E-03	3.08E-02
ENSG00000075388	FGF4	3.115	9.85E-07	2.01E-04
ENSG00000076356	PLXNA2	-1.906	3.70E-08	1.52E-05
ENSG00000080031	PTPRH	-1.921	9.41E-05	5.91E-03
ENSG00000088882	CPXM1	-2.096	1.80E-08	8.47E-06
ENSG00000094755	GABRP	1.101	9.12E-07	1.90E-04
ENSG00000099284	H2AFY2	-1.978	4.52E-09	2.59E-06
ENSG00000105880	DLX5	-3.956	1.00E-07	3.31E-05
ENSG00000113361	CDH6	-2.301	1.90E-05	1.85E-03
ENSG00000115138	POMC	2.711	1.42E-03	3.40E-02
ENSG00000115325	DOK1	-1.848	1.95E-05	1.88E-03
ENSG00000121351	IAPP	2.333	2.27E-04	1.05E-02
ENSG00000124721	DNAH8	-1.902	1.57E-07	4.40E-05
ENSG00000125144	MT1G	5.092	5.95E-30	1.40E-25
ENSG00000125414	MYH2	3.043	2.21E-09	1.62E-06
ENSG00000125848	FLRT3	-1.942	5.11E-12	7.51E-09
ENSG00000126010	GRPR	1.119	1.37E-04	7.49E-03
ENSG00000127124	HIVEP3	-3.624	6.85E-06	9.47E-04
ENSG00000127399	LRRC61	-2.176	9.38E-10	7.14E-07
ENSG00000130649	CYP2E1	-2.236	3.56E-06	5.76E-04
ENSG00000134201	GSTM5	4.547	1.07E-07	3.35E-05
ENSG00000134686	PHC2	-2.082	5.90E-11	7.70E-08
ENSG00000135248	FAM71F1	-1.758	3.33E-09	2.18E-06
ENSG00000142583	SLC2A5	-2.004	9.58E-11	1.07E-07
ENSG00000143195	ILDR2	-2.087	1.71E-05	1.76E-03
ENSG00000143369	ECM1	-2.288	1.05E-04	6.42E-03
ENSG00000143669	LYST	-1.961	1.52E-05	1.59E-03
ENSG00000144152	FBLN7	-2.435	3.29E-05	2.84E-03
ENSG00000144785	AC073896.1	-2.859	4.04E-04	1.53E-02
ENSG00000144810	COL8A1	-2.499	1.36E-04	7.45E-03
ENSG00000145247	OCIAD2	-2.600	2.65E-10	2.49E-07
ENSG00000146648	EGFR	-1.712	3.59E-05	3.04E-03
ENSG00000148516	ZEB1	-2.929	1.88E-05	1.84E-03

ENSG00000148848	ADAM12	-2.581	7.76E-05	5.24E-03
ENSG00000148948	LRRC4C	2.422	1.37E-03	3.35E-02
ENSG00000149294	NCAM1	-1.503	1.02E-05	1.19E-03
ENSG00000151376	ME3	-3.040	1.03E-07	3.35E-05
ENSG00000152208	GRID2	1.163	5.34E-04	1.81E-02
ENSG00000154146	NRGN	-3.547	4.44E-06	6.69E-04
ENSG00000154760	SLFN13	-1.354	2.91E-04	1.24E-02
ENSG00000155622	XAGE2	5.059	7.16E-06	9.79E-04
ENSG00000160097	FNDC5	-1.953	3.93E-05	3.22E-03
ENSG00000162344	FGF19	2.332	2.84E-06	4.90E-04
ENSG00000162909	CAPN2	-1.910	4.22E-05	3.37E-03
ENSG00000163492	CCDC141	2.539	2.51E-04	1.13E-02
ENSG00000165169	DYNLT3	4.395	2.34E-09	1.66E-06
ENSG00000166741	NNMT	-4.607	1.74E-05	1.76E-03
ENSG00000167785	ZNF558	3.243	4.96E-04	1.74E-02
ENSG00000168542	COL3A1	-6.832	6.75E-05	4.72E-03
ENSG00000169085	VXN	-2.719	2.36E-04	1.08E-02
ENSG00000169248	CXCL11	2.479	1.39E-06	2.76E-04
ENSG00000171004	HS6ST2	-1.592	1.53E-04	7.91E-03
ENSG00000172339	ALG14	-1.392	3.15E-04	1.30E-02
ENSG00000173809	TDRD12	2.449	4.61E-08	1.78E-05
ENSG00000175868	CALCB	2.568	1.65E-03	3.69E-02
ENSG00000182580	EPHB3	-2.031	9.42E-09	4.61E-06
ENSG00000182870	GALNT9	-2.793	7.00E-04	2.14E-02
ENSG00000186300	ZNF555	2.706	1.39E-05	1.48E-03
ENSG00000186439	TRDN	3.001	1.63E-06	3.14E-04
ENSG00000187105	HEATR4	1.737	1.73E-04	8.59E-03
ENSG00000187193	MT1X	1.799	1.74E-12	3.40E-09
ENSG00000188483	IER5L	-2.666	1.45E-10	1.48E-07
ENSG00000188707	ZBED6CL	-2.072	3.64E-09	2.25E-06
ENSG00000197415	VEPH1	1.342	7.03E-04	2.14E-02
ENSG00000197956	S100A6	3.185	8.68E-07	1.84E-04
ENSG00000198028	ZNF560	5.242	3.57E-12	5.60E-09
ENSG00000198417	MT1F	4.910	3.53E-08	1.48E-05
ENSG00000198732	SMOC1	-2.267	4.75E-06	6.97E-04
ENSG00000203685	STUM	3.235	2.33E-03	4.46E-02
ENSG00000213401	MAGEA12	-4.032	6.67E-20	7.84E-16
ENSG00000215386	MIR99AHG	-4.048	9.40E-04	2.57E-02
ENSG00000240184	PCDHGC3	-1.531	7.96E-07	1.75E-04
ENSG00000253230	LINC00599	1.777	1.80E-03	3.93E-02
ENSG00000253507	AC104257.1	2.128	1.18E-05	1.31E-03
ENSG00000255132	AC090138.1	4.569	5.36E-06	7.76E-04
ENSG00000258947	TUBB3	-1.090	1.38E-06	2.76E-04
ENSG00000258952	SALRNA1	-2.613	1.36E-13	3.99E-10

ENSG00000260362	AC007218.1	1.997	5.01E-05	3.85E-03
ENSG00000260518	BMS1P8	-3.491	4.74E-06	6.97E-04
ENSG00000261143	ADAMTS7P3	-4.857	1.64E-06	3.14E-04
ENSG00000263020	AL662899.2	-1.804	3.11E-04	1.29E-02
ENSG00000268119	AC010615.2	2.684	7.57E-11	8.89E-08
ENSG00000268861	AC008878.3	-7.323	6.53E-08	2.36E-05
144.3173154	HIST1H4F	0.471	1.22E-04	7.03E-03
7127.822855	AL161431.1	0.247	1.55E-07	4.38E-05
216.2395137	HIST1H2BB	0.321	1.69E-04	8.46E-03
56.77799995	HYDIN2	0.563	3.32E-13	8.66E-10
327.0661473	HIST1H3C	0.312	8.00E-06	1.05E-03
152.7581079	AC007846.1	0.516	2.30E-07	6.00E-05
17.12738923	AC000093.1	17.592	1.51E-04	7.88E-03
16.93240146	AC007846.2	27.999	8.32E-07	1.79E-04

6.2.1 Table of differentially expressed genes between WT and BRD3 KO in A1ATD1-c **iPSC** cells. Common differentially expressed genes between BRD3 KO iPSC and MKs highlighted in grey.

6.2.1 BRD3 KO MKs

Ensembl ID	gene name	log2FoldChange	pvalue	FDR
ENSG00000019991	HGF	5.261	4.320E-05	2.503E-03
ENSG00000064225	ST3GAL6	1.920	1.032E-03	2.829E-02
ENSG00000066382	MPPED2	1.829	7.550E-05	3.881E-03
ENSG00000081237	PTPRC	2.417	1.680E-06	1.889E-04
ENSG00000082781	ITGB5	1.178	1.800E-05	1.257E-03
ENSG00000085733	CTTN	1.508	1.808E-04	7.643E-03
ENSG00000102245	CD40LG	2.272	1.220E-05	9.038E-04
ENSG00000105767	CADM4	1.751	1.939E-04	8.074E-03
ENSG00000109705	NKX3-2	3.765	3.201E-04	1.149E-02
ENSG00000111186	WNT5B	2.752	8.430E-11	3.750E-08
ENSG00000111554	MDM1	1.264	1.460E-05	1.060E-03
ENSG00000116194	ANGPTL1	-1.636	5.820E-05	3.184E-03
ENSG00000117586	TNFSF4	1.690	2.180E-07	3.450E-05
ENSG00000118946	PCDH17	1.369	5.551E-04	1.759E-02
ENSG00000119283	TRIM67	-2.352	2.970E-15	3.370E-12
ENSG00000124406	ATP8A1	1.245	3.900E-06	3.795E-04
ENSG00000130508	PXDN	-1.049	7.350E-09	1.890E-06
ENSG00000130649	CYP2E1	-2.359	1.725E-03	4.044E-02
ENSG00000132932	ATP8A2	2.875	7.560E-06	6.378E-04
ENSG00000134871	COL4A2	3.788	2.670E-05	1.751E-03
ENSG00000136404	TM6SF1	1.378	7.439E-04	2.224E-02
ENSG00000137959	IFI44L	-1.394	1.930E-18	6.020E-15

ENSG00000139329	LUM	5.806	1.350E-07	2.340E-05
ENSG00000143226	FCGR2A	1.280	1.860E-04	7.811E-03
ENSG00000143333	RGS16	1.088	2.065E-04	8.345E-03
ENSG00000143367	TUFT1	1.737	1.453E-04	6.449E-03
ENSG00000144648	ACKR2	1.176	5.267E-04	1.680E-02
ENSG00000146555	SDK1	2.386	4.700E-07	6.690E-05
ENSG00000147804	SLC39A4	1.659	2.380E-06	2.560E-04
ENSG00000148926	ADM	-1.488	1.660E-07	2.750E-05
ENSG00000151491	EPS8	-1.421	8.410E-05	4.229E-03
ENSG00000151962	RBM46	4.910	8.920E-07	1.146E-04
ENSG00000152208	GRID2	2.529	1.620E-03	3.867E-02
ENSG00000152315	KCNK13	2.846	2.760E-08	5.880E-06
ENSG00000154217	PITPNC1	2.125	3.530E-06	3.504E-04
ENSG00000155158	TTC39B	1.576	1.120E-10	4.740E-08
ENSG00000155926	SLA	1.200	1.650E-10	6.860E-08
ENSG00000163898	LIPH	1.590	8.610E-06	6.928E-04
ENSG00000164691	TAGAP	2.390	1.158E-03	3.037E-02
ENSG00000165092	ALDH1A1	2.344	4.870E-09	1.290E-06
ENSG00000165169	DYNLT3	1.911	3.060E-05	1.917E-03
ENSG00000165949	IFI27	-1.849	1.870E-49	2.330E-45
ENSG00000166035	LIPC	1.164	4.250E-10	1.580E-07
ENSG00000169248	CXCL11	1.805	8.670E-05	4.300E-03
ENSG00000169946	ZFPM2	1.629	6.440E-10	2.320E-07
ENSG00000172819	RARG	1.489	8.220E-08	1.560E-05
ENSG00000173083	HPSE	1.335	1.860E-05	1.277E-03
ENSG00000173110	HSPA6	2.068	3.136E-04	1.127E-02
ENSG00000173334	TRIB1	1.211	1.550E-05	1.113E-03
ENSG00000174944	P2RY14	2.835	1.960E-05	1.335E-03
ENSG00000175556	LONRF3	2.626	4.500E-05	2.594E-03
ENSG00000179639	FCER1A	1.348	1.280E-08	2.960E-06
ENSG00000180353	HCLS1	1.380	1.212E-03	3.137E-02
ENSG00000182771	GRID1	1.975	5.046E-04	1.624E-02
ENSG00000183632	TP53TG3	-5.102	5.100E-09	1.340E-06
ENSG00000183785	TUBA8	1.549	5.880E-07	7.840E-05
ENSG00000186190	BPIFB3	1.841	1.299E-03	3.296E-02
ENSG00000186300	ZNF555	1.762	6.420E-07	8.430E-05
ENSG00000188219	POTEE	1.374	8.140E-06	6.621E-04
ENSG00000188959	C9orf152	2.595	1.098E-04	5.186E-03
ENSG00000196611	MMP1	2.137	9.580E-18	2.170E-14
ENSG00000197956	S100A6	3.657	1.626E-04	7.025E-03
ENSG00000198028	ZNF560	5.021	5.410E-07	7.410E-05
ENSG00000205609	EIF3CL	1.195	3.056E-04	1.109E-02
ENSG00000217644	AL355864.1	1.287	3.035E-04	1.105E-02
ENSG00000224400	AC010880.1	1.842	1.230E-06	1.454E-04

ENSG00000225255	AP000527.1	2.469	1.560E-07	2.630E-05
ENSG00000227550	TRBV7-5	2.801	3.432E-04	1.207E-02
ENSG00000229308	AC010737.1	1.982	1.711E-03	4.026E-02
ENSG00000230450	NEK2P4	4.778	3.920E-05	2.325E-03
ENSG00000231431	FAR2P4	1.716	1.110E-05	8.387E-04
ENSG00000232533	AC093673.1	1.097	8.116E-04	2.378E-02
ENSG00000234211	AL451067.1	3.527	2.636E-04	9.889E-03
ENSG00000234350	AC007405.1	-1.972	6.020E-06	5.459E-04
ENSG00000235288	AC099329.1	1.356	7.640E-05	3.922E-03
ENSG00000236956	NF1P8	3.829	4.720E-07	6.690E-05
ENSG00000244470	AC105918.1	1.788	6.250E-06	5.549E-04
ENSG00000248796	MED15P8	4.405	9.370E-07	1.181E-04
ENSG00000251301	LINC02384	1.919	4.860E-07	6.810E-05
ENSG00000254319	AC246817.2	-2.696	3.680E-07	5.390E-05
ENSG00000255446	AP003064.2	5.803	2.890E-06	3.018E-04
ENSG00000256683	ZNF350	1.068	1.264E-04	5.790E-03
ENSG00000260877	AP005233.2	2.347	5.801E-04	1.811E-02
ENSG00000261127	AC133548.2	-4.407	3.820E-19	1.590E-15
ENSG00000261466	AC136944.4	-2.827	1.330E-12	1.230E-09
ENSG00000261796	ISY1-RAB43	1.261	7.390E-06	6.286E-04
ENSG00000265799	AC090844.3	-2.039	1.010E-06	1.254E-04
ENSG00000278272	HIST1H3C	0.948	2.240E-11	1.210E-08
ENSG00000278996	FP671120.1	0.286	1.967E-04	8.150E-03

6.2.1 Table of differentially expressed genes between WT and BRD3 KO in A1ATD1-c **MK** cells. Common differentially expressed genes between BRD3 KO iPSC and MKs highlighted in grey. ZFPM2 (highlighted in red) has previously been associated with platelet traits in GWAS studies.

6.3. BET inhibition - appendix

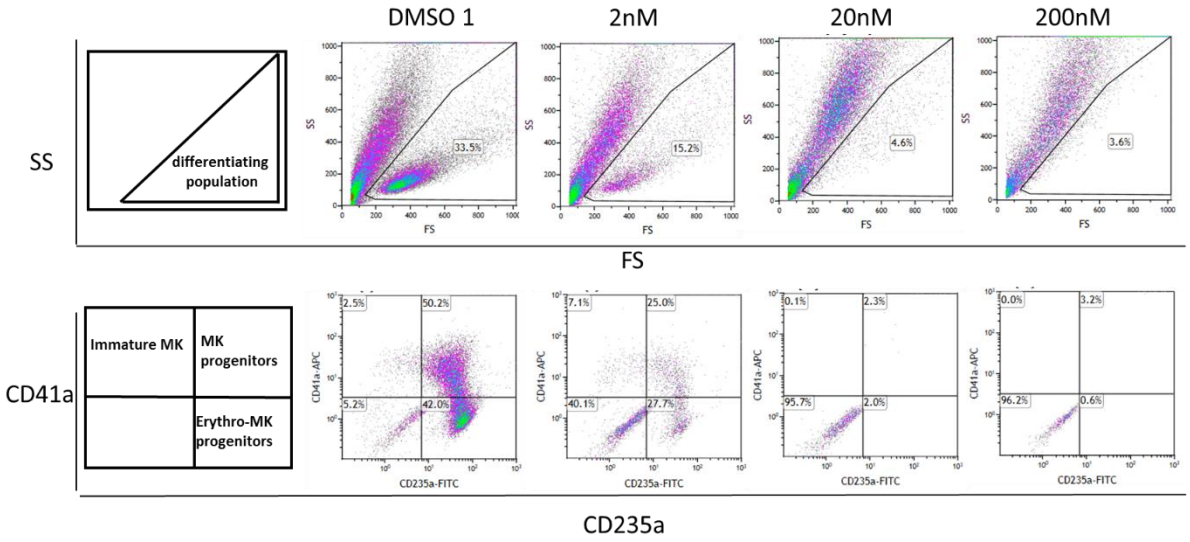

Figure 6.3.1. **Flow cytometry results at day 10 for cultures inhibited at day 1 (1i), related to figure 3.3.5.** FS vs SS plots (top panel) show gated differentiating cells. CD235a vs CD41a (bottom panel) show MK progenitor cells. BET inhibition at day 1 prevents the formation of MK progenitor population expected at day 10.

Acknowledgments

I would like to express my gratitude to my supervisor, Dr Mattia Frontini. Thank you for being a good mentor, and generous during life's unexpected circumstances.

I would like to thank Dr Denis Sereys for performing all the bioinformatics analysis in this thesis. Denis always had everything under control (or so it looked!), and consistently accommodated my interruptions with a smile on his face.

I would also like to thank other lab members, namely Dr John Lambourne for all his help with ChIP-seq; Mrs Frances Burden for her help with RNA-seq processing; Miss Giulia Artemi for taking on the BET project; my PhD colleagues Rita Tomé and Dr Tadbir Bariana for the good discussions and for your company in the late evenings at work. Thank you to all the other lab members for being so welcoming and helpful.

I would also like to acknowledge members of Dr Cedric Ghevaert's lab, in particular Dr Thomas Moreau, Dr Amanda Evans for the knowledge shared on generation of MKs and help tweaking the FoP protocol. Thanks to Dr Annette Muller for the plasmid for generation of KOs.

I would like to acknowledge Dr Marc Feary for running the rest of my daily life during my PhD studies. It was easier to pedal to the end with you in the support team.

A big thank you to all my family for understanding my absence during these years, and all my friends who believed that I would survive the PhD. So far, I did not let you down!

I would like to show my appreciation to BHF for generously financing the 3 years of my laboratorial work. Thank you for the opportunity.

And lastly, I would like to thank Newnham College for welcoming me to the University of Cambridge. Being a Newnhamite taught me that being confident and having high aspirations is a matter of healthy ambition requiring focus, discipline and self-believe.

Now… this is end of my thesis, but only the beginning of my science journey.

Thank you all.